

THE REPUBLIC OF INDONESIA
MINISTRY OF PUBLIC WORKS AND HOUSING

**THE PROJECT FOR ASSESSING AND INTEGRATING
CLIMATE CHANGE IMPACTS INTO
THE WATER RESOURCES MANAGEMENT PLANS
FOR BRANTAS AND MUSI RIVER BASINS**
(Climate Change Impact Assessment and Hydrological Simulation)

FINAL REPORT

MARCH 2017

JAPAN INTERNATIONAL COOPERATION AGENCY

THE UNIVERSITY OF TOKYO
NIPPON KOEI CO., LTD.

| |
|----------|
| GE |
| JR |
| 17 - 030 |

THE REPUBLIC OF INDONESIA

MINISTRY OF PUBLIC WORKS AND HOUSING

THE PROJECT FOR ASSESSING AND INTEGRATING

CLIMATE CHANGE IMPACTS INTO

THE WATER RESOURCES MANAGEMENT PLANS

FOR BRANTAS AND MUSI RIVER BASINS

(Climate Change Impact Assessment and Hydrological Simulation)

FINAL REPORT

MARCH 2017

JAPAN INTERNATIONAL COOPERATION AGENCY

THE UNIVERSITY OF TOKYO

NIPPON KOEI CO., LTD.



Location Map of the Study Area: Brantas River Basin

Abbreviations 略語表

| Abbreviation | English | Japanese |
|--------------|--|------------------|
| ADB | Asian Development Bank | アジア開発銀行 |
| AfWCCI | GEOSS African Water Cycle Coordination Initiative | アフリカ水循環調整イニシアチブ |
| AIEM | Advanced Integral Equation Model | 表面散乱モデル |
| AMSR-E | Advanced Microwave Scanning Radiometer for EOS | 改良型高性能マイクロ波放射計 |
| BAPPEDA | Regional body for planning and development | 南スマトラ州地域開発計画庁 |
| BATS | Biosphere–Atmosphere Transfer Scheme | 陸面過程モデル |
| BMKG | Agency for Meteorology, Climatology and Geophysics | 気候・気象・地球物理庁 |
| CMIP3 | The 3rd phase of Coupled Model Intercomparison Project | 第3次モデル相互比較プロジェクト |
| CMIP5 | The 5th phase of Coupled Model Intercomparison Project | 第5次モデル相互比較プロジェクト |
| C/P | Counterpart | カウンターパート |
| CRBOM | Center for River Basin Organizations and Management | 河川流域機関管理センター |
| DB | Database | データベース |
| DEM | Digital Elevation Model | 数値標高モデル |
| DF/R | Draft Final Report | ドラフト・ファイナルレポート |
| DGWR | Directorate General of Water Resources | 水資源総局 |
| DHM | Distributed Hydrological Model | 分布型水循環モデル |
| DMRT | Dense Medium Radiative Transfer | 放射伝達モデル |
| DNPI | National Council for Climate Change | 国家気候変動評議会 |
| DUWRMT | Dissemination Unit for Water Resources Management and Technology | 水資源管理技術普及ユニット |
| FAO | Food and Agriculture Organization of the United Nations | 国際連合食糧農業機関 |
| FPAR | Fraction of Photosynthetic Active Radiation | 光合成有効放射吸収率 |
| F/R | Final Report | ファイナル・レポート |
| GBHM | Geomorphology-Based Hydrological Model | 分布型流出モデル |
| GCM | General Circulation Model | 大気循環モデル |
| GEO | Group on Earth Observations | 地球観測作業部会 |
| GEOSS | Global Earth Observation System of Systems | 全球地球観測システム |

Location Map of the Study Area and Abbreviations

| | | |
|---------|---|---------------------|
| GOI | Government of Indonesia | インドネシア国政府 |
| GOJ | Government of Japan | 日本国政府 |
| GPS | Global Positioning System | 全球測位システム |
| GSMaP | Global Satellite Mapping of Precipitation | 全球降水マップ |
| ICHARM | International Centre for Water Hazard and Risk Management | 水災害・リスクマネジメント国際センター |
| IC/R | Inception Report | インセプション・レポート |
| IWRM | Integrated Water Resources Management | 統合水資源管理 |
| IPCC | Intergovernmental Panel on Climate Change | 気候変動に関する政府間パネル |
| IT/R | Interim Report | インテリム・レポート |
| JCC | Joint Coordinating Committee | 合同調整委員会 |
| JAXA | Japan Aerospace Exploration Agency | 宇宙研究開発機構 |
| JICA | Japan International Cooperation Agency | 国際協力機構 |
| JMA | Japan Meteorological Agency | 気象庁 |
| LAI | Leaf Area Index | 葉面積指数 |
| LDAS-UT | Land Data Assimilation System by Coupling AMSR-E and SiB2 | 陸面データ同化 |
| LSM | Land Surface Model | 地表面モデル |
| MM | Men Month | 人月 |
| M/M | Minutes of Meeting | 協議議事録 |
| NCDC | National Climatic Data Center | アメリカ国立気候データセンター |
| NOAA | National Oceanic and Atmospheric Administration | 米国海洋大気庁 |
| ODA | Official Development Assistance | 政府開発援助 |
| PDM | Project Design Matrix | プロジェクト・デザイン・マトリックス |
| PJT 1 | Jasa Tirta Public Corporation 1 | 水資源（水道）公社 1 |
| PO | Plan of Operation | 実行計画 |
| POLA | Water Resources Management Strategic Plan | 水資源管理戦略計画 |
| PU | Ministry of Public Works and Housing | 公共事業省 |
| PUSAIR | Water Resources Research and Development Center, Ministry of Public Works | 水資源研究センター |
| RBO | River Basin Organization | 河川流域機関（BBWS） |
| P/R | Progress Report | プロGRESS・レポート |
| R/D | Record of Discussions | 協議議事録 |
| RENCANA | Water Resources Management Implementation Plan | 水資源管理実施計画 |
| RMSE | Root Mean Squared Error | 2乗平均平方根誤差 |
| RTM | Radiative Transfer Model | 放射伝達モデル |

Location Map of the Study Area and Abbreviations

| | | |
|---------|--|------------------------|
| SEA | Strategic Environmental Assessment | 戦略的環境アセスメント |
| SiB2 | Simple Biosphere 2 | 単純植生モデル2 |
| SIMRIW | Simulation Model for Rice Weather Relations | 水稲生育モデル |
| SWI | Soil Wetness Index | 土壌湿潤指数 |
| USGS | United States Geological Survey | アメリカ地質調査所 |
| WEB-DHM | Water and Energy Budget based Distributed Hydrological Model | 分布型水循環モデル |
| WMO | World Meteorological Organization | 世界気象機関 |
| WRF | Weather Research and Forecasting Model | 次世代メソスケール数値天気予報モデルシステム |
| WSP | Water Security Plan | 水の安全保障計画 |

Table of Contents

| | |
|---|-----|
| Location Map of the Study Area: Brantas River Basin (Java Island) | |
| Location Map of the Study Area: Musi River Basin (Sumatra Island) | |
| Abbreviations | |
| | |
| CHAPTER 1 INTRODUCTION | 1-1 |
| 1.1 Background of the Project | 1-1 |
| 1.2 General outline of the Project | 1-2 |
| 1.2.1 Project Objectives | 1-2 |
| 1.2.2 Expected Project Outputs | 1-2 |
| 1.2.3 Project Area | 1-2 |
| 1.2.4 Implementing Organization in Indonesia | 1-3 |
| 1.3 General Outline of the Study (Climate Change Impact Assessment and Hydrological Simulation) | 1-3 |
| 1.3.1 Purpose of the Study | 1-3 |
| 1.3.2 Scope and Schedule of the Study | 1-4 |
| | |
| CHAPTER 2 IMPLEMENTATION POLICY | 2-1 |
| 2.1 Water Issue Recognition of Indonesia and its Needs | 2-1 |
| 2.2 Policy and Consideration for Project Implementation (Climate Change Impact Analysis and Hydrological Simulation) | 2-2 |
| 2.3 Input from the Japanese Side and Project Management | 2-3 |
| | |
| CHAPTER 3 PLAN OF OPERATION | 3-1 |
| 3.1 Technical Guideline | 3-1 |
| 3.1.1 Study Flow | 3-1 |
| 3.1.2 GCM Selection, Bias-correction and Spatial Downscaling | 3-3 |
| 3.1.3 Hydrologic simulation by Water and Energy Budget-based Distributed Hydrological Model (WEB-DHM) | 3-3 |
| 3.1.4 Simulation System Using a Coupled Model of a Distributed Hydrological Model (WEB-DHM) and rice growth model (SIMRIW) | 3-4 |
| 3.2 Implementation Method of the Study | 3-5 |
| 3.2.1 Preparatory Investigation | 3-5 |
| 3.2.2 Implementation of Rainfall-runoff Analysis Considering Climate Change Impact Assessment | 3-5 |

Table of Contents

| | | |
|-----------|--|-------|
| 3.2.3 | Assessment of Impacts on Food Production Caused by Climate Change in Musi River Basin | 3-12 |
| 3.3 | Assistance to Water Resources Management Plan Project Team | 3-14 |
| 3.2.1 | Science | 3-14 |
| 3.2.2 | Capacity Development | 3-14 |
| 3.4 | Report Schedule and Dispatch..... | 3-15 |
| | | |
| CHAPTER 4 | CLIMATE CHANGE IMPACT ASSESSMENT AND HYDROLOGICAL SIMULATION | 4-1 |
| 4.1 | Climate Change Impact Assessment on Water Cycle: Common Approaches | 4-1 |
| 4.1.1 | Review of Action Plan, and Collection and Analysis of Existing Information and Data | 4-1 |
| 4.1.2 | Climate Change Impact Assessment for Rainfall | 4-2 |
| 4.1.3 | Climate Change Impact Assessment for River Runoff, ET, and Soil Moisture..... | 4-14 |
| 4.1.4 | Selection of Future Scenarios and Assessment | 4-17 |
| 4.2 | Implementation of Rainfall-runoff Analysis Considering Climate Change Impact Assessment: Brantas River Basin | 4-20 |
| 4.2.1 | Overview of Targeted Basins..... | 4-20 |
| 4.2.2 | Climate Change Impact Assessment for Rainfall in the Brantas River Basin | 4-37 |
| 4.2.3 | Climate Change Impact Assessment for River Runoff, ET, and Soil Moisture..... | 4-48 |
| 4.2.4 | Selection of Future Scenarios in the Brantas River Basin | 4-65 |
| 4.2.5 | Runoff Analysis for Flood Risk Assessment | 4-71 |
| 4.3 | Implementation of Rainfall-runoff Analysis Considering Climate Change Impact Assessment: Musi River Basin | 4-84 |
| 4.3.1 | Overview of Targeted Basins | 4-84 |
| 4.3.2 | Development of WEB-DHM and its Validation..... | 4-100 |
| 4.3.3 | Selection of Future Scenarios in the Musi River Basin..... | 4-104 |
| 4.3.4 | Climate Change Impact Assessment for River Runoff, ET, and Soil Moisture.... | 4-107 |
| 4.3.5 | Runoff Analysis for Flood Risk Assessment | 4-113 |
| 4.4 | Implementation of Climate Change Impact Assessment on Food Production: Musi River Basin | 4-116 |
| 4.4.1 | Implementation of Field Survey Required for Preparing a Crop Model and Establishment of the Method | 4-116 |
| 4.4.2 | Development of a Coupling Hydrologic and Rice Growth Model..... | 4-119 |
| 4.4.3 | Implementation of Impact Assessment for Rice Production by the Coupling Model | 4-131 |
| 4.4.4 | Designing of Technology Education System for Wide Area Management | 4-136 |
| 4.5 | Implementation of Capacity Development..... | 4-142 |
| 4.5.1 | Implementation of the Seminar in Indonesia..... | 4-142 |
| 4.5.2 | Implementation of Training in Japan (Assistance)..... | 4-143 |

Table of Contents

| | |
|--|-------|
| 4.5.3 Handbook for Assessing and Integrating Climate Change Impacts into Water Resources Management Plan (Assistance)..... | 4-146 |
| CHAPTER 5 CONCLUSION AND RECOMMENDATION | 5-1 |
| 5.1 Climate Change Impact Assessment on Water Cycle | 5-1 |
| 5.1.1 General Remarks | 5-1 |
| 5.1.2 Summary in Brantas River Basin | 5-1 |
| 5.1.3 Summary in Musi River Basin | 5-1 |
| 5.2 Climate Change Impact Assessment on Food Production in Musi River Basin | 5-2 |
| 5.3 Recommendation | 5-2 |
| CHAPTER 6 OTHERS | 6-1 |
| 6.1 Undertaking of the Government of Indonesia | 6-1 |
| 6.2 References | 6-1 |
| <u>APPENDIX</u> | |
| Appendix A Meetings and Seminars | |
| A-1 Kick-off meeting and the First Seminar | |
| A-2 The Second Seminar in Jakarta and the First Seminar in Surabaya | |
| A-3 Workshop on Assessing and Integrating Climate Change Impacts into the Water Resources Management Plans for the Brantas and Musi River Basins (Interim Explanation-1) | |
| A-4 Interim Explanation of Musi River Basin Outputs and Overall Schedule of the Project (Interim Explanation-2) | |
| A-5 The Third Seminar in Jakarta and the First Seminar in Palembang | |
| Appendix B Field Surveys | |
| B-1 Field Survey for Crop Model in the Musi River Basin | |
| B-2 Field Survey for Hydrological Simulation in the Brantas River Basin | |
| B-3 Field Survey for Hydrological Simulation in the Musi River Basin | |
| B-4 Field Survey for Hydrological Simulation in the Brantas River Basin in Surabaya | |
| B-5 Field Survey for the Coupling Model in the Musi River Basin | |
| Appendix C Training in Japan (Climate Change Impact Assessment) | |
| C-1 The First Training Course (1st Training-1) | |
| C-2 The First Training Course (1st Training-2) | |
| C-3 The Second Training Course (Deep understanding) | |

CHAPTER 1

INTRODUCTION

CHAPTER 1 INTRODUCTION

CHAPTER 1 INTRODUCTION

1.1 Background of the Project

One of the impacts caused by climate change in Indonesia is considered to be changes in the water cycle. While rainfall tends to increase in Java, Bali, Nusa Tenggara, and Papua in the rainy season in particular, it tends to decrease in other regions. In the dry season, rainfall is projected to decrease in most of Java and South Sumatra. In addition, there are growing concerns about an increase in extreme weather events, such as droughts and floods, owing to the increasing frequency of El Niño. In addition to promoting development while taking these impacts into consideration, to achieve the goal of a 26% national reduction in greenhouse gas emissions by 2020, it is necessary to incorporate mitigation and adaptation strategies for climate change into development plans at both national and regional levels. However, no specific methodology has been organized in the various sectors. In the water resource management sector, each country has been seeking concrete ways to address climate change impacts in planning through trial and error, since no standard methods have been established worldwide. Therefore, it is becoming necessary to address planning theory and directionality of water resource management in Indonesia while considering climate change.

To properly manage water resources in Indonesia, the Water Resources Management Strategic Plan (POLA; which indicates the direction of river basin management) and the Water Resources Management Implementation Plan (RENCANA; a specific action plan for basin management based on POLA) are being developed. It is therefore necessary to formulate a water resources management plan corresponding to the impacts of future climate change and its uncertainty. In addition to measures against floods and droughts, peatland management for decrease in greenhouse gas emissions and increases in food production are viewed as particularly meaningful in the national action plan and necessary for policy reasons. Measures for peatland management should be taken on the basis of appropriate water resource management by treating these issues as key policies within the Ministry of Public Works (hereafter referred to as “PU”).

With respect to the above issues, projects for assessment and countermeasures of climate change impacts have been implemented with the assistance of various donors. However, some issues persist despite past efforts, such as: i) Meteorological and hydrological characteristics at the river-basin level are not reflected in climate change impacts, because those impacts are forecasted based on assessments on a larger scale or with certain assumptions; ii) climate change impacts cannot be reflected in water resource management plans (particularly RENCANA), because recommendations are neither quantitative nor specific; and iii) planning theory, such as how to reflect climate change impacts in formulating water resource management plans, has not been discussed within the Government of Indonesia (GOI), and a method applicable to river basins other than those targeted herein by the Indonesian side has not been developed.

Under these circumstances, the GOI has requested Technical Cooperation for Development Planning for the “Project for Assessing and Integrating Climate Change Impacts into the Water Resources Management Plan for Brantas and Musi River Basins” (herein referred to as “the project”) from the Government of Japan (GOJ). Upon receiving this request, the Japan International

CHAPTER 1 INTRODUCTION

Cooperation Agency (JICA) dispatched the Detailed Planning Survey Team to Indonesia in August 2012. As a result, a record of discussions on the project between the Directorate General of Water Resources (DGWR) of the PU and JICA was signed on November 6, 2012.

The project consists of two study components, namely, the “Water Resources Management Plan” and the “Climate Change Impact Assessment and Hydrological Simulation”. This Interim Report describes progress of the latter component.

1.2 General Outline of the Project

1.2.1 Project Objectives

To contribute to the implementation of water resource management in the Brantas and Musi river basins in Indonesia, recommendations should be formulated that reflect climate change impacts on water resource management plans, and guidelines applicable to those plans should be prepared for other river basins in Indonesia, while considering climate change issues.

1.2.2 Expected Project Outputs

Five expected outputs are described in the following list. The JICA Study Team for the study component Climate Change Impact Assessment and Hydrological Simulation (hereafter referred to as “the study team” and “the study”) mainly contributes to output (1) below, and assessment of the impact on food production considering climate change is reflected in output (3). The design of a technical guidance framework for regional expansion of that impact assessment is also included in the outputs.

- (1) Simulation of future rainfall for hydrologic simulation under projected climate change in target river basins
- (2) Assessment of water resource vulnerability and resilience under climate change, particularly in terms of floods and droughts in target basins
- (3) Formulation of recommendations for describing climate change impacts on water resource management plans (POLA and RENCANA)
- (4) Preparation of guidelines applicable to water resource management plans in other river basins of Indonesia, taking climate change issues into account
- (5) Strengthening the capability of the PU to formulate water resource management plans with strategies for climate change (investigations of planning theory through discussions, training courses for climate change prediction and water resource management planning, and preparations of training modules and materials)

1.2.3 Project Area

The target regions are the following two aforementioned basins. Maps of these basins are shown on the frontispiece of this report.

- Java island: Brantas River basin (approximately 12,000 km²)
- Sumatra island: Musi River basin (approximately 60,000 km²)

CHAPTER 1 INTRODUCTION

The Musi basin, for project purposes, includes downstream lowland swamp areas of the Banyuasin and Sugihan river basins, adjacent to the Musi basin.

1.2.4 Implementing Organizations in Indonesia

The following agencies are the main counterparts for the project.

- Implementing agency: Ministry of Public Works and Housing (MPWH)
- Related agencies: Agency for Meteorology, Climatology and Geophysics (BMKG)

1.3 General Outline of the Study (Climate Change Impact Assessment and Hydrological Simulation)

The project consists of two components, which are:

- Component-1: Climate Change Impact Assessment and Hydrological Simulation
- Component-2: Water Resources Management Plan.

This Draft Final Report (DF/R) describes the study “Climate Change Impact Assessment and Hydrological Simulation” by Component-1.

1.3.1 Purpose of the Study

- (1) Climate change impact assessments and hydrologic simulations of the Brantas and Musi river basins
- (2) Assessment of the impact on food production, considering the climate change impact assessment for the Musi River basin.

These outputs will be contributed to a vulnerability assessment for water resources under climate change impacts, and to the formulation of proposals for addressing climate change impacts in water resource management plans.

The study carried out based on meeting minutes (M/M) regarding the *Detailed Planning Survey on the Study on Adaptation Strategies for Climate Change Impacts for Two River Basins*, signed on August 10, 2010 by the DGWR of the PU, and the JICA, and the record of discussion (R/D) signed on November 6, 2012. The study team conducted its work according to the purpose of the study and expected project outputs described in the chapters of this document.

CHAPTER 1 INTRODUCTION

1.3.2 Scope and Schedule of the Study

The period of the study is 47 months (May 2013 through March 2017) and its schedule is presented in Figure 1.3.2-1 below.

Main study activities were done in Japan and their progress or challenges were reported to the Indonesian organizations during dispatch periods. Work done in Indonesia and in Japan are itemized in below.

(1) Work in Indonesia

Major activities in Indonesia are as follows.

- a) Submission, explanation, and discussion of each report, namely Inception Report (I/R), Interim Report (IT/R), and Draft Final Report (DF/R). Final Report (F/R) will be finalized by referring comments from JICA and the Indonesian side at the last discussion of the DF/R in Indonesia, January 2017.
- b) Holding seminars in Jakarta, Surabaya, and Palembang, with cooperation of the study team on the Water Resources Management Plan.
- c) Site visits to Brantas river basin and Musi river basin during each dispatch from 2013 to 2016. (The initial site observation of the Musi river basin was conducted under the framework of The University of Tokyo in September 2013 for need.)

(2) Work in Japan

Principal activities in Japan are as follows.

- a) Research and development of the study.
- b) Implementation of training in Japan, supporting the study team for the Water Resources Management Plan.
- c) Regular meetings for the study and the project meetings with JICA and the study team for the Water Resources Management Plan (Component-2).

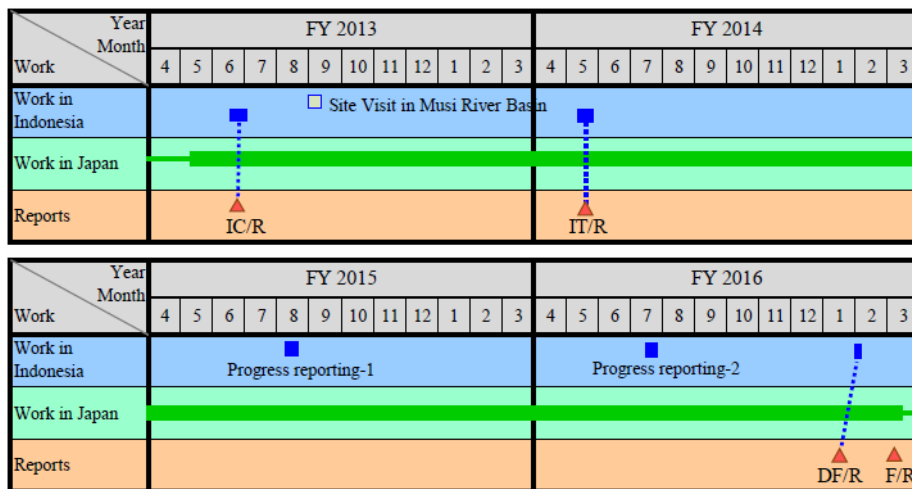


Figure 1.3.2-1 Schedule of the study

CHAPTER 2

IMPLEMENTATION POLICY

CHAPTER 2 IMPLEMENTATION POLICY

CHAPTER 2 IMPLEMENTATION POLICY

2.1 Water Issue Recognition of Indonesia and its Needs

Indonesia is in a tropical ocean area at the boundary between the Pacific and Indian Oceans. The global climate system is driven by processes in this area, with large amounts of solar energy absorbed by the ocean surface. There are various characteristic weather and climate anomalies that strongly affect the global climate. Clear interannual variability, including El Niño – Southern Oscillation (ENSO) and Indian Ocean Dipole (IOD), occurs in relation to equatorial wave propagation caused by strong ocean-atmosphere interactions, in contrast with cyclone-anticyclone activity at mid latitude. The strongest element of intraseasonal (30–60 days) variability in the tropical atmosphere is the Madden-Julian Oscillation (MJO). It is a large-scale coupling between atmospheric circulation and tropical deep convection. The MJO is migratory, propagating eastward above warm regions of the Indian and Pacific Oceans. Heavy rainfall events occur, associated with the propagation of cold surges from Siberia to the Maritime Continent. Mechanisms of these characteristic weather and climate anomalies are not fully understood, and they often cause serious water-related issues. This is why there is still much uncertainty in climate change projections for the region.

The IPCC Fourth Assessment Report (AR4) collected global data for the past 50 years, showing that heavy rainfall has increased since the 1990s. Simulation results with multiple models also demonstrate that more than 90% of member models produced an increasing trend of strong precipitation intensity worldwide. The AR4 analyzed global 100-year data to assess drought risk, indicating that drought-affected areas have increased over the past 20 years. In simulations with multiple models, more than two-thirds also suggested such an increase. Considering climate change projection on the global scale, it is a scientific challenge to assess climate change impacts on Indonesia with the characteristic weather and climate anomalies. A further challenge is providing useful information for decision-making regarding reducing water-related disaster damage and improving water use. In Indonesia, POLA and RENCANA are being developed to manage water resources properly, considering the impacts of future climate change and its uncertainty.

The government of Indonesia mainstreams climate change mitigation and adaptation, integrated water resource management, and increases in food productivity as part of key national policies. In addition to measures against floods and droughts, an increase in food production is viewed as particularly important in the national action plan, and is necessary for policy reasons.

Measures for peatland management should be taken on the basis of appropriate water resource management by treating these issues as key policies within the Ministry of Public Works. Considering the long-term and sustainable development of Indonesia, scientific and technological bases for addressing these issues should be enhanced by introducing integrated scientific knowledge and promoting human capacity. The capacity-building program should be designed and implemented effectively using our experience and human networks.

CHAPTER 2 IMPLEMENTATION POLICY

2.2 Policy and Consideration for Project Implementation (Climate Change Impact Analysis and Hydrological Simulation)

(1) Close cooperation with the JICA study team for Water Resources Management Plan

Existing meteorological and hydrological data plus new observation data, including survey data, were to be measured and collected by the Japan International Cooperation Agency (JICA) study team for the “Water Resources Management Plan”. Required data and observation sites were addressed and coordinated by this team.

Output of the study will contribute to assessments of water resource vulnerability under climate change impacts, and to the formulation of proposals for reflecting these impacts in water resource management plans. Therefore, analyzed data, related information, and schedules were shared in a timely fashion with other study team, Water Resources Management Plan. The draft proposal of this plan will benefit as necessary from advice concerning the evaluation of climate change impacts.

(2) Climate change impact assessment and hydrologic simulation

Water resource vulnerability and flood runoff in the Brantas and Musi river basins of Indonesia will be assessed using greenhouse gas emission scenarios, global climate models (GCM), and downscaling techniques for rainfall-runoff simulations, with consideration to future climate change in the target basins.

In runoff analyses, it was assumed that detailed models would simulate floods through drought conditions, with verification of its reproducibility of soil moisture through assimilation of satellite and other data.

(3) Target basin

The lowland swamp areas of the Banyuasin and Sugihan rivers were included in the targeted Musi River basin. However, accuracy on the same level as the Musi River was not possible, since flow and meteorological data for these swamp areas were insufficient compared with those from the Musi River.

It was assumed that simulations would be for the range mandated by the data measured by a newly established flow meter and satellite data, and that the water budget would be analyzed for swale portions where climatic variation would be considered.

Flood runoff was not analyzed for the Banyuasin and Sugihan rivers.

(4) Technology transfer

Technology transfers were made via seminars in Indonesia and training courses in Japan through the project. In order to share general knowledge and information related to the project and to have opportunities for discussions between both sides, seminars were held by the study team and the relevant agencies from Indonesia. On the other hand, for capacity development based on the

CHAPTER 2 IMPLEMENTATION POLICY

building up of technical knowledge, two levels of training were carried out for adequate engineers, those who have an incentive to learn how to assess climate change impacts and perform runoff analyses.

2.3 Input from the Japanese Side and Project Management

Tables 2.3-1 and 2.3-2 show the inputs to the project from the Japanese side. There has been continuous close cooperation with the Water Resource Management Plan team, as described in the above section.

Main activities in Japan involve research and development as in Section 4 supported from data management and coordination. To maintain communication and confirm update status, the study team held meetings regularly.

In addition, the joint meetings with the Water Resources Management Plan team had been held at the right time. In each of the joint meetings, considering the needs of Indonesian side, the possible and appropriate methods for the project based on science and technology aspects were discussed.

Table 2.3-1 Input 1 from Japan

Climate Change Impact Assessment and Hydrologic Simulation (the study)

| No. | Area of Expertise | Number of staff |
|-----|--|-----------------|
| 1 | Team Leader / Climate Change | 1 |
| 2 | Climate Change Impact Assessment | 2 |
| 3 | Food Production Impact Assessment | 3 |
| 4 | Operational Coordination / Data Collection | 2 |

Table 2.3-2 Input 2 from Japan

Study Team for Water Resources Management Plan

| No. | Area of Expertise | Number of staff |
|-----|--|-----------------|
| 1 | Team Leader / Climate Change Measures | 1 |
| 2 | Water Resource Management / River Management / Flood (Brantas and Musi rivers) | 2 |
| 3 | Sabo Management | 1 |
| 4 | Hydrology | 2 |
| 5 | Groundwater Management / Hydrogeology | 1 |
| 6 | River Facilities Management | 1 |
| 7 | Spatial Planning / Organizational and Institutional Capacity Development | 1 |
| 8 | Water Resource Management (Musi River) | 1 |

CHAPTER 2 IMPLEMENTATION POLICY

| | | |
|----|---|---|
| 9 | Water Supply and Sewerage | 1 |
| 10 | Agriculture / Irrigation | 1 |
| 11 | Environmental and Social Considerations | 1 |
| 12 | Wetland Management / Watershed Conservation / Environmental and Social Considerations | 1 |
| 13 | Implementation Plan / Cost Estimation | 1 |
| 14 | Economic Analysis/ Project Evaluation | 1 |
| 15 | Climate Change Analysis | 1 |
| 16 | Crop Production Impact Assessment | 1 |
| 17 | Project Coordinator / Water Resources Management Plan | 1 |

CHAPTER 3

PLAN OF OPERATION

CHAPTER 3 PLAN OF OPERATION

CHAPTER 3 PLAN OF OPERATION

3.1 Technical Guidelines

Coupled general circulation models (GCMs) are usually most widely applied to climate change impact assessments. However, there are large uncertainties associated with the outputs of these models. In particular, bias of precipitation projected by GCMs is too large. To reduce such uncertainties, it is necessary to conduct more analyses based on multi-model and multi-projection ensembles instead of single-model analyses. In addition, there is a large gap in the grid resolution between GCMs and catchment-scale hydrology models. To address this mismatch, downscaling of GCM data is essential for regional and local impact studies. There are two main types of downscaling: dynamic and statistical. Dynamic downscaling refers to nesting of fine-scale resolution within a large-scale resolution while preserving some spatial correlation. However, this method is computationally expensive and impossible for multi-decade simulations by different GCMs. Statistical downscaling based on the relationship between large-scale circulation and local-scale phenomena can be implemented within a reasonable range of computational costs.

Characteristics of the hydrologic analysis are summarized as follows:

- The model physically describes ET using a biophysical land surface scheme for simultaneously simulating heat, moisture, and CO₂ fluxes in soil-vegetation-atmosphere transfer (SVAT) processes.
- The hydrologic submodel describes overland, lateral subsurface, and groundwater flows using grid-hill slope discretization, followed by flow routing in the river network.
- The model has high efficiency for simulations of large-scale river basins while incorporating subgrid topography and effects of water resource management facilities.

How the water cycle varies with climate change and has a substantial influence on food production. How to develop and manage water resources for increased food production requires a crop model coupled with the aforementioned runoff analysis and some further developed simulation systems combined with various information, such as agriculture activities and water-use patterns in the target area. Even more important is that our developed system should be widely applicable to different areas of the target country. This necessitates the means for collecting required information for evaluation.

As stated above, to respond to each component problem and mutually-related issues as a whole in climate change analyses, runoff analyses and food production simulations, and for implementing the method in regional societies, we have applied the following method, which is already peer-reviewed and published in a scientific journal as described in the following sections.

3.1.1 Study Flow

Figure 3.1.1-1 shows the main flow of the study, Climate Change Impact Analysis and

CHAPTER 3 PLAN OF OPERATION

Hydrological Simulation, in the Project for Assessing and Integrating Climate Change Impact into the Water Resources Management Plan for Brantas and Musi River Basins.

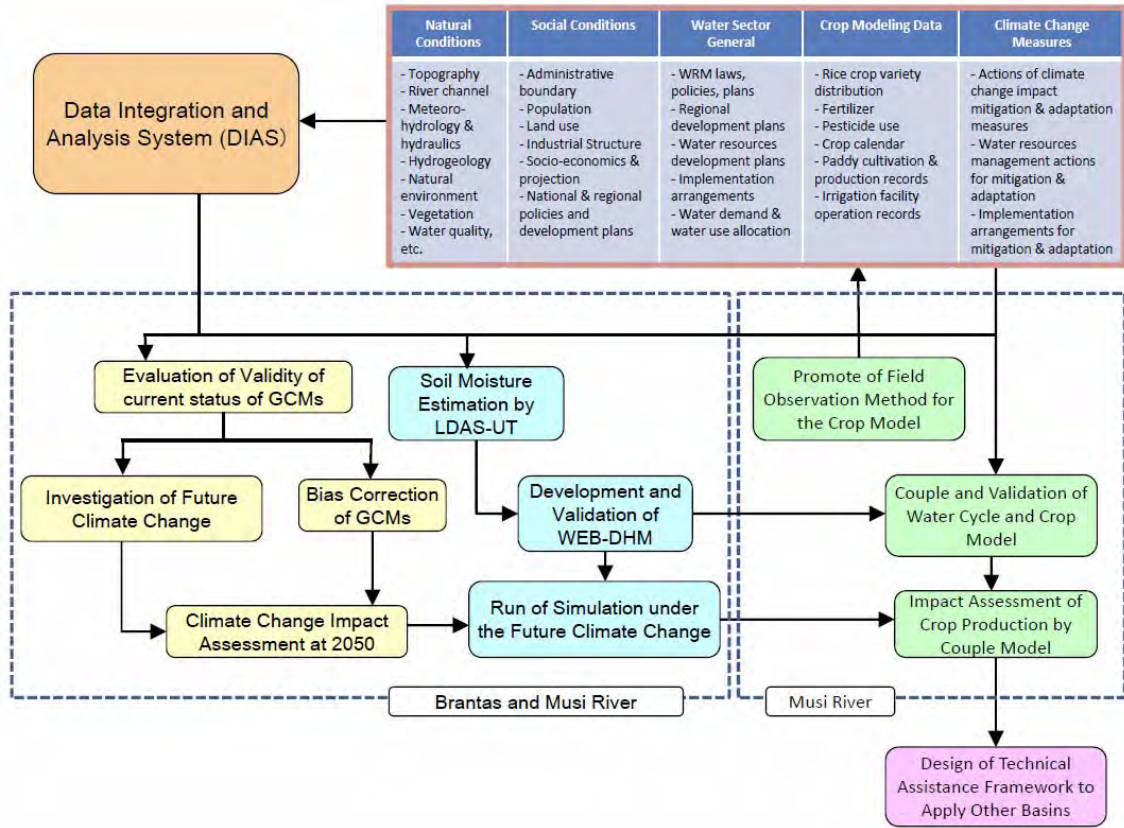


Figure 3.1.1-1 Main Flow of the Study
(Climate Change Impact Analysis and Hydrological Simulation)

Figure 3.1.1-2 indicates the assessment study and its system development.

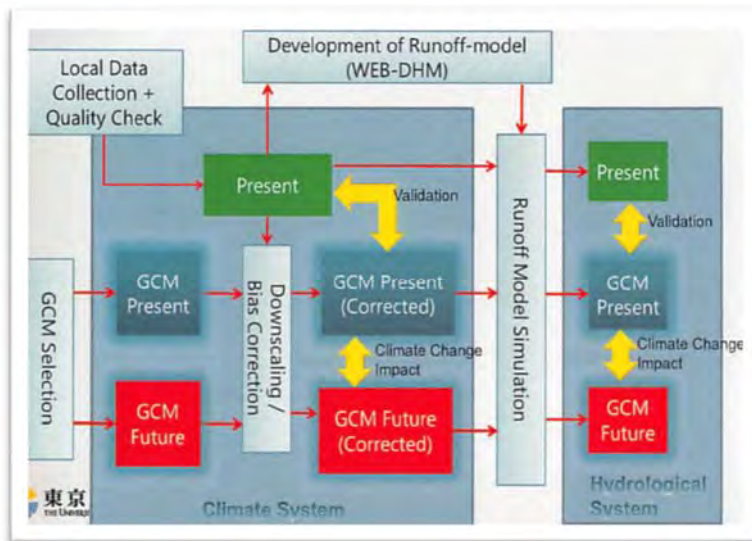


Figure 3.1.1-2 Assessment Study and System Development

CHAPTER 3 PLAN OF OPERATION

3.1.2 GCM Selection, Bias-correction and Spatial Downscaling

Selection of appropriate GCMs is crucial for multi-model analysis. Such selection is done based on the performance of GCMs participating in the Coupled Model Intercomparison Projects 3 and 5 (CMIP3 and CMIP5).

Most precipitation data in the GCMs show three main problems. These are the underestimation of heavy rainfall intensity, poor seasonal representation, and too many rainy days with very weak rainfall (referred to as drizzle). Within the current project, we focus on GCM bias correction to alleviate these problems. To accomplish this, annual maximum rainfall, normal rainfall, the and numbers of no-rain days are statistically bias-corrected.

3.1.3 Hydrologic Simulation by Water and Energy Budget-based Distributed Hydrological Model (WEB-DHM)

The WEB-DHM was developed by fully coupling a biosphere scheme (SiB2) and geomorphology-based hydrological model (GBHM). WEB-DHM is a distributed runoff model that enables the capture of geography and land use. The model can also reproduce spatially-biased rainfall, such as regionally intense rainfall, and can accurately simulate water loss and soil moisture, by combining surface and hillslope hydrologic processes. The model has been confirmed to reproduce the water cycle well for rainy or no-rain conditions. Therefore, the model can evaluate flood peak discharge accurately by estimating first-term loss without any halfway tuning when computing in a several-year order.

WEB-DHM characteristics are summarized as follows:

- i) Physically binding slope hydrology with atmosphere-surface interaction, the model can properly evaluate soil moisture, water cycle movement on the land surface, and groundwater. Computing heat and water fluxes simultaneously using a vegetation-physical scheme can more accurately predict water loss and, as a result, accurately estimate soil moisture and surface temperature.
- ii) Since the model can directly link to a GCM, it is possible to measure changes and differences in radiation and temperature.
- iii) The model can consider dam effects.

The required spatial resolution for a hydrologic model is 10 km and time resolution is one hour for observing rainfall.

Data from GCMs should be on a several-hundred kilometer scale, with a temporal resolution of 1 day. When there is dense land rainfall data, the model output data can be bias-corrected with in-situ observation data. However, when there is insufficient observation data, it is necessary to use a spatial downscaling method with satellite data.

Satellite-based, low-frequency microwave brightness temperature is strongly affected by near-

CHAPTER 3 PLAN OF OPERATION

surface soil moisture; therefore, it can be assimilated into a land surface model to improve modeling of soil moisture and the surface energy budget. The project uses the Land Data Assimilation System developed by The University of Tokyo (LDAS-UT) to estimate soil moisture and surface temperature. The LDAS-UT consists of a land surface model (LSM) used to calculate surface fluxes and soil moisture, a radiative transfer model (RTM) to estimate microwave brightness temperature, and an optimization scheme to search for optimal soil moisture values by minimizing the differences between modeled and observed brightness temperatures.

3.1.4 Simulation System Using a Coupled Model of a Distributed Hydrological Model (WEB-DHM) and rice growth model (SIMRIW)

We aim to evaluate the effects of changes in the hydrologic cycle on rice, a primary agricultural product of the area, by coupling the aforementioned WEB-DHM and SIMRIW (Simulation Model for Rice-Weather Relations). SIMRIW simulates the growth and potential production of rice using air temperature, solar radiation, and rice variety-dependent parameters, and has been used in the assessment of climate change and other phenomena. In the study, we will use SIMRIW-rainfed, in which the effects of water and nitrogen are taken into account as growth constraints on rice in actual agricultural fields. This model has been developed based on our own field investigation in northeast Thailand. Thus, the model is suitable for use in Southeast Asia, including Indonesia.

An interface for connecting various types of data must be developed to couple WEB-DHM and SIMRIW-rainfed. For both models, it is necessary to input meteorological data such as air temperature and solar radiation, and hydrologic data such as soil moisture, surface storage water depth, and others. WEB-DHM expects the output of rice growth as represented by the leaf area of rice from SIMRIW-rainfed. In addition, it is necessary to develop an irrigation scheme module to represent actual water use in a targeted area. The establishment of methods to obtain information on agricultural management and to discretize it into grids is also necessary, because SIMRIW-rainfed was developed on an individual farm scale whereas the coupled model with WEB-DHM simulates at basin-wide scale.

Furthermore, it is necessary to develop a method to optimize management under a climate change scenario. One type of management is the operation of an irrigation system that maximizes production while minimizing agricultural water use, and another is via planting date that minimizes water stress of rice under limited water resources.

The method to obtain information has not yet been established but is necessary to apply crop models, such as basin-wide agricultural management and characteristics of planted rice varieties. Thus, a research plan must be developed from a design level to obtain these data.

In the study, data stored by governments is collected as a first step, and then additional data should be collected by conducting field surveys. Data necessary for the coupled model are rice variety, amount of fertilization, and growing season. These should be certified by data of production amount and others, and then the model should be refined.

CHAPTER 3 PLAN OF OPERATION

3.2 Implementation Method of the Study

3.2.1 Preparatory Investigation

Outputs of the GCMs that participated in CMIP3 and CMIP5 are archived on the Data Integration and Analysis System (DIAS), which was developed by The University of Tokyo. From these GCMs, we will select models that can adequately describe climate characteristics in the Sumatra and Java island areas, including the Brantas and Musi river basins. In the study, we focus on rainfall, outgoing long-wave radiation, pressure fields, and sea surface temperature. We will compare this data with global datasets, such as those of satellite observation and reanalysis, and evaluate the capability to reproduce them based on the spatial correlation coefficient and root mean square error (RMSE). Using analysis results and in collaboration with the Japan International Cooperation Agency (JICA), we will select appropriate models for climate change impact assessment. We will then divide the region into subsections including the target basin for daily rainfall plus daily-average, daily-maximum, and daily-minimum air temperatures, based on outputs of the selected models. Since most of the archived models have temporally divided experimental results from 1960 to 2000 and 2045 to 2065, we will target the period through the year 2065.

3.2.2 Implementation of Rainfall-runoff Analysis Considering Climate Change Impact Assessment

(1) Evaluation of Future Climate Change Impact in Brantas and Musi River Basins

1) Evaluation of Validity of Current Status Simulations

Targeting outputs of the models selected per Section 3.2.1, we will evaluate the validity of simulations of the current status by comparison of statistical values produced by the models with observed rainfall and air temperature, which are closely related to floods and droughts. We will compare the following statistical values for 1980–2000.

- (i) Order statistics of daily rainfall, annual maximum daily rainfall, and annual maximum number of continuous non-rainy days for the past 20 years
- (ii) Twenty-year average monthly rainfall and monthly average air temperature
- (iii) Variations of monthly rainfall and monthly average air temperature during the past 20 years
- (iv) Twenty-year average daily maximum and daily minimum air temperatures for each month

For implementing (i) to (iv), observation data of daily rainfall plus daily average, daily maximum, and daily minimum air temperatures are required. These data should be available and accurate over the long term, without any data missing for the project area.

2) Examination of Future Climate Change Trends

From GCM simulation results, which continuously calculate from current conditions (1980–2000) through 2050, we will analyze climate change trends. Since these trends are

CHAPTER 3 PLAN OF OPERATION

strongly dependent on the climate sensitivity of each GCM, we will clarify similarities and differences of trends based on results from multiple GCMs.

3) Bias Correction of GCM Outputs

After selecting appropriate GCMs, biases for extremely heavy rainfall events, the number of no-rain days, and normal rainfall derived from the GCMs will be corrected as follows:

(i) Extremely heavy rainfall

The probability distribution function (PDF) giving the best fit of observed annual maximum daily rainfall from 1980 to 2000 will be identified. For correction, we will select the PDF that appropriately describes the distribution of extreme values, and estimate parameters via the maximum likelihood method. Finally, the conversion function will be applied to the annual maximum daily rainfall data derived from the GCM future outputs.

(ii) Number of no-rain days

The number of no-rain days will be corrected using the ranking order statistic. A threshold for each GCM rainfall event will be identified using the rank, which shows the least rainfall in descending order of observed rainfall. GCM rainfall data with values less than the threshold will be set to zero.

(iii) Normal rainfall

The range of normal rainfall will be defined as less than the minimum annual maximum daily rainfall from 1980 to 2000 and greater than the threshold of the no-rain days. A correction factor for each month will be calculated based on the difference between monthly average normal rainfall of the GCM and observed values.

Bias of the GCM future air temperature will be corrected using the ratio of the average observed and GCM daily averages, and the maximum and minimum air temperatures of each month from 1980 to 2000.

In general, it is difficult to confirm the scientific rationale of the bias correction methods described above, because future data are unavailable. However, we can apply these to GCM output at the beginning and middle of the 1900s (for example, from 1901 to 1920, 1921 to 1940, 1941 to 1960, and 1961 to 1980). If past observed data is available, we can estimate errors of the methods and compare them with changes projected by the GCMs. If the changes are greater than the errors, we can say that the projected changes are significant.

To implement this, we need long-term and quality controlled meteorological data, such as downward shortwave radiation, daily average air temperature, and maximum and minimum daily air temperature.

4) Climate Change Impact Assessment in Target Year 2050

CHAPTER 3 PLAN OF OPERATION

We will assess climate change impacts in the target year 2050 by merging the climate change trend and bias corrections. Given the likelihood of differences between the selected GCMs, daily rainfall and air temperature datasets will be generated for 20 years, centered on 2050.

(2) Implementation of Rainfall-runoff Simulation Considering Climate Change Impacts

1) Hydrologic Model Development and River Runoff Simulation

Although improvements over lumped hydrological models have been made by representing spatial heterogeneity, DHMs have large uncertainties when used to simulate water exchanges at the soil-atmosphere interface and temporal evolution of surface soil moisture, owing to the conceptual treatment of the land surface.

Lateral soil moisture redistributions by topographically driven runoff are usually not well formulated in most current LSMs (e.g., SiB2), since they were originally developed for application in GCMs. The coupling of LSMs and DHMs has the potential to improve land surface representation, benefiting streamflow prediction capabilities of the hydrologic models and providing improved estimates of water and energy fluxes into the atmosphere.

As mentioned in Section 3.1.2, WEB-DHM was developed by fully coupling SiB2 with GBHM. SiB2 describes the transfer of turbulent fluxes (energy, water, and carbon) between the atmosphere and land surface on each model grid. The GBHM redistributes water moisture laterally through simulation of both surface and subsurface runoff, using grid-hill slope discretization and subsequent flow routing in the river network.

(i) Overall Structure

Overall model structure is shown in Figure 3.2.2-1 and can be described as follows.

- i) A digital elevation model (DEM) is used to define the target area, after which the target basin is divided into sub-basins (Figure 3.2.2-1a). Within a given sub-basin, a number of flow intervals are specified to represent time lag and accumulation processes in the river network, according to distance to the outlet of the sub-basin. Each flow interval includes several model grids (Figure 3.2.2-1b).
- ii) For each model grid with one combination of land-use type and soil type, SiB2 is used to calculate turbulent fluxes (water, energy, CO₂) between the atmosphere and land surface independently (Figures 3.2.2-1c and 3.2.2-1d).
- iii) Hydrologic simulation is done on each model grid consisting of a river channel and two symmetric hill slopes. GBHM (Yang et al., 2000) is used to simulate surface flow, subsurface flow, and groundwater discharge. For simplicity, streams within one flow interval are lumped into a single virtual channel with the shape of a trapezoid. All runoff from the model grids in the given flow interval is accumulated into the virtual channel and led to the river basin outlet (Figures 3.2.2-2).

CHAPTER 3 PLAN OF OPERATION

(ii) Unsaturated and Saturated Zone Water Flows

Sib2 consists of three soil layers. The first is the surface layer where evaporation is calculated, the second is the root zone where transpiration is calculated, and the third, the deep zone, expresses the deepest unsaturated layer. The unsaturated zone water flow is described using a vertical one-dimensional Richards equation:

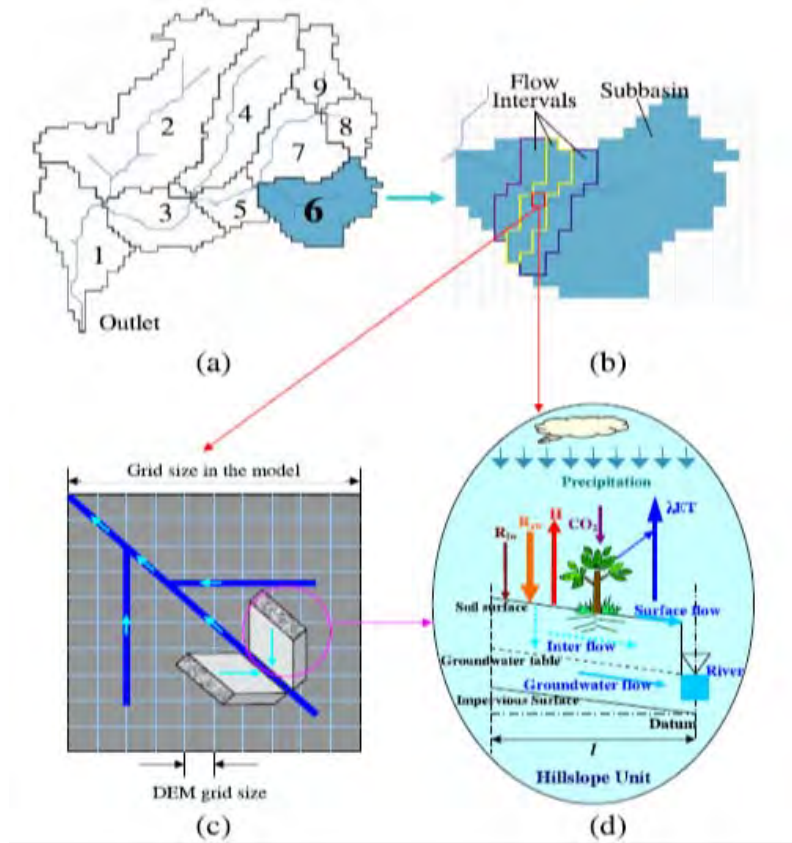


Figure 3.2.2-1 Overall model structure of WEB-DHM (Wang et al., 2009)

$$\frac{\partial \theta(z,t)}{\partial t} = -\frac{\partial q_v}{\partial z} + r(z,t) \quad (1)$$

Here, t and z are time and depth, respectively; $\theta(z,t)$ is volumetric water content; $r(z,t)$ is evapotranspiration; q_v represents soil moisture fluxes in the vertical direction, giving

$$\text{as } q_v = -K(\theta, z) \left[\frac{\partial \psi(\theta)}{\partial z} - 1 \right] \quad (2)$$

Here, $K(\theta, z)$ is the hydraulic constant; $\psi(\theta)$ is capillary suction (m); z is vertical

CHAPTER 3 PLAN OF OPERATION

distance from the surface, with downward positive (m). The basic equations used for the saturated zone are mass balance and Darcy's law. Discharge exchanged between aquifer and river per unit width $q_G(t)$ is calculated as

$$q_G(t) = K_g \frac{H_1 - H_2}{l/2} \frac{h_1 + h_2}{2} \quad (3)$$

Here, K_g is hydraulic conductivity of the unconfined aquifer; l is length of the hillslope (m); H_1 , H_2 , h_1 and h_2 are in meters (Figure 3.2.2-2).

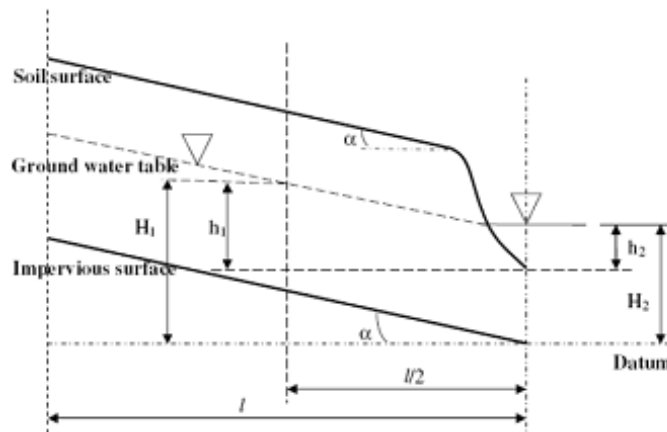


Figure 3.2.2-2 Hillslope model (Yang et al., 2000)

(iii) Input Data

To develop and validate WEB-DHM for the Brantas and Musi river basins, we require the meteorological forcing data, including air temperature, specific humidity, air pressure, wind speed, and downward solar and longwave radiation. Also needed are hydrologic data, including precipitation, river discharge, groundwater, dam inflow and outflow, existing dams, elevation, land use, and geological maps. The following data will also be used if there is a shortage of requested data.

i) Land-use type

Satellite analysis products via United States Geological Survey (USGS)

ii) Leaf Area Index (LAI) and Fraction of Photosynthetically Active Radiation (FPAR) via NASA/EOS Data Gateway

iii) Soil

Digital soil data via the Food and Agriculture Organization (FAO)

CHAPTER 3 PLAN OF OPERATION

The Global Satellite Mapping of Precipitation (GSMaP) project was established by the Japan Science and Technology Agency (JST) in 2002. The GSMaP_MVK product was developed by integrating passive microwave radiometer data with infrared radiometer (IR) data to provide high temporal (1 hour) and spatial (0.1 degree) resolution global precipitation estimates.

In our study, GSMaP_MVK daily precipitation from 2003 to 2008 will be used to obtain areal-average spatially distributed factors for GCM downscaling during each month. When dense in-situ surface rainfall data is available, the target data is bias-corrected by individual observation data and used for the distributed water cycle model with the Thiessen distribution method. If the surface observation data is relatively sparse, a spatial downscaling scheme with satellite data will be useful. For the latter case, the GSMaP can produce monthly mean precipitation datasets, and we can experiment with downscaling this precipitation data at 10-km GCM output scale. The data should be bias-corrected using the surface data.

In addition to validating soil moisture, we will apply LDAS-UT. Figure 3.2.2-3 shows the LDAS-UT algorithm, which includes a dual-pass assimilation technique. Both passes assimilate observed Tb from vertical polarization at lower (6.9 GHz) and higher (18.7 GHz) frequencies. This choice is critical to the production of stable and reliable estimates of soil moisture. Vertical polarization is more favorable than horizontal polarization, because it is relatively insensitive to vegetation coverage. Because the lower-frequency T_b is much more sensitive to near-surface soil moisture than the higher frequency, their difference is correlated based on soil wetness using a soil wetness index (SWI), which is defined by

$$SWI = 2(T_b^{18.7V} - T_b^{6.9V}) / (T_b^{18.7V} + T_b^{6.9V})$$

A high SWI value corresponds to a wet surface, and a low value to a dry surface.

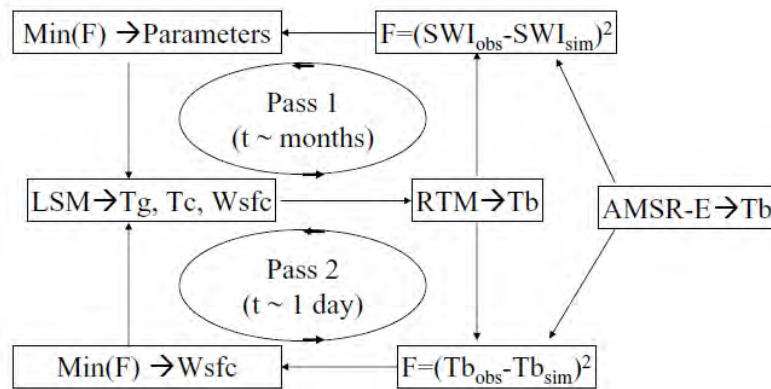


Figure 3.2.2-3 Overall structure of LDAS-UT

CHAPTER 3 PLAN OF OPERATION

Estimating T_b using RTM requires inputs near-surface soil water content (w_1), ground temperature (T_g), canopy temperature (T_c), vegetation water content (VWC), canopy parameters, surface roughness parameters, and soil texture. Simulation of surface variables (w_1 , T_g , T_c) by the LSM also requires a number of soil and vegetation parameters.

Accordingly, the modeled T_b is sensitive to several parameters in the LSM and RTM. In Pass 1, these parameters are obtained by minimizing a cost function that accounts for the difference between modeled and observed long-term T_b (t_{pass1} ; scale of two to three months). The cost function includes observation error and background error terms. The observation error term is defined by

$$F_{obs} = \sum_{t=0}^{t_{pass1}} \left[(T_{b,est}^{6.9V} - T_{b,obs}^{6.9V})^2 + (T_{b,est}^{18.7V} - T_{b,obs}^{18.7V})^2 \right] \quad (4)$$

where subscript *obs* denotes the observed value and *est* the modeled value. In Pass 1, the background error term is not directly accounted for in the cost function; rather, it is realized via adjustment of w_1 at each observation time so that the recalculated *SWI* value, which depends on w_1 , is close to $(SWI_{est} + SWI_{obs})/2$. This adjustment is implemented after adding the bias term $(T_{b,est} - T_{b,obs})^2$ into Eq. (4) (see details in Figure 3.2.2-3).

Given the existence of model deficiencies and errors in forcing data, the simulated soil moisture may become unrealistic without this adjustment, producing an absence of correlation between $T_{b,est}$ and $T_{b,obs}$, regardless of how the parameter values are tuned. Therefore, this adjustment is critical for optimizing the parameters.

The optimal parameter values are then transferred to Pass 2 for retrieval of soil moisture and the surface energy budget by assimilating T_b into the LSM. Pass 2 only optimizes the near-surface soil moisture, and its assimilation window (t_{pass2} ; ~1 day) is much shorter than that for Pass 1. The cost function for Pass 2 is defined by

$$F_{obs} = \sum_{t=0}^{t_{pass2}} \left[(T_{b,est}^{6.9V} - T_{b,obs}^{6.9V})^2 + (T_{b,est}^{18.7V} - T_{b,obs}^{18.7V})^2 \right] + \left[(T_{b0,bg}^{6.9V} - T_{b0}^{6.9V})^2 + (T_{b0,bg}^{18.7V} - T_{b0}^{18.7V})^2 \right] \quad (5)$$

where $T_{b0,bg}$ and T_{b0} are simulated T_b at the initial time of each assimilation cycle using the background $w_{1,bg}$ value and renewed $w_{1,0}$ value, respectively. Pass 1 requires just one execution, because the optimized parameters only include static model parameters and initial soil water conditions. Accordingly, this pass can be implemented using data prior to the real-time assimilation of satellite data in Pass 2.

CHAPTER 3 PLAN OF OPERATION

2) Simulation of Future Streamflow under Effects of Climate Change

Using the aforementioned outputs from the model of the Brantas and Musi rivers and the climate change impact assessment results for the designated target year 2050, future streamflow under the effects of climate change is estimated.

From the calculated future streamflow, we will analyze changes of high-water, low-water, and annual stream regimes from the current status and evaluate the effects of climate change. In addition, we will compare flood characteristics from model simulations for 1980–2000 and 2046–2065 and study changes in probability of flood frequency and flood scale.

3.2.3 Assessment of Impacts on Food Production Caused by Climate Change in Musi River Basin

(1) Implementation of Field Survey Required for Preparing a Crop Model and Establishment of the Method

It is necessary to collect data on agricultural management such as rice variety, growing season, and fertilizer amount as inputs for the growth and production models of rice, a primary agricultural product in the target area. This data is also required for verifying the models. Further, field surveys of actual water use are needed for the development of an irrigation module. For the data collection, we will assist the consultant responsible for the Water Resources Management Plan and establish methods (manuals) for the field survey. Government data collected for the targeted area is expected to be the primary source for this purpose. Contents of the collected data and their accuracies will be checked, and how the complimentary data was collected should be discussed. Then, actual data collection in the field and its manualization will be supported.

(2) Development of a Coupled Runoff and Crop Model

As described in Section 3.2.2, WEB-DHM can describe spatiotemporal distributions of soil moisture and river discharge with high accuracy and resolution at basin scale. The model of rice growth and production, SIMRIW-rainfed, can simulate the growth of rice as represented by LAI and rice production by considering yield decrease caused by stress from water and/or nitrogen deficits.

By dynamically coupling these two models, soil moisture distribution can be described by considering the soil characteristics and topography of a river basin, and then the growth and production of rice responding to soil moisture can be calculated over the entire basin.

Parameters in the crop model are set using data from the target area obtained in item (1) of this subsection. Based on the agricultural calendar and tables for characteristics of rice varieties, parameters such as those for phenological development processes are established for each variety. Parameters such as those for production properties are set for each variety based on yield data.

For coupling SIMRIW-rainfed and WEB-DHM, meteorological data such as air temperature, solar radiation, and so on, plus hydrologic data such as soil moisture and surface storage water depth output by WEB-DHM are input to SIMRIW-rainfed. Then, the data of rice growth as represented by leaf area of rice is output from SIMRIW-rainfed to WEB-DHM. Interfaces between the two models are thereby developed.

CHAPTER 3 PLAN OF OPERATION

The coupled model should include a module for irrigation management to investigate the effectiveness of water resource development. The irrigation-drainage system is regionally different and complicated. Consequently, an irrigation system model suitable to the target river basin should be developed by modifying the previously developed irrigation model⁴ based on the information obtained from field surveys of the target area, and then applied to the area.

The model should be verified by rice yield data for actual farms in the area. Data on yield and production of rice should be compared with the simulation result of the coupled model on the corresponding mesh, after expanding the field data to a larger area by satellite remote sensing. Average data of yield and production should be arranged by administrative unit, and they will be compared with the data obtained per item (1) of this subsection and discussed. Through the above efforts, accuracy of the coupled model will be verified, and the model should be improved by re-optimization of the parameters as needed.

(3) Implementation of Impact Assessment for Rice Production by Coupled Model

Rice production under climate change will be simulated using the coupled model developed in item (2) above, in which input data will be prepared using future rainfall obtained by multiple GCM runs (per Section 3.2.2 item (2)) after bias correction. Then, the data is compared with the simulation under present climate conditions to assess the effect of climate change on food production.

Furthermore, multiple alternative scenarios and adaptation strategies will be designed for agricultural management, such as planting season, fertilization, and so on. Simulations with such adaptation strategies will also be conducted and the effectiveness of each scenario will be discussed. For the planting varieties, several hypothetical ones in addition to the current ones will be addressed, and future direction for variety development will be discussed.

The simulation will be conducted for runoff and food production up to 2050, and the effectiveness of water resource development as adaptation strategies for future climate change, including the promotion of food production, will be examined.

(4) Designing of Technology Education System for Wide-Area Management

Information items from the field and how to collect them will be discussed, and the method to estimate parameters in the crop model using the above information will be addressed. The discussions should be oriented toward preparing manuals for required tasks.

Textbooks should be prepared to include the method for inputting current and future climate conditions into the coupled model of WEB-DHM and SIMRIW-rainfed and the method for impact assessment of food production under climate change. Training courses to build leaders' capacity should also be designed.

CHAPTER 3 PLAN OF OPERATION

3.3 Assistance to Water Resources Management Plan Project

3.3.1 Science

We provided the results from Sections 3.2.1 to 3.2.3 to the Water Resources Management Plan team (Component-2), the other study team, and proposed an appropriate water resource management plan that considers climate change impacts.

Particularly for the Brantas river basin, we gave technical advice on dam operations, accounting for runoff characteristic variations caused by climate change (how to alter storage of a target reservoir, or seasonal amendment of dam operation guidelines). For the Musi river basin, we provided technical advice on adaptation policies, including water resource development based on the climate change impact on food production.

3.3.2 Capacity Development

We cooperated with country-by-country training events designed to teach a runoff analysis method, in which the JICA and the Water Resources Management Plan team (Component-2) worked together in Japan. The project includes the following two types of training in Japan:

- 1) Training on climate change impact assessment, and
- 2) Training on the Water Resources Management Plan.

Local Indonesian operational staff were invited twice each time during the training session on assessment of climate change impacts.

The first training course of 4 weeks, which was the responsibility of the study team (Component-1), focused on WEB-DHM principles and application for three weeks. The other one week was allocated for coupling a crop model.

The second training, individual, was similar in content to the first, but its period was longer than the first.

The third 4-week training course, again our responsibility, focused on deepening understanding through study work by the attendees.

We also cooperated with the Water Resources Management Plan team in drafting training materials.

Outlines of this training course are compiled in Table 3.3.2-1. Appendix C shows the details of each training course.

Table 3.3.2-1 Program of training on climate change impact assessment

| Item | 1st Training | 2nd Training | 3rd Training |
|--------------|--|--------------------------------------|--------------------------------|
| Trainee | Group (4 persons) | Individual (1 person) | Group (3 persons) |
| Period | 4 weeks (April, 2014) | 2 months (January to March, 2015) | 4 weeks (May to June, 2015) |
| Course Title | Simulation and Evaluation of Climate Change Impacts by Downscaling and | | |

CHAPTER 3 PLAN OF OPERATION

| | | | |
|---------|---|---|----------------|
| | Hydrological Modeling | | |
| Purpose | To learn methods for assessment of climate change impacts and runoff analysis | | |
| Topics | Learning methods through lectures and practices | Deep understanding through study work by themselves | |
| Trainer | Study Team for “Climate Change Impact Assessment and Runoff Analysis” | | |
| Place | Tokyo | Tokyo | Tokyo, Tsukuba |

3.4 Report Schedule and Dispatch

(1) Summary of Reports

The following reports were prepared in the course of the project, as scheduled below.

Table 3.4-1 Summary of Report

| Report | Submission schedule (Dispatch period) | Volume and Submission |
|------------------------------|--|--|
| Inception Report (IC/R) | June 2013 (June 23 to 26, 2013) | - 40 copies (English) with simple binding - To JICA, Indonesian side |
| Interim Report (IT/R) | May 2014 (May 18 to 22, 2014) | - 40 copies (English) with simple binding - To JICA, Indonesian side |
| Draft Final Report (DF/R) | January 2017 (February 2 to 4, 2017) | - 40 copies (English) with simple binding. - To JICA, Indonesian side |
| Final Report (F/R) | March 2017 | - 39 copies (English) with hardcover and 3 CD-Rs - To JICA, Indonesian side |

1) Preparation and Discussion of Inception Report (IC/R)

The study team prepared the draft version of the IC/R, which included the study content and schedule covering the entire research period through the end of November 2014 originally. In the first dispatch, the IC/R was explained to, discussed, and agreed on with the Indonesian side on June 24, 2013. The final version of the report, reflecting comments from and confirmation by JICA, was submitted to and approved by JICA in June 2013.

2) Preparation and Discussion of Interim Report (IT/R)

The study team prepared the IT/R, which presents study outputs up until then. The procedure from the draft to final version was the same as the IC/R. Based on the IT/R in particular, results of the climate change impact assessment and hydrologic simulation for the

CHAPTER 3 PLAN OF OPERATION

Brantas and Musi river basins were explained and discussed regarding conduct of the impact assessment for food production considering the climate change impact assessment for the Musi Basin in the second dispatch. Submission of this report was just prior to the second dispatch, near the end of May 2014.

3) Preparation and Discussion of Draft Final Report (DF/R)

The study team prepared the DF/R, which presents the study outputs and recommendations covered in Chapter 4 and Chapter 5. After confirmation by JICA, contents of the DF/R were explained to and discussed with the Indonesian side. Submission of this report was the middle of January 2017 and the final dispatch was conducted on February second to fourth.

4) Preparation and Discussion of the Final Report (F/R)

The F/R, which reflected comments from JICA on the Draft Final Report, will be submitted to JICA near the beginning of March 2017.

These outputs will contribute to the vulnerability assessment of water resources under climate change impacts, and to the formulation of proposals reflecting climate change impacts on water resource management plans.

(2) Collected Materials

Materials and data collected via the study will be organized in certain areas and submitted to JICA as an edition of the collected materials, attaching the material list.

Table 3.4-2 Summary of collected materials

| Materials | Submission schedule | Volume and Submission |
|-----------------------------|----------------------------|---|
| Collected materials edition | Beginning of March 2017 | - One CD-ROM (electronic file, CD-ROM for Windows) - To JICA |

(3) Other Submissions

Reports and documents were submitted to JICA as suggested by Table 3.4-3.

Table 3.4-3 Other submissions

| Documents | Submission schedule | Volume and Submission |
|------------------|-------------------------------|--|
| Meeting minutes | Within 3 days of the meetings | To JICA |
| Monthly reports | End of every month | One original (Japanese) To JICA (supervisory staff) |
| Documents to | Prompt return | To Indonesia side |

CHAPTER 3 PLAN OF OPERATION

| | | |
|----------------|---------------|------------------------------|
| Indonesia side | | To JICA (supervisory office) |
| Others | Prompt return | To JICA |

1) Meeting Minutes

The minutes (A4 edition and typing), which explain and discuss each report in the meetings with the Indonesian government, were promptly submitted to JICA. Additionally, the minutes, including agenda, participants, and questions and answers in separate or special meetings, were composed and submitted to JICA.

2) Monthly Reports

Study progress was reported to JICA at the end of each month, which included the latest version of the business flowchart.

3) Documents to the Indonesian Side

The copies of documents submitted to the Indonesian government are to be promptly submitted to the JICA department in charge (JICA overseas office manager was also included when the study team was working in Indonesia during a dispatch period).

4) Others

Reports requested by JICA are to be also submitted.

CHAPTER 4

CLIMATE CHANGE IMPACT ASSESSMENT
AND
HYDROLOGICAL SIMULATION

CHAPTER 4 CLIMATE CHANGE IMPACT ASSESSMENT AND HYDROLOGICAL SIMULATION

CHAPTER 4 CLIMATE CHANGE IMPACT ASSESSMENT AND HYDROLOGICAL SIMULATION

4.1 Climate Change Impact Assessment on Water Cycle: Common Approaches

4.1.1 Review of Action Plan, and Collection and Analysis of Existing Information and Data

The study team investigated, reviewed, and analyzed existing data, information, materials, and references that were offered by the Water Resources Management Plan team and given in the Detailed Planning Survey (June 2013) of the Japan International Cooperation Agency (JICA).

Our outputs contribute to vulnerability assessments of water resources under climate change impacts, and to the formulation of proposals reflecting those impacts on water resource management plans. Therefore, the close relationship and timely information sharing with the Water Resources Management Plan team were considered by the project management aspect.

As a rule, the Water Resource Management Plan team is in charge of the observation data mentioned above so that selection of observation stations and method were properly advised and discussed. This has been coordinated and decided.

On the other hand, the study team has conducted five field surveys so far with the object of model development and validation properly. These field surveys are summarized in Table 4.1.1-1 below, and are also described in the Appendix-B.

Table 4.1.1-1 Field Survey in Indonesia

| Dispatch Period | Location | Observation / Overview | Refer |
|--|---|--|--------------|
| June 18 - 22, June 17 - July 6, 2013 (15 days) | Musi River basin: Palembang, Martapura | Implementation of field survey required for preparing crop model and establishment of the method. | Appendix B-1 |
| June 27 - July 2, 2013 (6 days) | Brantas River basin: Surabaya, Tulungagung | Implementation of field survey for model establishment of Brantas river basin. | Appendix B-2 |
| September 7 - 12, 2013 (6 days) * This mission is not included in the contract with JICA. | Musi River basin: Palembang, Talang, Saleh, Rambutan, Lempuing, Belitang, Bendung Perjaya, Lubuk Linggau, Tugumulyo, Lakitan, Bengkulu | Implementation of the field survey for model establishment of Musi river basin; screening or confirming the basin environment as tidal swamp, freshwater swamp, rainfed (dryland), or irrigated paddies. | Appendix B-3 |
| May 18 - 22, 2014 (5 days) | Brantas River basin: Surabaya | First seminar on climate change and the implementation of the field | Appendix B-4 |

CHAPTER 4 CLIMATE CHANGE IMPACT ASSESSMENT AND HYDROLOGICAL SIMULATION

| | | | |
|--------------------------------------|---|---|--------------|
| | | survey for model establishment and its validation | |
| May 15 - 17, 23-25, 2014 (6 days) | Bogor (Jakarta) Musi River basin Palembang, Martapura | Research meeting at Bogor Agricultural University. Implementation of field survey required for preparing crop model and establishment of the method. | Appendix B-5 |

4.1.2 Climate Change Impact Assessment for Rainfall

(1) Selection of GCMs

1) Methodology

A GCM is the most promising and advanced tool to increase our understanding of climate change and project future climate states. However, there is considerable discrepancy or bias between local climate conditions and simulated results. It is important to select appropriate GCMs before applying the model output to evaluation of climate change impacts on a target area. The selection of GCMs by The University of Tokyo was based on performance of the reproducibility of local climate conditions and the selection method.

There are 18 GCMs for which daily datasets are available to the public among the 24 GCMs in the Coupled Model Intercomparison Project 3 (CMIP3). The CMIP3 daily GCM datasets are archived in the DIAS of Japan, from which the study team obtained the 18 datasets with daily data.

Model selection was based on reproducibility of present climate conditions and climate variables important for evaluation of hydrologic conditions, namely, precipitation, air temperature at the ground surface, sea surface temperature, air pressure at sea level, outgoing radiation, meridional wind, and zonal wind.

At basin scale, selected global circulation models (GCMs) should be able to reproduce the seasonal pattern of precipitation. Spatial correlation (Scorr) and root mean square error (RMSE) were used to identify similarities and differences between the models and current observational global datasets. The Global Precipitation Climatology Project (GPCP) dataset was used for comparing similarities of average monthly precipitation, whereas the Japan Reanalysis (JRA25) output was used to compare other meteorological variables.

$$Scorr = r_{xy} = \frac{\sum_{i=1}^N (x_i - \bar{x})(y_i - \bar{y})}{(n-1)S_x S_y} = \frac{\sum_{i=1}^N (x_i - \bar{x})(y_i - \bar{y})}{\sqrt{\sum_{i=1}^N (x_i - \bar{x})^2 \sum_{i=1}^N (y_i - \bar{y})^2}} \quad (4.1.2-1)$$

$$RMSE = \sqrt{\frac{1}{N} \sum_{i=1}^N (R_{si} - R_{obs})^2} \quad (4.1.2-2)$$

CHAPTER 4 CLIMATE CHANGE IMPACT ASSESSMENT AND HYDROLOGICAL SIMULATION

To evaluate the ability of GCM to represent small-scale precipitation, additional screening should be done to eliminate the worst performing models. Three additional criteria should be used to achieve this:

- i. Long-term basin observed rainfall averages (climatology) should be compared with GCM data. If a GCM cannot represent seasonal variability, it should be eliminated.
- ii. If a GCM produces too little rainfall such that unreasonably dry days persist after a no-rain correction, then that model should also be eliminated.
- iii. Last, if observed rainfall within a basin is not uniformly distributed, basin subdivision climatological averages (based on areas of high, medium, and low rainfall usually related to elevation and land use) should be considered for the model selection comparison.

The climate in Indonesia is dominated by the Intertropical Convergence Zone (ITCZ) and conditions of the Pacific and Indian oceans. The El Niño - Southern Oscillation (ENSO) in the Pacific and Indian Ocean Dipole (IOD) are phenomena in which ocean water temperature is unevenly distributed. For example, La Niña, the cool phase of the ENSO, causes heavy rains over Indonesia. The eastern IOD tends to cause droughts in the country. The Asian summer monsoon, specifically, the Southeast Asian summer monsoon (0°N to 10°N; 90°E to 130°E) and Indian summer monsoon (5°N to 20°N and 40°E to 80°E) area also linked with the rainfall variations in Indonesia.

Considering these facts, the large area for evaluation of GCM performance was defined as 80°E–160°E and 20°S–20°N. This includes the Bay of Bengal, Indian Ocean, Philippine Sea, and Java Sea. The parameters considered are sea level pressure, air temperature (at 850 hPa), meridional wind (at 850 hPa), zonal wind (at 850 hPa), outgoing longwave radiation, and sea surface temperature. The local area for comparison of precipitation was set to 95°E–125°E and 16°S–9°N, which could cover GCM grids of more than 6 × 6. The two types of areas for the GCM performance evaluation are illustrated in Figure 4.1.2-1.

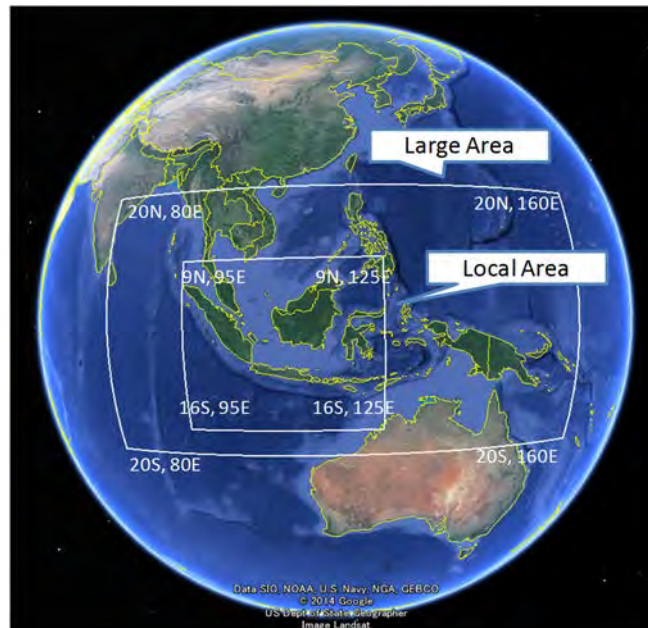


Figure 4.1.2-1 Local-scale (for precipitation) and large-scale (global circulation affecting other meteorological parameters) regions considered for model selection

2) Selected GCMs

In the study area, both the wet and dry seasons are very important for water management, so the spatial correlation (score) and root mean square error (RMSE) for each month was considered while prioritizing the models that showed high spatial correlation and low root mean square error during the wet season (May to September) and dry season (October to April). A simple index counter was used for identifying the models that had RMSE and score values above the average RMSE and score (if above average, index = 1, else index = 0).

The scorings of the 7 meteorological parameters for the wet season, dry season and for the whole year are given in Table 4.1.2-1~3. Table 4.1.2-4 is a summary of all the models selected. Primarily, models that had high scores (total scores above 1) are given priority. In addition, to ensure that the rainfall patterns are exhibited, only those models with above 0 score for precipitation were selected; incomplete data were rejected. Preference is given to the models selected based on the model's ability to represent the wet season and dry season as well as the yearly average rainfall conditions. Finally, 9 models were selected: *cccma_cgcm3_1*, *csiro_mk3_5*, *gfdl_cm2_0*, *gfdl_cm2_1*, *giss_aom*, *ingv_echam4*, *miub_echo_g*, *mpi_echam5*, and *mri_cgcm2_3_2a*. Among these selected models, *gfdl_cm2_1* was found to have best index during the wet season, dry season, and the annual average.

Figures 4.1.2-2 shows how the spatial distribution climatological average of annual rainfall over the region for these selected models shows similar patterns as those of GPCP. Figure 4.1.2-3 shows the grid size of the selected nine GCMs.

CHAPTER 4 CLIMATE CHANGE IMPACT ASSESSMENT AND HYDROLOGICAL SIMULATION

Table 4.1.2-1 Results from the average of the dry season analysis: May-Sep

| | Precipitation | Air Temperature | SST | OLR | SLP | Zonal Wind | Meridional Wind | TOTAL |
|-------------------|---------------|-----------------|-----|-----|-----|------------|-----------------|-------|
| bccr_bcm2_0 | -1 | 1 | -1 | 1 | 1 | 1 | -1 | 1 |
| cccma_cgcm3_1 | 1 | 1 | 1 | 1 | 1 | 1 | 1 | 7 |
| cccma_cgcm3_1_t63 | 1 | 1 | 1 | 1 | 1 | 1 | -1 | 7 |
| cnrm_cm3 | -1 | 0 | 0 | 0 | 1 | 0 | -1 | -1 |
| csiro_mk3_0 | 1 | 1 | -1 | -1 | 1 | 0 | -1 | 0 |
| csiro_mk3_5 | 1 | 0 | 0 | -1 | 1 | 1 | 0 | 2 |
| gfdl_cm2_0 | 0 | 1 | 1 | 1 | 1 | 1 | 1 | 6 |
| gfdl_cm2_1 | 1 | 1 | 1 | 1 | 1 | 1 | 1 | 7 |
| giss_aom | 1 | -1 | 1 | 1 | 1 | 1 | 0 | 4 |
| giss_model_e_h | -1 | 0 | -1 | -1 | -1 | -1 | -1 | -6 |
| giss_model_e_r | 1 | 1 | 1 | -1 | -1 | -1 | -1 | 1 |
| iap_fgoals1_0_g | 0 | 0 | -1 | 0 | 0 | -1 | -1 | -3 |
| ingv_echam4 | 1 | 0 | 1 | 1 | 0 | 1 | 1 | 5 |
| inmcm3_0 | 0 | -1 | -1 | -1 | 1 | -1 | 0 | -3 |
| ipsl_cm4 | 1 | 1 | 1 | 1 | 1 | 1 | 0 | 6 |
| miroc3_2_hires | 1 | 1 | -1 | 0 | -1 | -1 | 1 | 0 |
| miroc3_2_medres | 0 | 0 | 0 | 1 | 0 | -1 | 1 | 1 |
| miub_echo_g | 1* | 1 | 1 | 1 | 1* | * | * | 4 |
| mpi_echam5 | 0 | 1 | 1 | 1 | 1 | 1 | 1 | 6 |
| mri_cgcm2_3_2a | 0 | 0 | 1 | 1 | 0 | 0 | 0 | 2 |
| ncar_ccsm3_0 | -1 | 0 | 1 | 0 | 0 | 0 | 0 | 0 |
| ncar_pcm1 | -1 | -1 | -1 | -1 | -1 | -1 | -1 | -7 |
| ukmo_hadcm3 | -1 | 0 | -1 | -1 | 0 | 0 | -1 | -4 |
| ukmo_hadgem1 | 0 | 1 | 0 | 0 | 1 | 0 | -1 | 1 |

- 1 (GOOD) = spatial correlation (above average) AND root mean square error (below average)
0 (BAD) = spatial correlation (above average) OR root mean square error (below average)
-1 (VERY BAD) = spatial correlation (below average) and root mean square error (above average)
* = could not evaluate because of missing monthly data

Table 4.1.2-2 Results from the average of the wet season analysis: Oct-Apr

| | Precipitation | Air Temperature | SST | OLR | SLP | Zonal Wind | Meridional Wind | TOTAL |
|-------------------|---------------|-----------------|-----|-----|-----|------------|-----------------|-------|
| bccr_bcm2_0 | 1 | 1 | -1 | 0 | 0 | 0 | -1 | 0 |
| cccma_cgcm3_1 | 0 | 1 | 1 | 0 | 0 | 0 | 1 | 4 |
| cccma_cgcm3_1_t63 | -1 | 1 | 1 | 0 | 0 | 0 | 1 | 2 |
| cnrm_cm3 | 1 | 0 | -1 | 0 | 0 | 0 | -1 | -1 |
| csiro_mk3_0 | 0 | 1 | -1 | 0 | 1 | 1 | -1 | 1 |
| csiro_mk3_5 | 1 | 0 | 0 | 0 | 1 | 1 | -1 | 2 |
| gfdl_cm2_0 | 1 | 0 | 0 | 1 | 1 | 1 | 1 | 5 |
| gfdl_cm2_1 | 1 | 1 | 1 | 1 | 1 | 1 | 1 | 7 |
| giss_aom | 1 | 0 | 1 | 1 | 1 | -1 | 0 | 3 |
| giss_model_e_h | -1 | 0 | -1 | -1 | -1 | -1 | -1 | -6 |
| giss_model_e_r | 0 | 1 | 1 | 0 | 0 | 0 | 1 | 3 |
| iap_fgoals1_0_g | 1 | 1 | 0 | 1 | 1 | 1 | 0 | 5 |
| ingv_echam4 | 0 | 0 | 0 | 1 | -1 | 1 | 1 | 2 |
| inmcm3_0 | 1 | -1 | -1 | 0 | 1 | 1 | -1 | 0 |
| ipsl_cm4 | 0 | -1 | 1 | -1 | 1 | -1 | 1 | 0 |
| miroc3_2_hires | 1 | 1 | 1 | 1 | 0 | 0 | -1 | 3 |
| miroc3_2_medres | -1 | 0 | 0 | 1 | 0 | -1 | -1 | -2 |
| miub_echo_g | 1* | 1 | 1 | 1 | 0* | * | * | 3 |
| mpi_echam5 | 0 | 1 | 1 | 1 | 1 | 1 | 1 | 6 |
| mri_cgcm2_3_2a | 1 | 0 | 1 | 1 | 1 | 1 | 1 | 6 |
| ncar_ccsm3_0 | 0 | -1 | 1 | 0 | 1 | -1 | -1 | -1 |
| ncar_pcm1 | -1 | -1 | -1 | -1 | 0 | -1 | -1 | -6 |
| ukmo_hadcm3 | -1 | 0 | -1 | -1 | 0 | 0 | 0 | -3 |
| ukmo_hadgem1 | 0 | 1 | -1 | 0 | 1 | 0 | 1 | 2 |

- 1 (GOOD) = spatial correlation (above average) AND root mean square error (below average)
0 (BAD) = spatial correlation (above average) OR root mean square error (below average)
-1 (VERY BAD) = spatial correlation (below average) and root mean square error (above average)
* = could not evaluate because of missing monthly data

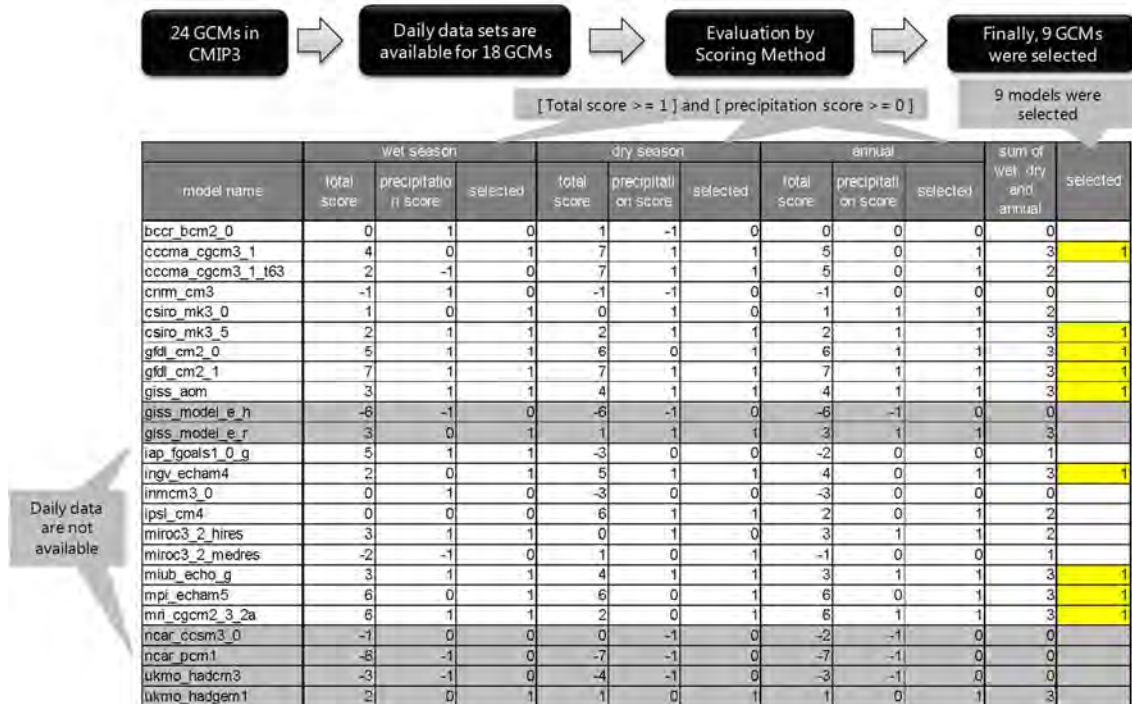
CHAPTER 4 CLIMATE CHANGE IMPACT ASSESSMENT AND HYDROLOGICAL SIMULATION

Table 4.1.2-3 Results from the average of the 12 month analysis

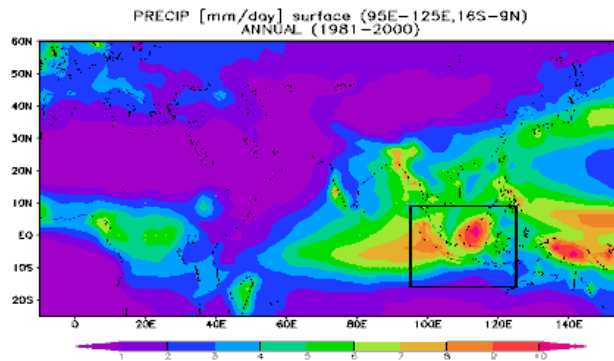
| | Precipitation | Air Temperature | SST | OLR | SLP | Zonal Wind | Meridional Wind | TOTAL |
|-------------------|---------------|-----------------|-----|-----|-----|------------|-----------------|-------|
| bccr_bcm2_0 | 0 | 1 | -1 | 0 | 1 | 0 | -1 | 0 |
| cccma_cgcm3_1 | 0 | 1 | 1 | 0 | 1 | 1 | 1 | 5 |
| cccma_cgcm3_1_t63 | 0 | 1 | 1 | 0 | 1 | 1 | 1 | 5 |
| cnrm_cm3 | 0 | 0 | -1 | 0 | 0 | 1 | -1 | -1 |
| csiro_mk3_0 | 1 | 1 | -1 | -1 | 1 | 1 | -1 | 1 |
| csiro_mk3_5 | 1 | 0 | 0 | 0 | 1 | 1 | -1 | 2 |
| gfdl_cm2_0 | 1 | 0 | 1 | 1 | 1 | 1 | 1 | 6 |
| gfdl_cm2_1 | 1 | 1 | 1 | 1 | 1 | 1 | 1 | 7 |
| giss_aom | 1 | 0 | 1 | 1 | 1 | 0 | 0 | 4 |
| giss_model_e_h | -1 | 0 | -1 | -1 | -1 | -1 | -1 | -6 |
| giss_model_e_r | 1 | 1 | 1 | 0 | 0 | -1 | 1 | 3 |
| iap_fgoals1_0_g | 0 | 0 | -1 | 0 | 0 | 0 | -1 | -2 |
| ingv_echam4 | 0 | 0 | 1 | 1 | 0 | 1 | 1 | 4 |
| inmcm3_0 | 0 | -1 | -1 | -1 | 1 | 0 | -1 | -3 |
| ipsl_cm4 | 0 | 0 | 1 | -1 | 1 | 0 | 1 | 2 |
| miroc3_2_hires | 1 | 1 | 1 | 0 | 0 | -1 | 1 | 3 |
| miroc3_2_medres | 0 | 0 | 0 | 1 | 0 | -1 | -1 | -1 |
| miub_echo_g | 1* | | 1 | 1 | 0 | * | | 3 |
| mpi_echam5 | 0 | 1 | 1 | 1 | 1 | 1 | 1 | 6 |
| mri_cgcm2_3_2a | 1 | 0 | 1 | 1 | 1 | 1 | 1 | 6 |
| ncar_ccsm3_0 | -1 | -1 | 1 | 0 | 1 | -1 | -1 | -2 |
| ncar_pcm1 | -1 | -1 | -1 | -1 | -1 | -1 | -1 | -7 |
| ukmo_hadcm3 | -1 | 0 | -1 | -1 | 0 | 0 | 0 | -3 |
| ukmo_hadgem1 | 0 | 1 | -1 | 0 | 1 | 0 | 0 | 1 |

- 1 (GOOD) = spatial correlation (above average) AND root mean square error (below average)
- 0 (BAD) = spatial correlation (above average) OR root mean square error (below average)
- 1 (VERY BAD) = spatial correlation (below average) and root mean square error (above average)
- * = could not evaluate because of missing monthly data

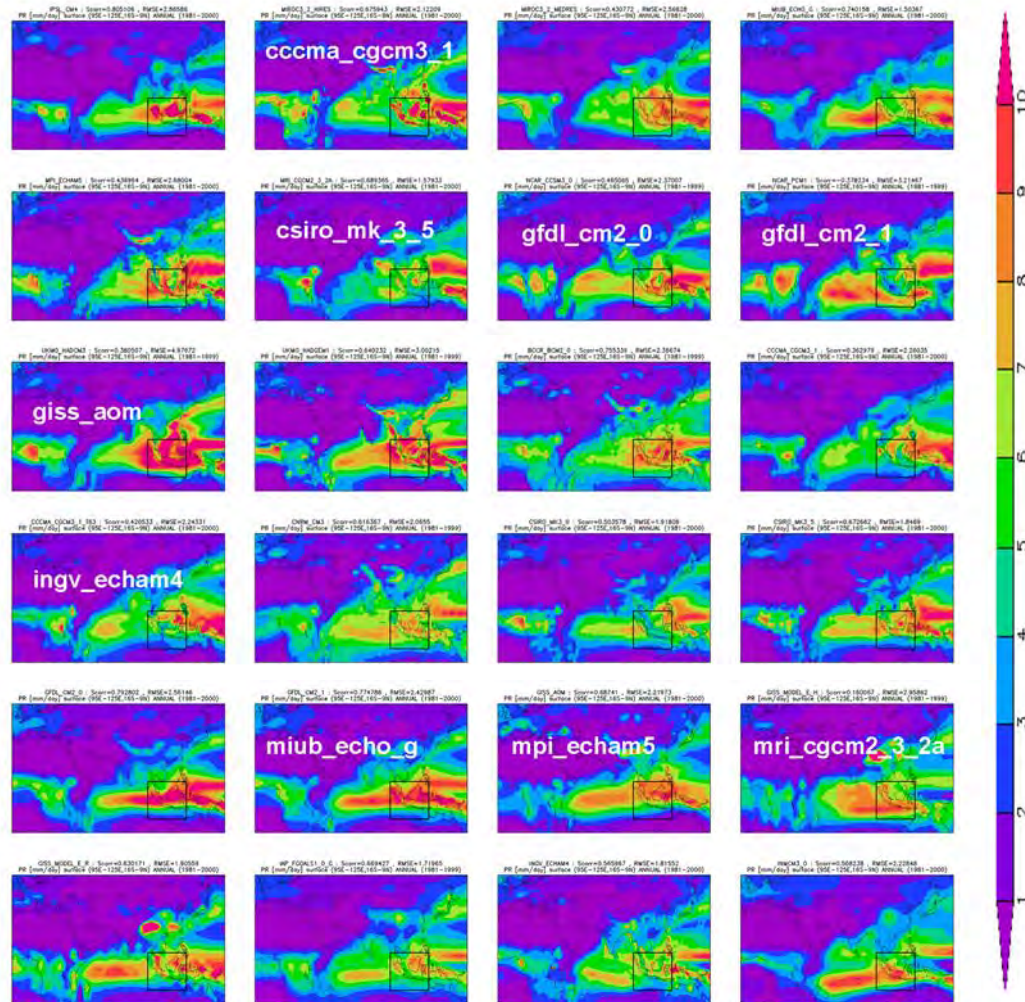
Table 4.1.2-4 Summary of model selection in indices for the wet season, dry season, and 12 month average



CHAPTER 4 CLIMATE CHANGE IMPACT ASSESSMENT AND HYDROLOGICAL SIMULATION



(a) Reference rainfall from GPCP



(b) Projected rainfall of the 24 GCMs. The names of selected nine GCMs are shown on the map.

Figure 4.1.2-2 Climatological average of annual mean rainfall of (a) GPCP and (b) 24 GCMs. The black boxes show the local scale precipitation region considered in the model selection.

CHAPTER 4 CLIMATE CHANGE IMPACT ASSESSMENT AND HYDROLOGICAL SIMULATION

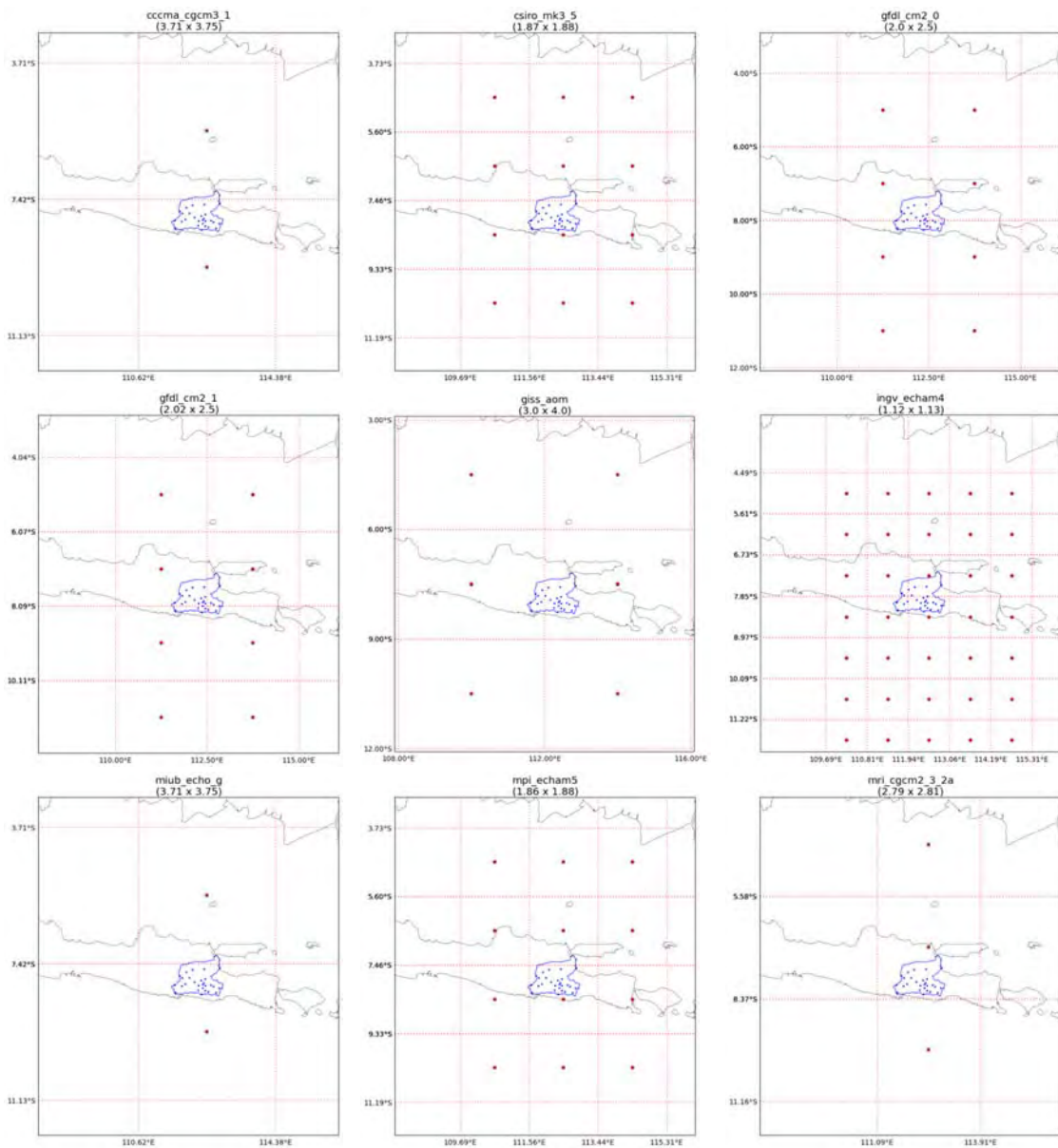


Figure 4.1.2-3 Grid size of selected Nine GCMs

(2) Methodology for Bias-correction of Rainfall Data

Most rainfall data in GCMs show three main problems. These are the underestimation of strong rainfall intensity, poor seasonal representation, and too many rainy days with very weak rainfall, referred to as drizzle. We focused on GCM bias correction to alleviate these problems. To accomplish this, annual maximum rainfall, normal rainfall, and numbers of no-rain days were statistically bias-corrected (Nyunt et al., 2012).

CHAPTER 4 CLIMATE CHANGE IMPACT ASSESSMENT AND HYDROLOGICAL SIMULATION

1) Three -Step Bias Correction Method

If realistic output is sought, precipitation outputs from the GCMs cannot be directly used to force hydrologic or other impact-assessment models without some form of prior bias correction (Ines and Hansen, 2006; Feddersen and Andersen, 2005; Sharma et al., 2007). If used directly, the models may magnify errors resulting from biases. Hence, it is necessary to correct the biases prior to the use of model outputs. Further, since there are differences between models, we investigated the use of a model ensemble (especially for precipitation, the most sensitive dynamic parameter affecting moisture) for basin water supply. A variety of tools for the evaluation, selection, and downloading of GCM data have been developed through the Data Integration & Analysis System (DIAS), and disseminated via its data access system.

To use GCM scenario outputs in a hydrologic study, appropriate downscaling is required. Two downscaling approaches are typically available, namely, dynamic and statistical. Dynamic downscaling involves the use of finer-resolution numerical weather prediction models with GCM output as initial and boundary conditions. Statistical downscaling includes the use of statistical relationships to convert large-scale projections from a GCM to higher spatial resolutions. This part of the report presents the steps necessary to achieve a simplified statistical approach based on statistics.

To achieve reasonable bias correction of precipitation, there is a need to separate no-rain, normal and extreme rain days. Because they do not incorporate parameterization schemes in their simulations, GCM outputs are characterized by many wet days (with substantial drizzle) and an inability to represent extreme events. This necessitates separation of the three types of rainfall events. To account for basins with extremely distinct seasons (e.g., very dry and wet), bias correction should be performed separately for these seasons. This should be done at monthly or bi-monthly scales, depending on basin climatology.

Bias correction using this approach is a three-step process, for dry days, normal days, and extreme rain days. Figure 4.1.2-4 illustrates how the three categories of rainfall are determined (Nyunt et al., 2012).

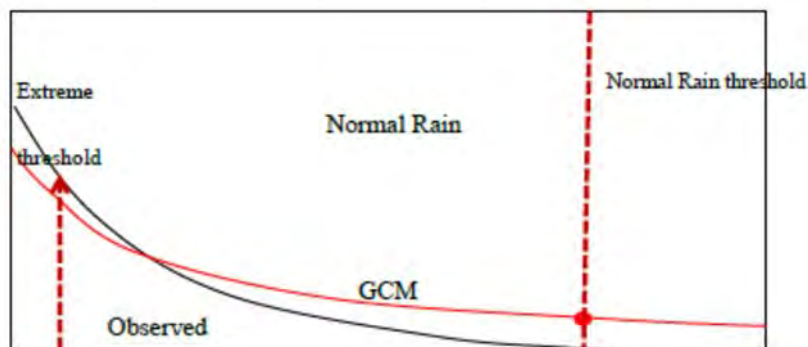


Figure 4.1.2-4 Three-step bias correction separating rainfall into extreme, normal, and no-rain days.

a) STEP 1: No-rain Day Correction

A common characteristic of all GCMs is an unrealistically high number of wet days. Most of these

CHAPTER 4 CLIMATE CHANGE IMPACT ASSESSMENT AND HYDROLOGICAL SIMULATION

are represented by drizzle and can be attributed to the lack of parameterization in GCMs. To correct for this, the following method was used.

- i. Both observations and present GCM-extracted values are ranked in descending order.
- ii. A threshold of 0 mm/day was established for no-rain days in the observations. The rank of this threshold is then used to determine the corresponding value of no-rain days in the GCMs.
- iii. All values equal to or below this rank in the GCM are set to zero.
- iv. No-rain day correction for the future GCM is based on the threshold for present GCMs.

b) STEP 2: Extreme Rainfall Correction

Most of the GCMs underestimate extreme rainfall compared with observations. To account for this, there should be appropriate correction for adjusting these values to match the distribution of the observations.

Annual maximum rainfall was selected for each year in the observation dataset. The smallest value of the annual maxima was selected as the threshold for the extreme events of observed rainfall. Values above this threshold were defined as extreme events. The number of such events was determined from observation stations and set to the same number of extreme events in present GCMs by ranking. Above this threshold, the generalized Pareto distribution (GPD) was fit to the data.

GPD fitting parameters for GCM corrected extremes were determined (shape, scale and location) using the method of moments (MOM) for parameterization, via the MOM equations below (Hosking and Wallis, 1987; Madsen et al., 1997). The best-fit GPD of GCM extreme events was determined by the minimum root mean square error (RMSE) between an inverse GPD of extreme events and those of observation stations (checked using trial and error with different thresholds). The same checking (present GCMs) and fitting procedure was applied to all extremes. GCM extremes for future projections were extracted and the transfer function of the present GCM extreme correction was applied.

All values greater than a threshold u ,
the distribution of excess x over u is defined by

$$F_u(y) = \Pr\{X - u \leq x | X > u\} = \frac{F(x) - F(u)}{1 - F(u)} \quad (4.1.2-3)$$

Generalized Pareto distribution (GPD) is given by :

$$G(x; K, \alpha, u) = 1 - \left(1 - K \frac{x - \mu}{\alpha}\right)^{1/\xi} \quad \xi \neq 0$$

$$1 - e^{-(x-\mu)/\sigma} \quad \xi = 0$$

$K = 0 \Rightarrow$ exponential distribution (medium-size tail)

$K < 0 \Rightarrow$ Pareto distribution (long-tailed)

$K > 0 \Rightarrow$ Pareto II type distribution (short-tailed)

CHAPTER 4 CLIMATE CHANGE IMPACT ASSESSMENT AND HYDROLOGICAL SIMULATION

$$\alpha = \frac{1}{2} \mu \left(\frac{\mu^2}{\sigma^2} + 1 \right) \quad (4.1.2-4)$$

$$\kappa = \frac{1}{2} \left(\frac{\mu^2}{\sigma^2} - 1 \right)$$

μ = sample mean

σ^2 = variance

Recurrences of extreme events for different return periods were calculated as shown in the equation below.

$$x_T = u + \frac{\alpha}{\kappa} \left[1 - (\lambda T)^{-\kappa} \right]$$

κ = shape parameter

α = scale parameter

λ = average number of events per year above threshold

T = return period in years

(4.1.2-5)

c) STEP 3: Normal Rainfall Correction

Normal rainfall is in the range between zero and extreme rainfall. Correction in this range is based on the gamma distribution function fit to observations and present GCMs. The following equation was adopted.

$$f(x) = \frac{\lambda^\beta x^{\beta-1} e^{-\lambda x}}{\Gamma(\beta)} \quad x \geq 0$$

$$\lambda = \frac{\bar{x}}{s_x^2}, \quad \beta = \frac{\bar{x}^2}{s_x^2}$$

(4.1.2-6)

\bar{x} = mean of sample

s_x^2 = variance of sample

$\Gamma(\)$ = Gamma function

The inverse of the gamma distribution for observed rainfall was used to correct for present GCM rainfall. This was then used as a transfer function for the future normal rainfall correction.

A summary of the three-step bias correction is given in Figure 4.1.2-5 below.

CHAPTER 4 CLIMATE CHANGE IMPACT ASSESSMENT AND HYDROLOGICAL SIMULATION


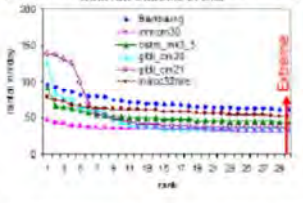
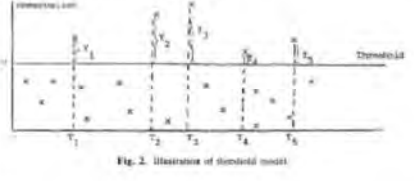

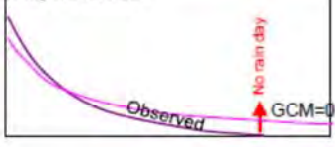

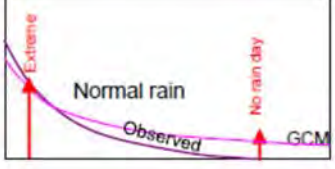
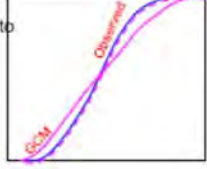
| Rain Type | Threshold | Correction |
|---|---|--|
| Extreme  | <ul style="list-style-type: none"> - Larger than minimum of annual maxima of station - count the number of extreme events in station (eg. Top of 30 rainfall by ranking all rainfall) - apply same number of extremes in GCM  | Generalized Pareto Distribution <ul style="list-style-type: none"> -Non every year statistics -Extreme (long or short tailed) fitting -Peak over threshold method  <p>Fig. 2. Illustration of threshold model.</p> |
| No rain day  |  | Ranking order statistics <ul style="list-style-type: none"> - frequency of no rain day in GCM is same as station - less than no rain day threshold change zero rainfall. |
| Normal  |  | Gamma Distribution <ul style="list-style-type: none"> - monthly CDF of GCM mapping to monthly CDF of station - inverse of Gamma CDF in each month is corrected rain  |

Figure 4.1.2-5 Summary of three-step bias correction

2) Adjustment for Areal Average Rainfall of GCMs

We have applied statistical downscaling and bias-correction for GCMs rainfalls to get adequate projections in basin scales. The applied methodology of statistical downscaling has been well verified for the reproducibility of statistical property (annual or monthly mean values and frequency distributions) for each point. However, the methodology has a limitation in representing rainfall space-time distributions. Even though the bias-corrected 1-day cumulative rainfall at each station match reasonably the observed 1-day rainfall, the method of bias correction does not guarantee matching of spatial and temporal (e.g. size of the rain spell) characteristics. For many hydrological assessments, the space-time series of rainfall is essential. Discharge is not only determined by magnitude of the daily rainfall but also by its spatial distribution and the size of the rain spell, particularly in the case of flooding. Impact of this problem on the hydrological phenomena will be different according to characteristics of subjected basins. If the subjected basin scale is adequately larger than the GCM grid size or the rainfall distribution over the basin is generally homogeneous, impact would be small. In the case of the reverse, impact would be large and care must be taken.

Comparisons of the grid size of nine GCMs with distribution of the rainfall observation sites in the Brantas River basin are illustrated in Figure 4.1.2-3. The GCM grid size is larger than the basin, thus all the observation sites are inside the same single grid. In this situation, based on the applied method, all sites are compared with the same grid value. As a result, rain occurs simultaneously at all sites, so the time correlation among the sites becomes very high. On the other hand, actual rainfall in the basin

CHAPTER 4 CLIMATE CHANGE IMPACT ASSESSMENT AND HYDROLOGICAL SIMULATION

is characterized by the active convective rainfall of the tropical climate, which causes very different rainfall rates across the basin. The examples of observed daily rainfall distributions are shown in Figure 4.1.2-6. Consequently, there is a big difference in rainfall distribution between downscaled GCM data with observed data. Basin average rainfall of GCM data becomes much larger than the observed one (see Figure 4.1.2-7 (a)), which may lead to significant increase in flood discharge.

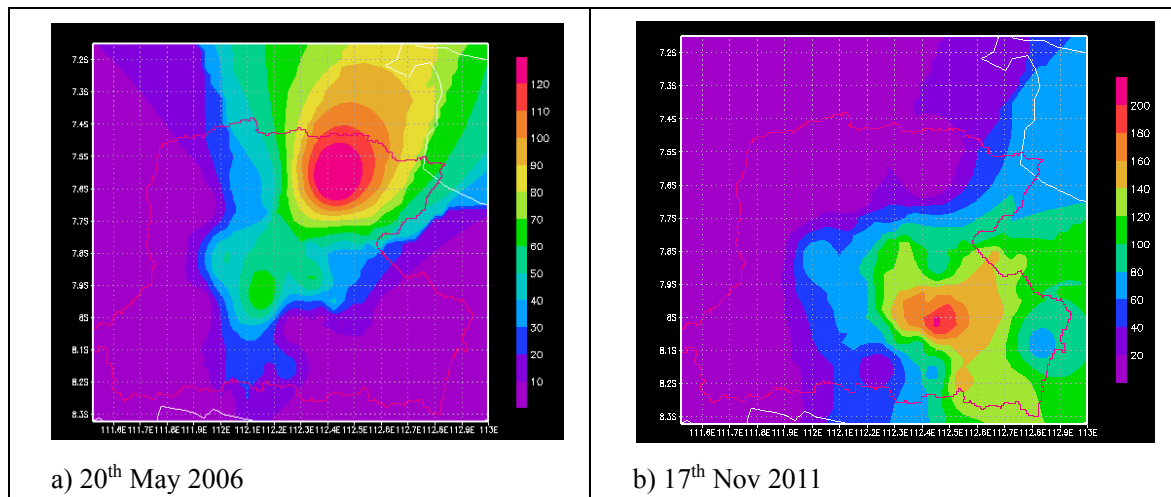


Figure 4.1.2-6 Examples of observed daily rainfall distribution in the Brantas River basin

The use of alternative downscaling methods (such as dynamic downscaling and stochastic models) may be one possible solution to overcome the mismatch in the time-spatial signatures. However, those methods are complicated, and they also have some limitations. In this study, we focused on removing the gap in the basin average rainfall to get a reasonable discharge. We adjusted the areal average rainfall over the catchment upstream via the following method:

- i. Areal average rainfall over the catchment upstream of New Lengkong was calculated using bias-corrected GCM dataset.
- ii. Methodology based on the same principle of GCM bias correction was applied to the areal average rainfall. Then, an adjustment factor for each rank of the rainfall was evaluated.
- iii. Original bias-corrected GCM grid data was adjusted by scaling it with the adjustment factor, resulting in the adjusted GCM grid data.

Consequently, this adjustment effectively removed the gap in the areal average rainfall over the catchment upstream of the New Lengkong (see Figure 4.1.2-7 (b)).

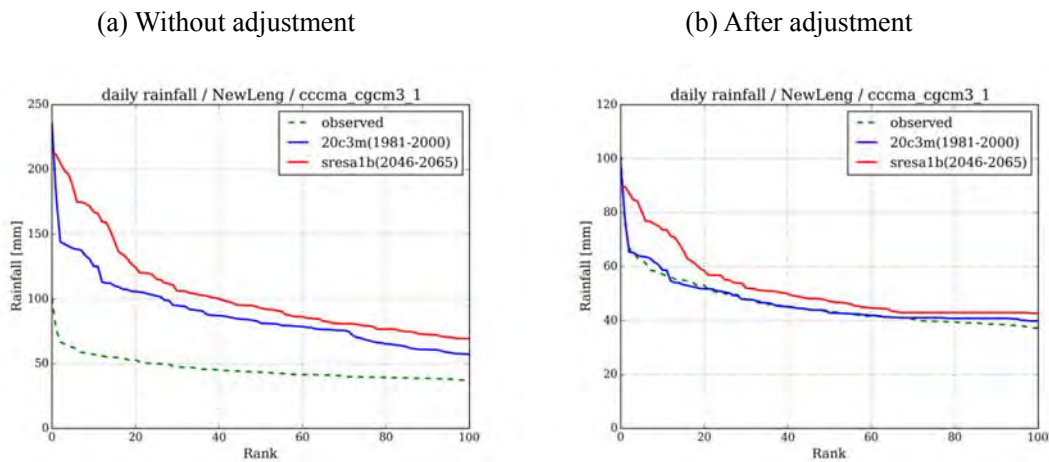


Figure 4.1.2-7 Top 100 of 20-year areal average daily rainfall for (a) without adjustment, (b) after adjustment (cccma_cgcm3_1) over the catchment upstream of the New Lengkong. Green dashed line: observed; Blue solid line: GCM present; Red solid line GCM future.

4.1.3 Climate Change Impact Assessment for River Runoff, ET, and Soil Moisture

(1) WEB-DHM Model Development

The Water and Energy Budget-based Distributed Hydrological Model (WEB-DHM) was developed by fully coupling a biosphere scheme (SiB2) with a geomorphology-based hydrological model (GBHM). The WEB-DHM has enabled consistent descriptions of water, energy, and CO₂ fluxes at basin scale (Wang et al., 2009a, 2009b). Characteristics of the model are summarized as follows.

- The model physically describes evapotranspiration (ET) using a biophysical land surface scheme for simultaneously simulating heat, moisture, and CO₂ fluxes in soil-vegetation-atmosphere transfer (SVAT) processes.
- The hydrologic sub-model describes overland, lateral subsurface, and groundwater flows using grid-hill slope discretization followed by flow routing in the river network.
- The model has high efficiency for simulations of large-scale river basins, and incorporates subgrid topography and effects of water resource management facilities.

Given possible limitations of in-situ data availability, it is necessary to consider satellite-based rainfall products, which can be widely applied to catchment-scale impact studies. Satellite-based, low-frequency microwave brightness temperature is strongly affected by near-surface soil moisture; therefore, it can be assimilated into a land surface model to improve the modeling of soil moisture and the surface energy budget. Our study uses the Land Data Assimilation System developed at The University of Tokyo (LDAS-UT) (Yang et al, 2007) for the Musi River basin to estimate soil moisture and surface temperature, and incorporates optimized soil parameters necessary for ongoing model calibration. The LDAS-UT consists of a land surface model (LSM) to calculate surface fluxes and soil moisture, a radiative transfer model (RTM) to estimate microwave brightness temperature, and an

optimization scheme to search for optimal soil moisture values by minimizing the difference between modeled and observed brightness temperatures.

1) Model Structure

Improvements over lumped hydrologic models have been made by representing spatial heterogeneity. However, DHMs have large uncertainties in simulating water exchanges at the soil-atmosphere interface and the temporal evolution of surface soil moisture, owing to the conceptual treatment of the land surface. In most current LSMs (e.g., SiB2), lateral soil moisture redistributions by topographically driven runoff are usually not well formulated since they were originally developed for application in general circulation models (GCMs).

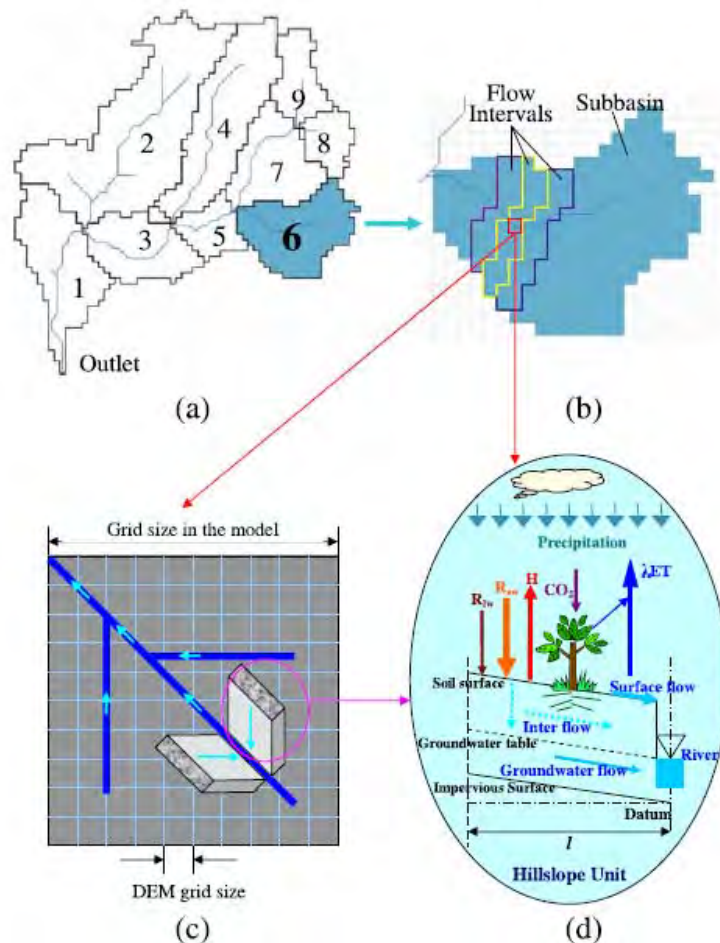


Figure 4.1.3-1 The WEB-DHM: (a) division from a basin to sub-basins; (b) subdivision from a sub-basin to flow intervals comprising several model grids; (c) discretization from a model grid to a number of geometrically symmetric hillslopes; (d) process descriptions of water moisture transfer from the atmosphere to river (Wang et al., 2009a, 2009b).

The coupling of LSMs and DHMs has the potential to improve land surface representation,

CHAPTER 4 CLIMATE CHANGE IMPACT ASSESSMENT AND HYDROLOGICAL SIMULATION

benefiting streamflow prediction capabilities of hydrologic models and providing improved estimates of water and energy fluxes into the atmosphere.

The WEB-DHM is a distributed biosphere hydrological model via the SiB2/GBHM coupling described above. SiB2 describes the transfer of turbulent fluxes (energy, water, and carbon fluxes) between the atmosphere and land surface at each model grid. The GBHM redistributes water moisture laterally through simulation of both surface and subsurface runoff, using grid-hill slope discretization and subsequent flow routing in the river network.

Overall model structure is shown in Figure 4.1.3-1 and is described as follows.

- A digital elevation map (DEM) is used to define the target area, after which the target basin is divided into sub-basins (Figure 4.1.3-1 (a)).
- Within a given sub-basin, a number of flow intervals are specified to represent time lag and accumulation processes in the river network according to distance to the outlet of the sub-basin. Each flow interval includes several model grids (Figure 4.1.3-1 (b)).
- For each model grid with one combination of land-use type and soil type, the SiB2 is used to calculate turbulent fluxes between the atmosphere and land surface independently (Figure 4.1.3-1 (b) and 4.1.3-1 (d)).

The GBHM is used to calculate runoff from a model grid with a sub-grid parameterization. Each model grid is subdivided into a number of geometrically symmetric hill slopes (Figure 4.1.3-1 (c)), which are the basic hydrological units (BHUs) of the WEB-DHM. For each BHU, the GBHM is used to simulate lateral water redistributions and calculate runoff (Figure 4.1.3-1 (c) and 4.1.3-1 (d)). Runoff in a model grid is the total response of all BHUs within it.

For simplicity, streams within one flow interval are lumped into a single virtual channel in a trapezoidal shape. All flow intervals are linked by the river network generated from the DEM. All runoff from model grids in a given flow interval is accumulated in the virtual channel and led to the river basin outlet.

2) Forcing Data

Meteorological atmospheric forcing data required by the WEB-DHM model are listed in Table 4.1.3-1. For rainfall alone, observed daily records were used. For other parameters such as temperature, surface pressure, wind speed, and specific humidity, data from the Japanese 25-year Reanalysis (JRA-25) and Japan Meteorological Agency (JMA) Climate Data Assimilation System (JCDAS) were used instead of real observations. For surface solar radiation parameters such as downward longwave and downward shortwave radiation, values were estimated using sunshine duration, air temperature, and relative humidity from JRA25. Equations for parameter estimations were based on Yang et al. (2006), Yang et al. (2001), and Todd and Claude (1998).

Table 4.1.3-1 Atmospheric forcing data

CHAPTER 4 CLIMATE CHANGE IMPACT ASSESSMENT AND HYDROLOGICAL SIMULATION

| Name | Data source | Time resolution |
|------------------------------|---|-----------------|
| Rainfall | Observed record at 49 stations | Daily |
| Temperature | JRA25 reanalysis with altitude correction | 6-hourly |
| Surface Pressure | JRA25 reanalysis with altitude correction | 6-hourly |
| Specific Humidity | JRA25 reanalysis | 6-hourly |
| Surface Wind | JRA25 reanalysis | 6-hourly |
| Downward longwave radiation | Estimated using JRA25 reanalysis | 6-hourly |
| Downward shortwave radiation | Evaluated using JRA25 reanalysis | Hourly |

4.1.4 Selection of Future Scenarios and Assessment

(1) Purpose

We have produced nine climate scenarios (nine ensemble projections) in the Brantas and Musi River basins by running hydrological model simulations with outputs of nine GCMs. In the next planning stage, other non-climatic social scenarios such as land-use changes or population changes will also be introduced to assess the climate change risk in various sectors. Therefore, if we use all the simulated climate scenarios together with possible social scenarios, the number of total combinations will be large. For the practical purpose of this study, considering all the combinations it is not feasible because of time, costs, and technical constraints. On the other hand, it is also not realistic to select one climate scenario, as climate predictions include uncertainty and the range of uncertainty could lead to a large variation in future water management planning. Plans should be based on the most likely range of change and should be flexible and adaptable to uncertain futures. Therefore, we selected a set of three scenarios listed below:

- High scenario (at the upper end of the likely range of future climate predictions):
- Medium scenario (central estimate of future climate predictions):
- Low scenario (at the low end of the likely range of future climate predictions).

The Medium Scenario describes the central estimate of the future, while the High and the Low scenarios describe the upper and the lower boundaries of possible futures respectively (see Figure 4.1.4-1).

The set of three scenarios are selected separately depending on the purpose of planning. For this study, the following two planning purposes were considered:

- Water resources management planning:
- Flood risk management planning.

CHAPTER 4 CLIMATE CHANGE IMPACT ASSESSMENT AND HYDROLOGICAL SIMULATION

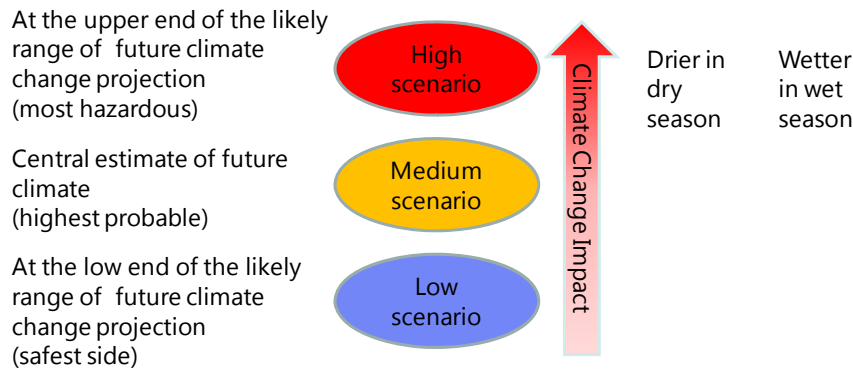


Figure 4.1.4-1 Set of three future scenarios

(2) Methodology

1) Box plot

A box plot was used to select the three scenarios. Box plots are one of several useful ways of graphically depicting ranges of distributions and identifying outliers. It is a nonparametric method. That means a box plot diagram displays variation in samples of a statistical population without making any assumptions of the underlying statistical distribution. Therefore, it is suitable when the number of samples is too small to apply a statistical distribution. In this study, the number of ensembles is only nine (we selected nine GCMs), so it is feasible to use a box plot instead of applying a statistical distribution.

The schematic image of a box plot is shown in Figure 4.1.4-2. The red line shows the median value and the blue dots show the mean value. The width of the box shows the spread of the models, the range of the 1st and 3rd quartiles. The upper and lower black lines show the highest and lowest values and the blue crosses represent the outliers, very different from all the other models. The box includes 50% of the samples.

The median value can be regarded as the Medium scenario, and the 1st and 3rd quartile can be regarded as High and Low scenarios respectively.

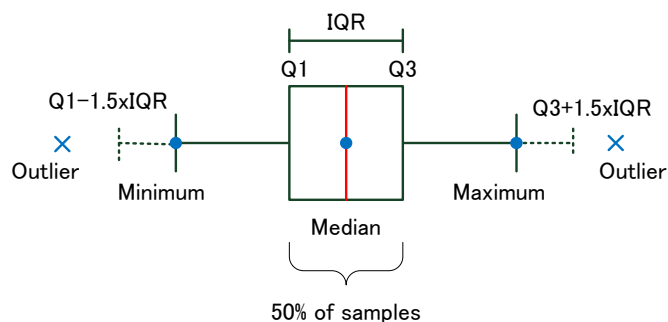


Figure 4.1.4-2 Schematic image of box plot

CHAPTER 4 CLIMATE CHANGE IMPACT ASSESSMENT AND HYDROLOGICAL SIMULATION

1) Future Scenario Selection for Water Resources Management

a) Indicator

Indicator was selected based on a discussion with the team for “Water Resources Management Plan”. In the stage of developing the water resources management plan, the most important indicator is the change in the basin’s low flow conditions. Therefore, the total discharge in dry season (June through October) and the annual flow duration curve were selected as the indicators for selecting futures scenario for water resources management.

1) Future Scenario Selection for Flood Risk Management

a) Indicator

Indicators were selected based on a discussion with the team for “Water Resources Management Plan”. In the stage of developing the flood risk management plan, the most important indicator is the change in magnitude of the daily flood peak and its frequency. Therefore, changes in the magnitude of the flood peak in a given return period can be used as indicators of change in the flood regime. However, there are limitations in the simulated discharge extremes based on GCM outputs. There are considerable differences between the observed and modeled mean daily flood peaks (as we have seen in Figure 4.2.3-8), so it is difficult to apply frequency analysis to simulated discharges directly. Therefore, we applied frequency analysis for the maximum annual daily rainfall instead of river discharge. The methodology is listed below.

Steps for evaluating present/future flood conditions

1. Select a representative flood hydrograph from observed discharge (if available) or simulated discharge with observed rainfall.

<Evaluation for present flood conditions>

2. Calculate the magnitude of daily rainfall intensity for T-year return period using observed rainfall record.
3. Stretch/shorten the peak of rainfall, which corresponds to the peak flow of the hydrograph, and adjust it with the intensity of T-year return period. Simulated discharge with this rainfall series can be regarded as the present flood event with T-year return period.

<Evaluation for future flood conditions>

4. Calculate the magnitude of the daily rainfall intensity for several return periods using GCM present/future rainfall records. Then, calculate the change ratio (ratio between GCM present and GCM future).
5. Stretch the peak of the hyetograph produced in Step 3 by scaling it with the change ratio. Simulated discharge with this rainfall series can be regarded to the future flood event with T-year return period.

Finally, we determined six indicators for selecting future scenarios for flood condition: the change ratio (future/present) of annual maximum 1-day rainfall intensity of the 2-, 5-, 10-, 30 (25)-, 50-, and 100-year return period events.

CHAPTER 4 CLIMATE CHANGE IMPACT ASSESSMENT AND HYDROLOGICAL SIMULATION

4.2 Implementation of Rainfall-runoff Analysis Considering Climate Change Impact Assessment: Brantas River Basin

4.2.1 Overview of Targeted Basins

(1) Brantas River Basin

1) Basin Characteristics

The Brantas River is located in East Java Province on the island of Java in the Republic of Indonesia. The river originates at the southern slope of Mount Kawi-Kelud-Butak, and its course has a clockwise semicircular or spiral shape that eventually flows into Madura Strait. The Brantas River basin is the second largest basin on Java. The basin has about 11,800 km² of catchment area, and the river runs a total length of about 320 km. The main river separates into two, namely the Surabaya and Porong rivers, in the lower basin.

Surabaya, the second largest city in Indonesia, is located at the mouth of the Mas River and along the edge of the Madura Strait. Surabaya is a very important city in East Java in terms of Indonesia's economy, culture, and education. Based on the 2010 census¹, the estimated population of the city was 2,757,232.

Development of the Brantas River basin began in 1961. Based on a series of earlier master plans, a large number of development activities have been implemented for flood protection, irrigation, electricity, drinking and industrial water supplies, and other purposes benefitting people. There is no doubt that proper management of water resources and efficient flood control in the basin is vital for the prosperity and sustainable development of East Java. In this regard, understanding the impacts of climate change in the region is necessary and relevant, and timely adaptation measures can be taken to help maintain socioeconomic growth of the country.

Major river facilities are listed in Table 4.2.1-1 (see location map on page i of this report).

Table 4.2.1-1 Major river facilities in the Brantas River basin

| Dam | Weir / Barrage / Gate |
|-----------------------------|------------------------|
| Sengguruh Dam | Tulungagung Gate |
| Lahor Dam | Mrican Barrage |
| Sutami Dam (Karankates Dam) | Jatimlerek Barrage |
| Wlingi Dam | Menturus Barrage |
| Lodoyo Dam | New Lengkong Barrage |
| Wonorejo Dam | Mrilip Gate |
| Selorejo Dam | New Gunungsari Barrage |
| Bening Dam | |

¹ Surabaya City home page, <http://www.surabaya.go.id/files.php?id=2065> (accessed April 13, 2014)

CHAPTER 4 CLIMATE CHANGE IMPACT ASSESSMENT AND HYDROLOGICAL SIMULATION

2) Climate

The climate in the Brantas River basin is tropical climate with wick warm temperatures throughout the year and a significant amount of precipitation. Like other tropical areas, there are two seasons, a wet season (November through May) and dry season (June through October). Annual rainfall in out study area varies from 1,600 to 4,800 mm. The average temperature in the lowland area is almost constant around 25 °C through the year.

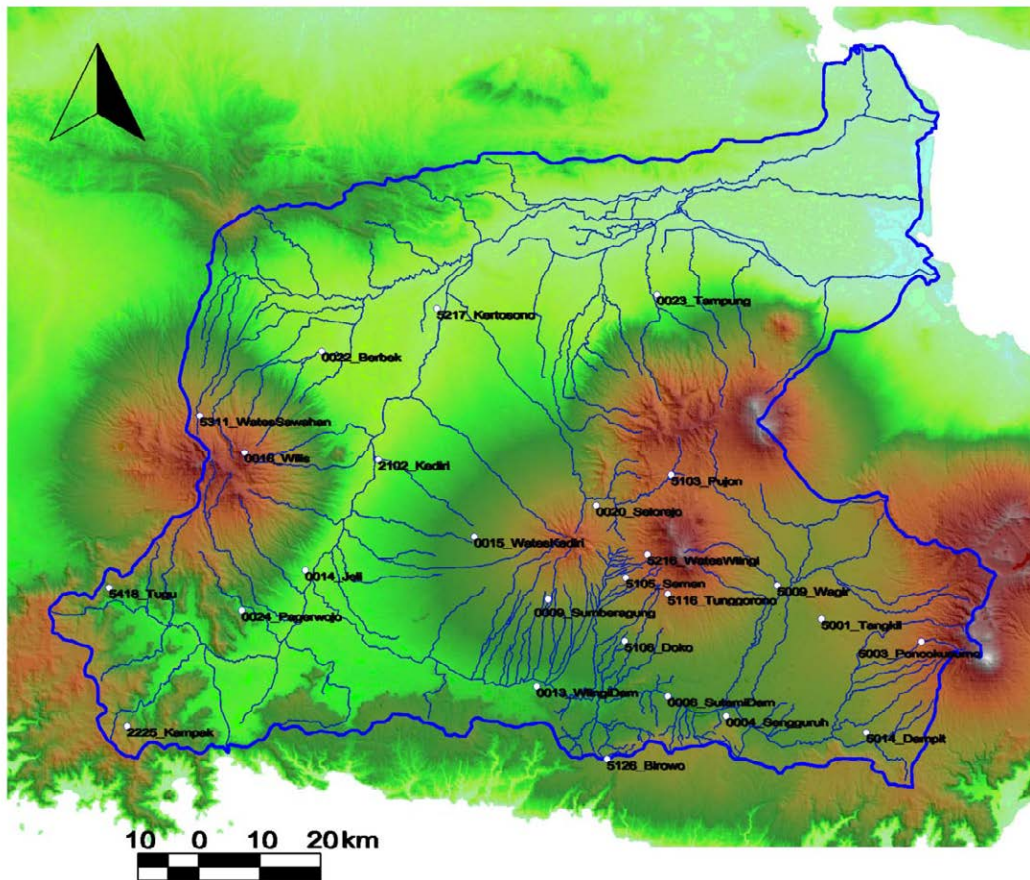
3) Observations and Data

a) Rainfall

The rainfall monitoring system was changed radically in 1991; the Jasa Tirta I Public Corporation (PJT-1) was established in 1990 and the rain gauge system in the Brantas River basin was reformed. Prior to 1990, the system was installed and managed by BMKG (Agency for Meteorology, Climatology and Geophysics). When the PJT-1 was established, the operation and management of all rain gauge stations was transferred to PJT-1. Availability of rainfall data for all stations is shown in Table 4.2.1-2 and information was based on daily rainfall data obtained from PJT-1. Some stations have daily rainfall records dating back to the 1950s. However, prior to 1991, data was recorded manually once per day at each station. After the system changed in 1991, instantaneous data has been recorded automatically. Aldrian and Djamil (2006) found an approximate 40% difference in monthly rainfall before and after 1991. This difference is mainly attributed to lack of accounting for daily evaporation prior to 1991.

Continuous daily rainfall data for at least 20 years is required for bias correction. Since there is a problem with consistency in rainfall data prior to 1991, stations with data after 1991 were selected for this study. A map of rain gauge stations used is shown in Figure 4.2.1-1. Details on the exact locations of the stations were unavailable, so the study team plotted estimated locations from a map in the operations room of the PJT-1 Malang office. Therefore, the locations shown in the figure may differ from the exact locations.

CHAPTER 4 CLIMATE CHANGE IMPACT ASSESSMENT AND HYDROLOGICAL SIMULATION

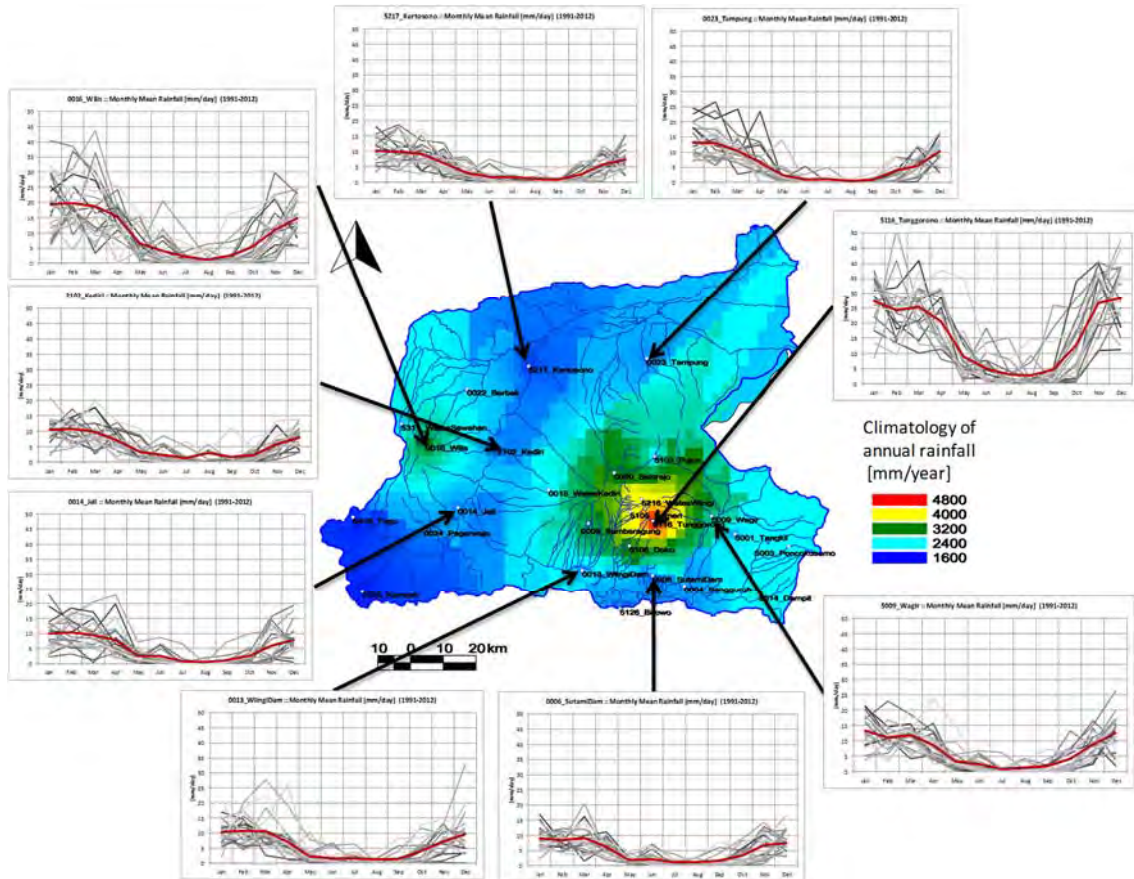


Source: JICA study team

Figure 4.2.1-1 Map of rainfall gauge stations used in the study (locations are estimated from a map in the operation room of the PJT-1 Malang office)

CHAPTER 4 CLIMATE CHANGE IMPACT ASSESSMENT AND HYDROLOGICAL SIMULATION

Figure 4.2.1-2 shows the climatology of annual and monthly rainfall under the present climate. The highest annual rainfall is about 4,800 mm/year, around Mount Arjuna and Mount Butak. Most of the area has an annual rainfall of over 2,000 mm/year.



Source: JICA study team

Figure 4.2.1-2 Climatology of annual and monthly rainfall under present climate from 1991 to 2010 in Brantas River Basin

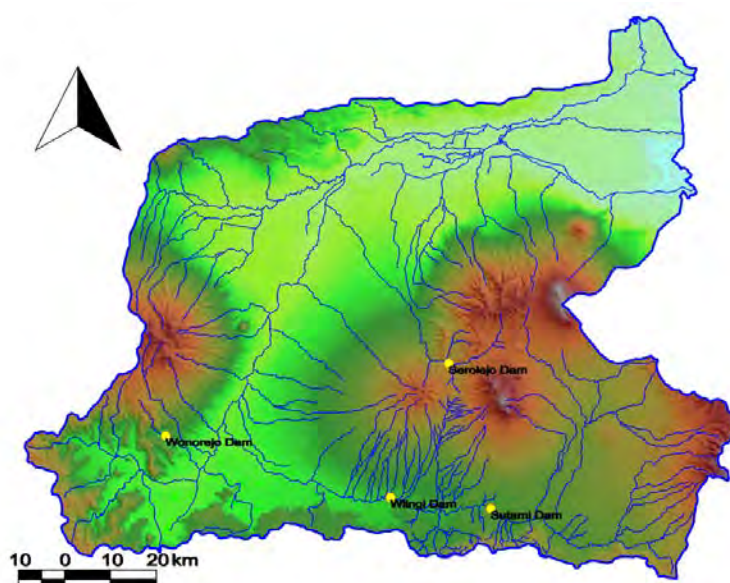
b) Temperature

Surface air temperature is a key observed variable for the evaluation of evapotranspiration. Figure 4.2.1-3 shows locations of the temperature observation stations managed by PJT1. Station names and data availability are tabulated in Table 4.2.1-3. Locations for only the temperature observation stations in the southern part of the Brantas River basin are shown in the figure. It is difficult to evaluate the spatial distribution from the four stations. In addition, the periods of data availability is less than 10 years; it is insufficient to analyze climate conditions.

CHAPTER 4 CLIMATE CHANGE IMPACT ASSESSMENT AND HYDROLOGICAL SIMULATION

Table 4.2.1-3 List of air temperature observation stations from PJT-1 and periods of data availability

| Station Name | Data collection period for air temperature | Time resolution |
|--------------|--|-----------------|
| Sutami Dam | 2006 – 2011 | daily |
| Wlingi Dam | 2005 – 2012 | daily |
| Selorejo Dam | 2003 – 2012 | daily |
| Wonorejo Dam | 2003 – 2012 | daily |



Source: JICA study team

Figure 4.2.1-3 Location map of air temperature observation stations from PJT-1

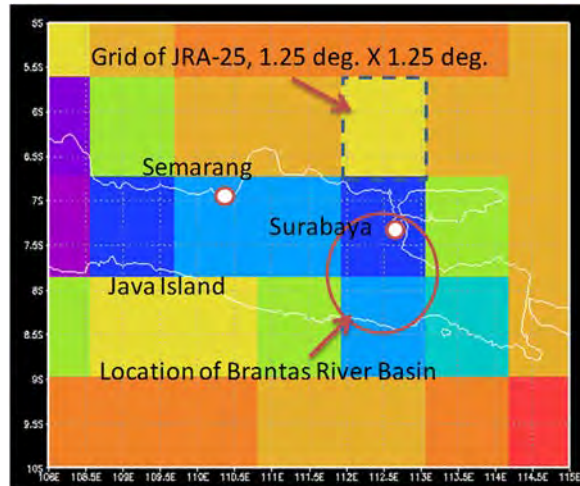
Because of the lack of data availability, the Japanese 25-year reanalysis product JRA-25 was used in this study. JRA-25 was obtained from the Japan Meteorological Agency (JMA) website.² The grid size of JRA-25 is 1.25 degrees in latitude and longitude, which is approximately 125 × 125 km. As shown in Figure 4.2.1-4, this grid size is too large to use directly in the study area. Therefore, an altitude correction was applied. The altitude correction assumes surface temperature decreases linearly with elevation, according to the lapse rate. The lapse rate was set as 0.005°C/m in this study. The correction procedure is described below:

- i. Normalize the JRA-25 grid value to an altitude of zero by applying the lapse rate.
- ii. Apply the spatial interpolation for the normalized grid value and make a fine grid.
- iii. Calculate surface temperature according to the fine elevation model grid by applying the lapse rate.

² JCDAS (JMA Climate Data Assimilation System) home page, http://jra.kishou.go.jp/JRA-25/index_en.html (accessed June 10, 2013)

CHAPTER 4 CLIMATE CHANGE IMPACT ASSESSMENT AND HYDROLOGICAL SIMULATION

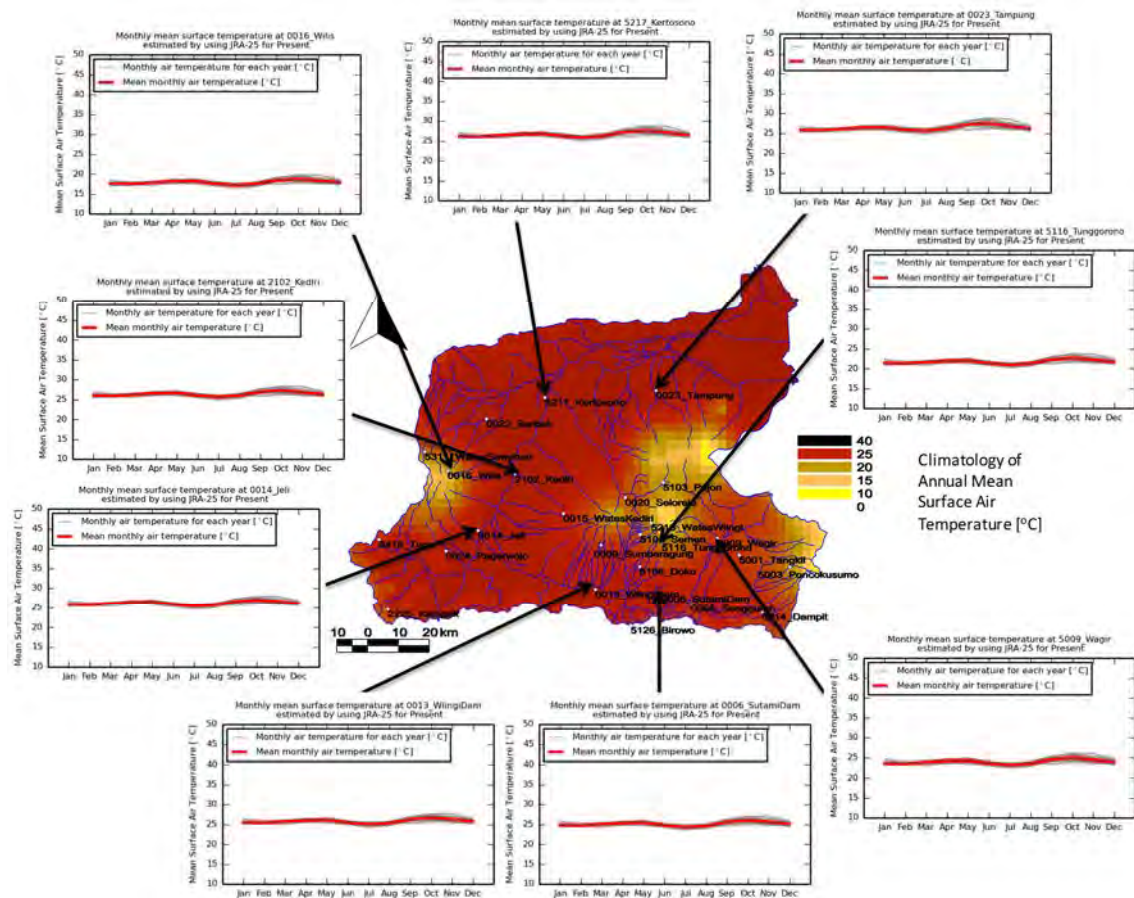
Monthly mean surface air temperatures at present conditions (1991 through 2010) were estimated for all grids in the Brantas River basin. Seasonal temperature changes at the observation stations and a map of the climatology of annual mean air temperatures are shown in Figure 4.2.1-5. Seasonal fluctuations of air temperatures in the Brantas River basin are about 2-3°C. The annual mean value is about 25°C in most of the study area.



Source: JICA study team

Figure 4.2.1-4 Comparison of size between grid size of JRA-25, island of Java, and target area

CHAPTER 4 CLIMATE CHANGE IMPACT ASSESSMENT AND HYDROLOGICAL SIMULATION



Source: JICA study team

Figure 4.2.1-5 Climatology of annual mean surface air temperature distribution estimated by altitude correction of JRA-25 for 1991–2010. Seasonal fluctuation charts for major observation stations were estimated from altitude-corrected JRA-25 grid data, not observed data.

c) Groundwater

Groundwater was monitored by ESDM (Kementarian Energi Dan Sumber Daya Mineral), from which observed groundwater level data was obtained. Observation wells for which we acquired monitoring data are listed in Table 4.2.1-4. Figure 4.2.1-6 provides a location map of the observation wells and charts of groundwater level fluctuation. Note that the observed periods of each chart in the figure are different.

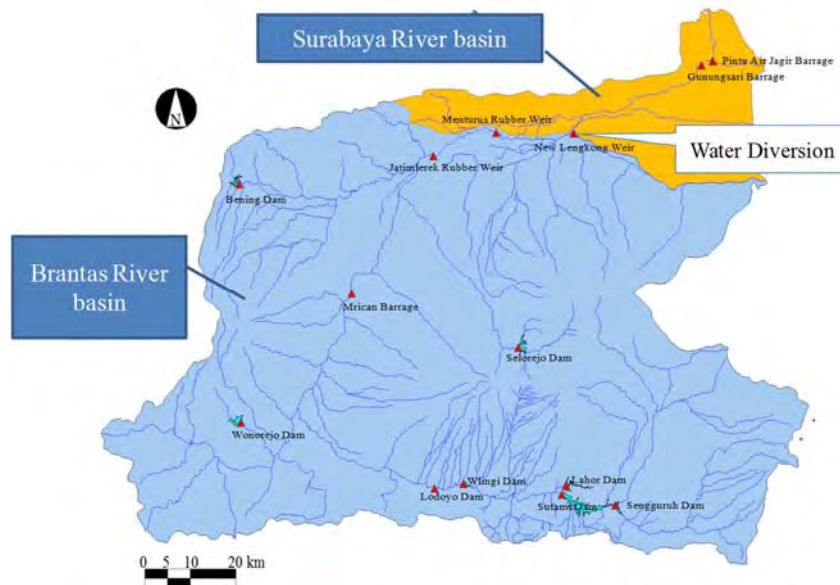
According to Figure 4.2.1-6, groundwater levels fluctuated seasonally in a range of 4-5 m in the lowlands along the main river channel. Most observation wells are in this lowland area along the river channels, where the groundwater level is shallow and near the ground. The seasonal change of rainfall amounts is a major reason for such seasonal fluctuations in groundwater levels. Another important reason is artificial water use, especially groundwater abstraction. It is difficult to remove such artificial effects from the observed groundwater level fluctuations.

The observed groundwater level data was used as a reference for parameter calibration of the

CHAPTER 4 CLIMATE CHANGE IMPACT ASSESSMENT AND HYDROLOGICAL SIMULATION

d) Topology

Figure 4.2.1-7 shows two river basins in the target area. At the New Lengkong barrage, water from the Brantas River diverted into the Surabaya River. The Water and Energy Budget-based Distributed Hydrological Model (WEB-DHM) was developed separately for these two river basins (Brantas and Surabaya River basins). The total area of the Brantas River basin is around 11,000 km² and that of the Surabaya is about 1,100 km².



Source: JICA study team

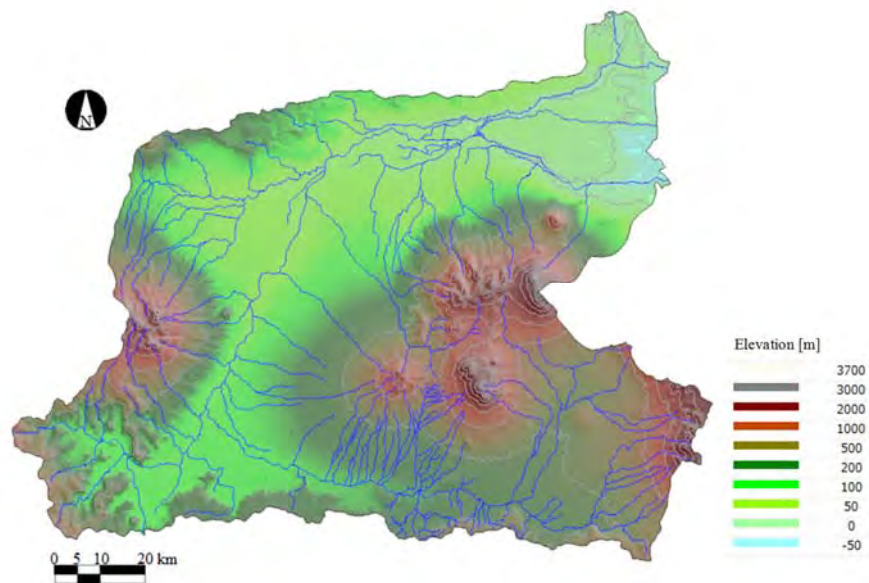
Figure 4.2.1-7 Brantas and Surabaya River basins

The HydroSHEDS Digital Elevation Model (DEM) is used to define the study area. HydroSHEDS is based on the Shuttle Radar Topography Mission (SRTM) dataset. No-data voids in the original SRTM dataset were filled using interpolation, and data was clipped at the ocean shoreline. The finest DEM resolution is 3 arc-second (about 90 m).

To use the DEM data in the runoff model, data of the original geographic coordinate system was projected into the Universal Transverse Mercator coordinate system (UTM), zone 49 South. The grid was re-sampled to 500-m size in the projection process. The re-sampled DEM data of the basin is shown in Figure 4.2.1-8. Elevation in the Brantas River basin varies from 0 m in the lower reach to around 3,600 m in mountainous areas.

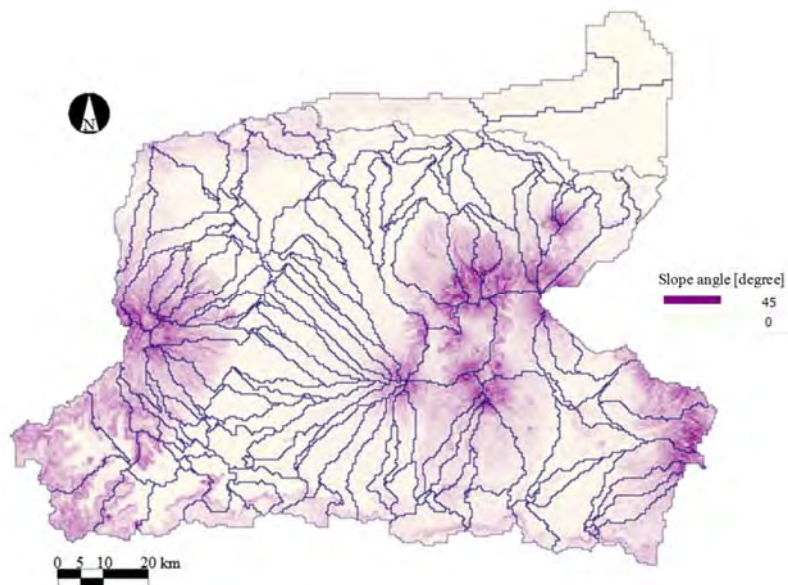
Next, the target basin was divided into smaller sub-basins. The Pfafstetter system, which performs this function on a main basin automatically, was not used. This is because the many dams and other facilities in the Brantas River basin make it difficult to divide sub-basins appropriately using that system. The numbers of flow intervals in a particular cell of WEB-DHM was specified for time lag and concentration processing in the river network according to distance to the sub-basin outlet. The divided sub-basins with distribution of hill-slope angle are shown in Figure 4.2.1-9.

CHAPTER 4 CLIMATE CHANGE IMPACT ASSESSMENT AND HYDROLOGICAL SIMULATION



Source: JICA study team for the HydroSHEDS datasets

Figure 4.2.1-8 Elevation in the Brantas River basin



Source: JICA study team for the HydroSHEDS datasets

Figure 4.2.1-9 Sub-basins with distribution of hill slope angle in the Brantas River basin

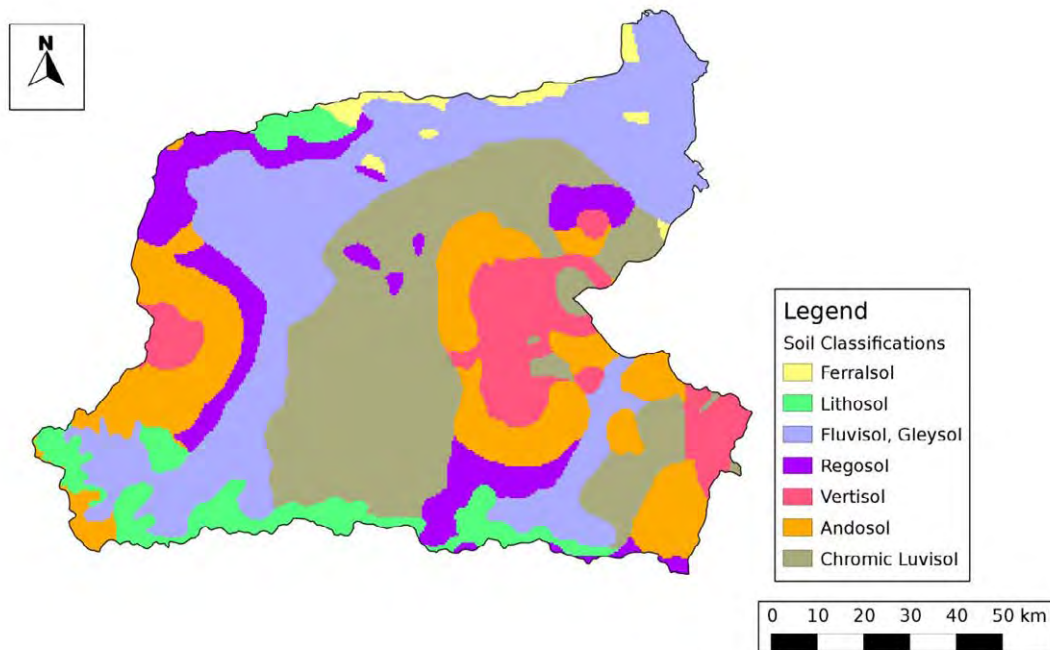
CHAPTER 4 CLIMATE CHANGE IMPACT ASSESSMENT AND HYDROLOGICAL SIMULATION

e) Soil Parameters

Local soil data provided by BBWS (Large River Basin Organization) Brantas were used for establishing soil parameters. Their classification was converted into those of the Food and Agriculture Organization (FAO) by overlaying the FAO soil map on the local map, as shown in Table 4.2.1-5. Soil parameters were based on intrinsic properties of each soil type taken from the FAO global dataset. Figure 4.2.1-10 shows the distribution of soil types as defined by the FAO classifications.

Table 4.2.1-5 Soil classification

| Soil Classification | | | coverage [%] |
|---|---------------|-------------------|--------------|
| Local Soil Classification | FAO soil code | Soil Class (FAO) | Brantas |
| Aluvial (Alluvium) | 4518 | Fluvisol, Gleysol | 23.5 |
| Andosol NCB Soil (Non-calcic Brown soil) | 4576 | Andosol | 18.6 |
| Grumosol (Grumusol) | 4573 | Vertisol | 10.1 |
| Latosol | 4490 | Ferralsol | 0.4 |
| Litosol (Lithosol) | 4509 | Lithosol | 7.5 |
| Mediteran (Mediterranean reddish brown soil, Terra rossa) | 4580 | Chromic Luvisol | 29.7 |
| Regosol | 4570 | Regosol | 10.2 |



Source: JICA study team for the BBWS Brantas and FAO datasets

Figure 4.2.1-10 Distribution of soil types for runoff simulations with FAO classification

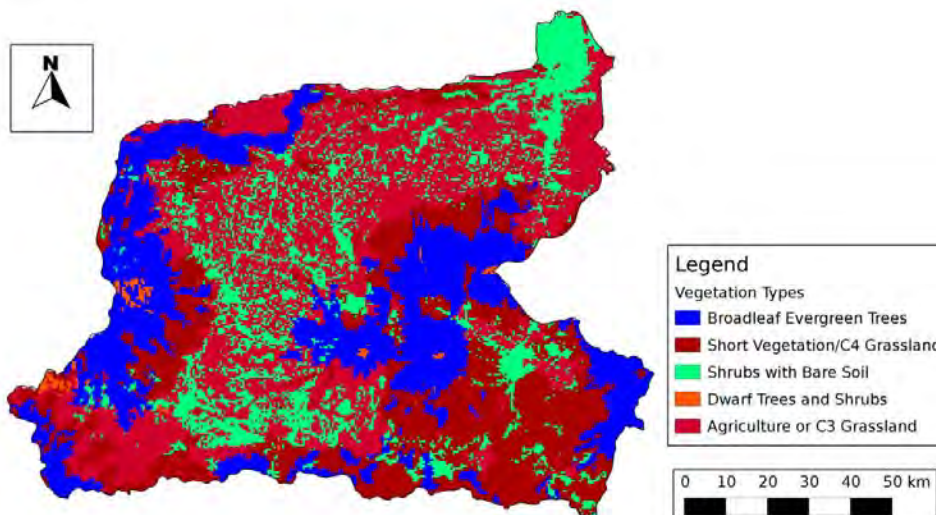
CHAPTER 4 CLIMATE CHANGE IMPACT ASSESSMENT AND HYDROLOGICAL SIMULATION

f) Vegetation Parameters

Local vegetation and land-use data provided by Ministry of Public Works (PU) were used for establishing vegetation parameters. The data was reclassified within the Simple Biosphere 2 (SiB2) model by overlaying the SiB2 land-use map on the local map. Table 4.2.1-6 shows the vegetation classifications and Figure 4.2.1-11 shows the distribution using SiB2 classifications.

Table 4.2.1-6 Vegetation classification

| No | Local Vegetation and Landuse Classification | | SiB2 Reclassification | coverage [%] |
|----|---|---|---------------------------------|--------------|
| | Indonesian | English | | Brantas |
| 1 | Perkebunan Hutan Lahan Kering Hutan Alam | Plantation Dryland Forests Natural Forests | 1-Broadleaf Evergreen Trees | 25.9 |
| 6 | Tegalan/Ladang | Moorland | 6-Short vegetation/C4 grassland | 25.3 |
| 7 | Permukiman Tambak/Empang Rawa Danau/Waduk/Situ | Settlement Dam/ Ponds Swamp Lake / Reservoir | 7-Shrubs with bare soil | 15.2 |
| 8 | Tanah Terbuka Semak/Belukar Mangrove Rawa | Open Land Bush / Shrub Mangrove | 8-Dwarf trees and Shrubs | 0.7 |
| 9 | Sawah Kebun Campuran | Rice field Mixed Garden | 9-Agriculture or C3 Grasslands | 32.9 |



Source: JICA study team with the PU

Figure 4.2.1-11 Distribution of vegetation classifications for runoff simulation with SiB2 classifications

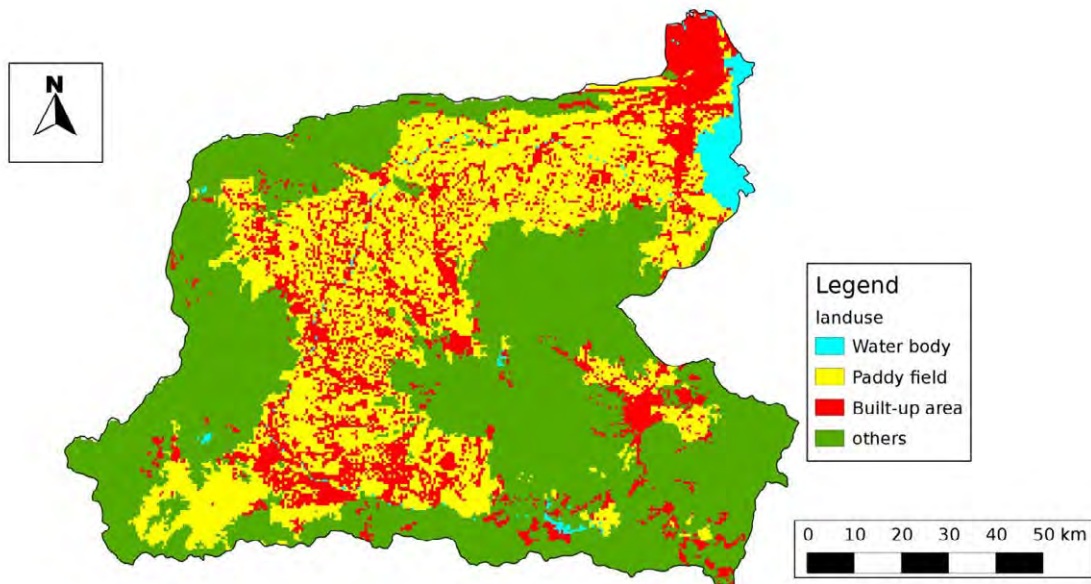
g) Land-use Parameters

The same local vegetation and land-use data used for vegetation parameters was applied to the establishment of land-use parameters. Local land use was classified into four types, i.e., body of water (dams, rivers, lakes, swamps and fish ponds), paddy field, built-up area, and other (e.g., forest and bush). According to these types, some model parameters were defined, such as the depression storage depth and equivalent roughness coefficient.

Table 4.2.1-7 shows the land-use classification and Figure 4.2.1-12 shows the distribution of land-use classified into four types.

Table 4.2.1-7 Land-use classification

| ID | Landuse Type | coverage |
|----|---------------|-------------|
| | | Brantas [%] |
| 1 | waterbody | 0.8 |
| 2 | paddyfield | 29.3 |
| 3 | Built up area | 14.8 |
| 4 | others | 55.1 |



Source: JICA study team with PU

Figure 4.2.1-12 Distribution of land-use types with runoff simulations

CHAPTER 4 CLIMATE CHANGE IMPACT ASSESSMENT AND HYDROLOGICAL SIMULATION

h) LAI and FPAR

The leaf area index (LAI), which is an important structural property of a plant canopy, is defined as one-sided green leaf area per unit ground surface area. In other words, LAI is the ratio of total upper leaf surface of vegetation divided by the surface area of the land on which the vegetation grows. LAI is a dimensionless value, typically ranging from zero (for bare ground) to six (for dense forest). The Fraction of Photosynthetically Active Radiation (FPAR) measures the proportion of available radiation in the photosynthetically-active wavelength band (400 to 700 nm) that a canopy absorbs. LAI and FPAR are biophysical variables that describe canopy structure and are derived from satellite data such as those from the Moderate Resolution Imaging Spectroradiometer (MODIS) and Advanced Very High Resolution Radiometer (AVHRR), which are provided by the National Aeronautics and Space Administration (NASA).

i) River Flow

The Planning and Controlling Unit of the Jasa Tirta I Public Corporation (PJT-1) is responsible for collecting hydrometeorological data in the Brantas River basin. Various types of data such as river discharge, river water level, dam inflow and outflow, irrigation water supply, and return flows are available for the basin. The following table shows the availability of hydrologic data in the basin and Figure 4.2.1-13 shows a location map.

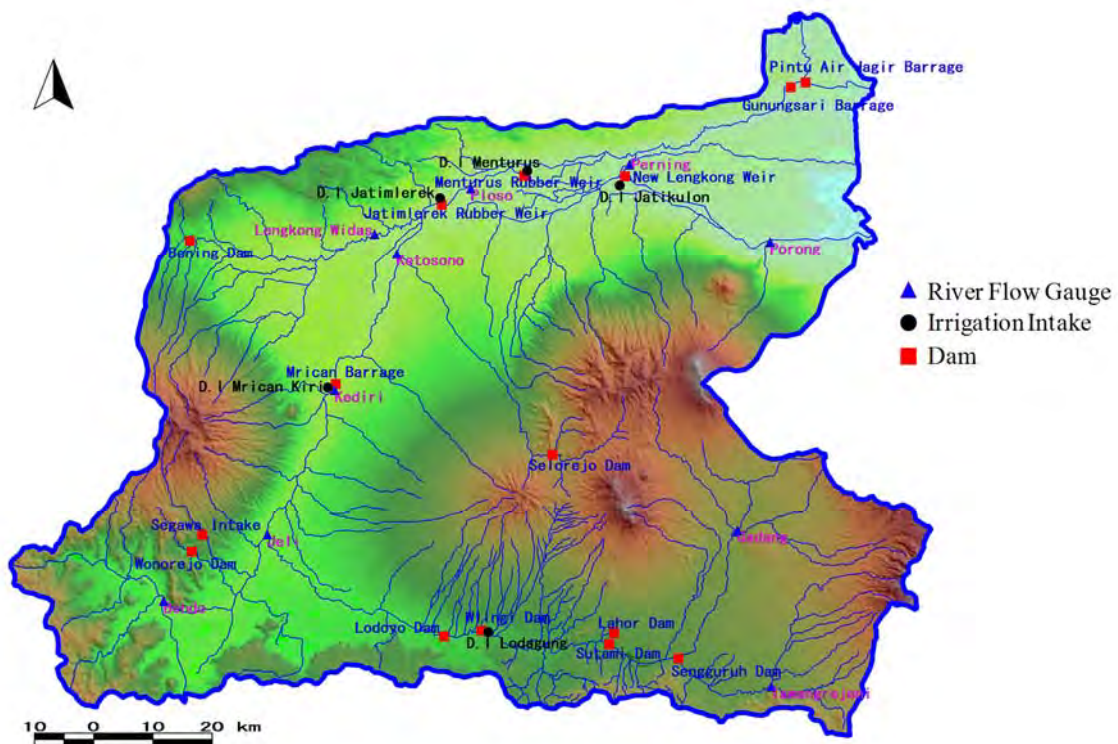
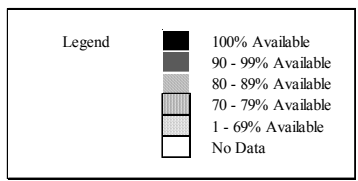


Figure 4.2.1-13 Flow measuring locations in the Brantas River basin

CHAPTER 4 CLIMATE CHANGE IMPACT ASSESSMENT AND HYDROLOGICAL SIMULATION

Table 4.2.1-8 Availability of hydrologic data in Brantas River basin

| Type | Name | Year | | | | | | | | | | | | | | | | | | | | | | | | | | | | | | | | | | |
|--------------|---------------------|------|------|------|------|------|------|------|------|------|------|------|------|------|------|------|------|------|------|------|------|------|------|------|------|------|------|------|------|------|------|------|------|--|--|--|
| | | 1981 | 1982 | 1983 | 1984 | 1985 | 1986 | 1987 | 1988 | 1989 | 1990 | 1991 | 1992 | 1993 | 1994 | 1995 | 1996 | 1997 | 1998 | 1999 | 2000 | 2001 | 2002 | 2003 | 2004 | 2005 | 2006 | 2007 | 2008 | 2009 | 2010 | 2011 | 2012 | | | |
| River Flow | H Bendo | | | | | | | | | | | | | | | | | | | | | | | | | | | | | | | | | | | |
| | H Gadang | | | | | | | | | | | | | | | | | | | | | | | | | | | | | | | | | | | |
| | H Jeli | | | | | | | | | | | | | | | | | | | | | | | | | | | | | | | | | | | |
| | H Kediri rev1 | | | | | | | | | | | | | | | | | | | | | | | | | | | | | | | | | | | |
| | H Kertosono rev1 | | | | | | | | | | | | | | | | | | | | | | | | | | | | | | | | | | | |
| | H Perning | | | | | | | | | | | | | | | | | | | | | | | | | | | | | | | | | | | |
| | H Ploso | | | | | | | | | | | | | | | | | | | | | | | | | | | | | | | | | | | |
| | H Porong | | | | | | | | | | | | | | | | | | | | | | | | | | | | | | | | | | | |
| | H Tawangrejeni | | | | | | | | | | | | | | | | | | | | | | | | | | | | | | | | | | | |
| H Widas | | | | | | | | | | | | | | | | | | | | | | | | | | | | | | | | | | | | |
| Dam Inflow | Wilingi | | | | | | | | | | | | | | | | | | | | | | | | | | | | | | | | | | | |
| | Wonokromo | | | | | | | | | | | | | | | | | | | | | | | | | | | | | | | | | | | |
| | Tulungagung Selatan | | | | | | | | | | | | | | | | | | | | | | | | | | | | | | | | | | | |
| | Tiudan | | | | | | | | | | | | | | | | | | | | | | | | | | | | | | | | | | | |
| | Sutami | | | | | | | | | | | | | | | | | | | | | | | | | | | | | | | | | | | |
| | Sengguruh | | | | | | | | | | | | | | | | | | | | | | | | | | | | | | | | | | | |
| | Segawe | | | | | | | | | | | | | | | | | | | | | | | | | | | | | | | | | | | |
| | NewLengkong | | | | | | | | | | | | | | | | | | | | | | | | | | | | | | | | | | | |
| | Mrican | | | | | | | | | | | | | | | | | | | | | | | | | | | | | | | | | | | |
| | Lodoyo | | | | | | | | | | | | | | | | | | | | | | | | | | | | | | | | | | | |
| | Lahor | | | | | | | | | | | | | | | | | | | | | | | | | | | | | | | | | | | |
| | Jagir | | | | | | | | | | | | | | | | | | | | | | | | | | | | | | | | | | | |
| | Gunungsari | | | | | | | | | | | | | | | | | | | | | | | | | | | | | | | | | | | |
| Gubeng | | | | | | | | | | | | | | | | | | | | | | | | | | | | | | | | | | | | |
| Wonorejo | | | | | | | | | | | | | | | | | | | | | | | | | | | | | | | | | | | | |
| Dam outflow | Gubeng | | | | | | | | | | | | | | | | | | | | | | | | | | | | | | | | | | | |
| | Wonokromo | | | | | | | | | | | | | | | | | | | | | | | | | | | | | | | | | | | |
| | Wonorejo | | | | | | | | | | | | | | | | | | | | | | | | | | | | | | | | | | | |
| | Wilingi | | | | | | | | | | | | | | | | | | | | | | | | | | | | | | | | | | | |
| | Tulungagung Selatan | | | | | | | | | | | | | | | | | | | | | | | | | | | | | | | | | | | |
| | Sutami | | | | | | | | | | | | | | | | | | | | | | | | | | | | | | | | | | | |
| | Sengguruh | | | | | | | | | | | | | | | | | | | | | | | | | | | | | | | | | | | |
| | Segawe | | | | | | | | | | | | | | | | | | | | | | | | | | | | | | | | | | | |
| | Segawe ke Tunnel | | | | | | | | | | | | | | | | | | | | | | | | | | | | | | | | | | | |
| | New Lengkong | | | | | | | | | | | | | | | | | | | | | | | | | | | | | | | | | | | |
| | Mrican | | | | | | | | | | | | | | | | | | | | | | | | | | | | | | | | | | | |
| | Mlirip | | | | | | | | | | | | | | | | | | | | | | | | | | | | | | | | | | | |
| | Lodoyo | | | | | | | | | | | | | | | | | | | | | | | | | | | | | | | | | | | |
| Lahor | | | | | | | | | | | | | | | | | | | | | | | | | | | | | | | | | | | | |
| Kanal Tiudan | | | | | | | | | | | | | | | | | | | | | | | | | | | | | | | | | | | | |
| Jagir | | | | | | | | | | | | | | | | | | | | | | | | | | | | | | | | | | | | |
| Gunungsari | | | | | | | | | | | | | | | | | | | | | | | | | | | | | | | | | | | | |
| Irrigation | Mrican Kanan | | | | | | | | | | | | | | | | | | | | | | | | | | | | | | | | | | | |
| | Menturus | | | | | | | | | | | | | | | | | | | | | | | | | | | | | | | | | | | |
| | Lodagung(Wilingi) | | | | | | | | | | | | | | | | | | | | | | | | | | | | | | | | | | | |
| | Jatimlerek | | | | | | | | | | | | | | | | | | | | | | | | | | | | | | | | | | | |
| | Jatikulon | | | | | | | | | | | | | | | | | | | | | | | | | | | | | | | | | | | |
| | Delta Brantas | | | | | | | | | | | | | | | | | | | | | | | | | | | | | | | | | | | |
| Mrican Kiri | | | | | | | | | | | | | | | | | | | | | | | | | | | | | | | | | | | | |



Some of the river discharge data was incomplete, but dam inflow/outflow and irrigation data (intake and return flow) was available at several locations for a period of 10 years (2003 to 2012). The natural flow, without any artificial flow control or diversions, is necessary for the water resources management study, therefore, we have developed the WE-DHM model without components for reservoir and irrigation water supplies (details in Section 4.2.3). The model simulates natural flows in the basin. To calibrate the model, it is necessary to construct a discharge dataset without such artificial controls (hereafter such flow is called “natural”). Even though observed river discharge records are available from 1981 to 1993 from some river gauging stations shown in Table 4.2.1-8, the natural flow

CHAPTER 4 CLIMATE CHANGE IMPACT ASSESSMENT AND HYDROLOGICAL SIMULATION

cannot be computed since artificial flow control data is unavailable for that period. Therefore, river flow data observed at river gauging stations was not used for model calibration. Instead, natural flow at seven locations shown in the schematic diagram of the Brantas River system (Figure 4.2.1-14) for the aforementioned 10-year period was calculated using available dam input/output data and irrigation water supply/return flow records. Because of limited availability, industrial water intake and discharge were not considered for natural flow computations. Then, the calculated natural flow at each location was used for calibrating WEB-DHM.

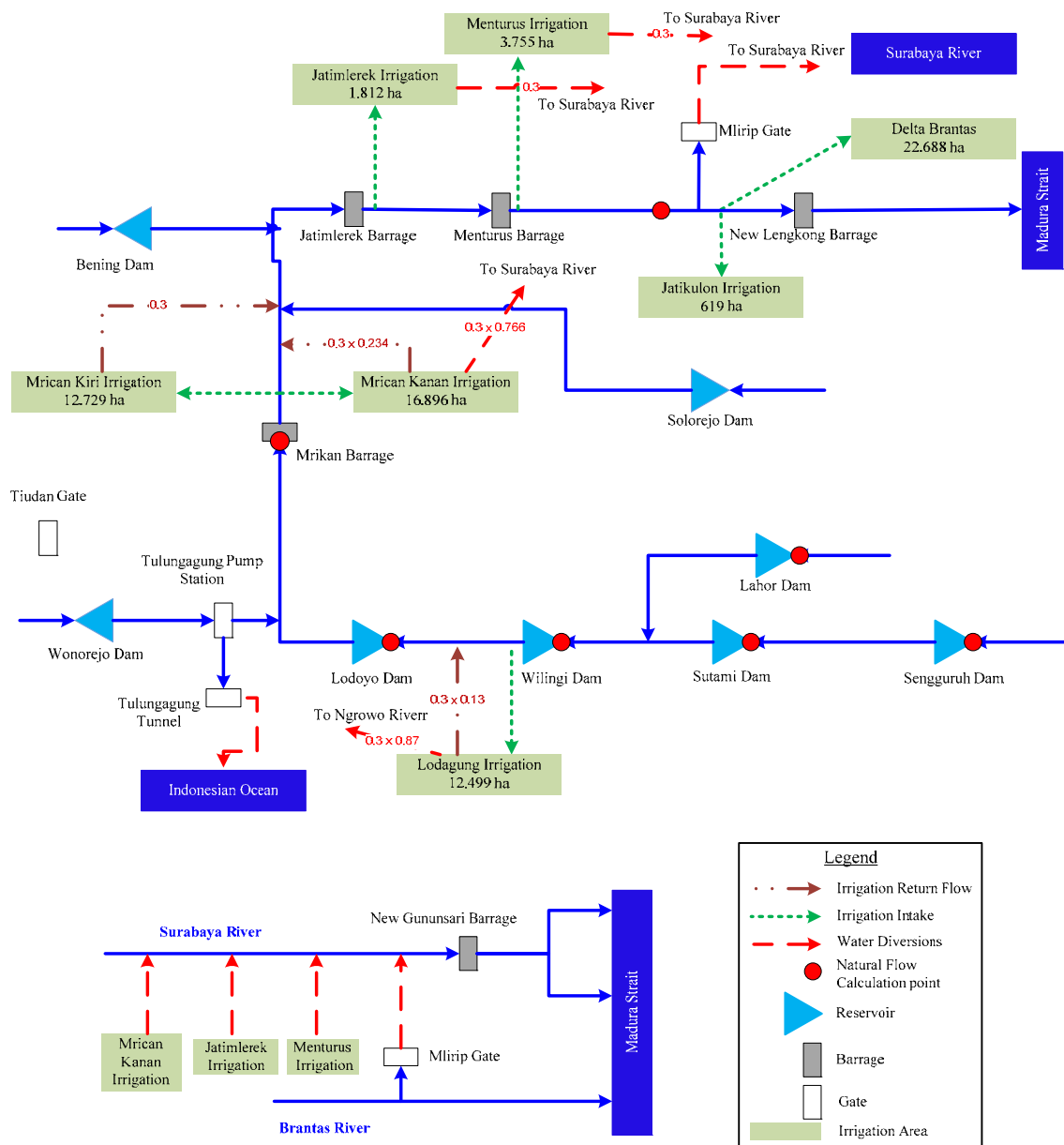


Figure 4.2.1-14 Schematic diagram of the Brantas and Surabaya River system

CHAPTER 4 CLIMATE CHANGE IMPACT ASSESSMENT AND HYDROLOGICAL SIMULATION

The equation used for calculating natural flow at New Lengkong Barrage $(NF_{Lengkong})_i$ is

$$(NF_{Lengkong})_i = (Q_{out})_i + \sum(Irr_{Supply})_i - \sum(Irr_{Return})_i + \sum(\nabla S)_i, \quad (4.2.1-1)$$

where $\sum(Irr_{Supply})_i$ is the sum of all upstream irrigation water supply; $\sum(Irr_{Return})_i$ is the sum of all irrigation return flow drained upstream of the New Lengkong Barrage; $\sum(\nabla S)_i$ is the sum of storage change in all upstream reservoirs; i is the corresponding natural flow calculation date. ∇S for each reservoir is calculated using inflow and outflow data of the corresponding reservoir. Return flow from each irrigation area is assumed to be 30% of irrigation water supply based on “The study on comprehensive management plan for the water resources on the Brantas River basin in the Republic of Indonesia (JICA, 1998)”.

The calculated natural flow and observed outflow at New Lengkong are shown below.

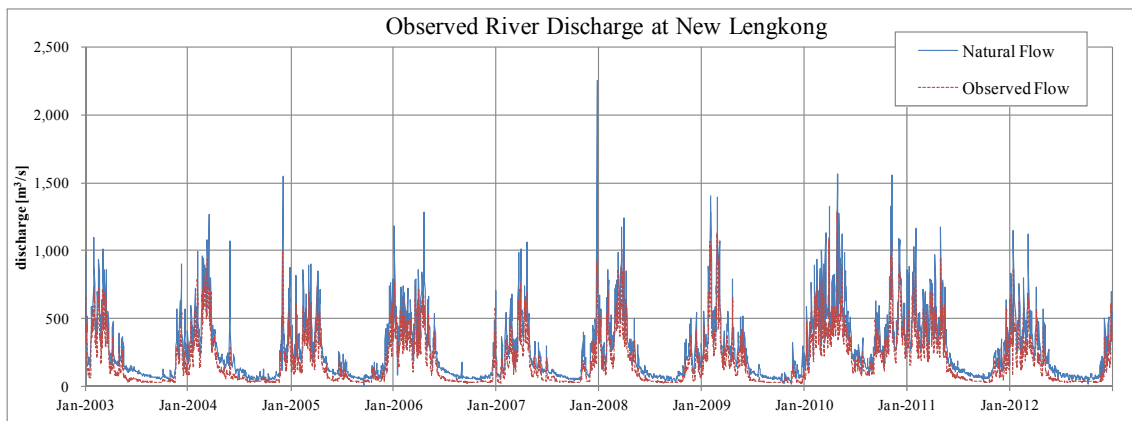


Figure 4.2.1-15 Observed flow and natural flow (calculated using observed dataset) at New Lengkong Barrage

Using a similar approach, natural flow at the other seven locations was calculated and used for WEB-DHM model calibration. Figure 4.2.1-15 shows observed flow and calculated natural flow at New Lengkong.

4.2.2 Climate Change Impact Assessment for Rainfall in the Brantas River Basin

(1) Results of Bias Correction

Based on the method described above, we collected bias in GCM-projected rainfall data using observed rainfall data for the 1991–2010 period. After bias correction, seasonal climatology and extremes of the bias-corrected data were validated against those of observed data.

CHAPTER 4 CLIMATE CHANGE IMPACT ASSESSMENT AND HYDROLOGICAL SIMULATION

1) Seasonality

Figure 4.2.2-1 compares average monthly rainfall of bias-corrected data and raw GCM data at the Sutami Dam rain gauge station. The result shows that bias of seasonal rainfall in the raw GCM data was effectively removed by the bias correction. Seasonal variability was captured very well in the bias-corrected rainfall.

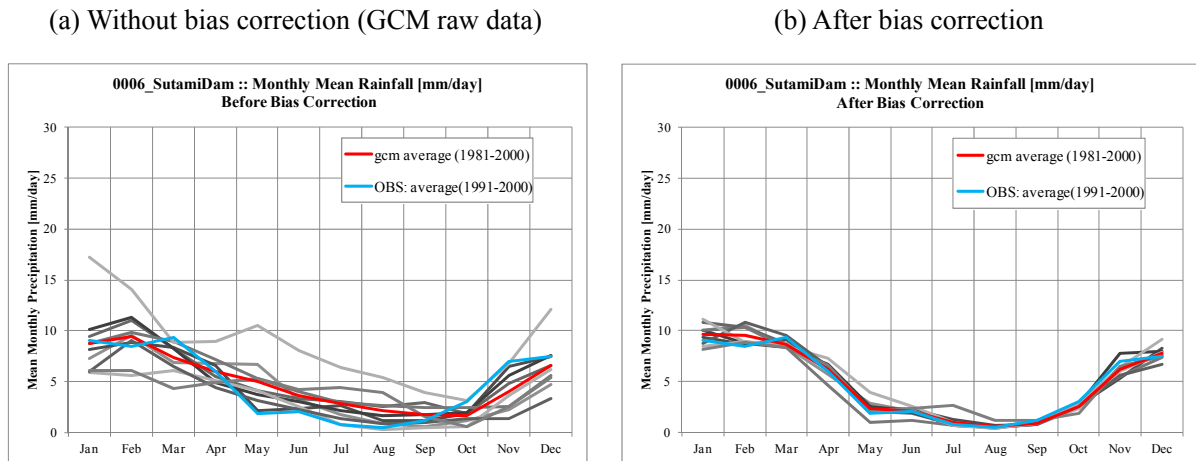


Figure 4.2.2-1 Comparison of monthly rainfall variation for (a) without bias correction (GCM raw data), (b) after bias correction at the Sutami Dam rain gauge station

2) Top 20

Figure 4.2.2-2 compares the top 20 of 20-year daily rainfalls of bias-corrected data and raw GCM data at the Sutami Dam rain gauge station. The result shows that bias of extreme rainfall in the raw GCM data was effectively removed by the bias correction. Extreme rainfall variability was captured very well by the bias-corrected rainfall.

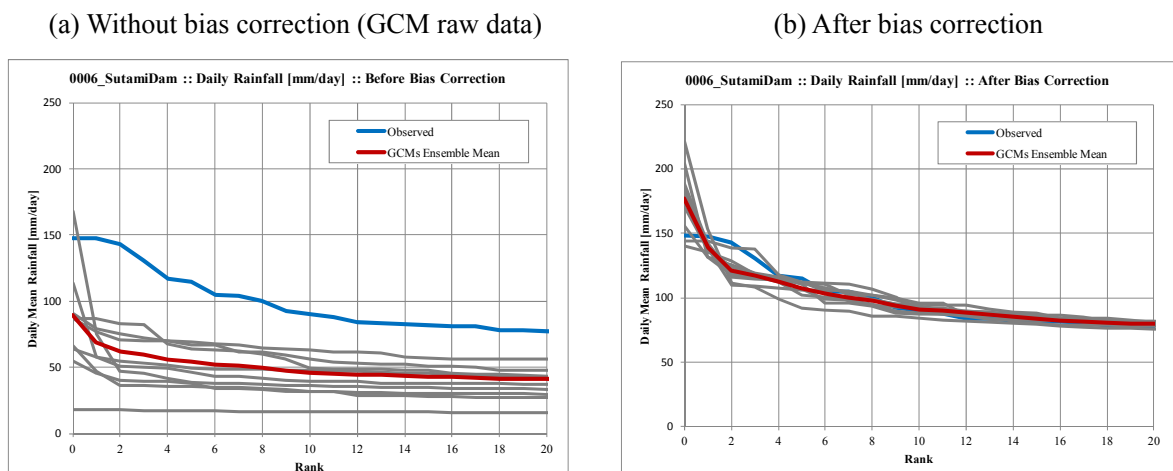
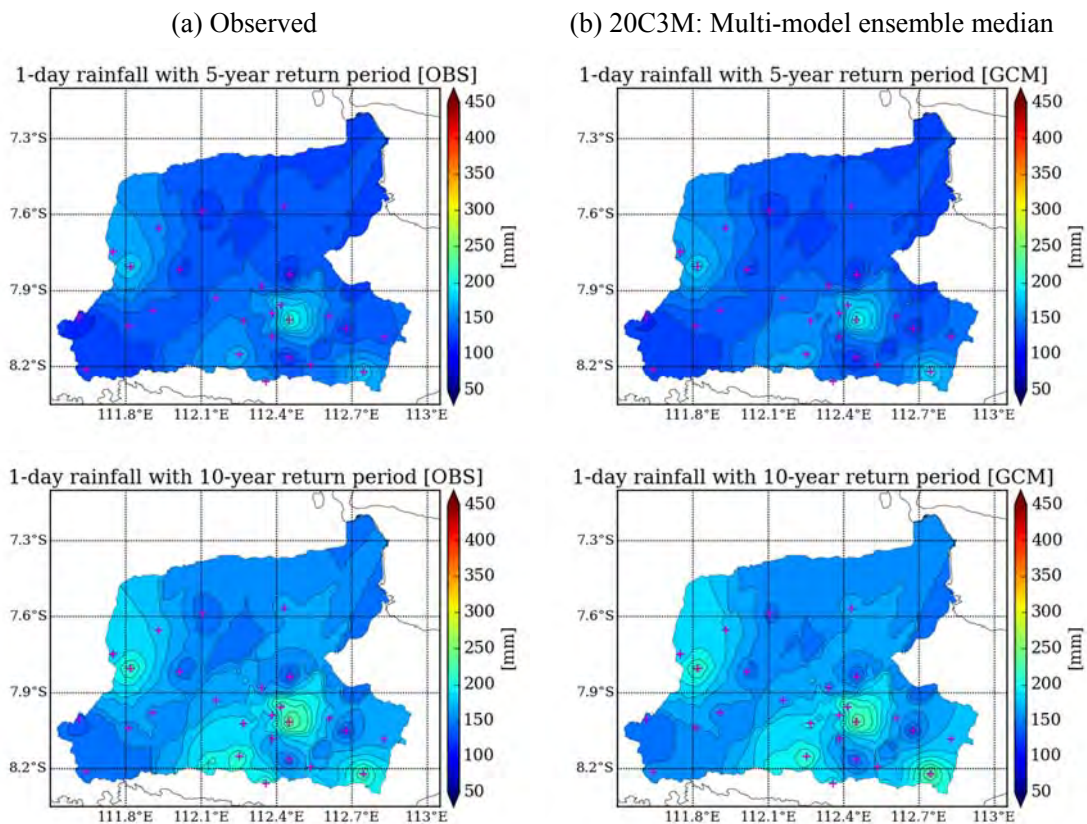


Figure 4.2.2-2 Comparison of top 20 of 20-year daily rainfalls for (a) without bias correction (GCM raw data), (b) after bias correction at the Sutami Dam rain gauge station

3) Return Periods

Annual maximum 1-day cumulative rainfall was extracted for each year and gauge station from the observed rainfall data and from the bias-corrected GCM rainfall data. Then, the generalized extreme value (GEV) distribution was fitted independently for each case, and we used the fitted distributions to calculate rainfall with five different return periods: 5-, 10-, 20-, 50- and 100-year. Finally, the rainfall values for each return period and gauge station were spatially interpolated and rainfall distribution maps were prepared for each return period. Figure 4.2.2-3 compares observed and bias-corrected GCM 1-day cumulative rainfall with the five return periods. According to the figures, the maps for 5-, 10-, 20- and 50-year return periods from the observed data match reasonably well with those from the bias-corrected GCM data. This furnishes evidence to prove that the bias correction is effective. However, the maps corresponding with the 100-year return period are somewhat different (Figure 4.2.2-4). There are several reasons for these differences:

- We used only 20 samples of annual maximum rainfall to fit the probability distribution, owing to lack of data. This may cause some errors in calculating extreme rainfalls with longer return periods.
- Limitations of the bias correction.



CHAPTER 4 CLIMATE CHANGE IMPACT ASSESSMENT AND HYDROLOGICAL SIMULATION

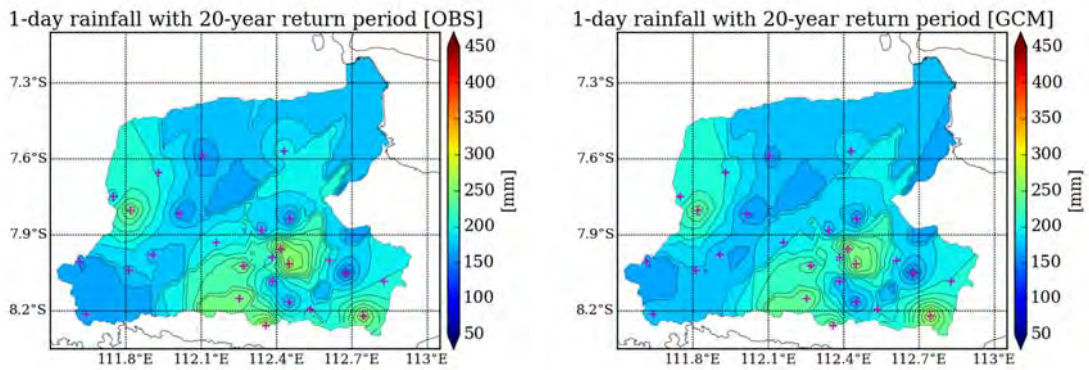


Figure 4.2.2-3 Comparison of 1-day rainfall with various return periods (observed vs. GCMs; 5-, 10-, 20-, 50- and 100-year). Red crosses show rainfall measuring locations. (Part 1)

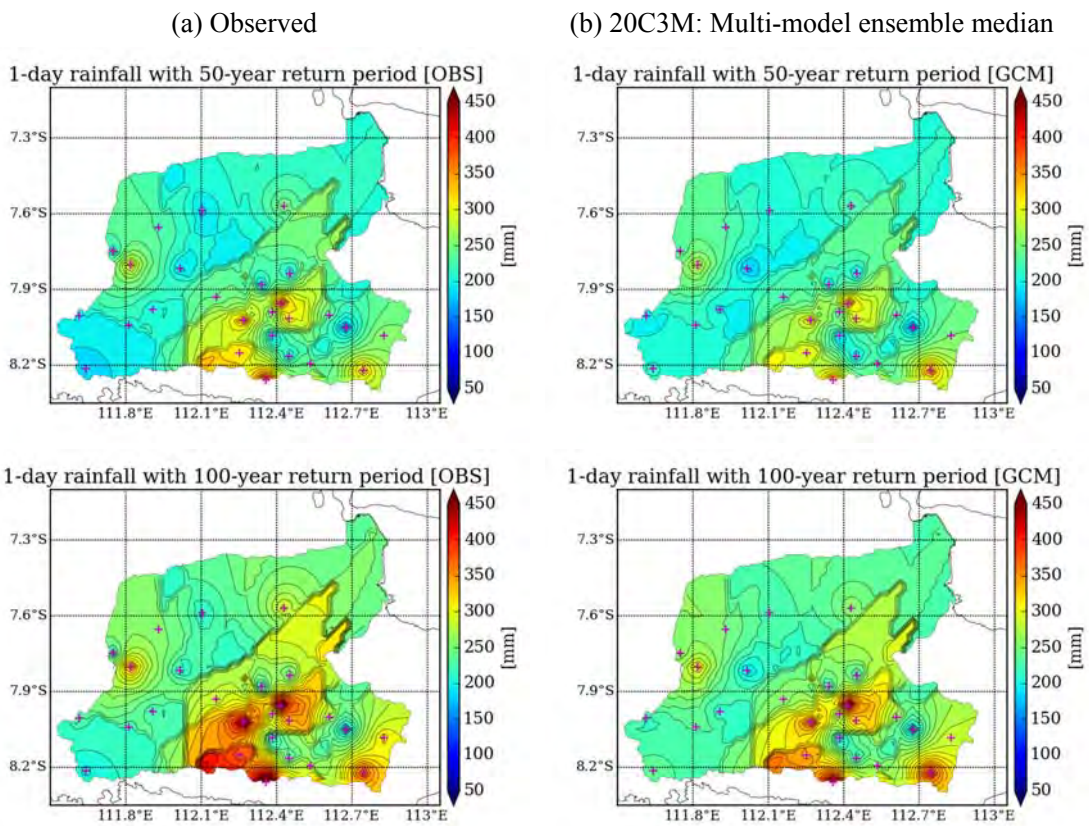


Figure 4.2.2-4 Comparison of 1-day rainfall with various return periods (observed vs. GCMs; 5-, 10-, 20-, 50- and 100-year). Red crosses show rainfall measuring locations. (Part 2)

(2) Changes of Rainfall

To analyze implications of climate change for annual, seasonal, and extreme rainfall in the Brantas River basin, we used bias-corrected and adjusted rainfall data from nine climate models for the following time-slice experiments.

CHAPTER 4 CLIMATE CHANGE IMPACT ASSESSMENT AND HYDROLOGICAL SIMULATION

- Present: 1981 through 2000
- Future: 2046 through 2065

1) Annual

Figure 4.2.2-5 shows annual mean changes of rainfall for the 2046–2065 period compared with the 1981–2000 period. The multi-model mean was calculated using nine GCMs. The probability of increase represents how many models agree on the sign of change. It was evaluated by applying a t-distribution to the multi-model distribution of changes.

According to the figures, the annual mean rainfall over the basin increases slightly with a mean change to the maximum about 50 mm except for the region around the Mt. Kawi where the annual rainfall decrease slightly to the maximum about 80 mm. However, confidence is low. Half the models show decreasing trends and the remaining half increasing ones. The probability of increase is about 50% over the basin.

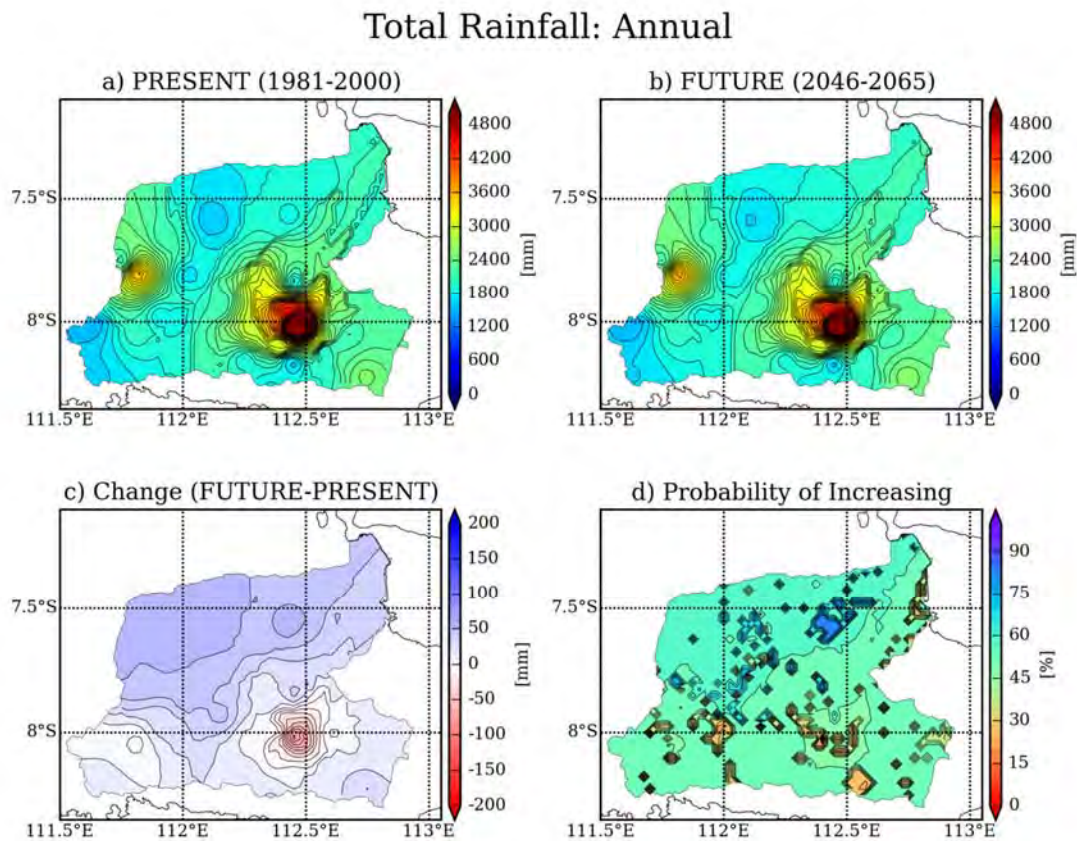


Figure 4.2.2-5 Changes of CMIP3 multi-model annual average rainfall: (a) multi-model mean of annual average rainfall for present (1991–2000); (b) multi-model mean of annual average rainfall for the future (2046–2065); (c) difference between (b) and (a); (d) probability of increase evaluated using variation of model ensemble.

CHAPTER 4 CLIMATE CHANGE IMPACT ASSESSMENT AND HYDROLOGICAL SIMULATION

2) Seasonal

Figure 4.2.2-6 shows seasonal variability of monthly mean areal averaged rainfall over the upstream of New Lengkonng. Change trends are not consistent with seasons and models. In the middle of the wet season (January-February-March), more than half (six of nine) of the GCMs showed an increasing trend, whereas in the middle of the dry season (July-August-September), more than half (six of nine) of the GCMs showed a decreasing trend.

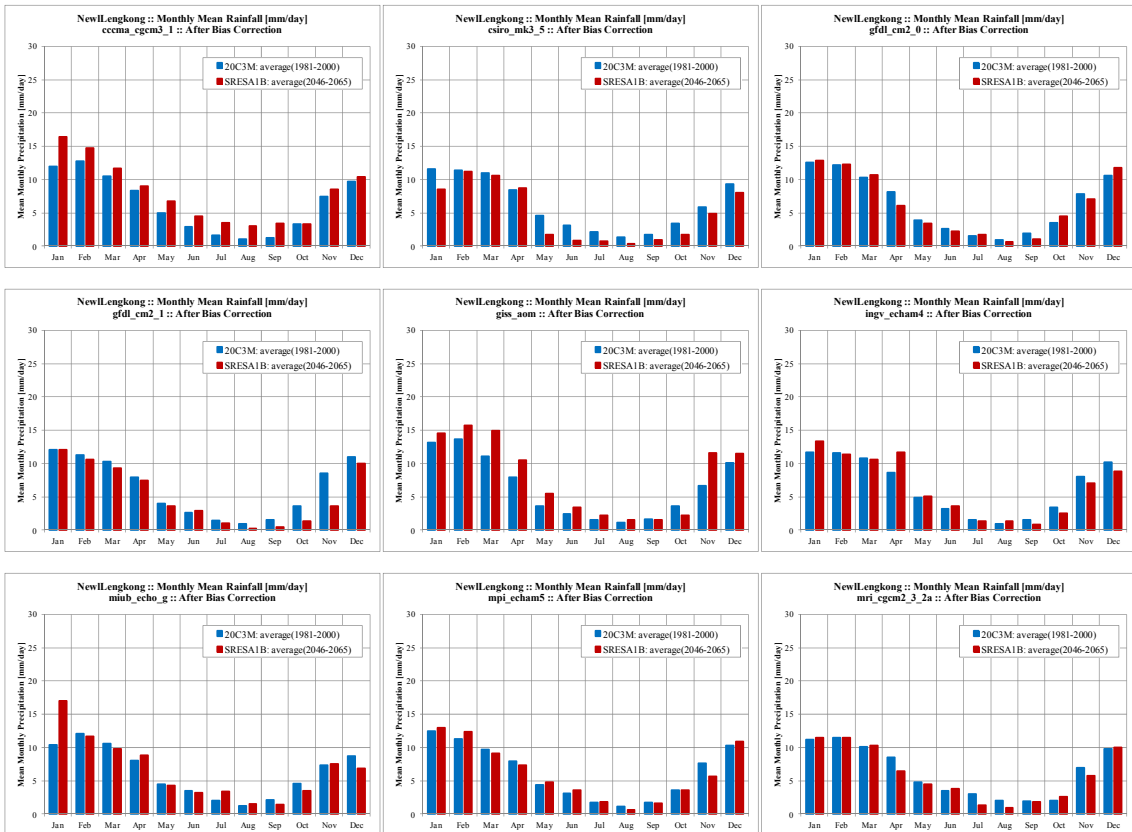


Figure 4.2.2-6 Change of monthly mean areal average rainfall over the upstream of New Lengkonng for different GCMs. Blue bar: GCM present; Red bar: GCM future.

3) Top 20

To evaluate the change of extreme rainfall, changes in the top 20 maximum rainfalls were evaluated by comparing the present and future of each GCM. The top 20 were identified by ranking the 20-year daily rainfall values from highest to lowest (7305 values).

Figure 4.2.2-7 shows the top 20 daily areal average rainfalls over upstream of New Lengkonng. According to the figures for the top 20, six of nine GCMs showed increasing trends, whereas two of 11 (csiro_mk3_5 and mri_cgcm2_3_2a) showed decreasing trends. The remaining station (gfdl_cm2_1) showed little change.

CHAPTER 4 CLIMATE CHANGE IMPACT ASSESSMENT AND HYDROLOGICAL SIMULATION

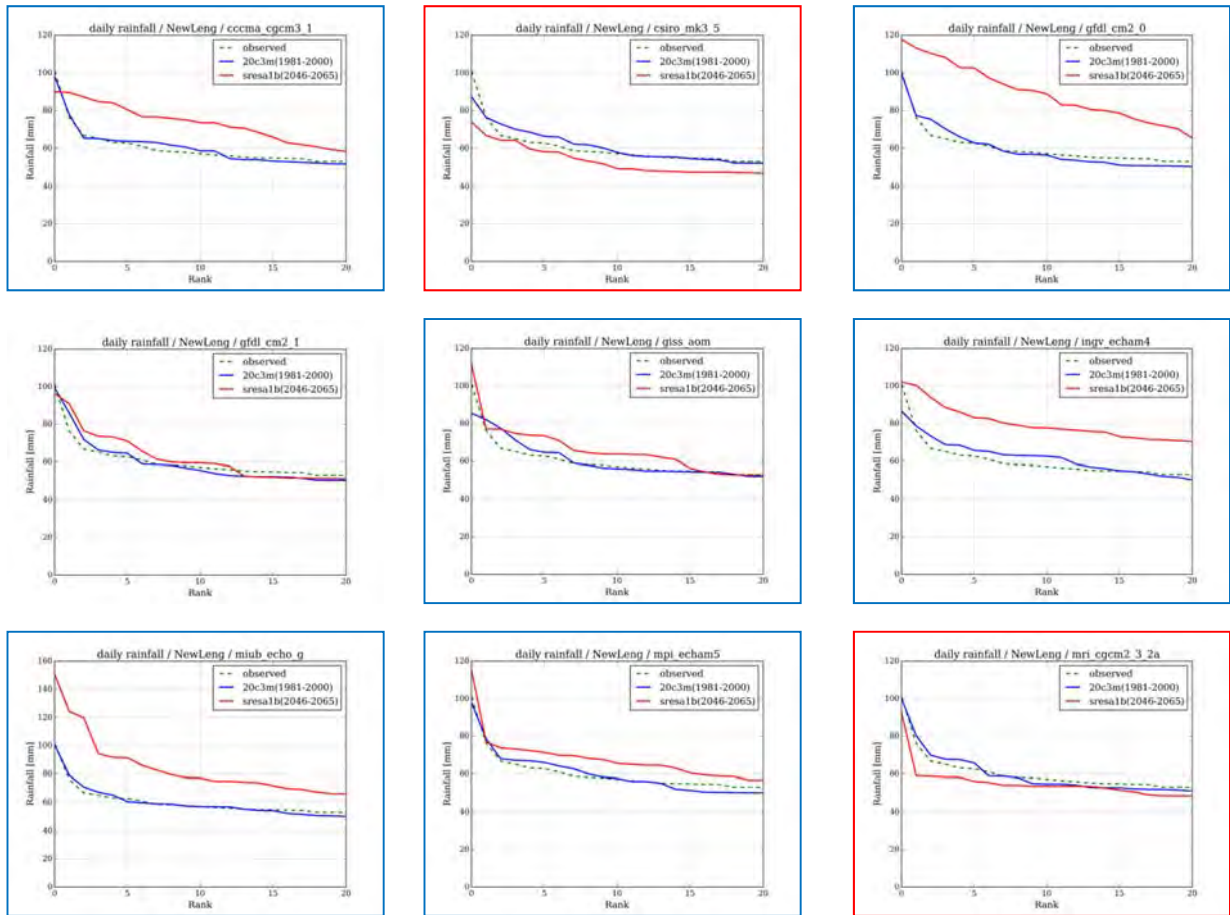


Figure 4.2.2-7 Changes in the top 20 of 20-year daily areal average rainfall over the upstream of New Lengkong. Green dashed line: observed; Blue solid line: GCM present; Red solid line: GCM future.

4) Return Periods

To evaluate rainfall return periods of extreme events, the GEV distribution was fit for 1-day rainfall, using the annual maximum values. Then, the 5-, 10-, 20-, 50- and 100-year return period rainfalls were obtained using the fitted GEV distribution for each case, and the change ratio (future/present) was calculated. Areal average rainfall over the upstream of New Lengkong was used for the evaluation.

Table 4.2.2-1 shows 1-day cumulative areal average rainfall for the present and future climate and for the five return periods. Figure 4.2.2-8 shows the change ratio of areal average rainfall from different climate models for the five return periods. It is shown that in all of the cases, the median change ratio is greater than one. Therefore, we can expect that rainfall with the 5-, 10-, 20-, 50- and 100-year return period in the Brantas River basin will increase in the future.

CHAPTER 4 CLIMATE CHANGE IMPACT ASSESSMENT AND HYDROLOGICAL SIMULATION

Table 4.2.2-1 Rainfall of 20C3M, SRES A1B rainfall, and the change ratio for 1-day cumulative areal average rainfall over the upstream of New Lengkong for various return periods

Areal Average Rainfall Upstream of New Lengkong

20C3M[1981-2000]

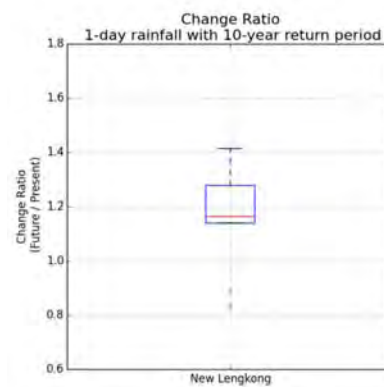
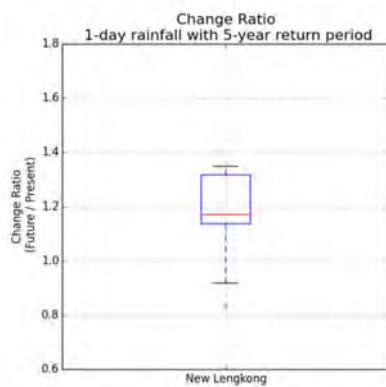
| Return Period/ Years | cccma_cg cm3_1 | csiro_mk3 _5 | gfdl_cm2_0 | gfdl_cm2_1 | giss_aom | ingv_ech am4 | miub_ech o_g | mpi_echa m5 | mri_cgcm 2_3_2a | Observed |
|-------------------------|-------------------|-----------------|------------|------------|----------|-----------------|-----------------|----------------|--------------------|----------|
| 5 | 63.9 | 67.2 | 66.7 | 57.9 | 61.7 | 67.3 | 65.1 | 60.9 | 64.0 | 62.5 |
| 10 | 73.7 | 75.1 | 76.6 | 68.5 | 67.7 | 74.7 | 74.4 | 69.8 | 74.0 | 69.7 |
| 20 | 83.8 | 82.1 | 86.6 | 81.3 | 73.1 | 81.8 | 84.8 | 81.4 | 85.1 | 78.1 |
| 50 | 97.8 | 90.6 | 100.3 | 102.9 | 79.7 | 90.8 | 100.4 | 102.2 | 101.9 | 91.7 |
| 100 | 109.0 | 96.4 | 111.0 | 123.7 | 84.4 | 97.6 | 114.0 | 123.7 | 116.7 | 104.3 |

SRES A1B[2046-2065]

| Return Period/ Years | cccma_cg cm3_1 | csiro_mk3 _5 | gfdl_cm2_0 | gfdl_cm2_1 | giss_aom | ingv_ech am4 | miub_ech o_g | mpi_echa m5 | mri_cgcm 2_3_2a |
|-------------------------|-------------------|-----------------|------------|------------|----------|-----------------|-----------------|----------------|--------------------|
| 5 | 72.8 | 56.3 | 90.0 | 68.0 | 71.5 | 88.6 | 86.7 | 72.0 | 59.0 |
| 10 | 84.3 | 62.5 | 108.4 | 79.5 | 81.9 | 95.6 | 103.4 | 81.6 | 65.7 |
| 20 | 95.9 | 69.2 | 126.9 | 91.8 | 92.7 | 101.1 | 123.0 | 91.5 | 72.8 |
| 50 | 111.8 | 79.2 | 151.9 | 109.5 | 108.3 | 106.8 | 154.8 | 105.8 | 82.8 |
| 100 | 124.4 | 87.8 | 171.6 | 124.3 | 121.2 | 110.3 | 184.5 | 117.7 | 91.1 |

Change Ratio[SRES A1B/20C3M]

| Return Period/ Years | cccma_cg cm3_1 | csiro_mk3 _5 | gfdl_cm2_0 | gfdl_cm2_1 | giss_aom | ingv_ech am4 | miub_ech o_g | mpi_echa m5 | mri_cgcm 2_3_2a | Median |
|-------------------------|-------------------|-----------------|------------|------------|----------|-----------------|-----------------|----------------|--------------------|--------|
| 5 | 1.14 | 0.84 | 1.35 | 1.17 | 1.16 | 1.32 | 1.33 | 1.18 | 0.92 | 1.17 |
| 10 | 1.14 | 0.83 | 1.41 | 1.16 | 1.21 | 1.28 | 1.39 | 1.17 | 0.89 | 1.17 |
| 20 | 1.14 | 0.84 | 1.46 | 1.13 | 1.27 | 1.24 | 1.45 | 1.13 | 0.86 | 1.14 |
| 50 | 1.14 | 0.87 | 1.52 | 1.06 | 1.36 | 1.18 | 1.54 | 1.04 | 0.81 | 1.14 |
| 100 | 1.14 | 0.91 | 1.55 | 1.00 | 1.44 | 1.13 | 1.62 | 0.95 | 0.78 | 1.13 |



CHAPTER 4 CLIMATE CHANGE IMPACT ASSESSMENT AND HYDROLOGICAL SIMULATION

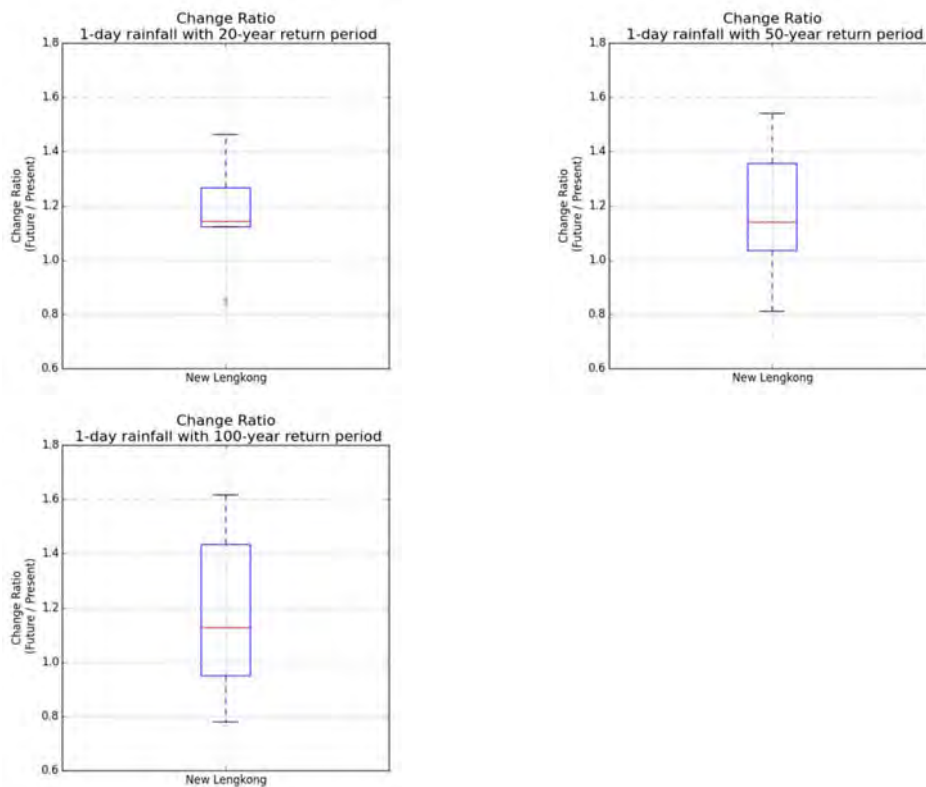


Figure 4.2.2-8 Change ratio of different climate models for 1-day cumulative areal average rainfall over the upstream of New Lengkong. Red line: median values; Lower and upper blue-color box edges: first and third quartiles; Upper and lower black lines: highest and lowest values within the 1.5-times inter-quartile range from the third and first quartiles. Blue crosses: outliers.

5) Trend Analysis

We analyzed monthly rainfall data from selected GCM models for the Brantas River basin to identify annual dry season (June through October) and wet season (November through May) trends under climate change. Because monthly rainfall data from *csiro_mk3_5* (one of the nine selected models) was not available, we used results from eight GCM models.

Figure 4.2.2-9 shows trends observed in each GCM models for annual rainfall. According to the results, two of eight models show positive trends and others do not show any trend significant at the 5% level. We can say the trend for annual rainfall is not so significant. Figure 4.2.2-10 and Figure 4.2.2-11 show trends for dry-season and wet-season rainfall respectively. For the dry-season rainfall, two of eight models show negative trends and others do not show any trend. For the wet-season rainfall, six of eight models show positive trends. We can say the trend is not so significant for dry-season rainfall, whereas there is positive trend for wet-season rainfall.

CHAPTER 4 CLIMATE CHANGE IMPACT ASSESSMENT AND HYDROLOGICAL SIMULATION

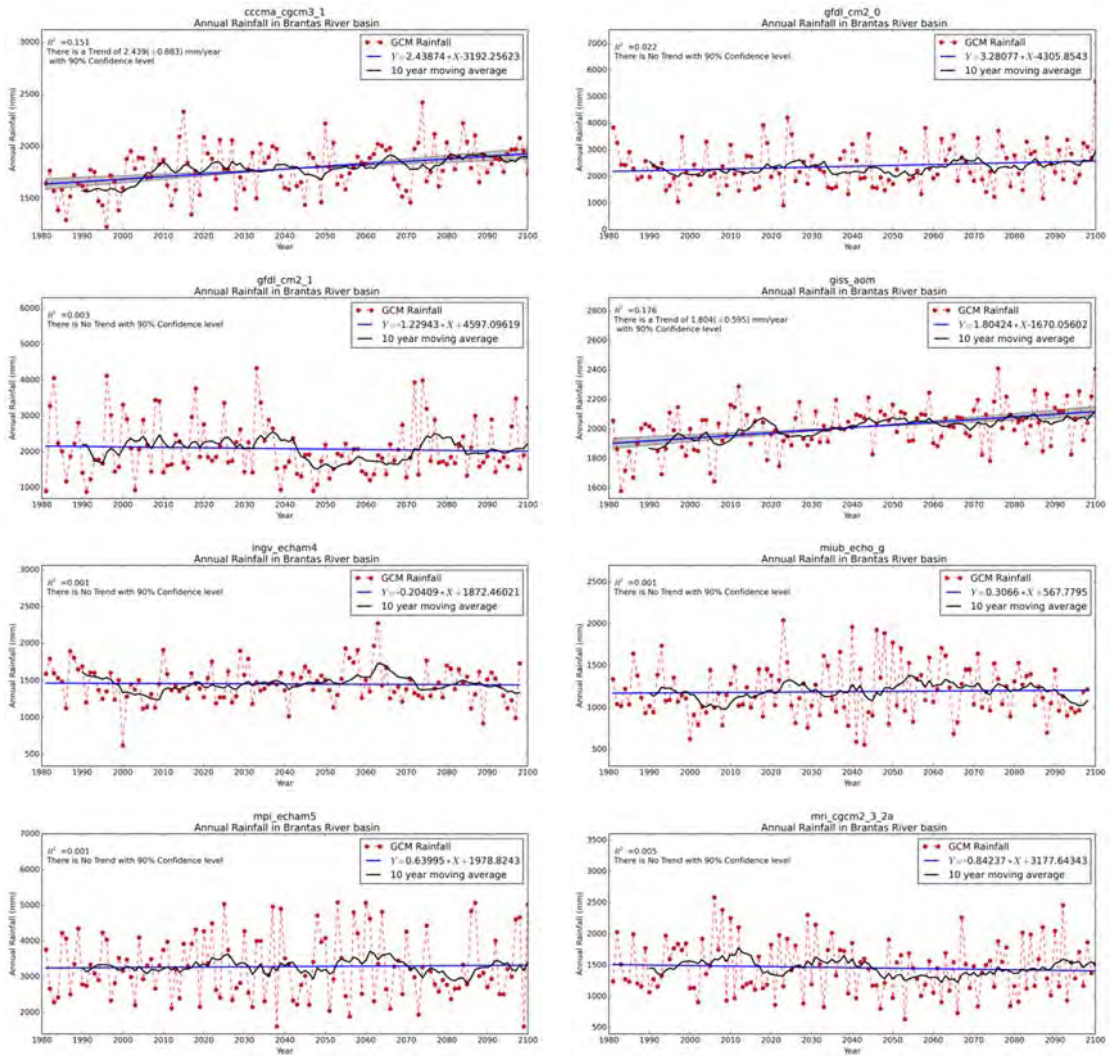
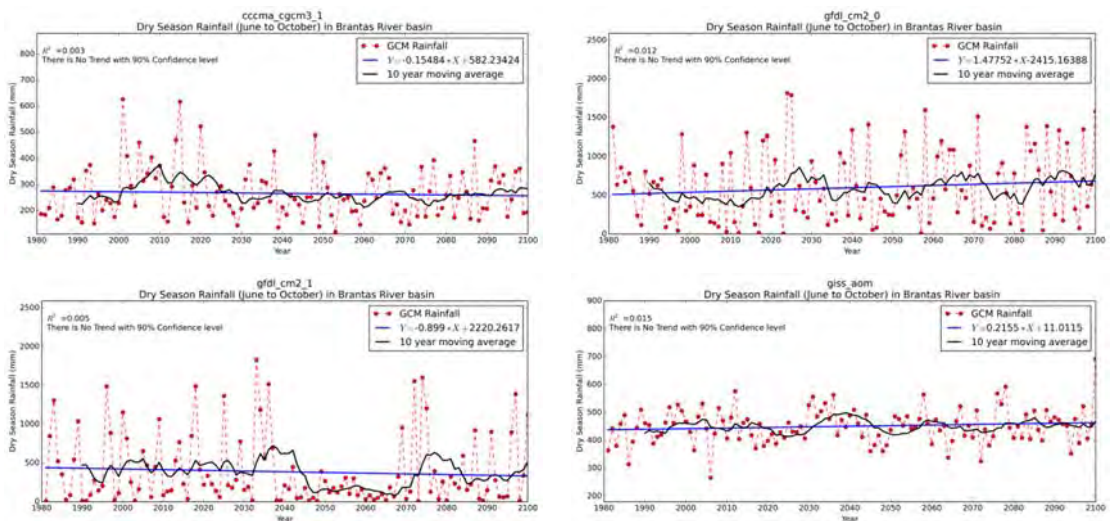


Figure 4.2.2-9 Annual trends (1981 through 2100) in eight GCM models



CHAPTER 4 CLIMATE CHANGE IMPACT ASSESSMENT AND HYDROLOGICAL SIMULATION

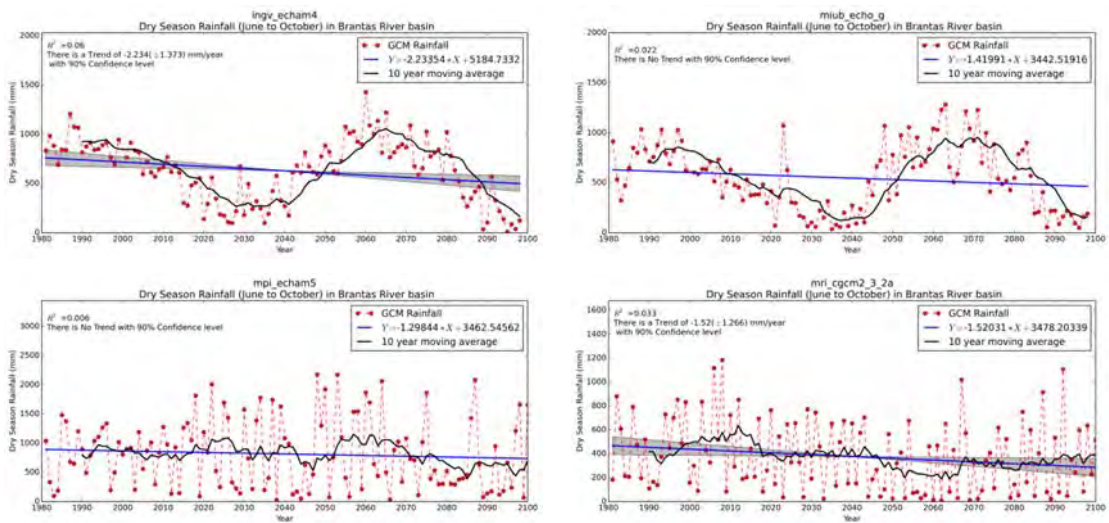


Figure 4.2.2-10 Dry seasonal trends (1981 through 2100) in eight GCM models

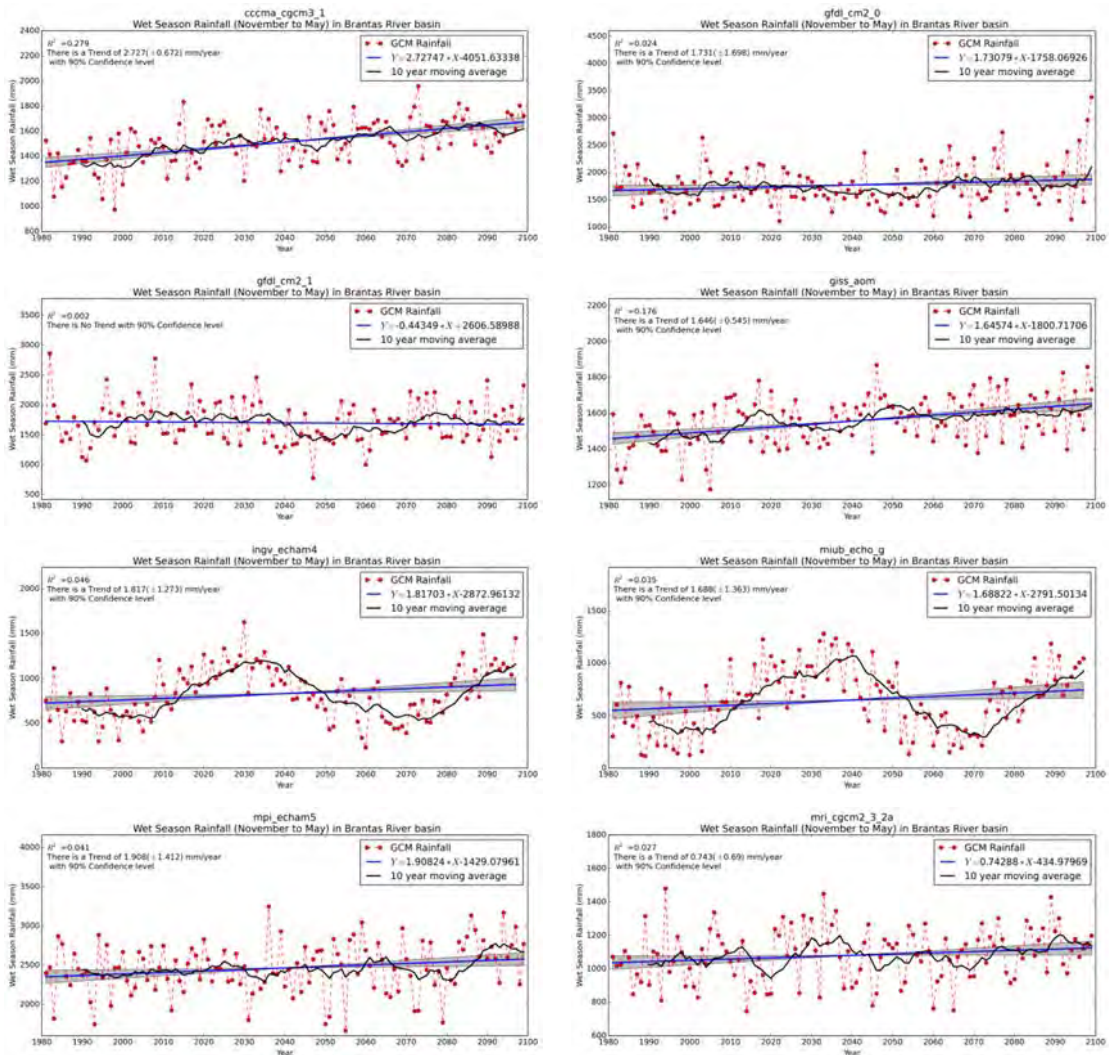


Figure 4.2.2-11 Wet seasonal trends (1981 through 2100) in eight GCM models

4.2.3 Climate Change Impact Assessment for River Runoff, ET, and Soil Moisture

(1) Development of WEB-DHM and its Validation

1) Target Area

The WEB-DHM was developed separately for Brantas and Surabaya River basin as shown in Figure 4.2.1-7. Total area of the Brantas River basin is around 11,000 km², and that of the Surabaya is about 1,100 km².

2) Model Calibration and Validation

The WEB-DHM model was calibration by comparing simulated daily discharges with natural flow derived from observed streamflow records. Because of a limited availability of hourly rainfall data in the basin, daily rainfall data was used in the modeling and thus it was difficult to fit the peak flows well. Hence, calibration was done mainly focusing on baseflow.

Efficiency criteria of Nash-Sutcliffe model efficiency (NS) and relative error (RE) were used to evaluate model performance. Runoff ratio, the percent of drainage basin rainfall that becomes stream flow, was also calculated for each of the observed and simulated flows.

$$NS = 1 - \frac{\sum_{i=1}^N \{q_o(i) - q_s(i)\}^2}{\sum_{i=1}^N \{q_o(i) - q_{av}\}^2} \quad (4.2.3-1)$$

$$q_{av} = \frac{1}{N} \sum_{i=1}^N q_o(i) \quad (4.2.3-2)$$

Where NS is Nash Sutcliffe model efficiency ,N is number of samples, q_o(i) is observed flow at time i, q_s(i) is simulated flow at time i, and q_{av} is the average of observed flow.

(NS ≥ 0.7: good performance, NS = 1.0: perfect prediction)

$$RE = \frac{\sum_{i=1}^N |q_o(i) - q_s(i)|}{\sum_{i=1}^N |q_o(i)|} \times 100 \quad [\%] \quad (4.2.3-3)$$

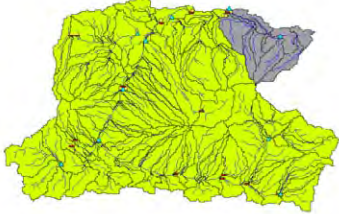
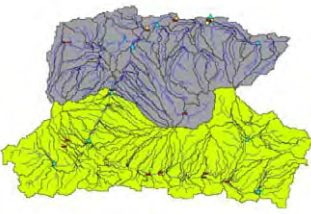
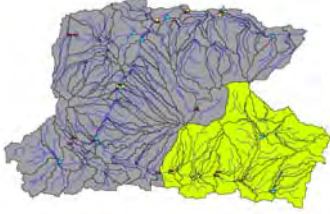
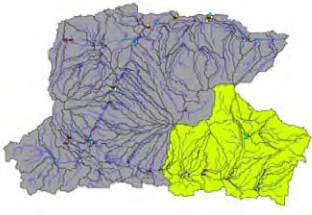
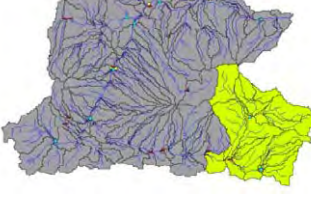
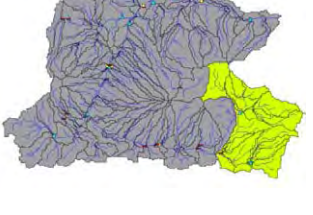

Where RS is relative error, q_o(i) is observed flow at time i, and q_s(i) is simulated flow at time i. (RE = 0.0: perfect prediction)

Natural flow data at seven locations in the Brantas and Surabaya River basin for calibrating

CHAPTER 4 CLIMATE CHANGE IMPACT ASSESSMENT AND HYDROLOGICAL SIMULATION

parameters and evaluating model performance are shown in Table 4.2.3-1.

Table 4.2.3-1 Calibration points in Brantas and Surabaya River basin (catchment upstream of the calibration points are shown in light green)

| Calibration points in the Brantas River basin | | |
|---|---|---|
| New Lengkong Barrage (~9,908 km ²) | Mrican Barrage (~5,981 km ²) | Lodoyo Dam (~2,970 km ²) |
|  |  |  |
| Wlingi Dam (~2,829 km ²) | Sutami Dam (~1,993 km ²) | Sengguruh Dam (~1,637 km ²) |
|  |  |  |
| Calibration point in the Surabaya River basin | | |
| New Gunungsari Barrage (~1,637 km ²) | | |
|  | | |

3) Model Performance

Brantas River Basin

It was found that the model simulates with high accuracy, especially for the most downstream locations: New Lengkong and Mrican. Details of model simulations at each location are given below.

Figure 4.2.3-1 and Figure 4.2.3-2 compare simulated discharge and observed natural flow at all six calibration points in the Brantas River basin for 2005. With regard to the New Lengkong, WEB-DHM simulated daily discharge with NS of 0.87 and RE of 18.6%, indicating reasonably good accuracy. Other years also revealed good performance. However, as for 2007, 2008, and 2010, in

CHAPTER 4 CLIMATE CHANGE IMPACT ASSESSMENT AND HYDROLOGICAL SIMULATION

which there was relatively heavy rainfall in the basin, simulated flood discharge was considerably greater than the observed discharge. In conclusion, the model is capable of simulating discharge with high accuracy at New Lengkok except for the flood discharges in 2007, 2008, and 2010. The results of Mrican and Lodoyo also show the same trend. With regard to the Wlingi, Stami, and Sengguruh, simulated flood discharges for 2005 was slightly greater than observed flow, and the differences were more significant for years from 2007 to 2010. These differences may originate from uncertainty in the observed data or in the hydrologic model parameters and from limitations of hydrologic process modeling in mountainous areas. In general, the spatial variation of rainfall was very high, especially in mountainous areas, and this might have produced large errors in the simulated flow. Therefore, one must be careful when using the simulated flow in mountainous small basins for any specific tasks.

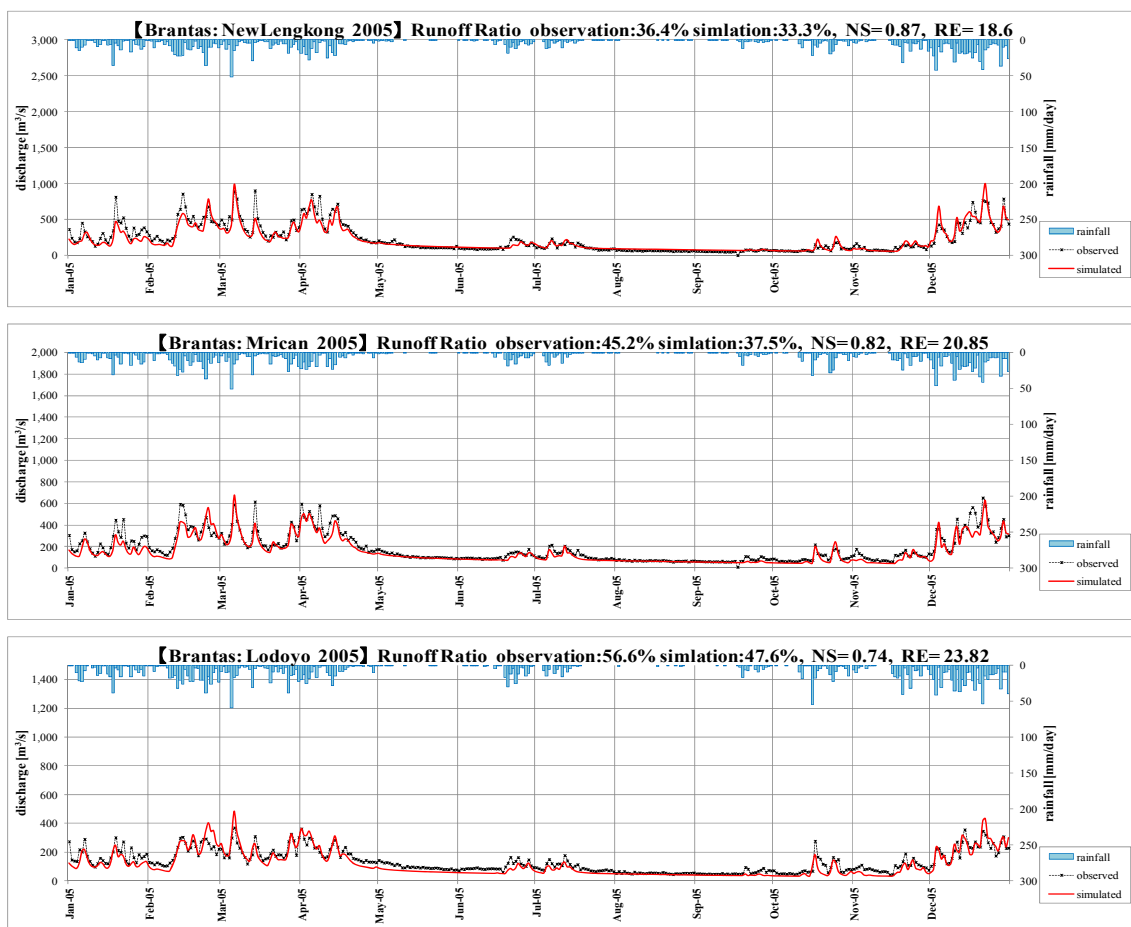


Figure 4.2.3-1 Comparisons between observed and simulated natural flows at New Lengkok, Mrican, and Lodoyo for 2005. Red solid line: simulated discharge with observed rainfall; Black dashed line: observed discharge.

CHAPTER 4 CLIMATE CHANGE IMPACT ASSESSMENT AND HYDROLOGICAL SIMULATION

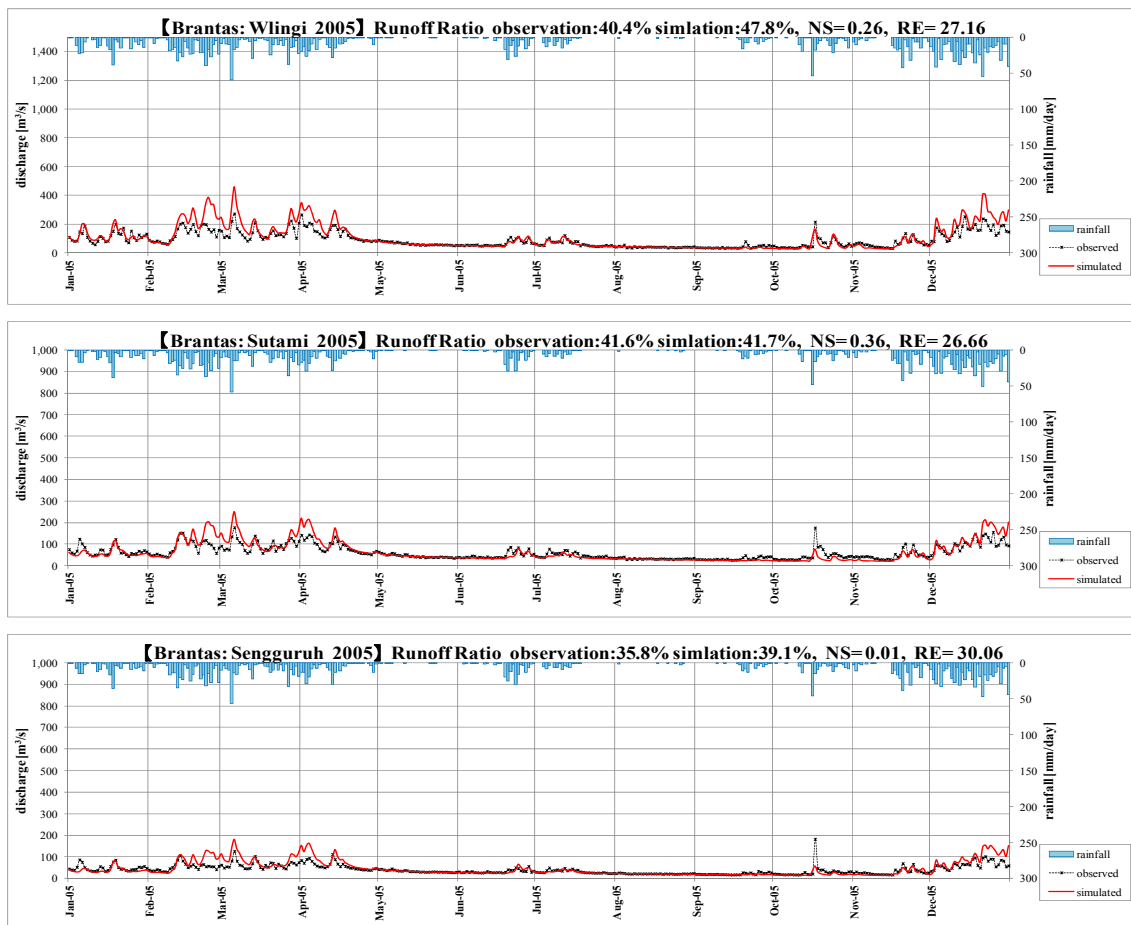


Figure 4.2.3-2 Comparisons between observed and simulated natural flows at Wilingi, Sutami, and Sengguruh for 2005. Red solid line: simulated discharge with observed rainfall; Black dashed line: observed discharge.

Surabaya River Basin

There is only one calibration point in the Surabaya River basin, New Gunungsari barrage. In the Surabaya River basin, water is supplied from the Brantas River through the Mrilip gate, especially in the dry season. The dominant component of river discharge over the region downstream of Mrilip gate is the supplied water from the Brantas River. Figure 4.2.3-3 shows a comparison of observed discharge and natural flow, which are calculated as a remaining of observed discharge after the deduction of diversion discharge. The calculated natural flow is significantly smaller than the observed discharge and sometimes it decreases to zero, so its accuracy is expected to be low. In addition, downstream of the Surabaya River basin are lowland flood areas, and the river water tends to spread across the delta. Runoff modeling in such areas are very difficult. For the above reasons, it was difficult to make simulated discharge fit well with observed natural flow. Therefore, we focused on matching a volume of wet season discharge in the calibration process for the Surabaya River basin model.

Figure 4.2.3-4 shows result for 2009 at New Gunungsari gauging station in the Surabaya River basin. The runoff ratio of simulated discharge (14.1%) matches well with that of observed discharge (13.4%).

CHAPTER 4 CLIMATE CHANGE IMPACT ASSESSMENT AND HYDROLOGICAL SIMULATION

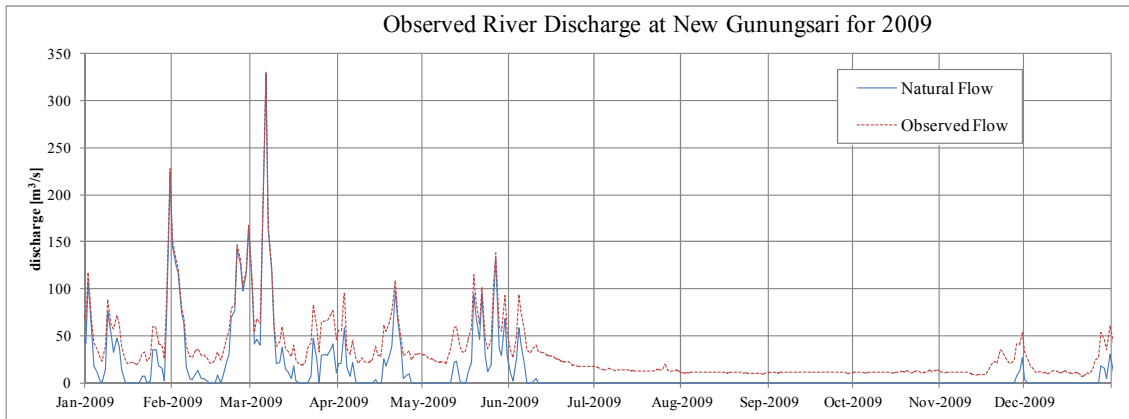


Figure 4.2.3-3 Observed flow and natural flow (calculated using observed dataset) at New Gunungsari Barrage. Red dashed line: observed river discharge; Blue solid line: natural flow.

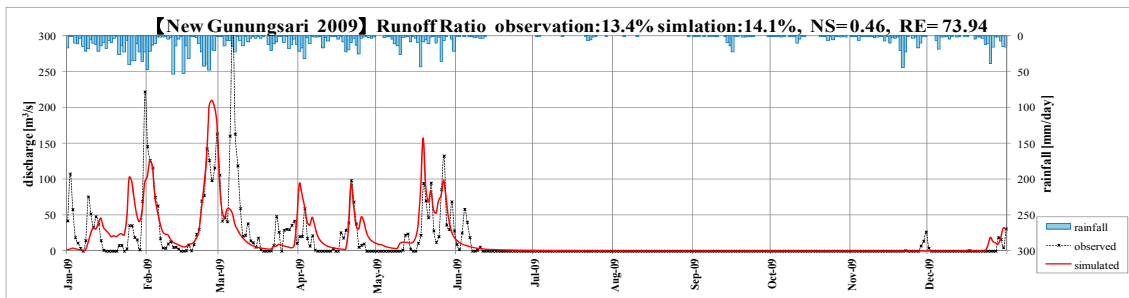


Figure 4.2.3-4 Comparison between observed and simulated natural flows at New Gunungsari for 2009. Red solid line: simulated discharge with observed rainfall; Black dashed line: observed river discharge.

4) Calibrated Model Parameters

Calibrated model parameters for each soil type, vegetation class, and land-use type are summarized in Tables 4.2.3-2~6. Saturated hydraulic conductivities were calibrated for the Brantas and Surabaya river basins, respectively. Manning's roughness coefficient of the riverbed was set at 0.05 for both basins.

CHAPTER 4 CLIMATE CHANGE IMPACT ASSESSMENT AND HYDROLOGICAL SIMULATION

Table 4.2.3-2 Soil parameters for the Brantas River basin model

| Soil Classification | | Soil water parameters | | | | | | | | | | |
|---------------------|-------------------|-------------------------|------------------------|-------------------------|-------------------------|---|------------|---|------------|------------|---|------|
| FAO soil code | Soil Class (FAO) | theta_s | theta_r | alpha | n | ks1 | | ks2 | | ksg | | GWcs |
| | | Saturated water content | Residual water content | van Genuchten parameter | van Genuchten parameter | Saturated Hydraulic conductivity for soil surface [mm/hr] (*) | calibrated | Saturated Hydraulic conductivity for unsaturated zone [mm/hr] | default | calibrated | Hydraulic conductivity for unconfined aquifer [mm/hr] | |
| - | - | - | - | - | - | default | calibrated | default | calibrated | default | calibrated | - |
| 4518 | Fluvisol, Gleysol | 0.446 | 0.076 | 0.016 | 1.432 | 18.674 | 933.69 | 1.867 | 93.37 | 0.934 | 9.34 | 0.15 |
| 4576 | Andosol | 0.502 | 0.092 | 0.015 | 1.364 | 62.207 | 3,110.33 | 6.221 | 311.03 | 3.110 | 31.10 | 0.3 |
| 4573 | Vertisol | 0.473 | 0.054 | 0.021 | 1.551 | 153.006 | 7,650.30 | 15.301 | 765.03 | 7.650 | 76.50 | 0.4 |
| 4490 | Ferralsol | 0.488 | 0.089 | 0.025 | 1.400 | 55.139 | 2,756.94 | 5.514 | 275.69 | 2.757 | 27.57 | 0.3 |
| 4509 | Lithosol | 0.495 | 0.082 | 0.016 | 1.427 | 53.008 | 2,650.41 | 5.301 | 265.04 | 2.650 | 26.50 | 0.3 |
| 4580 | Chromic Luvisol | 0.472 | 0.054 | 0.022 | 1.719 | 204.388 | 10,219.40 | 20.439 | 1,021.94 | 10.219 | 102.19 | 0.3 |
| 4570 | Regosol | 0.444 | 0.058 | 0.024 | 1.789 | 176.801 | 8,840.05 | 17.680 | 884.01 | 8.840 | 88.40 | 0.3 |

(*) the value of ks1 decreased by 0.1 in the build up area, decreased by 0.5 in the Wet Lowland area

Table 4.2.3-3 Soil parameters for the Surabaya River basin model

| Soil Classification | | Soil water parameters | | | | | | | | | | |
|---------------------|-------------------|-------------------------|------------------------|-------------------------|-------------------------|---|------------|---|------------|------------|---|------|
| FAO soil code | Soil Class (FAO) | theta_s | theta_r | alpha | n | ks1 | | ks2 | | ksg | | GWcs |
| | | Saturated water content | Residual water content | van Genuchten parameter | van Genuchten parameter | Saturated Hydraulic conductivity for soil surface [mm/hr] (*) | calibrated | Saturated Hydraulic conductivity for unsaturated zone [mm/hr] | default | calibrated | Hydraulic conductivity for unconfined aquifer [mm/hr] | |
| - | - | - | - | - | - | default | calibrated | default | calibrated | default | calibrated | - |
| 4518 | Fluvisol, Gleysol | 0.446 | 0.076 | 0.016 | 1.432 | 18.674 | 18.674 | 1.867 | 1.867 | 0.934 | 0.934 | 0.15 |
| 4490 | Ferralsol | 0.488 | 0.089 | 0.025 | 1.400 | 55.139 | 55.139 | 5.514 | 5.514 | 2.757 | 2.757 | 0.3 |
| 4509 | Lithosol | 0.495 | 0.082 | 0.016 | 1.427 | 53.008 | 53.008 | 5.301 | 5.301 | 2.650 | 2.650 | 0.3 |
| 4570 | Regosol | 0.444 | 0.058 | 0.024 | 1.789 | 176.801 | 176.801 | 17.680 | 17.680 | 8.840 | 8.840 | 0.3 |

(*) the value of ks1 decreased by 0.1 in the build up area, decreased by 0.5 in the Wet Lowland area

Table 4.2.3-4 Soil depth in the Brantas and Surabaya River basin model

| soil depth | | |
|-------------------------------|---|-------------|
| Dsfc | Dsub | Dg |
| first layer of subsurface [m] | subsurface [m] | aquifer [m] |
| 0.05 | 2: in the catchment upstream of Sutami. 4 in the other areas | 6 |

Table 4.2.3-5 Vegetation parameters for the Brantas and Surabaya River basin model

| SiB2 Reclassification | Hydraulic conductivity anisotropy ratio | Rooting depth [m] |
|---------------------------------|---|-------------------|
| 1-Broadleaf Evergreen Trees | 1 | 1.5 |
| 6-Short vegetation/C4 grassland | 3 | 1 |
| 7-Shrubs with bare soil | 1 | 1 |
| 8-Dwarf trees and Shrubs | 2 | 1 |
| 9-Agriculture or C3 Grasslands | 3 | 1 |

Table 4.2.3-6 Land-use parameters for the Brantas and Surabaya River basin model

| ID | Landuse Type | Equivalent Roughness Coefficient | Surface depression storage [mm] |
|----|--------------|----------------------------------|---------------------------------|
| 1 | Waterbody | 0.03 | 0.1 |
| 2 | Wet Lowland | 2 | 50 |
| 3 | Dry Upland | 0.5 | 5 |
| 4 | Settlements | 0.1 | 5 |
| 5 | Forest | 1 | 7 |

CHAPTER 4 CLIMATE CHANGE IMPACT ASSESSMENT AND HYDROLOGICAL SIMULATION

(2) Simulation of River Flow under Effects of Climate Change

Runoff was simulated by feeding bias-corrected GCM data into the developed basin model. Meteorological forcing datasets (rainfall, temperature and radiation) were obtained from each GCM. For other required parameters for the WEB-DHM model that were unavailable, the same data used in the calibration stage was applied. Temporal interpolation from daily maximum and minimum data into hourly temperature was implemented based on an empirical model called the “TM model”, proposed by Cesaraccio (2001).

Three types of simulations were run, namely, “simQobs”, “simQgcmp”, and “simQgcmf”. The simQobs represents simulated flows from 1991 to 2010, driven by observed meteorological data. The simQgcmp represents simulated flows from 1981 to 2000, driven by bias-corrected present meteorological conditions reproduced by GCMs. The simQgcmf represents simulated flows for 2046–2065, driven by future meteorological conditions obtained from bias-corrected GCM outputs. As mentioned earlier, the nine GCMs selected in order of performance were used for rainfall-runoff analyses. The simulations were done for two basins, respectively. The total number of simulations was 38, as shown in Table 4.2.3-7.

Table 4.2.3-7 List of simulations in the Brantas and Surabaya river basins

| Basin Name | Brantas River basin | | | Surabaya River basin | | |
|----------------|---------------------|------------------------|---------------|----------------------|------------------------|---------------|
| | simQobs | simQgcm | simQgcmf | simQobs | simQgcm | simQgcmf |
| (Scenario) | - | p | SRESA1B | - | p | SRESA1B |
| (Period) | 1991- 2000 | 20C3M 1981- 2000 | 2046- 2065 | 1991- 2000 | 20C3M 1981- 2000 | 2046- 2065 |
| observed data | ✓ | | | ✓ | | |
| cccma_cgcm3_1 | | ✓ | ✓ | | ✓ | ✓ |
| csiro_mk3_5 | | ✓ | ✓ | | ✓ | ✓ |
| gfdl_cm2_0 | | ✓ | ✓ | | ✓ | ✓ |
| gfdl_cm2_1 | | ✓ | ✓ | | ✓ | ✓ |
| giss_aom | | ✓ | ✓ | | ✓ | ✓ |
| ingv_echam4 | | ✓ | ✓ | | ✓ | ✓ |
| miub_echo_g | | ✓ | ✓ | | ✓ | ✓ |
| mpi_echam5 | | ✓ | ✓ | | ✓ | ✓ |
| mri_cgcm2_3_2a | | ✓ | ✓ | | ✓ | ✓ |

Total: 38 simulations

CHAPTER 4 CLIMATE CHANGE IMPACT ASSESSMENT AND HYDROLOGICAL SIMULATION

(3) Changes of Hydrological Parameters

1) River Runoff

a) Seasonal

Figure 4.2.3-5 shows seasonal variability of monthly mean discharge at New Lengkong. According to the figure, simQgcmp (blue solid line) match reasonably simQobs (blue dashed line). When compared with simQgcmp and simQgcmf (red solid line), five of nine GCMs (csiro_mk3_5, gfdl_cm2_0, gfdl_cm2_1, mpi_echam5 and mri_cgcm2_3_2a) showed decreasing trends of monthly discharge in almost all seasons, whereas two of nine (cccma_cgcm3_1 and giss_aom) showed increasing trends. The remaining two (ingv_echam4 and miub_echo_g) showed little change and a sign of changes varying with the seasons.

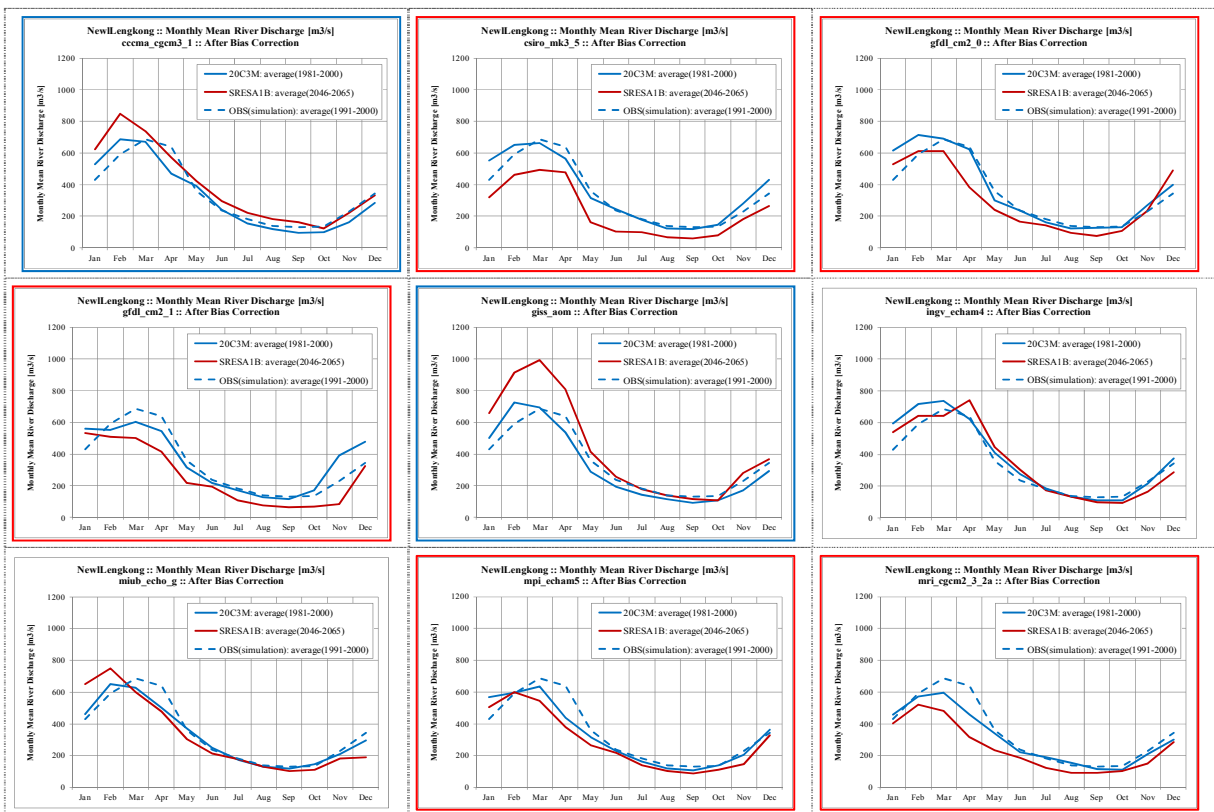


Figure 4.2.3-5 20-year mean monthly discharge at New Lengkong. Blue dashed line: simulation with observed rainfall; Blue solid line: simulation with GCM present; Red solid line: simulation with GCM future.

To evaluate the magnitude of predicted change and its uncertainty quantitatively, percentage increases for monthly mean discharges were calculated using projected present and future discharges. Figure 4.2.3-6 shows percentage increases of the monthly mean river discharge from different climate models at New Lengkon. According to the figures, the multi-model ensemble median/mean discharge shows a decreasing trend. The median discharge decreases around 5 - 20%, and the third quartile discharge decreases around 10 - 40%. Other locations also show the same trend. Therefore, we expect

that the total rainfall amount in the Brantas River basin will likely decrease in the future throughout the year. Besides, the multi-model ensemble spread varied between about -50 and 50%, meaning that monthly discharge trends among the GCMs were inconsistent. Thus, it is also important to bear in mind a possibility of 50% increase or 50% decrease in monthly discharges.

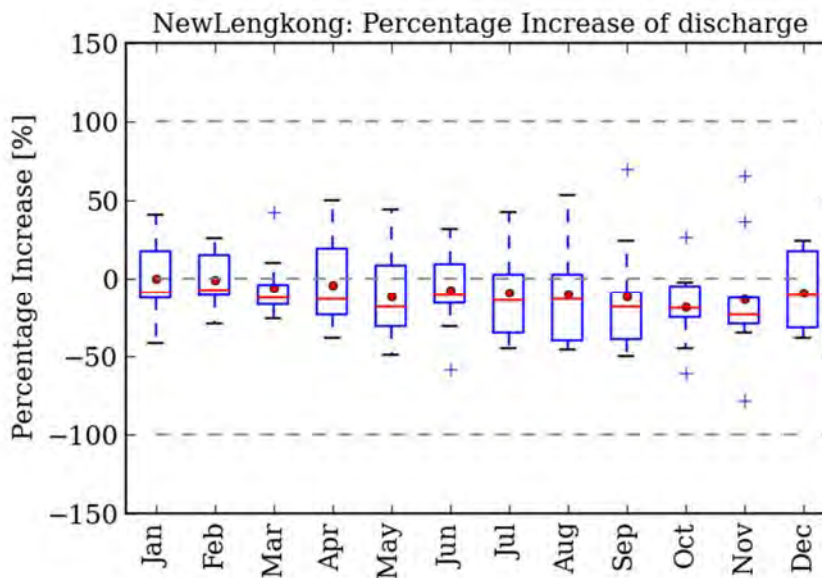


Figure 4.2.3-6 Percentage increase of 20-year mean monthly discharge at New Lengkong. Red line: median values; Red dots: mean values. Lower and upper blue-color box edges: first and third quartiles; Upper and lower black lines: highest and lowest values within the 1.5-times inter-quartile range from the third and first quartiles. Blue crosses: outliers.

b) Annual Flow Duration Curve

Figure 4.2.3-7 shows annual mean duration curves at New Lengkong for the present and future. According to the figure, simQgcmp (blue solid line) match reasonably simQobs (green dashed line). When compared with simQgcmp and simQgcmf (red solid line), seven of nine GCMs (csiro_mk3_5, gfdl_cm2_0, gfdl_cm2_1, ingv_echam4, miub_echo_g, mpi_echam5 and mri_cgcm2_3_2a) had decreasing trends and others (cccma_cgcm3_1 and giss_aom) increasing trends.

Figure 4.2.3-8 shows the top 10% of flow duration curves at New Lengkong. It should be noted that there is a considerable gap between simQgcmp (blue solid line) and simQobs (green dashed line). The result shows the differences between the observed and modeled mean daily flood peaks is considerably large. The main reason for this problem is the lack of temporal and spatial coherence of the GCM rainfalls as we have described in section 4.2.2. Therefore, careful consideration is needed when using the simulated flood discharge directory. In this section, we compared with simQgcmp and simQgcmf to evaluate the change trend of flood discharge. Focusing on the top 2%, six of nine GCMs (cccma_cgcm3_1, gfdl_cm2_0, gfdl_cm2_1, giss_aom, ingv_echam4 and miub_echo_g) showed

CHAPTER 4 CLIMATE CHANGE IMPACT ASSESSMENT AND HYDROLOGICAL SIMULATION

increasing trends, whereas 2 of 9 (csiro_mk3_5 and mri_cgcm2_3_2a) showed decreasing ones. The remaining one (mpi_echam4) showed little change.

In order to evaluate the magnitude of predicted change and its uncertainty quantitatively, the percentage increase of discharge at each rank was calculated using present and future discharges. Figure 4.2.3-9 shows the result at New Lengkong. The black thick line shows the multi-model ensemble mean of probability of increase and the red and blue dashed lines show the maximum and minimum values, respectively. Regarding the multi-model ensemble mean, flood discharges with less than 5% exceedance probability slightly increased around 10%, and normal and low flows (upper 20% of exceedance probability) declined around 15%. Therefore, we expect that dry season discharge will likely decrease, whereas flood discharge will likely increase in the future. Beside, the multi-model ensemble spread of normal and low flows varied between -50 and 40%, meaning that discharge trends among the GCMs were inconsistent. Thus, it is also important to bear in mind a possibility of 50% increase or 40% decrease in normal and low flows.

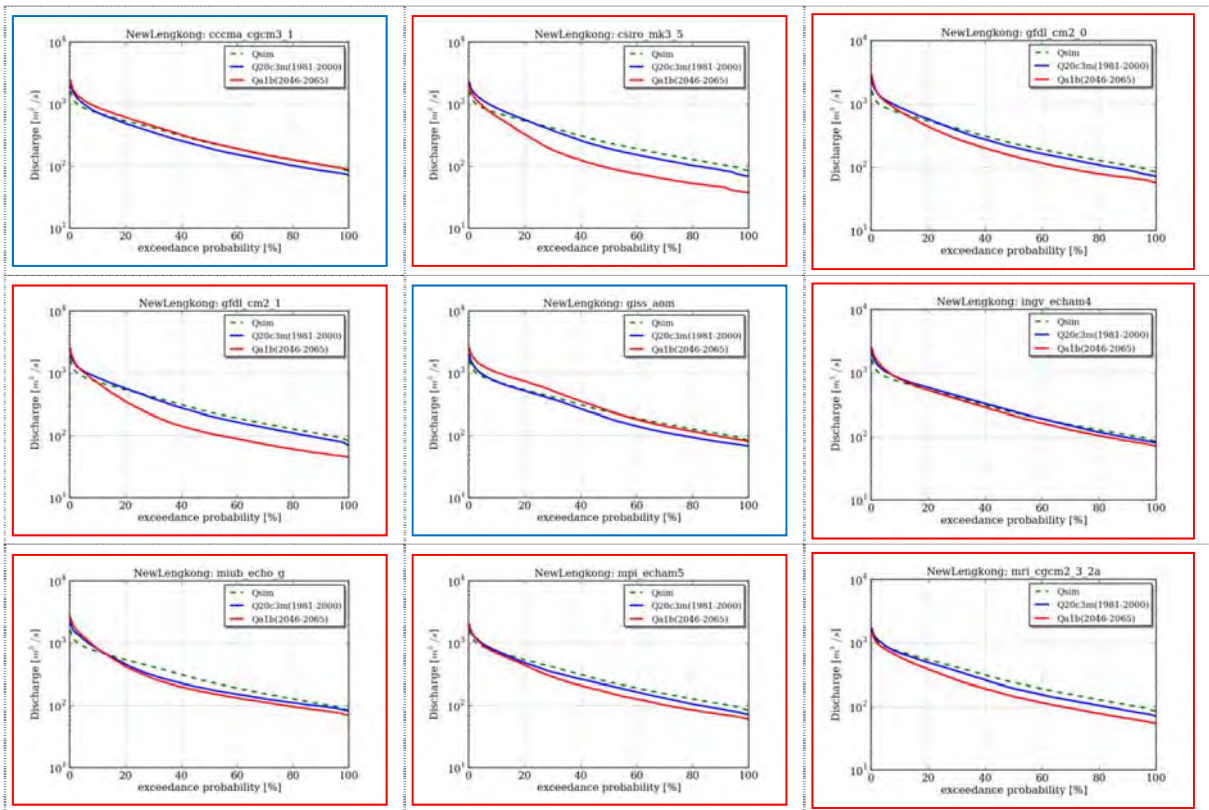


Figure 4.2.3-7 Flow duration curve at New Lengkong. Green dashed line: simulation with observed rainfall; Blue solid line: simulation with GCM present; Red solid line: simulation with GCM future.

CHAPTER 4 CLIMATE CHANGE IMPACT ASSESSMENT AND HYDROLOGICAL SIMULATION

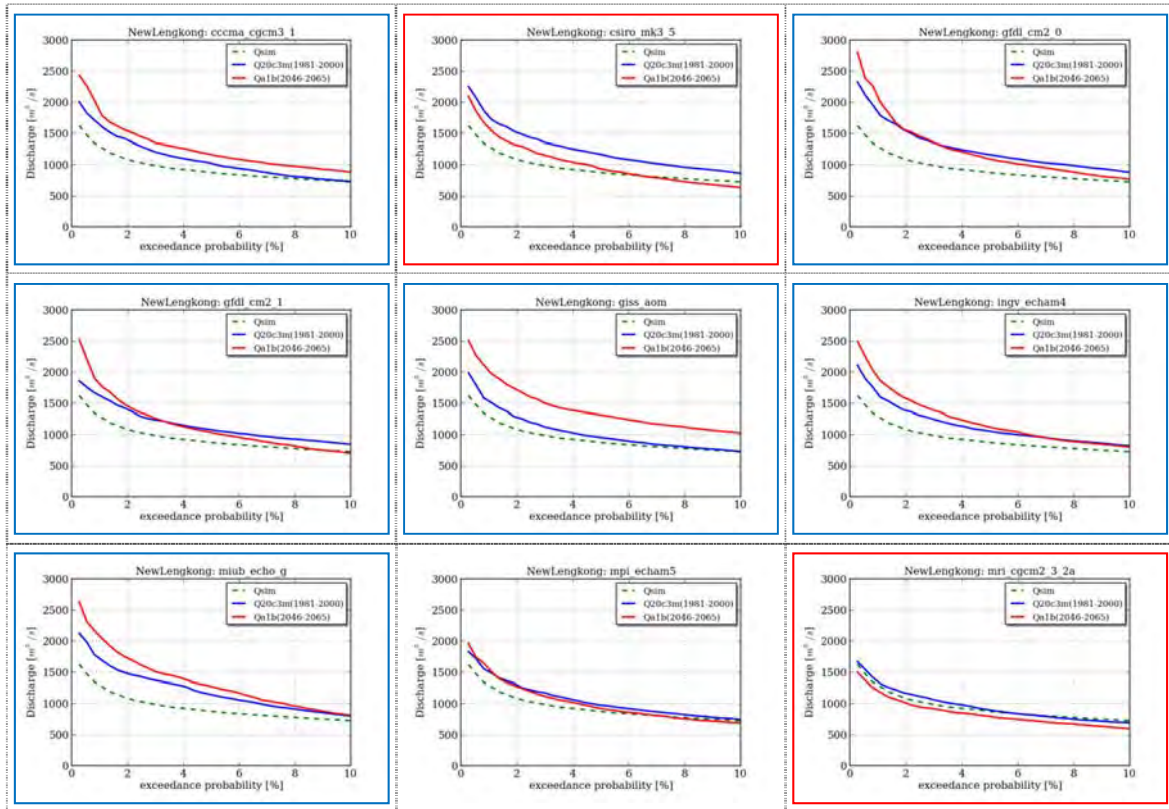


Figure 4.2.3-8 Top 10% of flow duration curves at New Lengkok. Green dashed line: simulation with observed rainfall; Blue solid line: simulation with GCM present; Red solid line: simulation with GCM future.

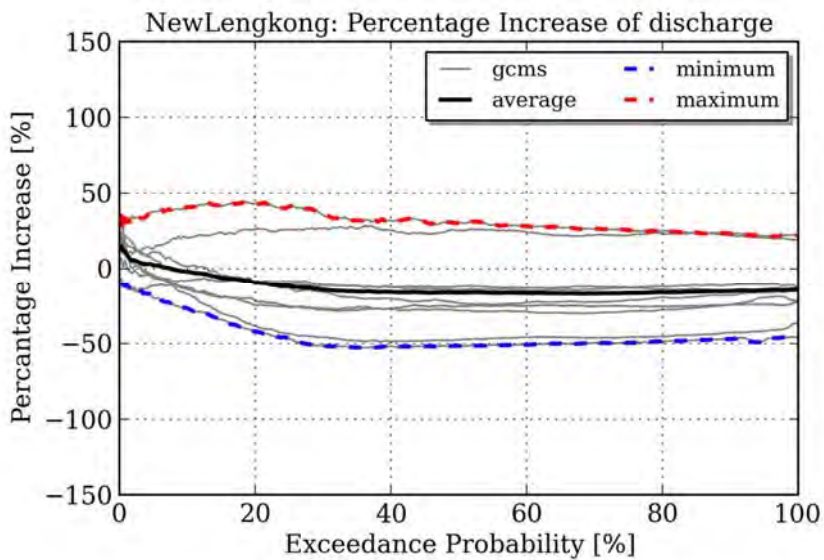


Figure 4.2.3-9 Percentage increase of river discharge at New Lengkok. Black thick line: multi-model ensemble mean of probability of increase; Red and blue dashed line: maximum and minimum values.

CHAPTER 4 CLIMATE CHANGE IMPACT ASSESSMENT AND HYDROLOGICAL SIMULATION

c) Drought

Climate change impacts on drought in the Brantas River basin are some of the most important concerns. To evaluate changes of drought discharge, the following indices were used.

- Annual drought discharge (average of 355th rank of daily discharge)
- Number of days in a year in which river discharge was less than the present drought discharge
- The 10% non-exceedance probability of present annual drought discharge
- Number of days in a year in which the river discharge was below the 10% non-exceedance probability of present annual drought discharge
- Longest number of days in a year in which the river discharge was less than the present annual drought discharge

Table 4.2.3-8 lists the calculated drought indices at New Lengkong barrage for each climate simulation. This shows that seven of nine climate models had increasing trends of drought conditions in the future climate, and two models showed decreasing trends. Because more than 78% of the models predicted severe drought conditions in the future, it is vital to include effective countermeasures against water scarcity in future water resource management plans for the Brantas Basin. Other locations also show the same trend.

Table 4.2.3-8 Drought indices at New Lengkong Barrage

| GCM Model | Annual Drought Discharge (m ³ /s) | | # of days/year that baseflow < present drought discharge | | 10% Non Exceedance Probability of Annual Drought Discharge (m ³ /s) | | # of days/year that baseflow < present 1/10 drought discharge | | Longest # of days for each year below average drought discharge | |
|----------------|--|--------|--|--------|--|--------|---|--------|---|--------|
| | <i>(average 355th rank)</i> | | | | <i>(10th percentile of 355th rank)</i> | | | | | |
| | Present | Future | Present | Future | Present | Future | Present | Future | Present | Future |
| ccma_cgcm3_1 | 77.38 | 94.16 | 26 | 13 | 46.91 | 65.68 | 2 | 0 | 125 | 63 |
| csiro_mk3_5 | 72.94 | 39.22 | 55 | 165 | 44.58 | 21.15 | 2 | 68 | 207 | 304 |
| gfdl_cm2_0 | 76.44 | 62.09 | 48 | 90 | 44.39 | 40.47 | 6 | 9 | 204 | 183 |
| gfdl_cm2_1 | 80.37 | 47.42 | 82 | 143 | 37.35 | 27.36 | 4 | 20 | 202 | 324 |
| giss_aom | 71.70 | 86.11 | 31 | 1 | 54.82 | 74.46 | 2 | 0 | 79 | 13 |
| ingv_echam4 | 85.68 | 76.81 | 30 | 53 | 61.64 | 48.51 | 3 | 14 | 91 | 168 |
| miub_echo_g | 87.70 | 75.71 | 37 | 60 | 59.77 | 51.47 | 3 | 7 | 120 | 151 |
| mpi_echam5 | 77.50 | 65.18 | 42 | 66 | 48.92 | 48.10 | 3 | 5 | 170 | 149 |
| mri_cgcm2_3_2a | 76.70 | 58.12 | 36 | 80 | 51.29 | 41.87 | 3 | 18 | 117 | 191 |

Red = drier in future; greater frequency of drought conditions

Blue = wetter in future; less frequency of drought conditions

2) Surface Air Temperature

Figure 4.2.3-10 shows the annual mean changes of surface air temperature for 2046–2065 relative to 1981–2000. The multi-model mean was calculated using nine GCMs. The probability of an increase represents how many models agreed on the sign of change. This probability was evaluated by applying the t-distribution to the multi-model distribution of changes.

According to the figures, annual mean surface air temperatures over the basin increased with a mean change of about 2.3°C in the future. The probability of increase was nearly 100% over the entire

basin, indicating that nearly all models had increasing trends. Therefore, confidence is very high.

Mean Surface Air Temperature: Annual

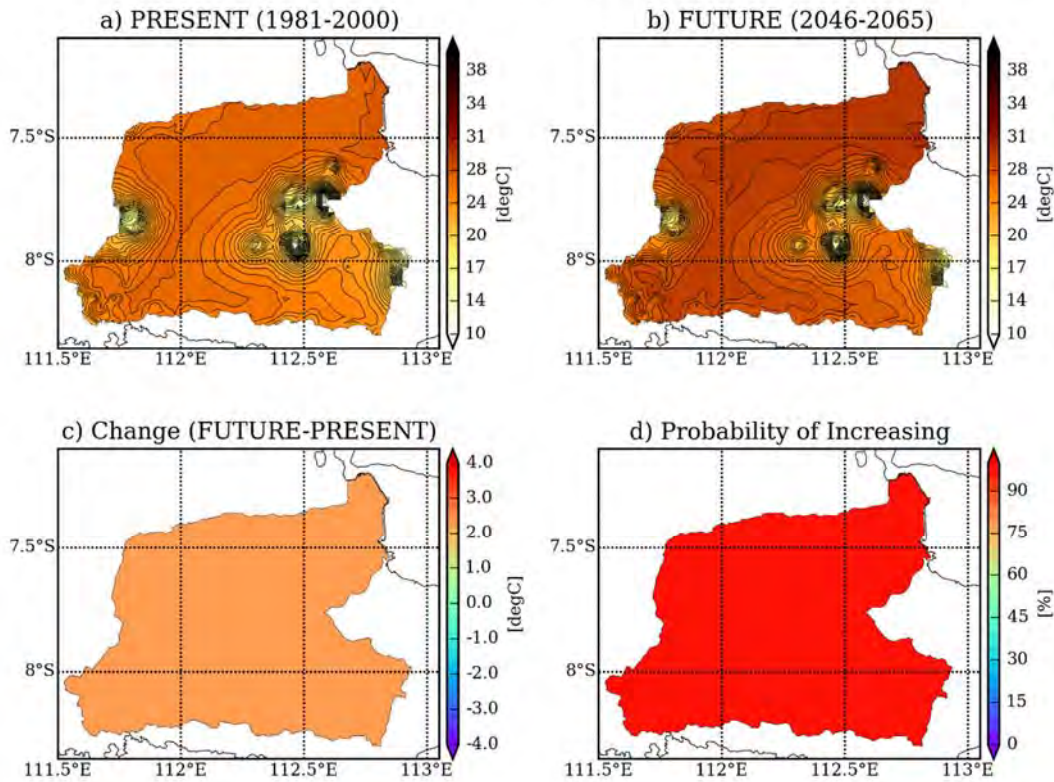
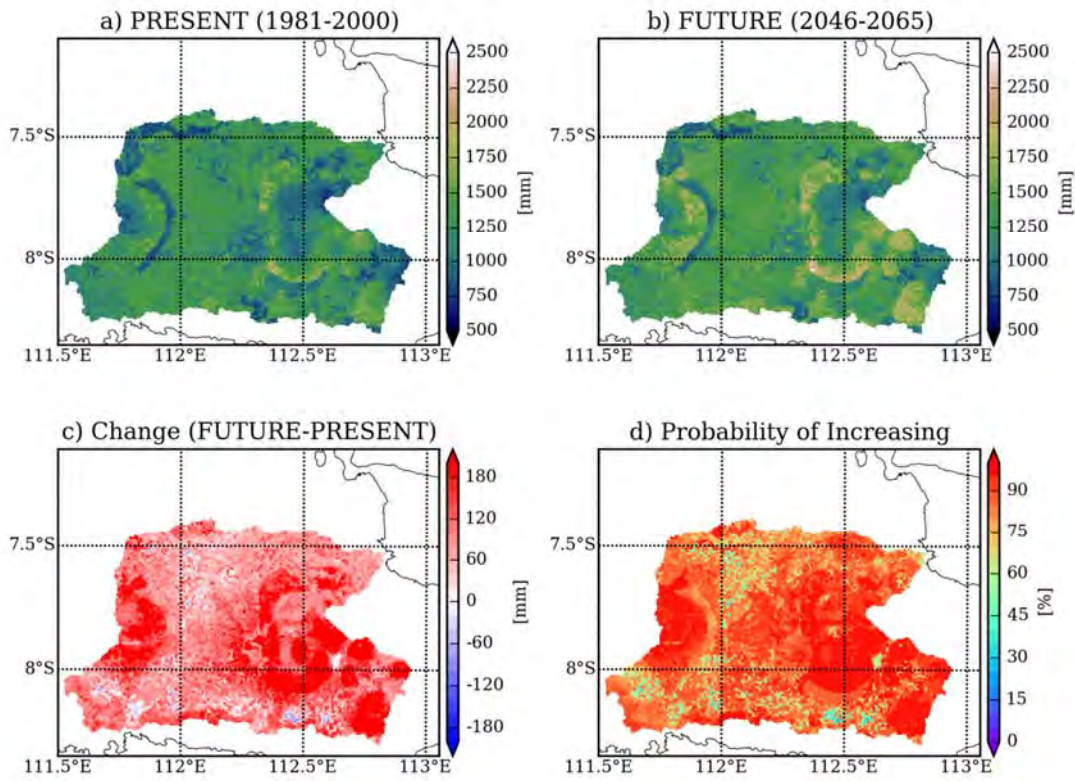


Figure 4.2.3-10 Changes of CMIP3 multi-model annual average temperature: (a) multi-model mean of annual average rainfall for the present (1991–2000); (b) multi-model mean of annual average rainfall for the future (2046–2065); (c) difference between (b) and (a); (d) probability of an increase, evaluated using variations of the model ensemble

3) ET (Precipitation Minus Evapotranspiration)

Figure 4.2.3-11 shows annual mean changes of projected ET for 2046–2065 with respect to 1981–2000 in the Brantas and Surabaya river basins. There were increasing trends of ET in both river basins. As for the Brantas River basin, almost all changes for the annual mean ET are increasing, generally averaging an increase of around 150 mm in the future. The probability of an increase was around 80%, with high confidence. As for the Surabaya River basin, almost all changes for annual mean ET are increasing, generally averaging an increase of around 80 mm in the future. The probability of an increase was around 50-80%.

Total Evapotranspiration: Annual



Total Evapotranspiration: Annual

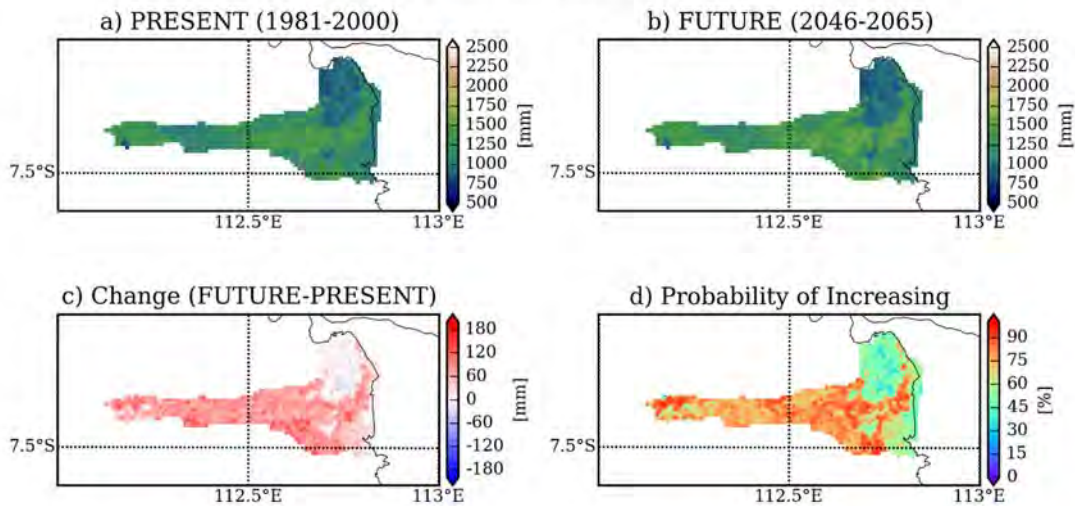


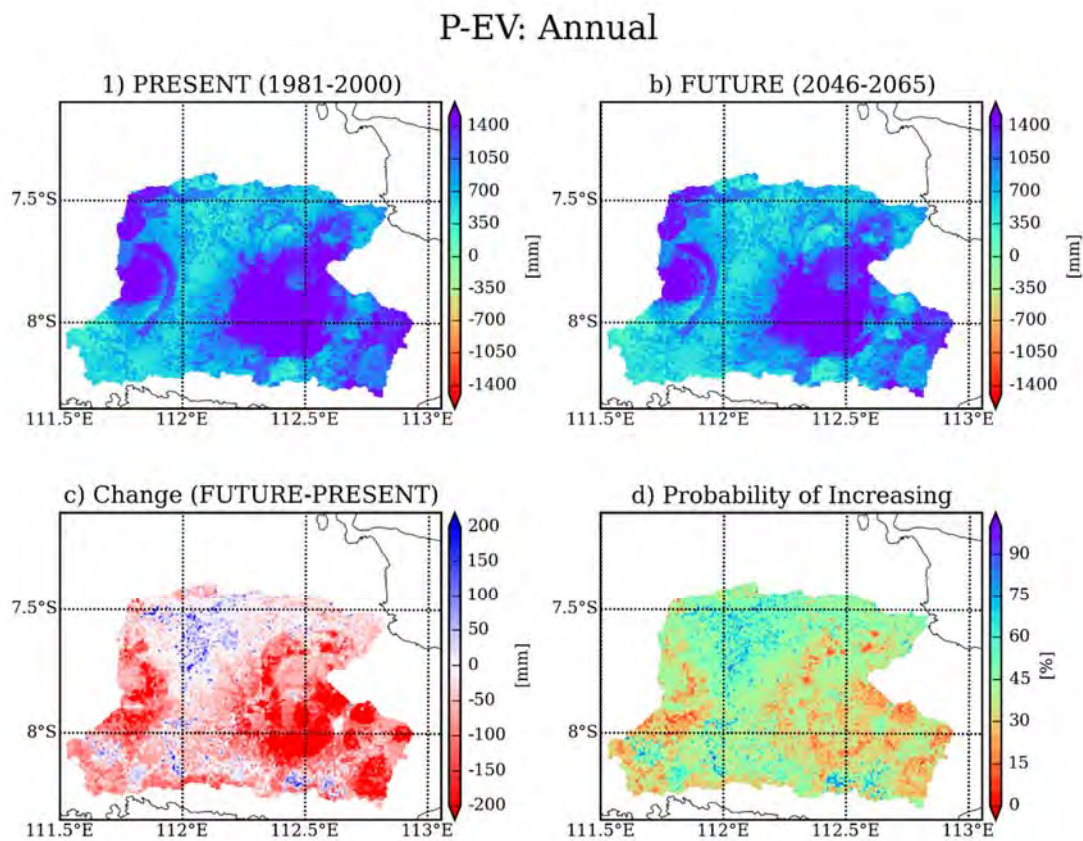
Figure 4.2.3-11 Changes of CMIP3 multi-model annual average ET in Brantas (upper) and Surabaya River basin (lower): (a) multi-model mean of annual average rainfall for present (1991–2000); (b) multi-model mean of annual average rainfall for future (2046–2065); (c) differences between (b) and (a); (d) probability of an increase, evaluated using variations of the model ensemble

CHAPTER 4 CLIMATE CHANGE IMPACT ASSESSMENT AND HYDROLOGICAL SIMULATION

4) Changes of P–E

Precipitation minus ET (P–E) describes the flux of water between the atmosphere and land surface, and provides important information for understanding the impacts of climate change on water resources. After conducting the WEB-DHM simulations, we obtained the projected future and present ET. Using these data, P–E for each GCM was calculated.

Figure 4.2.3-12 shows annual mean changes of P–E for 2046–2065 relative to 1981–2000 in the Brantas and Surabaya river basins. In the Brantas River basin, changes of annual mean P–E decreased about 200mm, whereas increased about 100 mm in some parts of the alluvial area. The probability of an increase varied between 30 and 70%, indicating confidence is low. Regarding the Surabaya River basin, annual mean P–E decreased in the downstream of the Surabaya River basin, whereas increased about 50% in the other area. The probability of increase was around 50%, indicating very low confidence. In conclusion, the change of P–E is not so significant over the Brantas and Surabaya river basins.



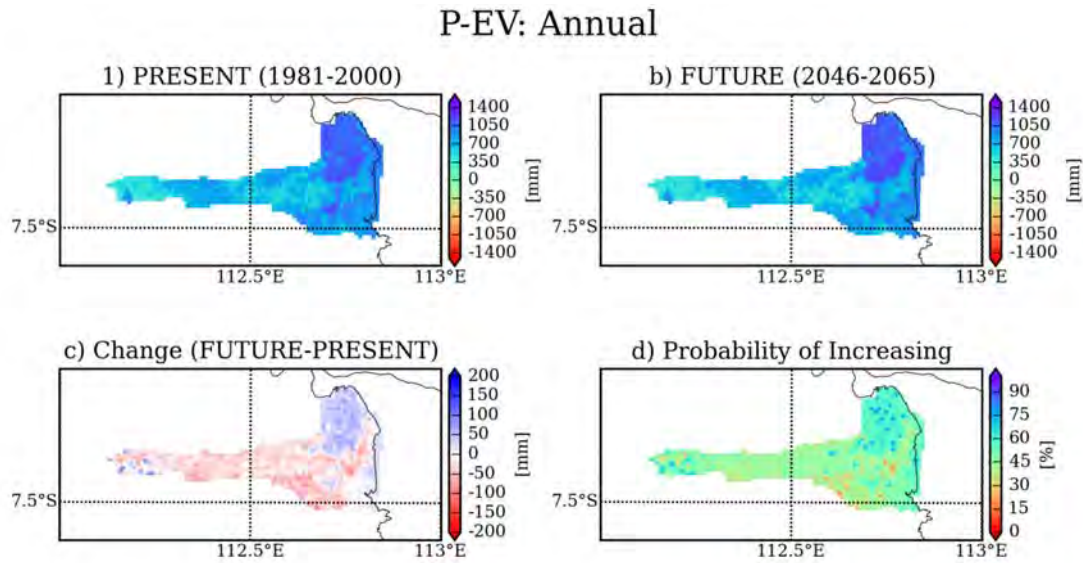
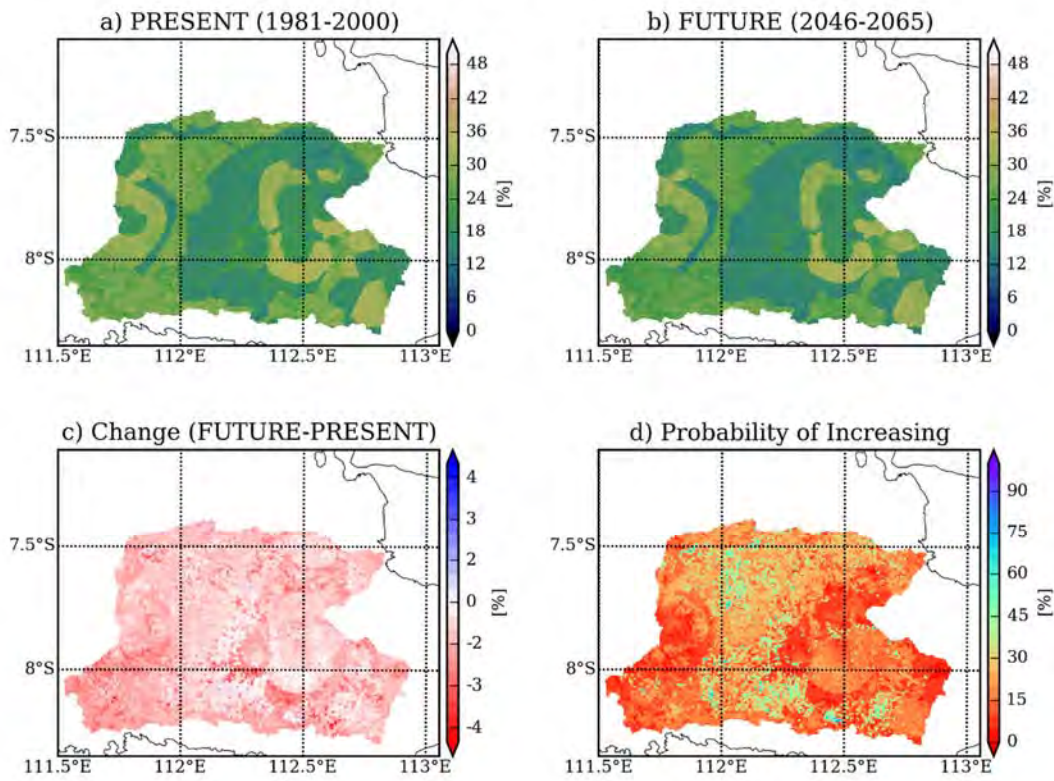


Figure 4.2.3-12 Changes of CMIP3 multi-model annual average P-E in Brantas (upper) and Surabaya River basin (lower): (a) multi-model mean of annual average rainfall for present (1991–2000); (b) multi-model mean of annual average rainfall for future (2046–2065), (c) differences between (b) and (a); (d) probability of an increase, evaluated using variations of the model ensemble

5) Soil Moisture

The WEB-DHM model is also capable of simulating soil moisture and its change. Figure 4.2.3-13 shows annual mean changes of soil moisture for 2046–2065 relative to 1981–2000 in the Brantas and Surabaya River basin. This shows that annual mean soil moisture over both basins decreased around 1–3%. The probability of an increase was around 15%, indicating that the confidence level of a decreasing trend is high.

Mean Soil Moisture: Annual



Mean Soil Moisture: Annual

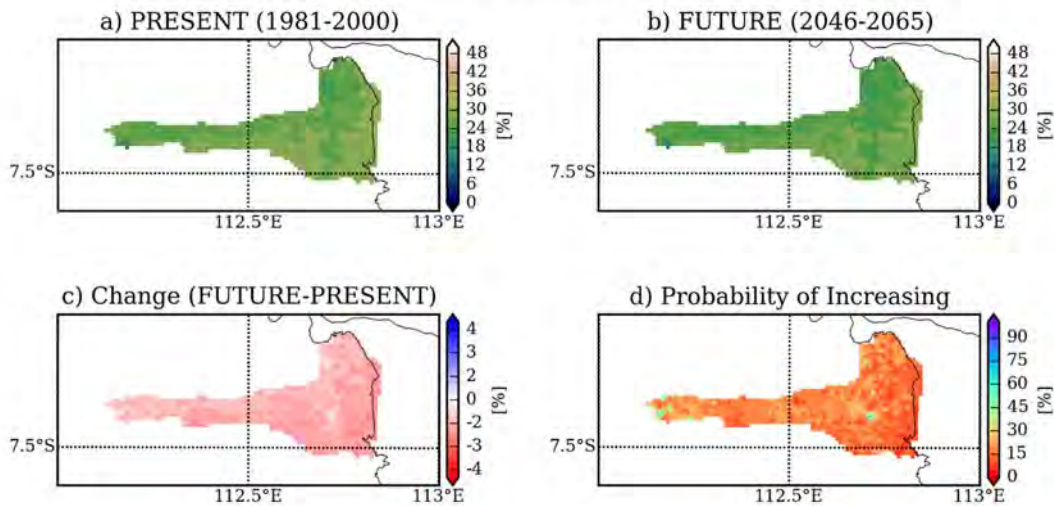


Figure 4.2.3-13 Changes of CMIP3 multi-model annual average soil moisture in Brantas (upper) and Surabaya River basin (lower): (a) multi-model mean of annual average rainfall for present (1991–2000); (b) multi-model mean of annual average rainfall for future (2046–2065); (c) differences between (b) and (a); (d) probability of increase, evaluated using variations of the model ensemble.

CHAPTER 4 CLIMATE CHANGE IMPACT ASSESSMENT AND HYDROLOGICAL SIMULATION

(4) Summary of Climate Change Impact in the Brantas River Basin

We evaluated climate change impacts on water resources in the Brantas River basin. Through multi-model ensemble analysis, we quantitatively evaluated the projected change and its uncertainty.

The projected climate change in the basin is summarized below.

- i. Surface air temperature will increase by 2.0°C by 2050, with high confidence.
- ii. Annual total rainfall will increase slightly. However, this trend was not consistent among the GCMs, so confidence is low.
- iii. Rainfall with 5-, 10-, 20-, 50-, and 100-year return periods will increase in the future.
- iv. Evapotranspiration will increase slightly, with a high probability.
- v. P–E (Precipitation minus Evapotranspiration) will not change significantly, and trends were inconsistent among the GCMs.

The projected change in water resources is summarized below.

- i. There is a relatively high degree of agreement among GCMs about the future direction of drought conditions over the entire basin. The ensemble mean change of low flows is around -15% by the 2050s, indicating severe drought conditions in the future climate.
- ii. There is a relatively high degree of agreement among GCMs about the future direction of flood conditions over the entire basin. The ensemble mean a change of the top 2% of the duration curve is around 10% by the 2050s, indicating severe flooding conditions in the future climate.

4.2.4 Selection of Future Scenarios in the Brantas River Basin

(1) Future Scenario Selection for Water Resources Management

1) Indicator

Indicator was selected based on a discussion with the team for “Water Resources Management Plan”. In the stage of developing the water resources management plan, the most important indicator is the change of the basin’s low flow conditions. Therefore, total discharge in the dry season (June through October) was selected as the indicator. Altogether four evaluation sites of the discharge were selected at strategic points along the Brantas River (shown in Figure 4.2.4-1). The sites are the New Lengkong barrage, Sutami dam, Mrican barrage, and the mouth of the Widas River (where the Widas and Brantas rivers meet).

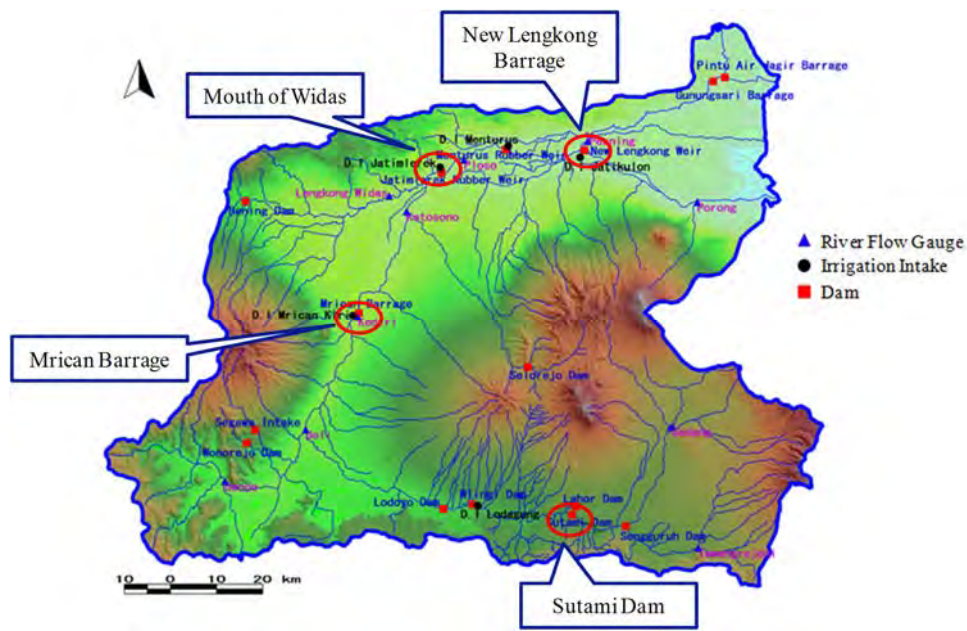


Figure 4.2.4-1 Evaluation sites of the discharge

2) Results of Scenario Selection

Figure 4.2.4-2 shows box plots for percentage increase of total discharge in dry season at each of the evaluation sites by the year 2050. Except for Widas, all the other sites shows similar ensemble spreads (widths of the boxes), which are around -25% to 0%. This means that there is a possibility of 25% decrease or nearly unchanged low flow condition at those sites by the year 2050. At Widas, the ensemble spread varies from around -20% to +10%. With respect to the order of the models, there is a consistency among the sites. The median and 1st and 3rd quartile models are very similar among the sites. According to the results, we selected three models to represent High, Medium, and Low scenarios of future discharged in the dry season as listed below.

- “ingv_echam4” as Low scenario (the safest scenario)
- “mpi_echam5” as Medium scenario (scenario of highest probability)
- “gfdl_cm2_0” as High scenario (the most hazardous scenario)

CHAPTER 4 CLIMATE CHANGE IMPACT ASSESSMENT AND HYDROLOGICAL SIMULATION

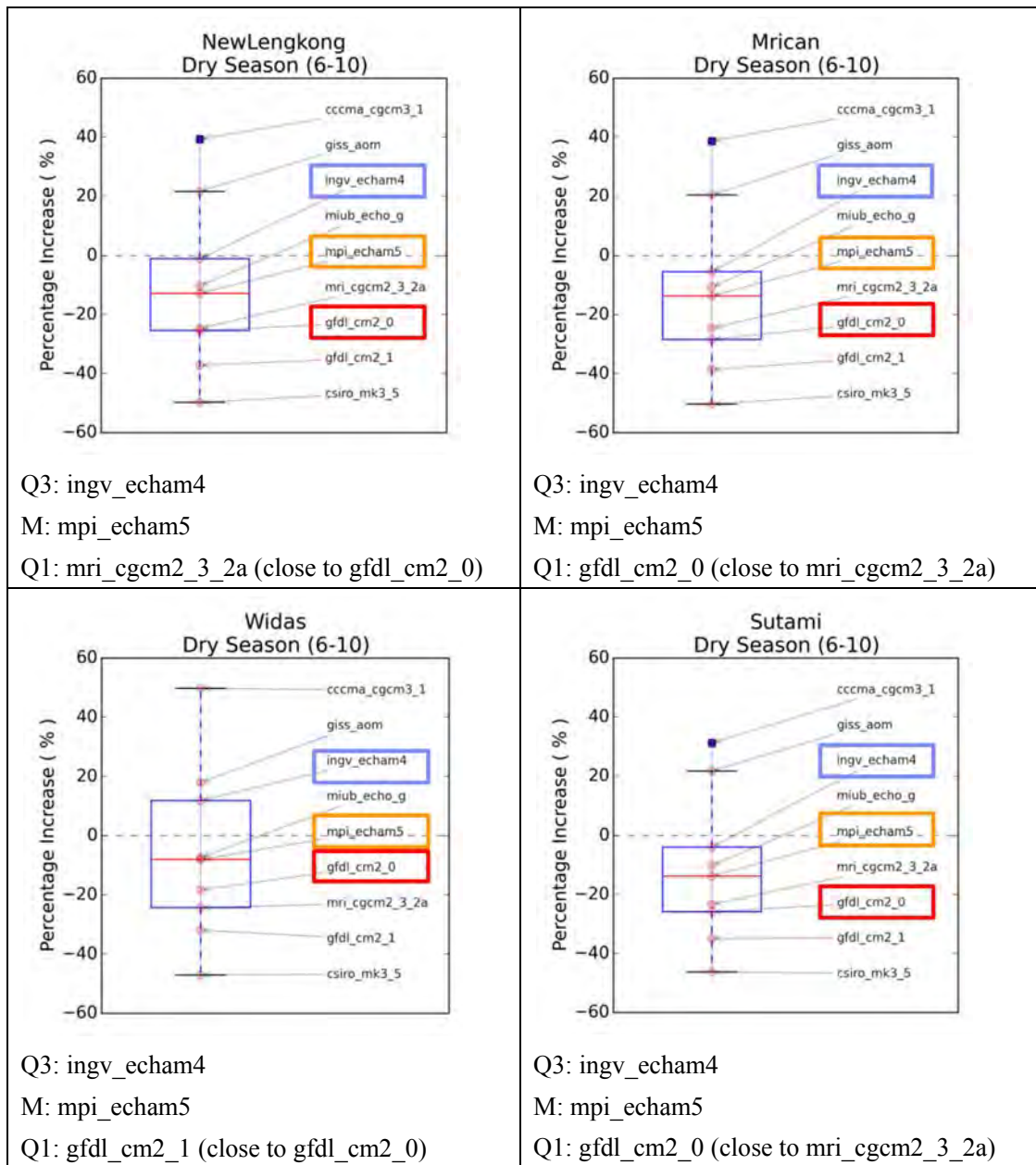


Figure 4.2.4-2 Box plots for percentage increases of total dry season discharges at four evaluation sites by 2050. Q1: 1st quartile; M: median; Q3: 3rd quartile.

(2) Future Scenario Selection for Flood Risk Management

1) Indicator

Indicators were selected based on a discussion with the team for “Water Resources Management Plan”. In the stage of developing the flood risk management plan, the most important indicator is the change of the magnitude of the daily flood peak and its frequency. Therefore, changes in the magnitude of the flood peak in a given return period can be used as the indicators of change in the flood regime. However, there are limitations of the simulated discharge extremes based on GCM outputs. There are considerable differences between the observed and modeled mean daily flood peaks (as we have seen

CHAPTER 4 CLIMATE CHANGE IMPACT ASSESSMENT AND HYDROLOGICAL SIMULATION

in Figure 4.2.3-8), so it is difficult to apply frequency analysis for simulated discharge directly. Therefore, we applied frequency analysis for maximum annual daily rainfall instead of river discharge. The methodology is described in Figure 4.2.4-3.

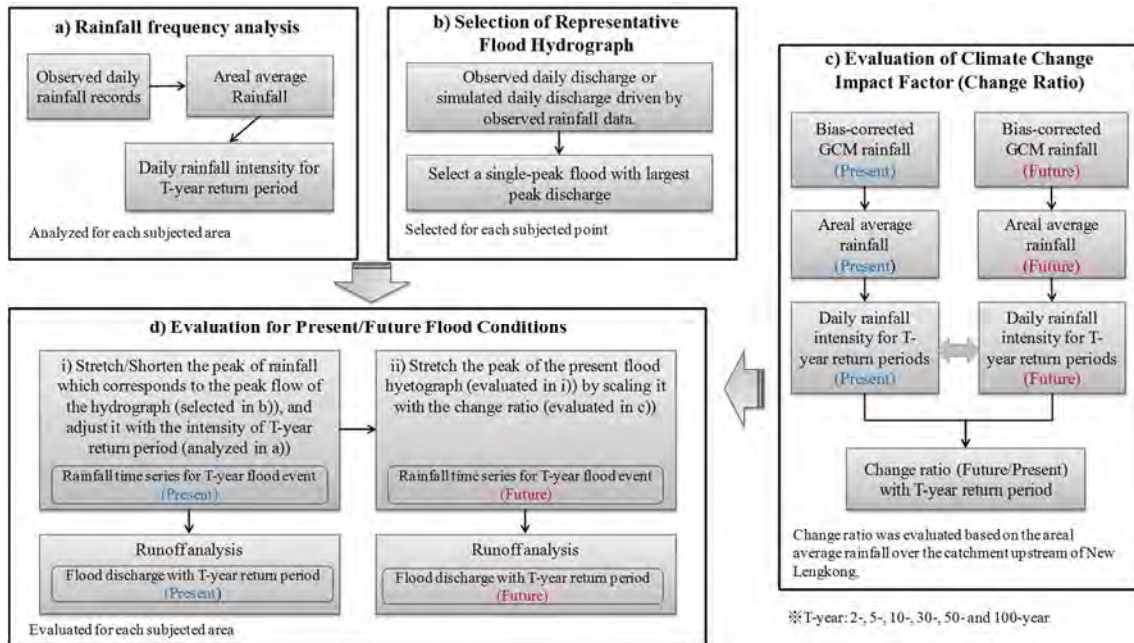


Figure 4.2.4-3 Methodology of evaluation for present/future flood conditions

Finally, we determined six indicators for selecting future scenarios for flood conditions: the change ratio (future/present) of annual maximum 1-day rainfall intensity of the 2-, 5-, 10-, 30-, 50- and 100-year return period events. Areal average rainfall over the upstream of New Lengkong was used for the rainfall frequency analysis. The results of evaluation for present/future flood conditions based on this method are described in the next section (4.2.5).

2) Results of Scenario Selection

Figure 4.2.4-4 shows change ratios (future/present) of extreme rainfall for different return periods. A set of three change factors for extreme rainfall is evaluated for each return period considering the uncertainty of the GCM projection.

CHAPTER 4 CLIMATE CHANGE IMPACT ASSESSMENT AND HYDROLOGICAL SIMULATION

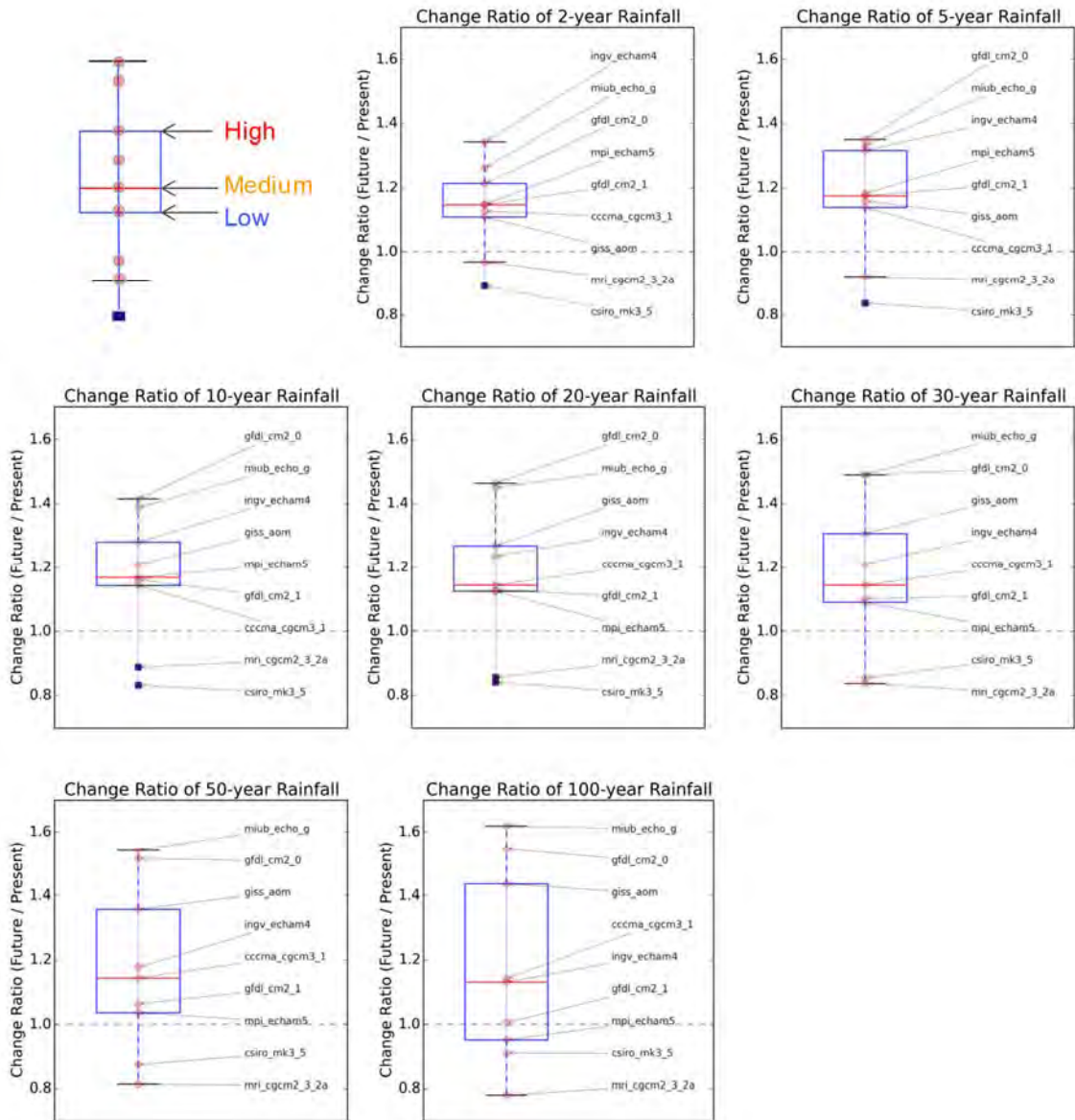


Figure 4.2.4-4 Box plots for change factors (future/present) of extreme rainfall for different return periods

Figure 4.2.4-5 shows change ratio versus return periods for different future scenarios. There exists a linear trend in the plot of change ratios and return periods: the increasing trend in the High scenario and the decreasing trend in the Low scenario. Regarding the Medium scenario, the change ratios show almost a constant value (1.15) for each return period.

CHAPTER 4 CLIMATE CHANGE IMPACT ASSESSMENT AND HYDROLOGICAL SIMULATION

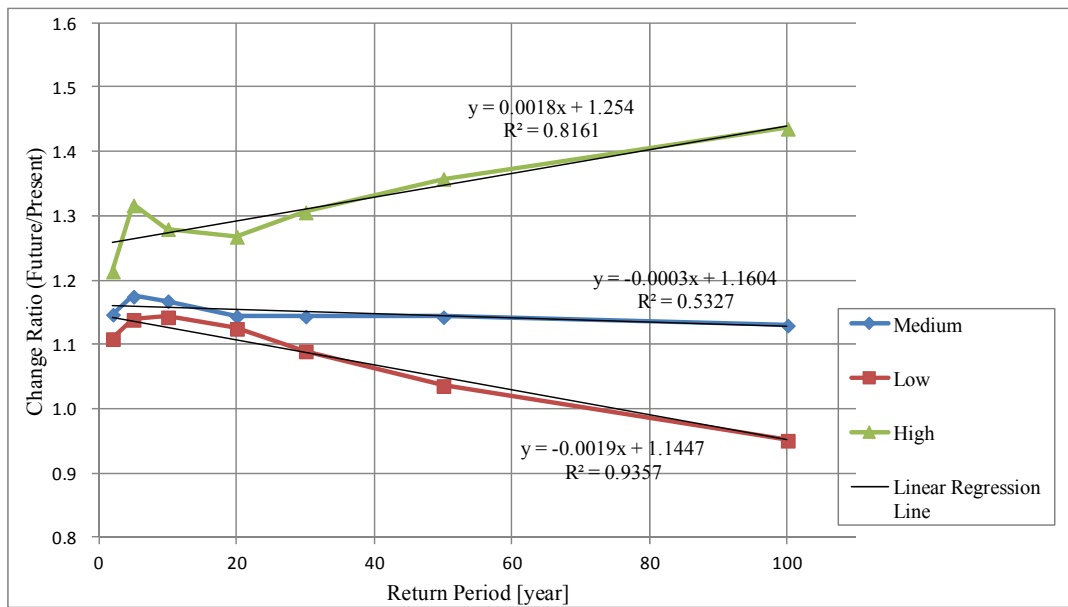


Figure 4.2.4-5 Change Ratio vs. Return Period for different future scenarios

Table 4.2.4-1 summarizes the change factors for extreme rainfall associated with each of the three climate change scenarios. The value on the linear regression line was applied. In addition, the value was rounded up/down in units of 0.05. Finally, the change ratios for extreme rainfall associated with each of the three climate change scenarios are determined.

Table 4.2.4-1 Summary of the change factors for extreme rainfall associated with each of three climate change scenarios (rounded values were applied)

| Return Period | Original Value | | | Value on the regression line | | | Rounded value | | |
|---------------|----------------|--------|------|------------------------------|--------|------|---------------|--------|------|
| | High | Medium | Low | High | Medium | Low | High | Medium | Low |
| 2 | 1.21 | 1.15 | 1.11 | 1.26 | 1.15 | 1.14 | 1.25 | 1.15 | 1.15 |
| 5 | 1.32 | 1.18 | 1.14 | 1.26 | 1.15 | 1.14 | 1.25 | 1.15 | 1.15 |
| 20 | 1.27 | 1.14 | 1.13 | 1.29 | 1.15 | 1.11 | 1.30 | 1.15 | 1.10 |
| 30 | 1.31 | 1.14 | 1.09 | 1.31 | 1.15 | 1.09 | 1.30 | 1.15 | 1.10 |
| 50 | 1.36 | 1.14 | 1.04 | 1.34 | 1.15 | 1.05 | 1.35 | 1.15 | 1.05 |
| 100 | 1.44 | 1.13 | 0.95 | 1.43 | 1.15 | 1.00 | 1.40 | 1.15 | 1.00 |

CHAPTER 4 CLIMATE CHANGE IMPACT ASSESSMENT AND HYDROLOGICAL SIMULATION

4.2.5 Runoff Analysis for Flood Risk Assessment

Runoff calculations were done for four subjected catchments to evaluate future river flood conditions based on the methodology described in section 4.2.4. Land-use changes were also considered as well as extreme rainfall increases.

(1) Brantas River Basin

1) Subjected Catchments

The subjected catchments for flood risk assessment were selected by the team for “Water Resources Management Plan”. Four river catchments were selected: Sadar, Brankal, Widas, and Ngrowo (shown in Figure 4.2.5-1). River discharges from those catchments flow into main stream of the Brantas River, and floods are likely to occur at the junctions of branch and main stream (outlets of subjected catchments). We imposed same climate change factors on all of the subjected catchments and analyzed the responses of peak flows to these changes.

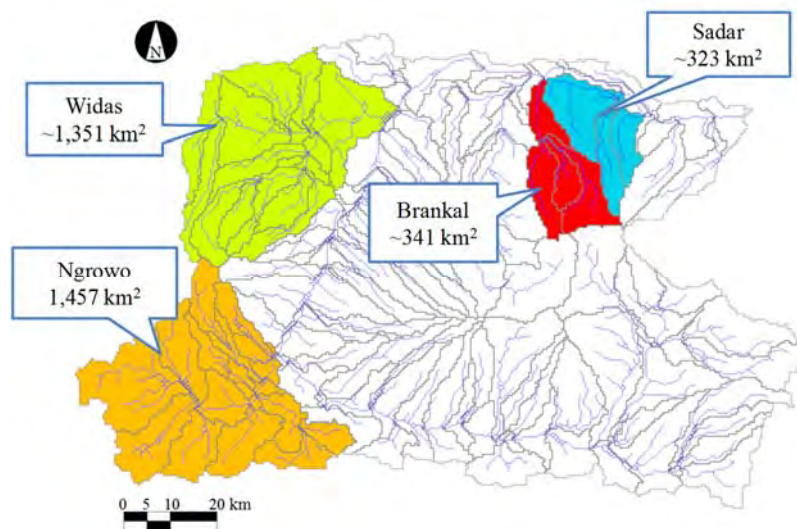


Figure 4.2.5-1 Subjected areas for flood risk assessment in the Brantas River basin

2) Land-use Change

Future land-use in the Brantas River basin was evaluated by the term for “Water Resources Management Plan”. Figure 4.2.5-2 and Figure 4.2.5-3 show present and projected future land-use distribution, respectively. Across the whole basin, change of paddy field to build-up area is dominant. However, change area is limited. The expected percentage of change area is around 8% in the Ngrowo River catchment, and around 3% in the Widas River catchment. No change is expected in the Brankal and Sadar River catchments.

CHAPTER 4 CLIMATE CHANGE IMPACT ASSESSMENT AND HYDROLOGICAL SIMULATION

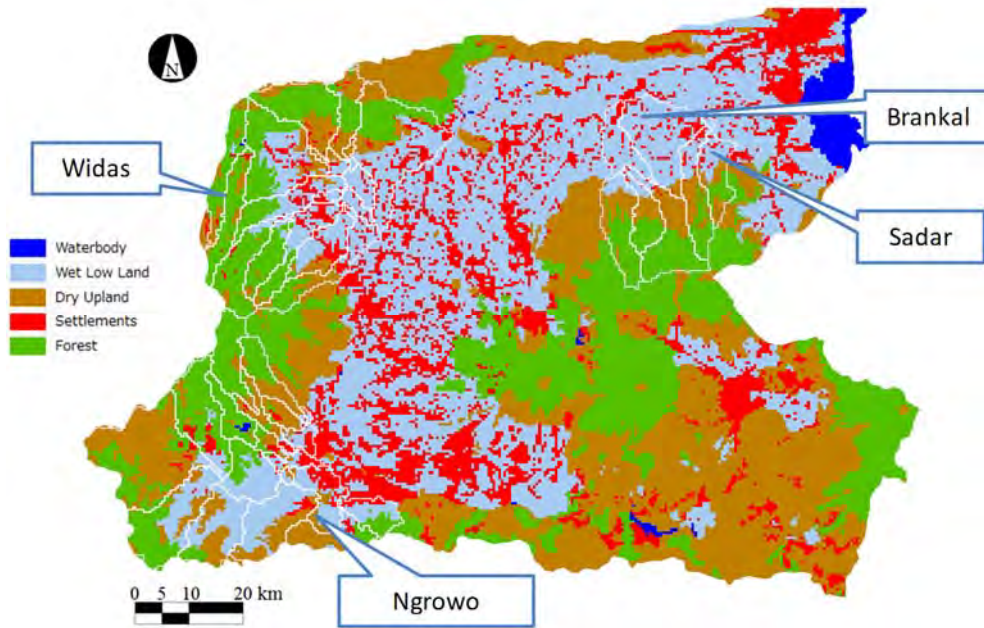


Figure 4.2.5-2 Present Land-use (2010)

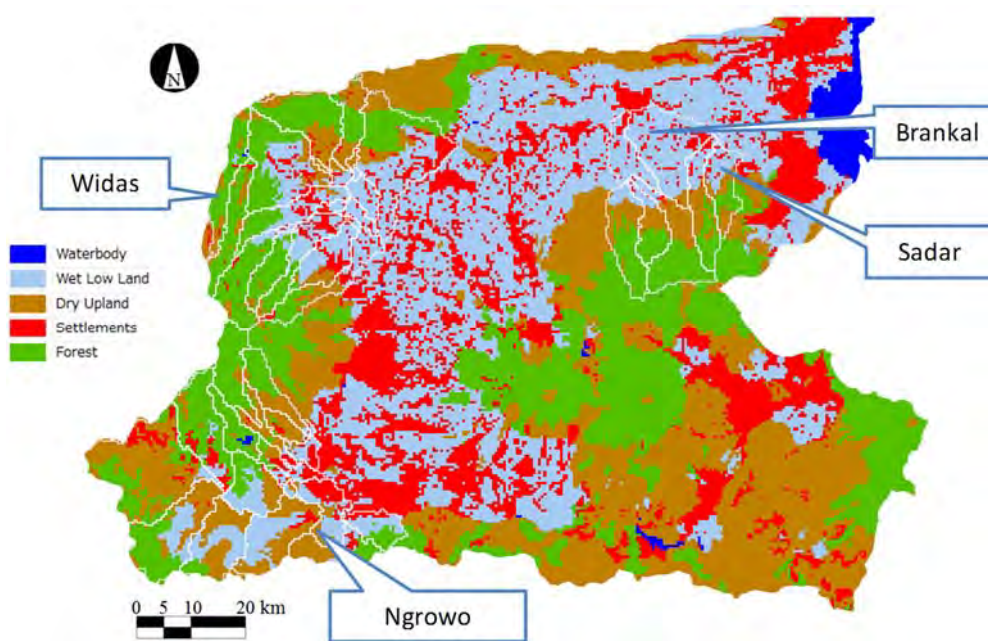


Figure 4.2.5-3 Projected Future Land-use (2050)

CHAPTER 4 CLIMATE CHANGE IMPACT ASSESSMENT AND HYDROLOGICAL SIMULATION

3) Selection of Representative Flood Hydrograph

We selected representative flood hydrographs from simulated discharge with observed rainfall for each subjected catchment. Observed discharge was not used because no data was available at the outlet of subjected catchments.

We extracted the top five flood events (in terms of peak discharge) from the period in which the runoff model was validated This showed good accuracy from 1991 to 2011, except for February-June 2007, February-June 2008, and 2010. Next, we selected a single-peak flood showing clear response to the rain peaks from the extracted five flood events. The top five floods for each catchment are listed in Tables 4.2.5-1~4, and the selected hydrographs are shown in Figures 4.2.5-4~7.

Table 4.2.5-1 Top five floods at the outlet of the Brankal River

| Brankal | | | | | |
|-------------------------------|------|---------------|------|--------|----------|
| discharge [m ³ /s] | | rain [mm/day] | | peak | selected |
| 20-Mar-2006 | 67.7 | 20-Mar-2006 | 97.5 | 1 peak | ✓ |
| 27-Feb-2009 | 64.9 | 27-Feb-2009 | 52.9 | 2 peak | |
| 18-May-2009 | 64.3 | 18-May-2009 | 85.9 | 4 peak | |
| 31-Mar-2009 | 54.3 | 31-Mar-2009 | 50.0 | 1 peak | |
| 17-Jan-2006 | 50.3 | 17-Jan-2006 | 66.6 | 1 peak | |

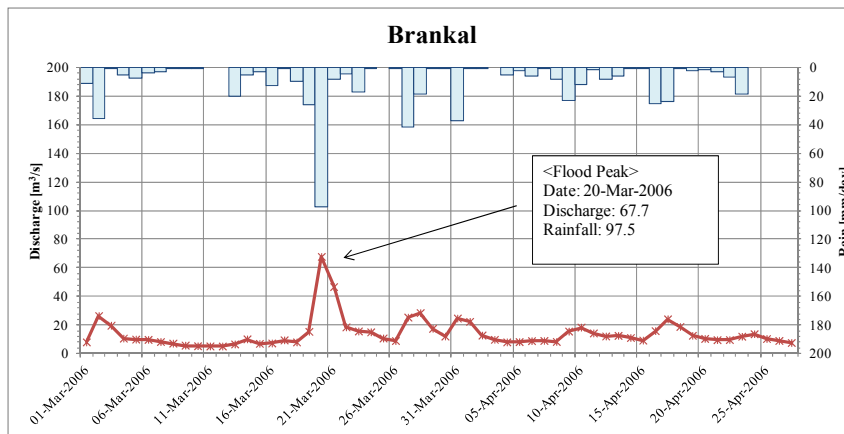


Figure 4.2.5-4 Representative flood hydrograph and hyetograph for the Brankal River catchment

CHAPTER 4 CLIMATE CHANGE IMPACT ASSESSMENT AND HYDROLOGICAL SIMULATION

Table 4.2.5-2 Top 5 floods at the outlet of the Sadar River

| Sadar | | | | | |
|-------------|-------------------------------|---------------|-------|----------|---|
| date | discharge [m ³ /s] | rain [mm/day] | peak | selected | |
| 27-Feb-2009 | 89.5 | 27-Feb-2009 | 58.8 | 2 peak | |
| 18-May-2009 | 72.3 | 18-May-2009 | 95.0 | 4 peak | |
| 20-Mar-2006 | 71.7 | 20-Mar-2006 | 110.9 | 1 peak | ✓ |
| 26-May-2009 | 58.5 | 26-May-2009 | 47.4 | 4 peak | |
| 25-Dec-2007 | 54.6 | 25-Dec-2007 | 97.0 | 1 peak | |

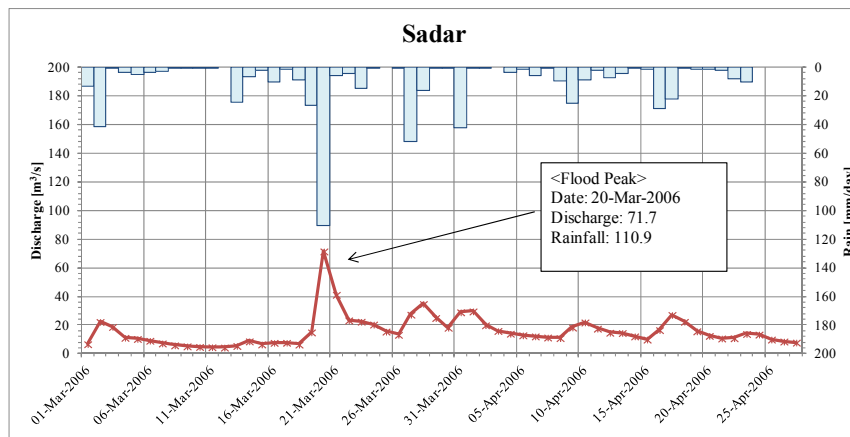


Figure 4.2.5-5 Representative flood hydrograph for the Sadar River catchment

Table 4.2.5-3 Top five floods at the outlet of the Widas River

| Widas | | | | | |
|-------------|-------------------------------|---------------|---------|----------|---|
| date | discharge [m ³ /s] | rain [mm/day] | peak | selected | |
| 3-Dec-2007 | 366.100 | 2-Dec-2007 | 138.190 | 1 peak | ✓ |
| 26-Dec-2007 | 291.702 | 25-Dec-2007 | 106.710 | 1 peak | |
| 31-Jan-2009 | 258.471 | 30-Jan-2009 | 70.378 | 1 peak | |
| 25-Feb-2009 | 250.466 | 24-Feb-2009 | 45.284 | 1 peak | |
| 4-Feb-2004 | 241.326 | 3-Feb-2004 | 86.737 | 1 peak | |

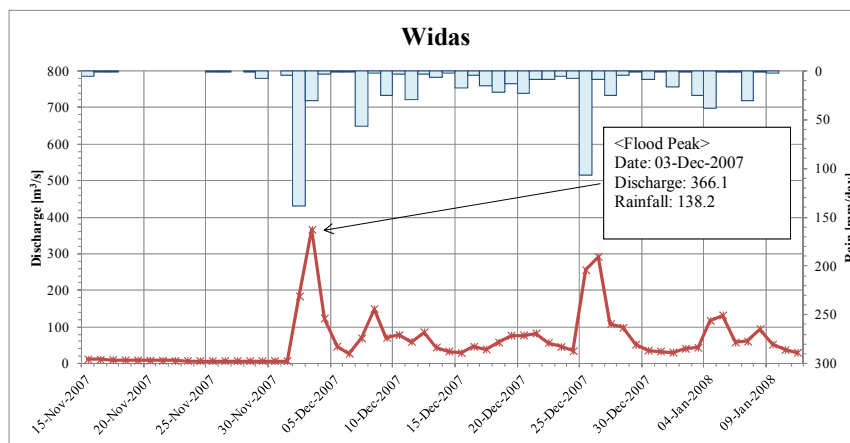


Figure 4.2.5-6 Representative flood hydrograph for the Widas River catchment

Table 4.2.5-4 Top five floods at the outlet of the Ngrowo River

| Ngrowo | | | | | |
|-------------------------------|---------|---------------|--------|--------|----------|
| discharge [m ³ /s] | | rain [mm/day] | | peak | selected |
| 29-May-2004 | 155.388 | 29-May-2004 | 85.600 | 1 peak | ✓ |
| 26-Dec-2007 | 103.066 | 25-Dec-2007 | 80.682 | 1 peak | |
| 14-Apr-2006 | 88.248 | 14-Apr-2006 | 24.536 | 2 peak | |
| 20-Apr-2006 | 83.361 | 19-Apr-2006 | 20.596 | 2 peak | |
| 9-Dec-2003 | 80.164 | 9-Dec-2003 | 55.658 | 1 peak | |

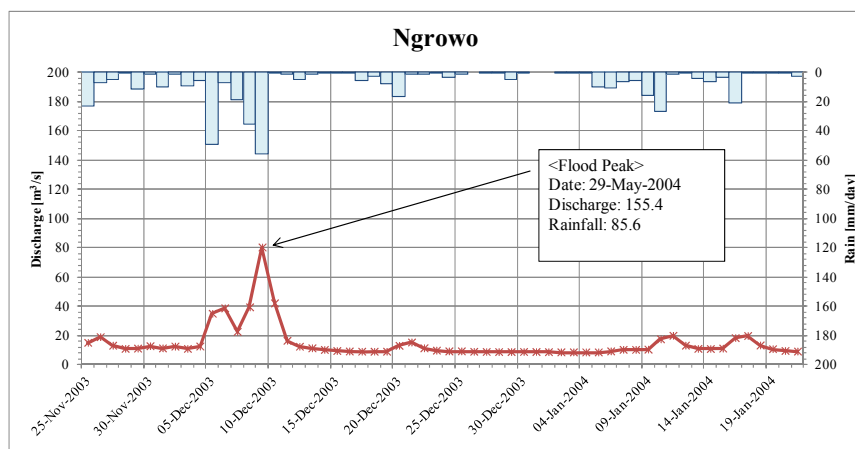


Figure 4.2.5-7 Representative flood hydrograph for the Ngrowo River catchment

4) Stretch/Shorten Ratios for Present and Future Conditions

The stretch/shorten ratios were calculated for each representative flood peak of present and future conditions. We evaluated the magnitude of daily rainfall intensity for 2-, 5-, 10-, 30-, 50-, and 100-year return periods (hereafter referred to as T-year return period) using observed annual maximum daily rainfall records. The results for each catchment are shown in Table 4.2.5-5 and Figure 4.2.5-8. The fitness of probability distribution provided by frequency analysis is appropriate according to Figure 4.2.5-8. Next, we evaluated the magnitude of the peak rainfall intensity, which corresponds to the peak flow of the flood hydrograph. Using the results, the stretch/shorten ratio for T-year return period for the present flood condition was calculated as a ratio of the daily rainfall intensity for T-year return period to the peak rainfall intensity of the flood event. By scaling it with the change ratio for T-year return period (shown in Table 4.2.5-6), the stretch/shorten ratio for T-year return period for the future flood condition was evaluated. The calculated stretch/shorten ratios are summarized in Table 4.2.5-7.

Rainfall series with the intensity of present/future T-year return period can be created by scaling the peak of 1-day rainfall, which corresponds to the peak flow of the hydrograph with the stretch/shorten ratio. Simulated discharge with this rainfall series can be regarded as the present/future flood event with T-year return period.

CHAPTER 4 CLIMATE CHANGE IMPACT ASSESSMENT AND HYDROLOGICAL SIMULATION

Table 4.2.5-5 Return periods of 1-day areal average rainfall for each catchment

| Catchment | Brankal | Sadar | Widas | Ngrowo |
|---------------|---------------------|---------------------|---------------------|---------------------|
| Return Period | 1-day Rainfall [mm] | 1-day Rainfall [mm] | 1-day Rainfall [mm] | 1-day Rainfall [mm] |
| 2-year | 79.8 | 87.1 | 80.2 | 65.9 |
| 5-year | 103.4 | 115.4 | 100.7 | 82.2 |
| 10-year | 119.6 | 135.8 | 115.0 | 93.5 |
| 30-year | 145.3 | 169.5 | 138.0 | 111.4 |
| 50-year | 157.4 | 186.1 | 149.0 | 119.9 |
| 100-year | 174.3 | 209.7 | 164.4 | 131.7 |

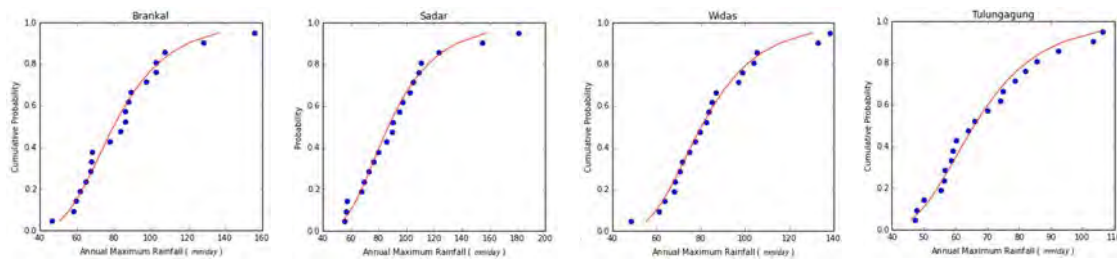


Figure 4.2.5-8 Cumulative probability distributions and plotting positions. Red line: fitted cumulative distribution; Blue dot: Weibull plotting position for observed rainfall data.

Table 4.2.5-6 Change ratios of extreme rainfall for each future scenario (evaluated in section 4.2.4)

| Return Periods | Scenarios | | |
|----------------|-----------|--------|------|
| | High | Medium | Low |
| 2-year | 1.25 | 1.15 | 1.15 |
| 5-year | 1.25 | 1.15 | 1.15 |
| 10-year | 1.25 | 1.15 | 1.10 |
| 30-year | 1.30 | 1.15 | 1.10 |
| 50-year | 1.35 | 1.15 | 1.05 |
| 100-year | 1.40 | 1.15 | 1.00 |

CHAPTER 4 CLIMATE CHANGE IMPACT ASSESSMENT AND HYDROLOGICAL SIMULATION

Table 4.2.5-7 Stretch/shorten ratios for different catchments, return periods, and future scenarios

| Catchment | Brankal | | | | Widas | | | |
|-----------------|-----------------|-----------|-----------|-----------|-----------------|-----------|-----------|-----------|
| Date | 20-Mar-2006 | | | | 2-Dec-2007 | | | |
| Rainfall Amount | 103.06 [mm/day] | | | | 138.19 [mm/day] | | | |
| Return Period | Present | Future(L) | Future(M) | Future(U) | Present | Future(L) | Future(M) | Future(U) |
| 2-year | 0.819 | 0.942 | 0.942 | 1.024 | 0.581 | 0.668 | 0.668 | 0.726 |
| 5-year | 1.060 | 1.219 | 1.219 | 1.325 | 0.729 | 0.838 | 0.838 | 0.911 |
| 10-year | 1.227 | 1.350 | 1.411 | 1.534 | 0.832 | 0.916 | 0.957 | 1.041 |
| 30-year | 1.490 | 1.639 | 1.714 | 1.937 | 0.998 | 1.098 | 1.148 | 1.298 |
| 50-year | 1.615 | 1.695 | 1.857 | 2.180 | 1.078 | 1.132 | 1.240 | 1.455 |
| 100-year | 1.787 | 1.787 | 2.055 | 2.502 | 1.190 | 1.190 | 1.368 | 1.665 |
| Catchment | Sadar | | | | Ngrowo | | | |
| Date | 20-Mar-2006 | | | | 25-Dec-2007 | | | |
| Rainfall Amount | 110.89 [mm/day] | | | | 78.341 [mm/day] | | | |
| Return Period | Present | Future(L) | Future(M) | Future(U) | Present | Future(L) | Future(M) | Future(U) |
| 2-year | 0.785 | 0.903 | 0.903 | 0.981 | 0.770 | 0.885 | 0.885 | 0.962 |
| 5-year | 1.040 | 1.196 | 1.196 | 1.300 | 0.960 | 1.104 | 1.104 | 1.200 |
| 10-year | 1.225 | 1.347 | 1.408 | 1.531 | 1.092 | 1.202 | 1.256 | 1.366 |
| 30-year | 1.528 | 1.681 | 1.758 | 1.987 | 1.302 | 1.432 | 1.497 | 1.692 |
| 50-year | 1.678 | 1.762 | 1.930 | 2.265 | 1.401 | 1.471 | 1.611 | 1.891 |
| 100-year | 1.891 | 1.891 | 2.175 | 2.648 | 1.539 | 1.539 | 1.770 | 2.155 |

5) Results

Runoff calculations were conducted for the future/present flood event with 2-, 5-, 10-, 30-, 50-, and 100-year return period with future/present land-use conditions.

a) Impact of Land-use Change on the Flood Regime

To check the effects of land-use changes on the flood regime, we compared simulated discharges with future land-use condition and that with present land-use conditions. The comparison was done for three river sites: the outlet of the Widas River, outlet of the Ngrowo River, and the New Lengkong. The results showed almost no differences between the present and future (see in Figure 4.2.5-9, 4.2.5-10, and 4.2.5-11). Projected land-use changes proved to have a negligible impact on the basin. This is because the change area is too small (less than 10%) to have an effect on the flood discharge.

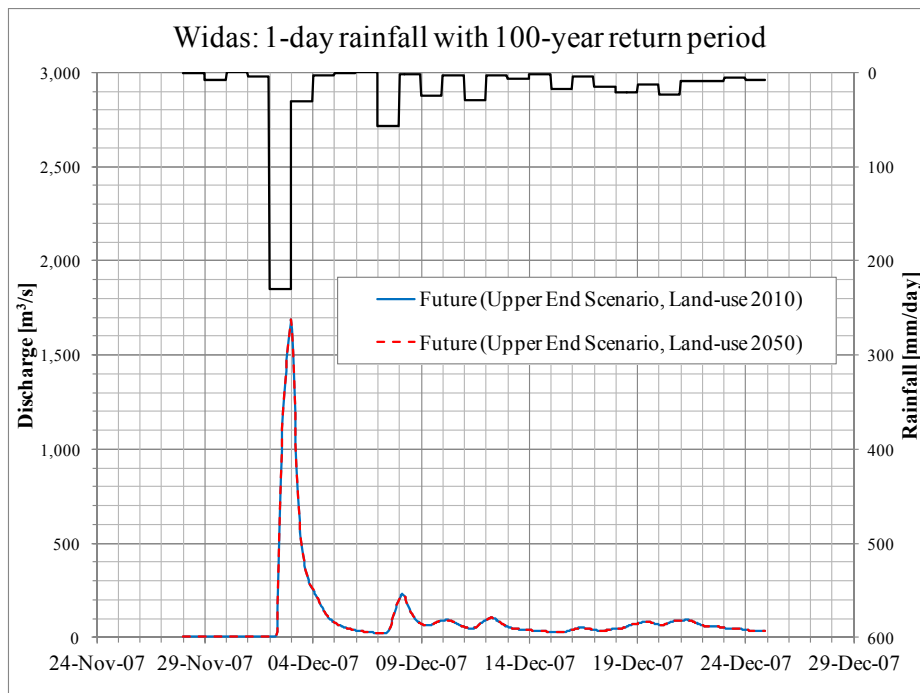


Figure 4.2.5-9 Simulated flood discharge driven by 100-year return period rainfall at the outlet of the Widas River. Blue solid line: under present land-use (2010); Red solid line: under projected future (2050) land-use.

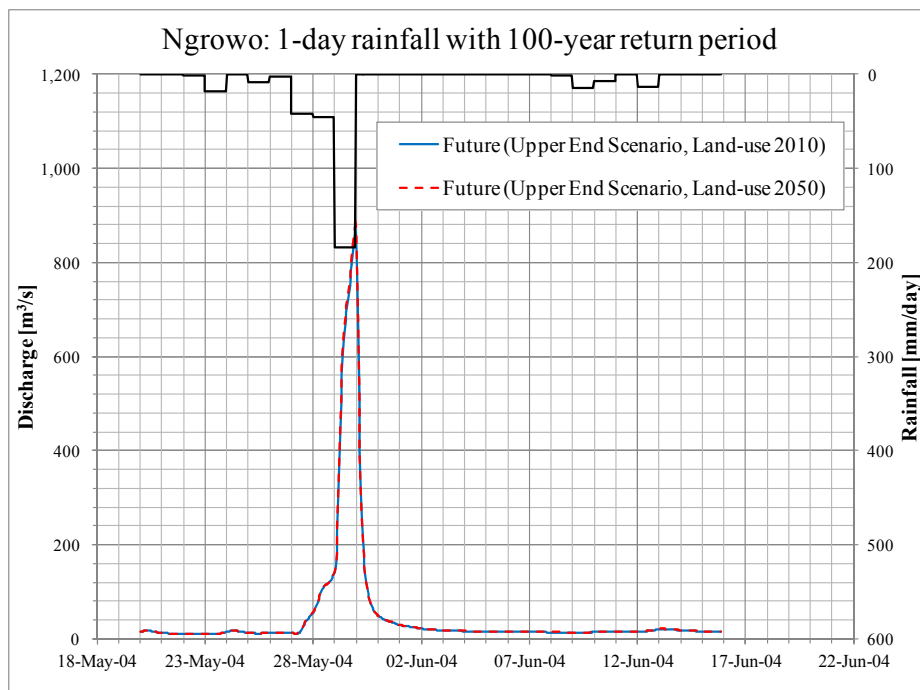


Figure 4.2.5-10 Same as Figure 4.2.5-9 but for the outlet of the Ngrowo River

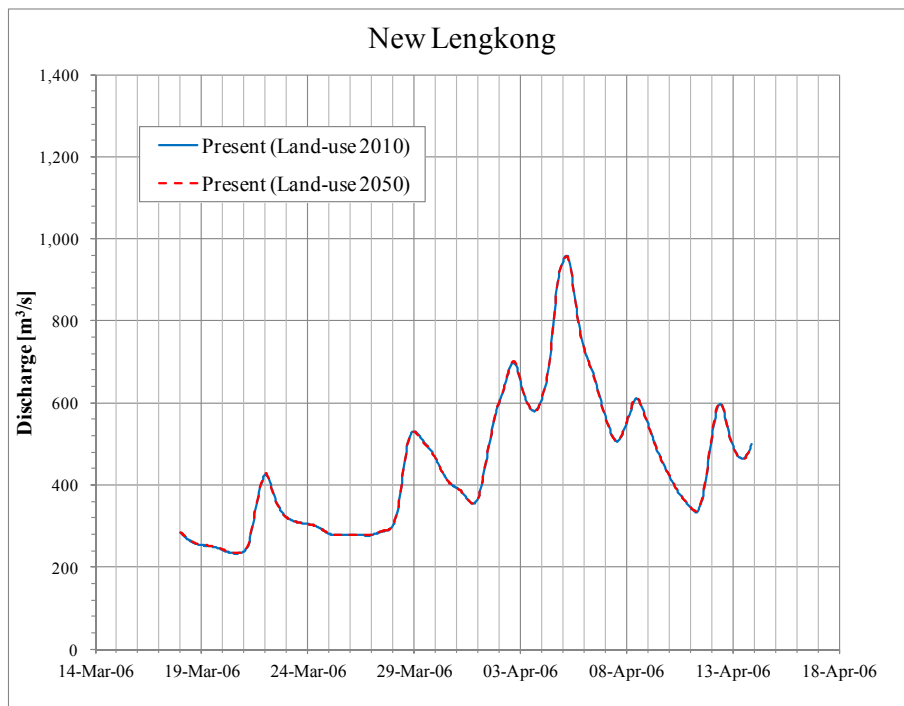


Figure 4.2.5-11 Simulated flood discharge at New Lengkong with observed rainfall. Blue solid line: present land-use (2010) was applied; Red solid line: projected future (2050) land-use was applied.

b) Impact of Climate Change on the Flood Regime

The impact of climate change on the flood regime was evaluated by comparing simulated flood discharges with different extreme rainfall scenarios (present and three sets of future scenarios). The simulated hydrograph are shown in Figures 4.2.5-12~15. Change ratios of flood peak discharge for a given return period were calculated as ratio of the future flood peak discharge to the present flood peak discharge and shown in Tables 4.2.5-8~11.

The change in flood peak discharge is more significant than that of rainfall when the magnitude of flood discharge is large. Regarding the Brankal River basin for the 100-year return period, the increase in the intensity of rainfall of 40% causes a raise in peak discharge of the flood hydrograph by 90%, showing the change of flood peak discharge is more than twice as large as that of rainfall. This is because water generally flows faster as its volume increases.

The results indicate severe flooding conditions in the future climate. Inundation simulations will be carried out using the evaluated present/future flood hydrograph, and future flood risk will be analyzed in the subsequent study component for “Water Resources Management Plan”.

CHAPTER 4 CLIMATE CHANGE IMPACT ASSESSMENT AND HYDROLOGICAL SIMULATION

Table 4.2.5-8 Intensity and change ratios of simulated flood peak discharges for different future scenarios and different return periods at the outlet of the Brankal River

| Return Periods | Peak Discharge [m ³ /s] | | | | Change Ratio of Peak Discharge (Future/Present) | | |
|----------------|------------------------------------|------------|------------|------------|---|------------|------------|
| | Present | Future (L) | Future (M) | Future (H) | Future (L) | Future (M) | Future (H) |
| RP2 | 75.3 | 86.2 | 86.2 | 93.5 | 1.14 | 1.14 | 1.24 |
| RP5 | 96.8 | 112.0 | 112.0 | 124.5 | 1.16 | 1.16 | 1.29 |
| RP10 | 112.8 | 127.9 | 136.1 | 155.6 | 1.13 | 1.21 | 1.38 |
| RP30 | 147.8 | 175.5 | 189.8 | 239.5 | 1.19 | 1.28 | 1.62 |
| RP50 | 170.9 | 186.2 | 220.7 | 299.0 | 1.09 | 1.29 | 1.75 |
| RP100 | 204.8 | 204.8 | 267.5 | 388.8 | 1.00 | 1.31 | 1.90 |

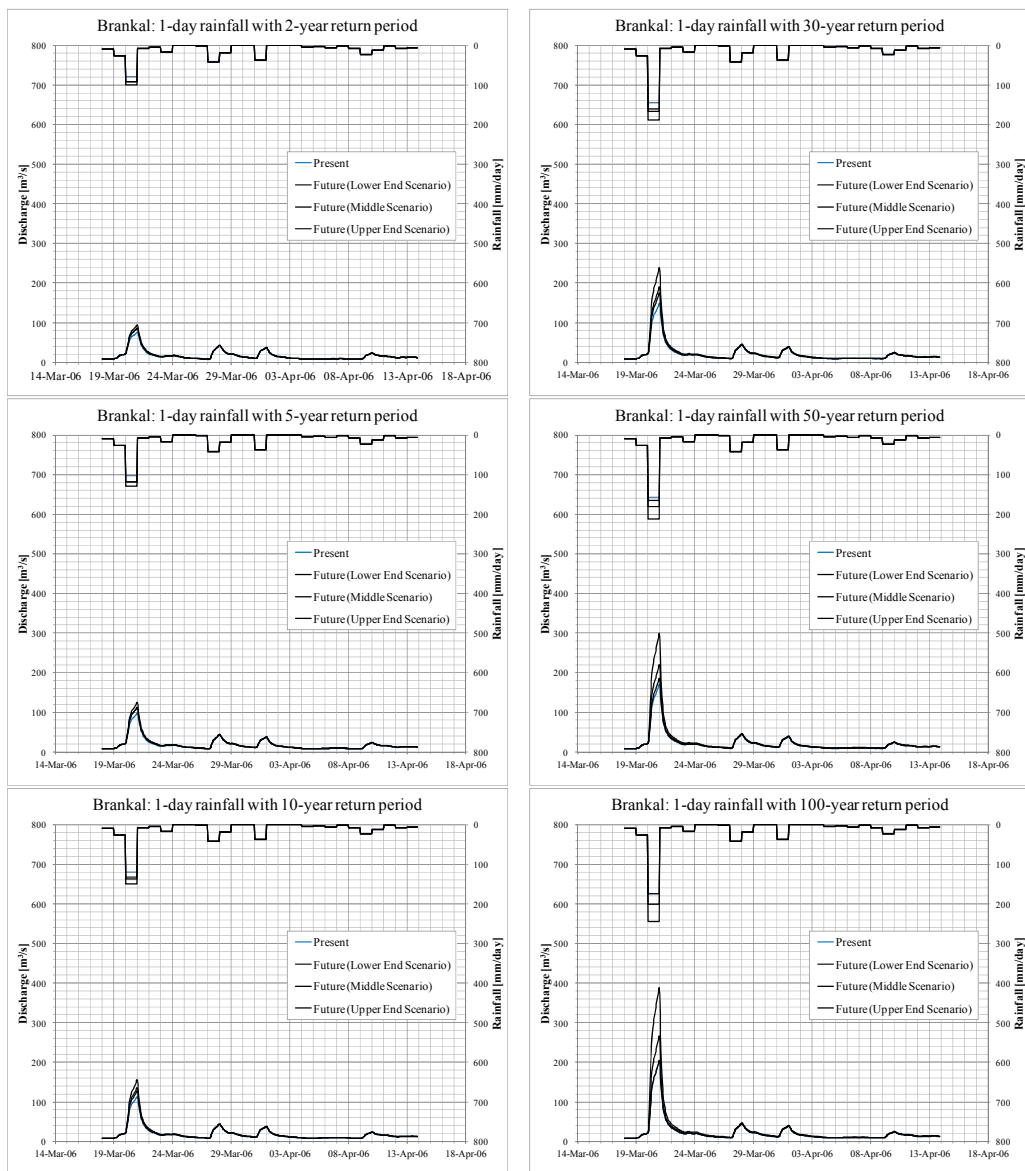


Figure 4.2.5-12 Results of runoff simulation for different return periods and different scenarios at the outlet of the Brankal River. Blue solid line: present condition; black solid line: future conditions for three scenarios.

CHAPTER 4 CLIMATE CHANGE IMPACT ASSESSMENT AND HYDROLOGICAL SIMULATION

Table 4.2.5-9 Same as Table 4.2.5-8 but for the outlet of the Sadar River

| Return Periods | Peak Discharge [m^3/s] | | | | Change Ratio of Peak Discharge (Future/Present) | | |
|----------------|--|------------|------------|------------|---|------------|------------|
| | Present | Future (L) | Future (M) | Future (H) | Future (L) | Future (M) | Future (H) |
| RP2 | 72.2 | 83.3 | 83.3 | 90.4 | 1.15 | 1.15 | 1.25 |
| RP5 | 96.0 | 111.3 | 111.3 | 121.4 | 1.16 | 1.16 | 1.26 |
| RP10 | 114.1 | 126.1 | 132.1 | 144.5 | 1.11 | 1.16 | 1.27 |
| RP30 | 144.1 | 160.6 | 169.4 | 199.9 | 1.11 | 1.18 | 1.39 |
| RP50 | 160.2 | 170.1 | 192.1 | 252.8 | 1.06 | 1.20 | 1.58 |
| RP100 | 186.4 | 186.4 | 234.1 | 357.3 | 1.00 | 1.26 | 1.92 |

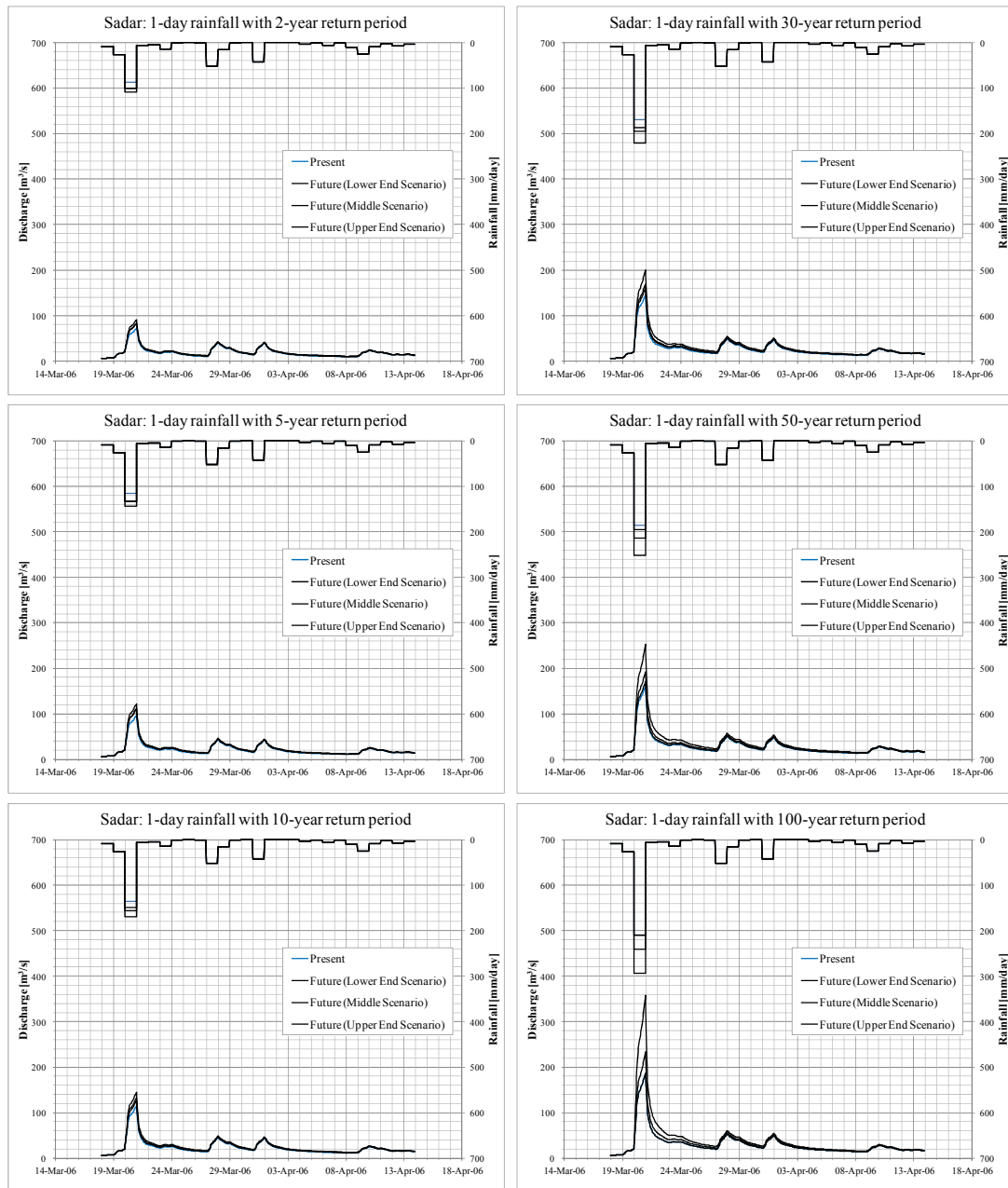


Figure 4.2.5-13 Same as Figure 4.2.5-12 but for the outlet of the Sadar River

CHAPTER 4 CLIMATE CHANGE IMPACT ASSESSMENT AND HYDROLOGICAL SIMULATION

Table 4.2.5-10 Same as Table 4.2.5-8 but for the outlet of the Widas River

| Return Periods | Peak Discharge [m^3/s] | | | | Change Ratio of Peak Discharge (Future/Present) | | |
|----------------|--|------------|------------|------------|---|------------|------------|
| | Present | Future (L) | Future (M) | Future (H) | Future (L) | Future (M) | Future (H) |
| RP2 | 264.5 | 335.5 | 335.5 | 383.0 | 1.27 | 1.27 | 1.45 |
| RP5 | 385.5 | 476.7 | 476.7 | 539.5 | 1.24 | 1.24 | 1.40 |
| RP10 | 471.7 | 544.1 | 583.0 | 671.1 | 1.15 | 1.24 | 1.42 |
| RP30 | 624.3 | 739.1 | 804.5 | 1032.2 | 1.18 | 1.29 | 1.65 |
| RP50 | 714.4 | 783.0 | 938.7 | 1303.3 | 1.10 | 1.31 | 1.82 |
| RP100 | 863.0 | 863.0 | 1150.2 | 1688.4 | 1.00 | 1.33 | 1.96 |

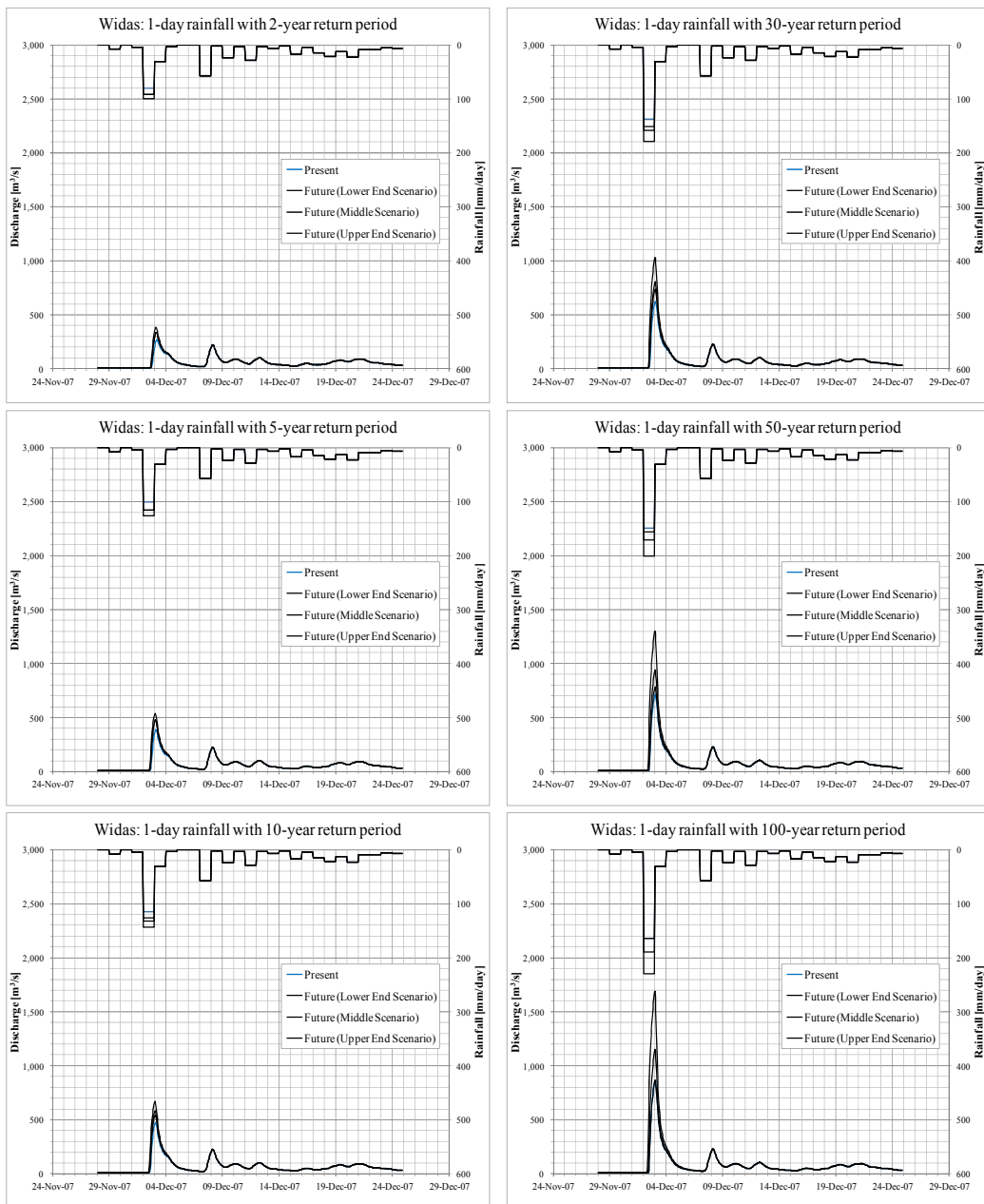


Figure 4.2.5-14 Same as Figure 4.2.5-12 but for the outlet of the Widas River

CHAPTER 4 CLIMATE CHANGE IMPACT ASSESSMENT AND HYDROLOGICAL SIMULATION

Table 4.2.5-11 Same as Table 4.2.5-8 but for the outlet of the Ngrowo River

| Return Periods | Peak Discharge [m^3/s] | | | | Change Ratio of Peak Discharge (Future/Present) | | |
|----------------|--|------------|------------|------------|---|------------|------------|
| | Present | Future (L) | Future (M) | Future (H) | Future (L) | Future (M) | Future (H) |
| RP2 | 143.0 | 144.0 | 144.0 | 155.4 | 1.01 | 1.01 | 1.09 |
| RP5 | 155.0 | 185.5 | 185.5 | 212.9 | 1.20 | 1.20 | 1.37 |
| RP10 | 182.7 | 213.6 | 231.6 | 274.8 | 1.17 | 1.27 | 1.50 |
| RP30 | 248.8 | 304.7 | 338.9 | 463.6 | 1.22 | 1.36 | 1.86 |
| RP50 | 290.2 | 324.6 | 407.8 | 620.2 | 1.12 | 1.41 | 2.14 |
| RP100 | 363.1 | 363.1 | 522.0 | 877.8 | 1.00 | 1.44 | 2.42 |

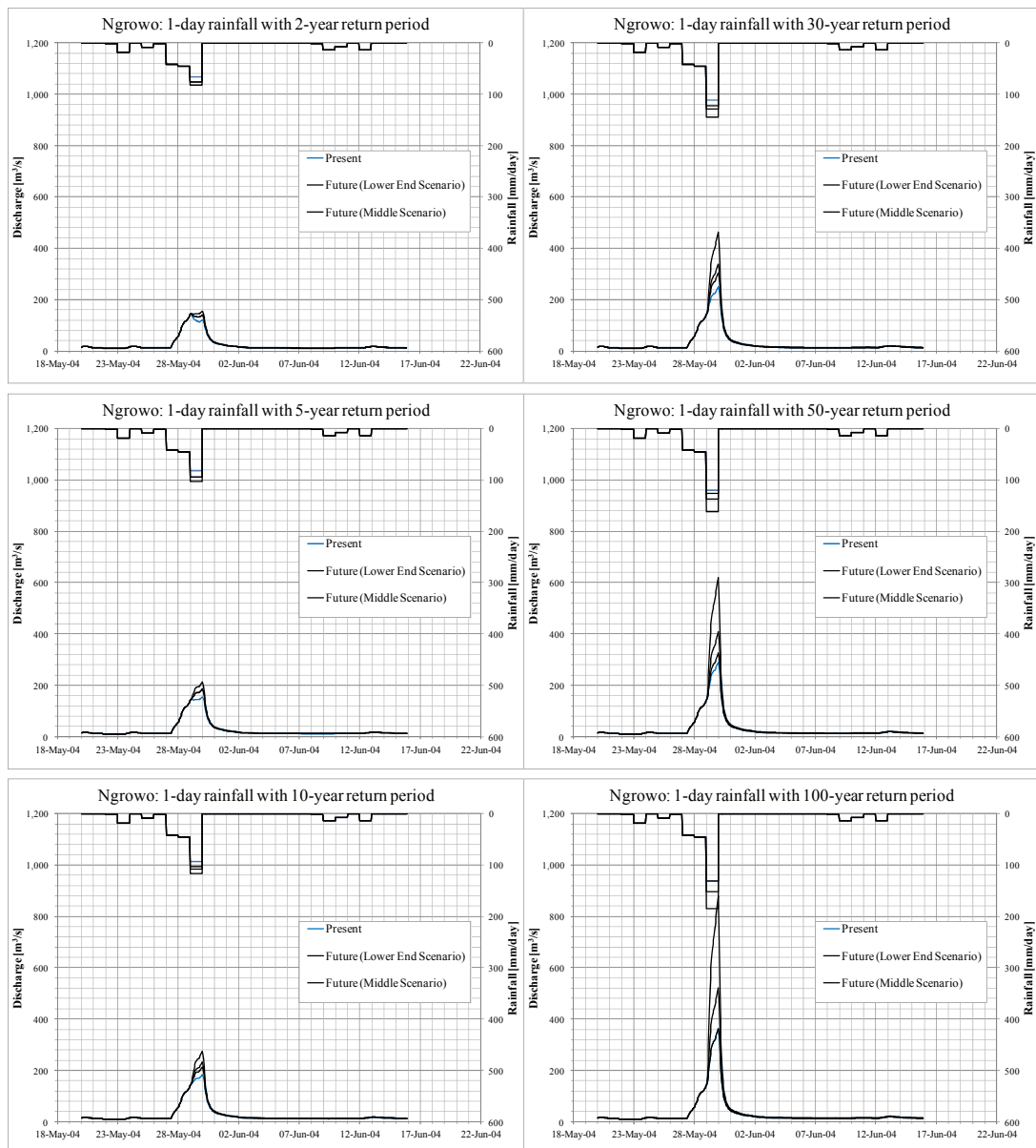


Figure 4.2.5-15 Same as Figure 4.2.5-12 but for the outlet of the Ngrowo River

CHAPTER 4 CLIMATE CHANGE IMPACT ASSESSMENT AND HYDROLOGICAL SIMULATION

4.3 Implementation of Rainfall-runoff Analysis Considering Climate Change Impact Assessment: Musi River Basin

4.3.1 Overview of Targeted Basins

(1) Musi River Basin

1) Basin Characteristics

The Musi river basin is located in the southern part of Sumatra Island, with a total catchment area of 60,000 km². This is a typical tropical rainforest basin, well-developed in its agricultural (rice) production methods. There are four types of agricultural rice production systems in Musi: tidal swamp paddy, freshwater swamp paddy, irrigated rice, and rain-fed rice systems. Table 4.3.1-1 gives short descriptions and sample figures for each type.

Table 4.3.1-1 The four types of agricultural rice production systems.

| | |
|---|---|
|  |  |
| <p><i>Tidal Swamp Paddy:</i> the main irrigation source is the upsurge in the tide from the nearby river.</p> | <p><i>Freshwater Swamp Paddy:</i> the main irrigation source is rain that pools as a swamp/marshland.</p> |
|  |  |
| <p><i>Irrigated Paddy:</i> a rice production system with a sophisticated irrigation system. Water is transported from a reservoir via canals.</p> | <p><i>Rain-fed Paddy:</i> a rice production system that is wholly dependent on rainfall for irrigation.</p> |

CHAPTER 4 CLIMATE CHANGE IMPACT ASSESSMENT AND HYDROLOGICAL SIMULATION

Palembang (Figure 4.3.1-1), the most populated (1,742,186 people (2013, Pemerintah Kota Palembang)) and second largest city (capital) on the island, is located 100 km from the mouth of the Musi River basin. Musi River basin drains through Palembang and then joins several other rivers, including the Banyuasin River, to form a delta near the city of Sungsang. The river (about 750 km long with a depth of about 6.5 meters), is navigable by large ships as far as Palembang, which is the site of major port facilities (for petroleum, rubber, and coal exports).



Figure 4.3.1-1 Downstream of Musi: Ampera Bridge, Palembang, South Sumatra.

Upstream of the basin on the west coast of Sumatra is the Musi Hydro-electric power plant (Figure 4.3.1-2). This power plant was first proposed in 1965 considering the need for electric power in Sumatra and to anticipate the ever increasing demand for electricity in the future, especially for the Southern Sumatra (Musi) region. A detailed study on the dam was conducted in 1981-1983 prior to its construction. The hydropower plant is located in the district of Musi Rejang Lebong (upstream Musi river basin) while the outflow sections are in the Susup Village area of the district Taba Penanjung, North Bengkulu (outside Musi river basin). (See location map page ii for this river basin)



Figure 4.3.1-2 Upstream of Musi: PLTA Musi (Pembangkitan Sumbagsel-Sektor Pembangkitan Bengkulu).

CHAPTER 4 CLIMATE CHANGE IMPACT ASSESSMENT AND HYDROLOGICAL SIMULATION

2) Climate

The typical climate in the Musi river basin is a tropical rainforest climate with relatively high humidity and winds ranging from 2.3 km/h to 4.5 km/h. Air temperature ranges from 23.4 to 31.7° C . Annual rainfall ranges from 2000 mm to 3000 mm. Humidity ranges from 75% to 89% with an average of 45% annual sunshine. During the wettest months, the city's marshlands (freshwater swamp paddies) are inundated. Average temperatures are nearly identical throughout the year.

3) Observations and Data

Data collection has proven to be very challenging in this basin.

a) Dynamic Parameters

a-1) Other Meteorological Parameters

The meteorological parameters were taken from the Japan Reanalysis data (JRA-25), (surface air temperature (K); relative humidity (%); total cloud cover (%); downward long wave and short wave radiation flux at surface (W/m²), (surface pressure (Pa); surface 10 m zonal wind (m/s) and surface 10 m meridional wind (m/s)). The downward solar radiation was estimated from sunshine duration, temperature, and humidity using a hybrid model developed by Yang et al. (2006). The longwave radiation was estimated from temperature, relative humidity, surface pressure, and solar radiation using the relationship between solar radiation and longwave radiation (Crawford and Duchon, 1999).

a-2) Rainfall

One of the primary datasets collected is rainfall. Due to the remote conditions of this basin, good quality rainfall data is quite difficult to obtain. Historical rainfall provided by PUSAIR was well distributed throughout the basin, however, there were many long breaks (months or even years) in the daily data provided. Because of this, additional rainfall sources were analyzed to see if they could be used as substitute for the missing rainfall data during the data breaks.

Figure 4.3.1-3 shows the locations. This data, although well distributed throughout the basin, shows some problematic/incomplete data is available at very few stations. This sparse availability of data requires some inclusion of additional information either from satellite data or from other global data sources.

For Monsoon Asia, the APHRODITE (Asian precipitation-highly resolved observational data integration towards the evaluation of water resources management dataset) was explored on whether or not it could represent the seasonality in this region. APHRODITE contains a dense network of daily rain-gauge data for Asia, including the Himalayas, South and Southeast Asia, and mountainous areas in the Middle East. The number of valid stations was between 5,000 and 12,000, representing 2.3 to 4.5 times the data available through the Global Telecommunication System network, which were used for most daily grid precipitation products. It is a long-term, continental scale 52-year gridded (0.25o x 0.25o; 0.5o x 0.5o) daily precipitation dataset (1951-2007).

The APHRODITE dataset was also run in the WEB-DHM and was found to completely

CHAPTER 4 CLIMATE CHANGE IMPACT ASSESSMENT AND HYDROLOGICAL SIMULATION

misrepresent the discharges (both frequency and intensity) by a couple of months, as the seasonality of the APHRODITE is different from that typically observed in South Sumatra.

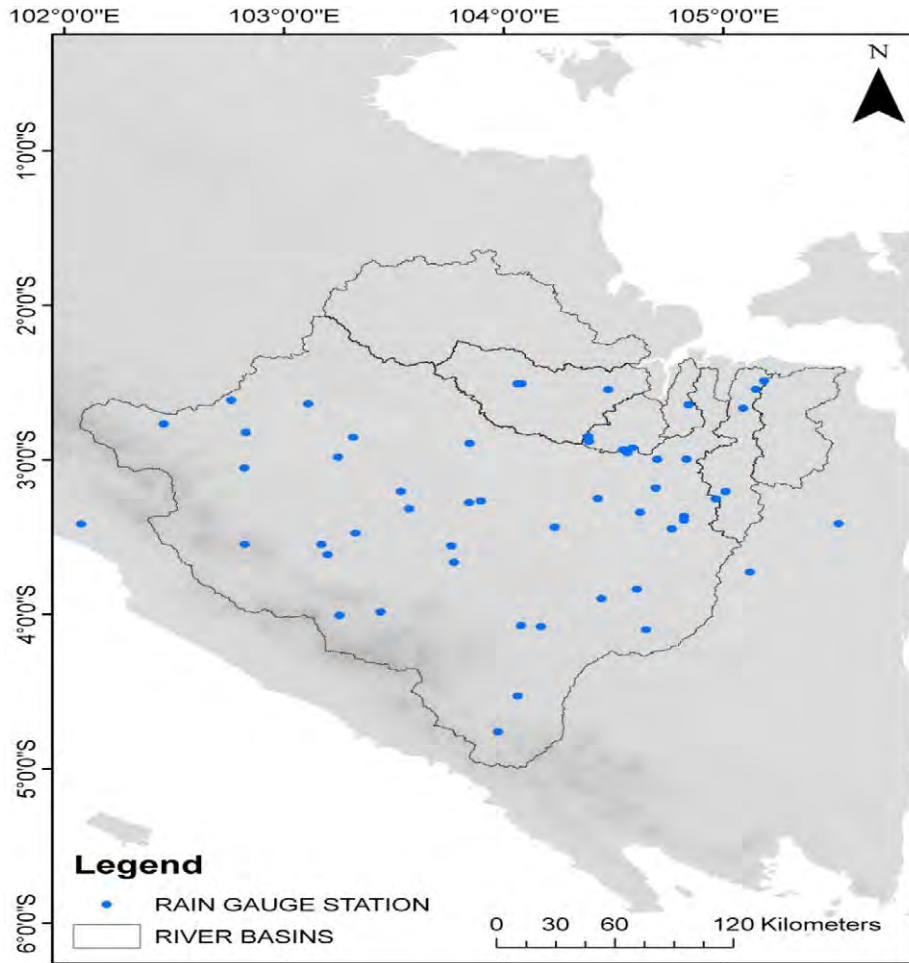


Figure 4.3.1-3 Fifty-Three (53) rainfall gauges distributed throughout the seven basins.

The interpolated rain gauge data was also incorporated into the model and was found to either overestimate or underestimate (intensity issues) depending on the available data for that year. But, it was found to at least have similar frequency as that of observed discharges (peak discharges occur on the correct months as compared to trial simulations for APHRODITE). From the results of this trial run, we recommend to utilize the sparse rainfall data available thru PUSAIR instead of APHRODITE. To compensate the low spatial density and data quality, the daily data from BMKG was added. After the detail data quality assessment, the 21 rain gauge station data was selected as shown in Table 4.3.1-2.

CHAPTER 4 CLIMATE CHANGE IMPACT ASSESSMENT AND HYDROLOGICAL SIMULATION

Table 4.3.1-2 Selected rainfall data and its availability per year.

| No. | Gauging Station Name | Longitude | Latitude | Source Agency | 1980 | 1981 | 1982 | 1983 | 1984 | 1985 | 1986 | 1987 | 1988 | 1989 | 1990 | 1991 | 1992 | 1993 | 1994 | 1995 | 1996 | 1997 | 1998 | 1999 | 2000 | 2001 | 2002 | 2003 | 2004 | 2005 | 2006 | 2007 | 2008 | 2009 | 2010 | 2011 | 2012 | 2013 |
|--------------------|----------------------|-----------|----------|---------------|------|------|------|------|------|------|------|------|------|------|------|------|------|------|------|------|------|------|------|------|------|------|------|------|------|------|------|------|------|------|------|------|------|------|
| 001 | alicia | 104.544 | -2.938 | BMKG | | | | | | | | | | | | | | | | | | | | | | | | | | | | | | | | | | |
| 010 | Gelumbang | 104.429 | -3.254 | BMKG | | | | | | | | | | | | | | | | | | | | | | | | | | | | | | | | | | |
| 020 | Karang Jawa | 102.758 | -2.615 | BMKG | | | | | | | | | | | | | | | | | | | | | | | | | | | | | | | | | | |
| 026 | Kenten (2) | 104.710 | -3.000 | BMKG | | | | | | | | | | | | | | | | | | | | | | | | | | | | | | | | | | |
| 032 | Lahat | 103.562 | -3.782 | BMKG | | | | | | | | | | | | | | | | | | | | | | | | | | | | | | | | | | |
| 043 | Melania | 104.564 | -2.958 | BMKG | | | | | | | | | | | | | | | | | | | | | | | | | | | | | | | | | | |
| 048 | Muara Beliti I | 103.038 | -3.246 | BMKG | | | | | | | | | | | | | | | | | | | | | | | | | | | | | | | | | | |
| 062 | Pampangan | 105.012 | -3.209 | BMKG | | | | | | | | | | | | | | | | | | | | | | | | | | | | | | | | | | |
| 070 | Pendopo | 102.960 | -3.790 | BMKG | | | | | | | | | | | | | | | | | | | | | | | | | | | | | | | | | | |
| 089 | SMB II | 104.701 | -2.900 | BMKG | | | | | | | | | | | | | | | | | | | | | | | | | | | | | | | | | | |
| 094 | Sampang Campang | 103.769 | -4.516 | BMKG | | | | | | | | | | | | | | | | | | | | | | | | | | | | | | | | | | |
| 095 | Srilaton | 102.922 | -3.203 | BMKG | | | | | | | | | | | | | | | | | | | | | | | | | | | | | | | | | | |
| 099 | Sumber Harta | 102.960 | -3.050 | BMKG | | | | | | | | | | | | | | | | | | | | | | | | | | | | | | | | | | |
| 110 | Tebing Tinggi | 103.075 | -3.598 | BMKG | | | | | | | | | | | | | | | | | | | | | | | | | | | | | | | | | | |
| 119 | 006 Beltang | 104.648 | -4.106 | PU | | | | | | | | | | | | | | | | | | | | | | | | | | | | | | | | | | |
| 122 | 009 Cilika | 104.822 | -3.369 | PU | | | | | | | | | | | | | | | | | | | | | | | | | | | | | | | | | | |
| 127 | 017 KupangTB Tinggi | 103.195 | -3.616 | PU | | | | | | | | | | | | | | | | | | | | | | | | | | | | | | | | | | |
| 136 | 027 Pagar Alam | 103.249 | -4.011 | PU | | | | | | | | | | | | | | | | | | | | | | | | | | | | | | | | | | |
| 140 | 031 Pangkajene Bahai | 104.389 | -2.884 | PU | | | | | | | | | | | | | | | | | | | | | | | | | | | | | | | | | | |
| 150 | 042 Terawas | 102.824 | -3.223 | PU | | | | | | | | | | | | | | | | | | | | | | | | | | | | | | | | | | |
| 20stations Average | | | | | 0.10 | 0.15 | 0.21 | 0.29 | 0.29 | 0.75 | 0.44 | 0.83 | 0.87 | 0.87 | 0.98 | 0.86 | 0.82 | 0.76 | 0.78 | 0.75 | 0.73 | 0.65 | 0.73 | 0.69 | 0.66 | 0.74 | 0.55 | 0.45 | 0.68 | 0.60 | 0.56 | 0.57 | 0.68 | 0.68 | 0.55 | 0.63 | 0.71 | 0.43 |

| | |
|--|----------------------|
| | 100% - Available |
| | 90 - 99% - Available |
| | 80 - 89% - Available |
| | 70 - 79% - Available |
| | 1 - 69% - Available |
| | 0% - No Data |

a-3) Discharge and water level gauges

Discharge data is one of the primary sources of information for basin calibration. The terrain of the basin (densely forested and mountainous) makes it quite challenging to maintain good quality data. Selected water level gauging sites were considered (Figure 4.3.1-4) to account for the water level and discharge measurements for calibration of the hydrological models (WEB-DHM for discharge, 1D model for the water level fluctuations at different sites; IRA for inundation). A list of all the gauge stations is given in Table 4.3.1-3. However, due to poor accessibility and maintenance of the discharge gauges, only the years marked in red filled circles have complete discharge data from PUSAIR (red circles) and PSDA (blue circles) have complete information. While those marked with unfilled (white) circles have complete water level data from BBWS. Unfortunately, only a few stations have available data. The highlighted stations (in grey) show the selected discharge stations we selected for our model calibrations. Data in these strategic stations are also incomplete, but we will be using some of the better quality datasets for our basin calibration. For the continuity of our analysis, after calibration of the basins, the simulated outputs will be used to complement the limited information provided by the observation gauge stations.

CHAPTER 4 CLIMATE CHANGE IMPACT ASSESSMENT AND HYDROLOGICAL SIMULATION





























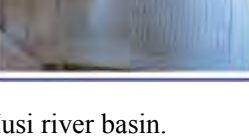
| | | | | |
|----|--------------------|---|--|---|
| 1 | Boom Baru |  |  |  |
| 3 | Selat Jaran |  |  |  |
| 4 | Kampung Upang |  |  |  |
| 5 | Tanjung Buyut |  |  |  |
| 6 | S.Rotan |  |  | |
| 7 | Kalang Agung |  |  | |
| 8 | Nusantara/Jalur 27 |  |  | |
| 9 | Skanak |  |  |  |
| 10 | Srijabo |  |  |  |
| 11 | Sekayu |  |  | |
| 12 | Sukabumi |  |  |  |

Figure 4.3.1-4 Summary of discharge and water level gauges in Musi river basin.

CHAPTER 4 CLIMATE CHANGE IMPACT ASSESSMENT AND HYDROLOGICAL SIMULATION

How to calculate Q_{out} after hydropower generation:

$$- 1.06\text{m}^3/\text{kWh} \times \text{kWh}/\text{yr produced} / 365\text{days}/\text{yr} = \text{total volume per day} \quad (< 40 \text{ m}^3/\text{s})$$

From the underground tunnel $Q_{in} = 37.9 \text{ m}^3/\text{s}$ on average and outflow to Simpang air river is around $15\text{-}40 \text{ m}^3/\text{s}$.

After the trip, additional data for some months in 2009 were provided as well as the power generation from 2006-2013. For 2009, sample average reductions for the months of May to November are: 35.96, 28, 22.16, 22.11, 25.43, 36.66, 30.11 m^3/s . This averages at around $27\text{m}^3/\text{s}$.

Using the same calculation method as above, we are able to estimate discharge reductions from the dam as follows:

- For year < 2006, no reductions since dam op was started 2006
- For 2006: $1.06\text{m}^3/\text{KWh} \times 528.85\text{GWh}/\text{yr} \times 1 \text{ year}/365 \text{ days} \times 1 \text{ day}/86400\text{s} = 17.77 \text{ m}^3/\text{s}$
- For 2007: $1.06\text{m}^3/\text{KWh} \times 710.04\text{GWh}/\text{yr} \times 1 \text{ year}/365 \text{ days} \times 1 \text{ day}/86400\text{s} = 23.866 \text{ m}^3/\text{s}$
- For 2008: $1.06\text{m}^3/\text{KWh} \times 861.04\text{GWh}/\text{yr} \times 1 \text{ year}/365 \text{ days} \times 1 \text{ day}/86400\text{s} = 28.9416 \text{ m}^3/\text{s}$
- For 2009: $1.06\text{m}^3/\text{KWh} \times 901.27\text{GWh}/\text{yr} \times 1 \text{ year}/365 \text{ days} \times 1 \text{ day}/86400\text{s} = 30.2938 \text{ m}^3/\text{s}$
- For 2010: $1.06\text{m}^3/\text{KWh} \times 1077.05\text{GWh}/\text{yr} \times 1 \text{ year}/365 \text{ days} \times 1 \text{ day}/86400\text{s} = 36.2022 \text{ m}^3/\text{s}$
- For 2011: $1.06\text{m}^3/\text{KWh} \times 792.92\text{GWh} / \text{yr} \times 1 \text{ year}/365 \text{ days} \times 1 \text{ day}/86400\text{s} = 26.6519 \text{ m}^3/\text{s}$
- For 2012: $1.06\text{m}^3/\text{KWh} \times 824.83\text{GWh}/\text{yr} \times 1 \text{ year}/365 \text{ days} \times 1 \text{ day}/86400\text{s} = 27.7244 \text{ m}^3/\text{s}$
- For 2013: (same assumption for year >2013) $1.06\text{m}^3/\text{KWh} \times 569.52\text{GWh} / \text{yr} \times 1 \text{ year}/365 \text{ days} \times 1 \text{ day}/86400\text{s} = 19.1429 \text{ m}^3/\text{s}$

The 2009 value (at $30 \text{ m}^3/\text{s}$.) is quite similar to the measured value provided by the Musi Hydropower plant engineers (at $27 \text{ m}^3/\text{s}$). Therefore, the calculated values above are used as assumptions in our hydrological model simulations regarding discharge reductions from the dam.

a-4) Water Level information

As inputs to the 1D model for determining tidal effects at the mouth of the basin, five water level check stations have been provided. These are at Tanjung Buyut, Kampung Upang, Selat Jaran, Sungai Lais, and Boom Baru (Figure 4.3.1-5).

CHAPTER 4 CLIMATE CHANGE IMPACT ASSESSMENT AND HYDROLOGICAL SIMULATION

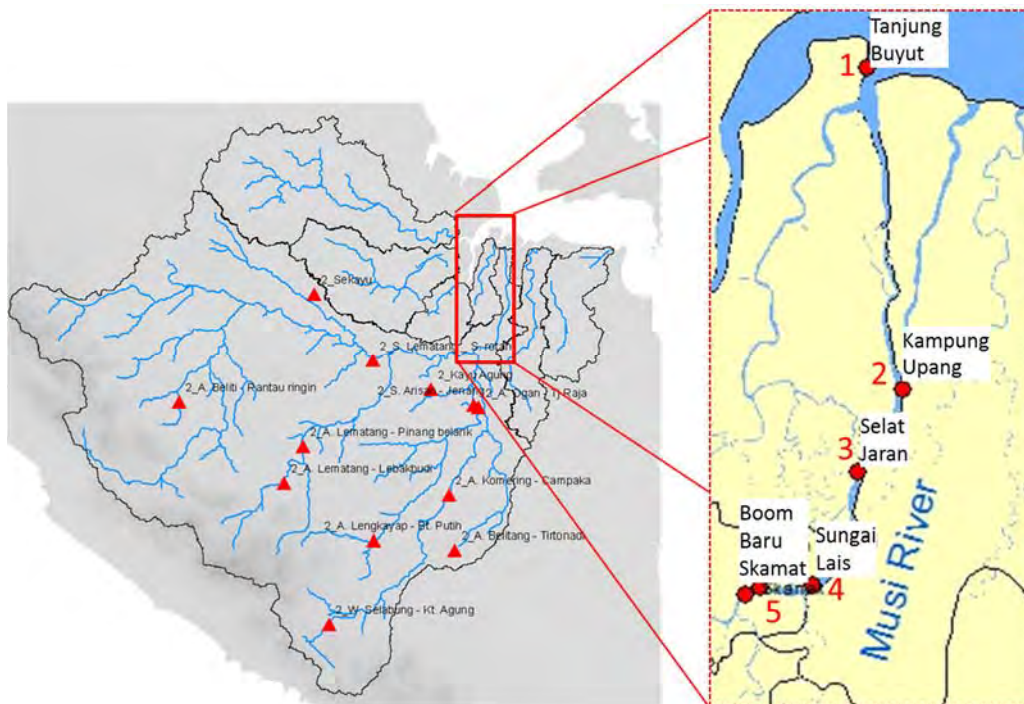


Figure 4.3.1-5 Five (5) water level check stations in Musi for analyzing tidal effects into the basin.

Currently, water level data from 1997 to 2013 has been collected and, together with the river cross-sections (see Figure 4.3.1-6), is now being incorporated into the 1D model.

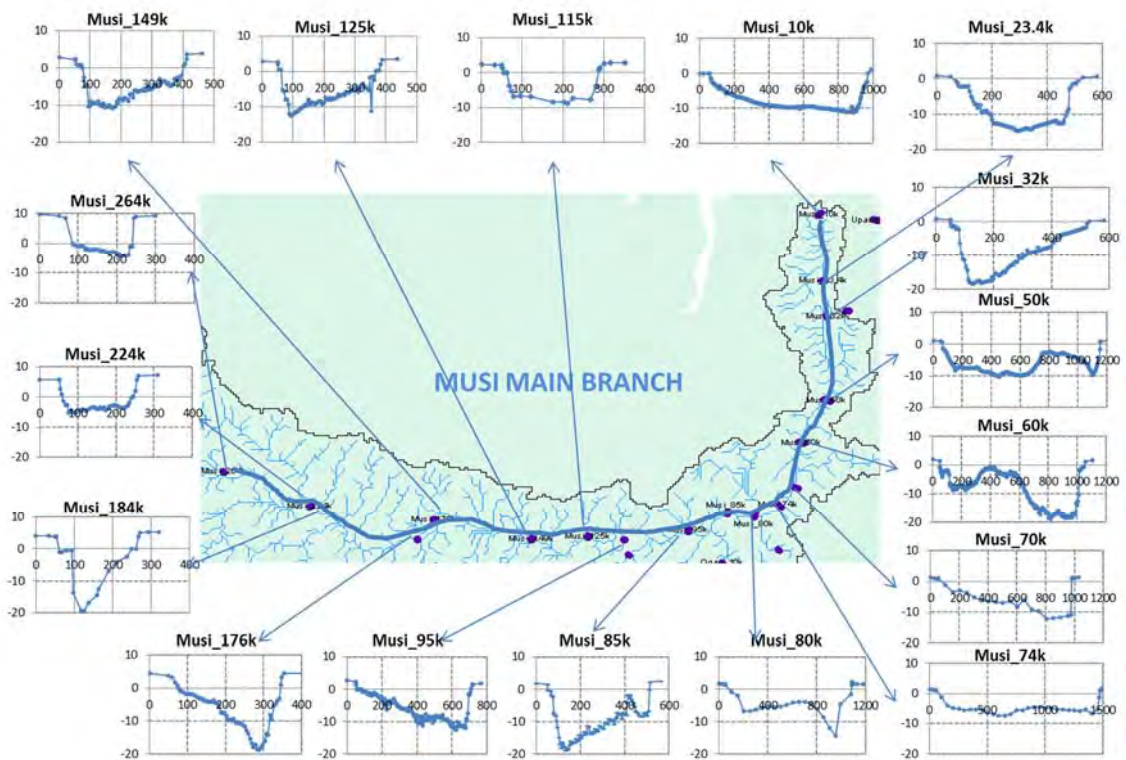


Figure 4.3.1-6 Cross sections at the main branches of the Musi River.

b) Static Parameters

b-1) Soil maps

Local soil was unavailable for this basin, so the Food and Agriculture Organization (FAO) global soil map was used. The global FAO soil map was processed and resampled to a 500 m x 500 m grid, and the soil parameters were modified to reflect the optimized hydraulic conductivities (ksat) provided by the optimized LDAS-UT soil parameters

b-2) Soil texture from LDAS-UT

To drive the LDAS-UT, AMSR-E Brightness temperature was used for the assimilation dataset. Global Land Data Assimilation System (GLDAS) output (<http://ldas.gsfc.nasa.gov/>), which provides 0.25° spatial resolution every three hours (GLDAS_NOAH025SUBP_3H), was used for the forcing data. The MODIS LAI, ISLSCP-II data are prepared as inputs in the initial condition.

The input and output data of the LDAS-UT is shown in Figure 4.3.1-7.

Specific details are given in the succeeding subsections.

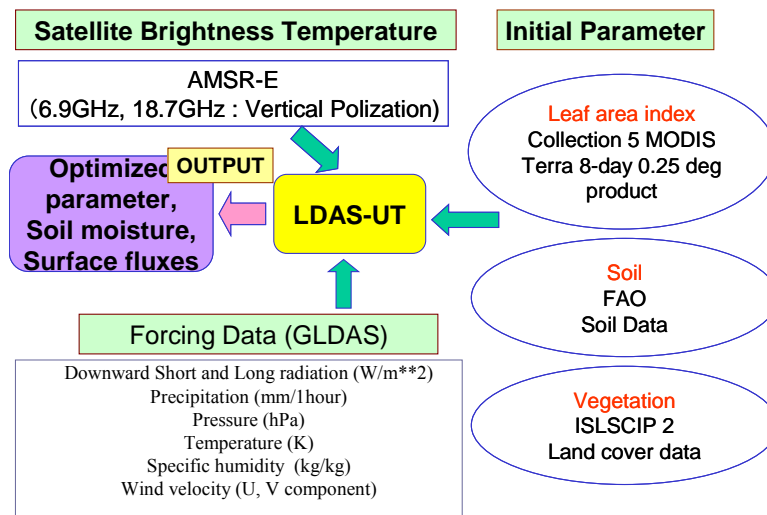


Figure 4.3.1-7 Input and Output data of the LDAS-UT

b-2-1) AMSR-E

AMSR-E is a multi-frequency and dual-polarized passive microwave radiometer that detects microwave emissions from the Earth's surface as well as from the atmosphere. It measures brightness temperature at 6.925, 10.65, 18.7, 23.8, and 89.0 GHz. It maintains a constant Earth incident angle of 55°, covering a swath of 1,445 km on the Earth's surface, and has a spatial resolution of individual measurements that vary from 5.4 km at 89.0 GHz to 56 km at 6.9 GHz. This study employed a vertical polarization of 6.925 and 18.7 GHz to retrieve the soil moisture data.

CHAPTER 4 CLIMATE CHANGE IMPACT ASSESSMENT AND HYDROLOGICAL SIMULATION

b-2-2) GLDAS

For the GLDAS output (<http://ldas.gsfc.nasa.gov/>), which provides 0.25° spatial resolution every three hours (GLDAS_NOAH025SUBP_3H), air temperature, specific humidity, wind speed and direction, downward short wave radiation, downward long wave radiation, and precipitation were used as forcing data.

b-2-3) Leaf Area Index from MODIS

The Leaf Area Index (LAI), provided by Boston University estimated using a Moderate-resolution Imaging Spectroradiometer (MODIS), was used as the initial condition of the vegetation (<http://cliveg.bu.edu/>)

b-2-4) ISLSCP-II

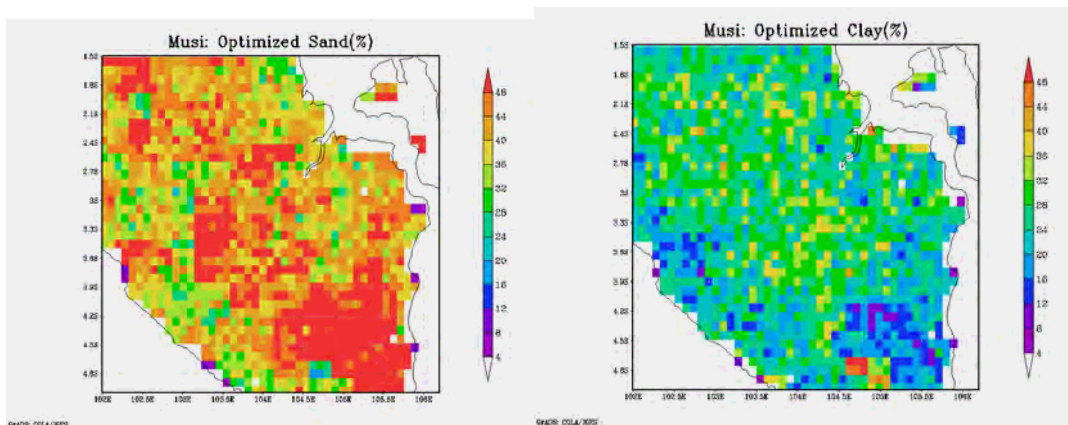
The initial condition of land cover data was used from the International Satellite Land Surface Climatology Project, Initiative II (ISLSCP II) Project (https://daac.ornl.gov/ISLSCP_II/islscpii.shtml).

b-2-5) FAO Soil data

The initial condition of soil characteristics was taken from Food and Agriculture Organization (FAO) data (<http://www.fao.org/nr/land/soils/en/>).

b-2-6) Soil texture optimization

The LDAS-UT was applied to the Musi river basin during the dry season (July to August 2010) to get optimal soil parameters. Figure 4.3.1-8 shows the optimized soil parameters (Upper left: sand , Upper right: clay, Lower left: unsaturated hydraulic conductivity, lower right: porosity) for the Musi river basin.



CHAPTER 4 CLIMATE CHANGE IMPACT ASSESSMENT AND HYDROLOGICAL SIMULATION

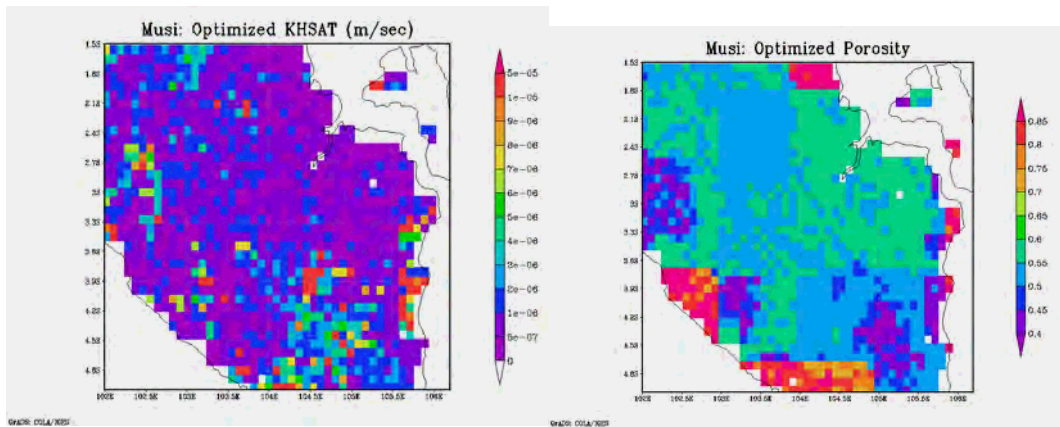


Figure 4.3.1-8 Optimized soil parameters (Upper left: sand , Upper right: clay, Lower left: unsaturated hydraulic conductivity, lower right: porosity) for the Musi river basin.

Figure 4.3.1-8 shows the optimized soil parameters for Musi river basin. These maps will be incorporated as an additional layer to provide improvements in the crop model simulations in the near future. For now, these parameters are compared using sample points with FAO soil characteristics. If the FAO soil values are significantly different from the sample point data, the optimized value is used instead of the FAO value. This procedure is currently ongoing since we are still in the process of finalizing our calibration of soil parameters.

Figure 4.3.1-9 shows the distribution of the different soil classes in the Musi river basin based on the classification by FAO. There is a maximum of 19 soil classes in the basin majority of which consists of acrisols.

CHAPTER 4 CLIMATE CHANGE IMPACT ASSESSMENT AND HYDROLOGICAL SIMULATION

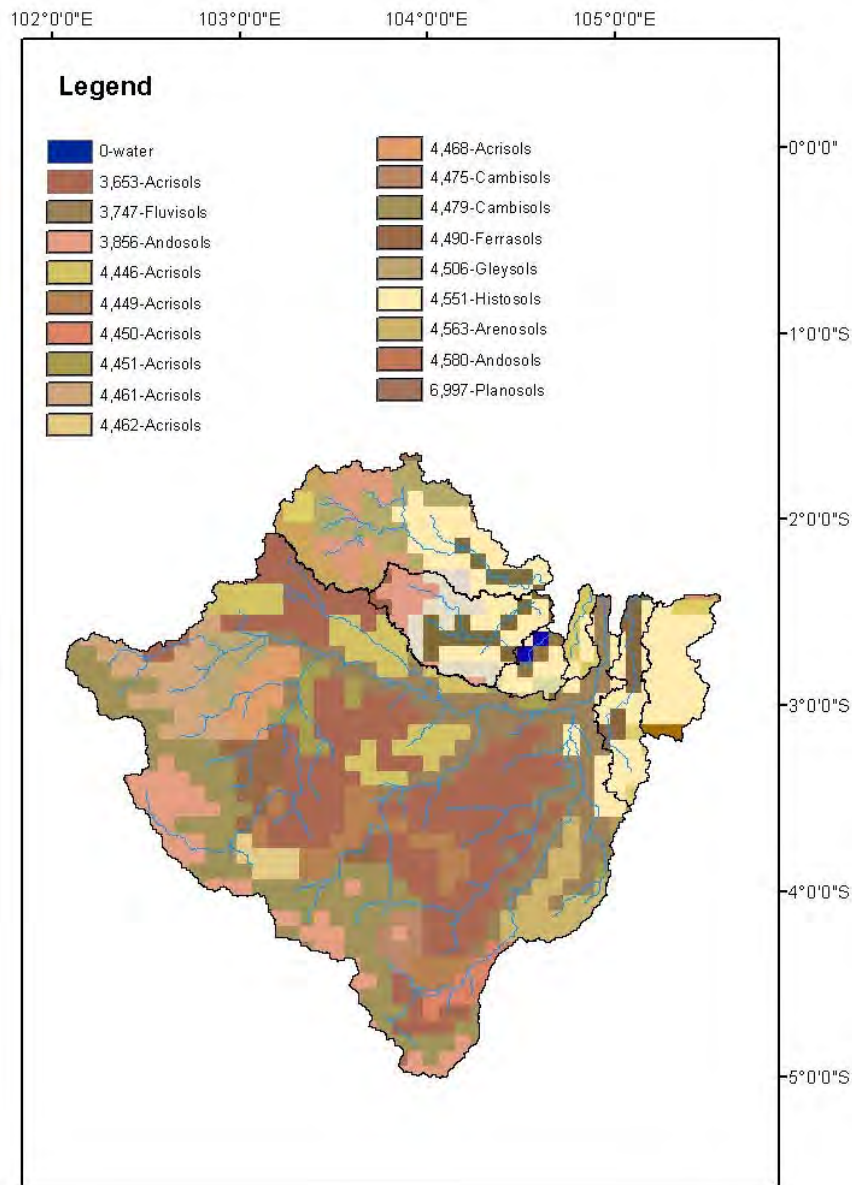


Figure 4.3.1-9 FAO soil classes in the Musi River basin.
(Legend shows FAO number and soil class)

Each grid has a homogeneous soil type. The area distributions of different types of land cover and soil are represented using one-dimensional functions with respect to flow distance from the outlet. In a flow interval at any flow distance, the area fraction of each land cover (and soil) type is known. For representation of the heterogeneity of land cover and soil inside a hillslope, one hillslope is divided into a number of smaller elements along the direction of the slope. Each element corresponds to one type of land use-soil combination, which is the simulation unit of the unsaturated zone. The top soil is considered the unsaturated zone, and the maximum depth of the unsaturated zone is around 4 meters. Below the top soil, the minimum simulation unit of the unconfined aquifer, is the whole hillslope above the impermeable bed rock, which is the common groundwater storage of all elements in this hillslope.

CHAPTER 4 CLIMATE CHANGE IMPACT ASSESSMENT AND HYDROLOGICAL SIMULATION

Non-uniform vertical distribution of soil water property of root zones is represented assuming an exponentially decreasing function (Robinson and Sivapalan, 1996; Singh et al., 2002):

$$K_s(z) = K_0 \exp(-fz) \quad (4.3.1-1)$$

where $K_s(z)$ is the saturated hydraulic conductivity, z is the distance taken positive in downward direction normal to surface, K_0 is the saturated hydraulic conductivity of the surface soil, and f is a constant parameter. Many soils, especially forest soils, are anisotropic with a higher conductivity parallel to the hillslope. For such soils, an anisotropy ratio can be defined as (Jackson, 1992; Singh et al., 2002):

$$r_a = \frac{K_{sp}}{K_{sn}} \geq 1 \quad r_a = \frac{K_{sp}}{K_{sn}} \geq 1 \quad (4.3.1-2)$$

where r_a is the anisotropy ratio, K_{sp} and K_{sn} is the saturated hydraulic conductivity in the directions normal (n) and parallel (p) to the slope respectively.

These soil parameters were taken from the FAO global soil dataset. Soil parameterization at each basin was done by applying factors to the saturated hydraulic conductivity at the soil surface, the hydraulic conductivity decay factor, hydraulic conductivity in groundwater, manning's roughness for each sub-basin, and the soil anisotropic ratio for each sub-basin.

b-3) Land use maps

Local land-use was available in Musi river basin. For the purpose of WEB-DHM simulation, SiB2 land-use classification is needed. Additionally, specific details on the location of the 4 agricultural rice production systems is needed to be able to incorporate the coupled crop model into the basin. The land-use data from PU was made available for this purpose. Additional field surveys (interviews) were also conducted to learn the details of the crop growing methods in different parts of Musi as well as geographically locate where the exact locations of these land use types are. Satellite information (Figure 4.3.1-10) was also overlaid to further identify these. Figure 4.3.1-11 shows how the land-use classifications were translated from Bahasa to English to the specific SiB2 land use classification + the 4 agricultural land-use types. Corresponding numbers from 1 to 14 were included to identify the modified land-use types (Figure 4.3.1-12).

CHAPTER 4 CLIMATE CHANGE IMPACT ASSESSMENT AND HYDROLOGICAL SIMULATION

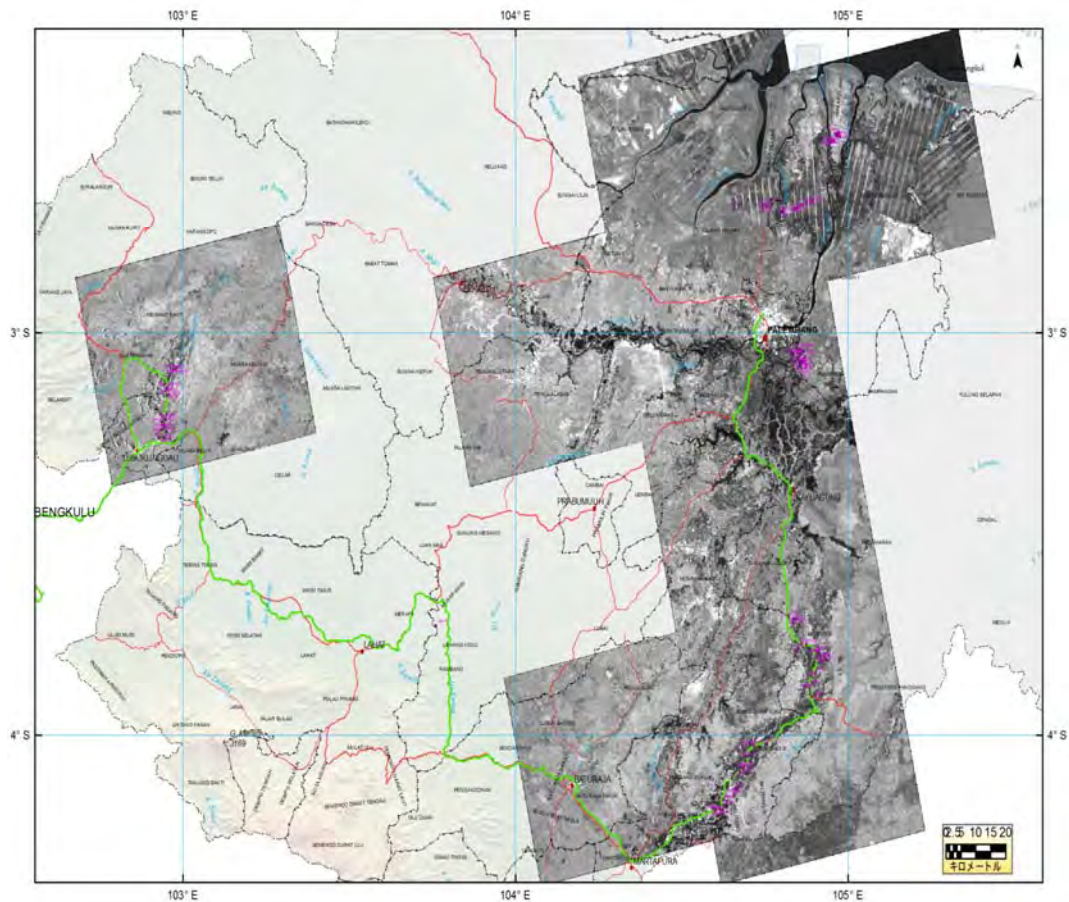


Figure 4.3.1-10 Overlay of satellite imagery on the selected survey areas.

| FID | Shape ^ | PL | Luas_PL | Landuse | Landuse_Si | Sib_number |
|-----|---------|--------------------|--------------|-------------------|---------------------------|------------|
| 0 | Polygon | Danau | 142.732402 | Lake | water/wetland | 10 |
| 1 | Polygon | Hutan Alam | 7894.848172 | Natural Forest | Broadleaf evergreen tree | 1 |
| 2 | Polygon | Hutan Lahan Kering | 7944.412752 | Forest (Dry land) | Broadleaf & Needleleaf tr | 3 |
| 3 | Polygon | Kebun Campuran | 21831.834846 | Mixed Garden | Agriculture/c3 grassland | 9 |
| 4 | Polygon | Mangrove | 1949.508823 | Mangrove | Broadleaf Deciduous Tre | 2 |
| 5 | Polygon | Perkebunan | 16017.473455 | Plantation | Tidal Swamp | 14 |
| 6 | Polygon | Pemukiman | 1892.71436 | Settlement | Irrigated Agriculture | 12 |
| 7 | Polygon | Rawa | 6572.335506 | Swamp | Freshwater swamp | 13 |
| 8 | Polygon | Sawah | 4807.075302 | Wetland | Rainfed Agriculture | 11 |
| 9 | Polygon | Semak/Belukar | 8439.02854 | Shrubs/bush | Freshwater swamp | 13 |
| 10 | Polygon | Sungai | 940.406388 | river | water/wetland | 10 |
| 11 | Polygon | Tambak/Empang | 378.809762 | fish pond | water/wetland | 10 |
| 12 | Polygon | Tanah Terbuka | 1837.155682 | open area | Shrubs with bare soil | 7 |
| 13 | Polygon | Tegalan/Ladang | 6139.346134 | field/moore | Agriculture/c3 grassland | 9 |

Figure 4.3.1-11 Modified land-use classification from Bahasa to English to SiB2 Classification + 14 land-uses.

CHAPTER 4 CLIMATE CHANGE IMPACT ASSESSMENT AND HYDROLOGICAL SIMULATION

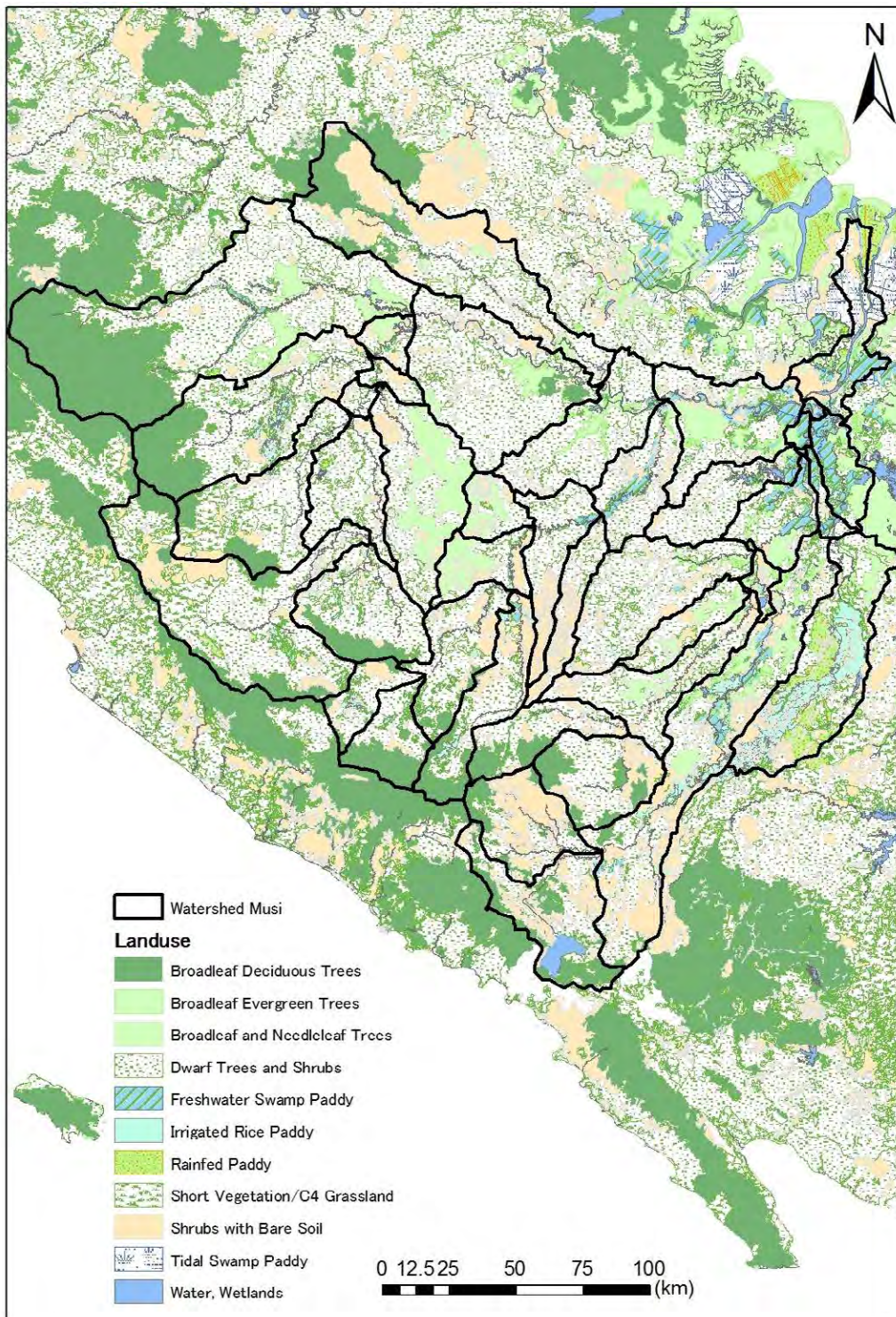


Figure 4.3.1-12 Land-use types.

CHAPTER 4 CLIMATE CHANGE IMPACT ASSESSMENT AND HYDROLOGICAL SIMULATION

4.3.2 Development of WEB-DHM and its Validation

(1) Target Area and Data

The WEB-DHM was developed for the Musi River as shown in Figure 4.1.3-1. The total area of the Musi River is around 60,000 km².

Because of the critically limited availability of rainfall and streamflow data with enough accuracy in the basin, we tried to identify reasonable data sets to be used for the model calibration.

There are so many, around 170, daily rain gauge stations in Musi River. Due to the large amount of data discontinuity, however, twenty-one rain gauge stations were selected by considering data availability with relatively small amounts of long-term and/or frequent data missing. The data sets at two stations located closely to one other were merged into one. Then, twenty station data were used for this assessment. To produce a gridded hourly rainfall product which was used as an input into the WEB-DHM, we tried to apply i) Thiessen Method by using a weighted average of the selected measurements based on the size of each one's polygon; ii) Inverse Distance Weighting (IDW) by using a weighted average of the values available at the known twenty points for calculation of values of unknown points; iii) Tropical Rainfall Measuring Mission (TRMM) products, and; iv) reanalysis product after bias correction by using the observed data. We finally decided to use a simple Thiessen Method after various performance checks, not only by applying the calibrations and validations but the long-term past climate simulations. After making the gridded rainfall product, an hourly version was generated by dividing it by twenty-four, and thus it was difficult to fit the peak flows well.

We found series of suspicious-looking streamflow data. After careful checking the possibility of data fabrication and abnormal runoff ratio as well as data continuity, we identified the four stations as candidates to be used for calibration and validation. Through the validation, two of the four, small sub-basins, showed no reasonable consistency to the rainfall signal which came from the gridded rainfall product by using the twenty rain gauges with the sparse distribution as described above. Then, we adopted two stations, Lematang Rotan and Komering Campaka, as calibration and validation sites.

Considering such a critical situation concerning the effective data availability for the Musi River, we simplified the model as much as possible and evaluated the model calibration and validation qualitatively but not quantitatively.

(2) Model Calibration

The WEB-DHM was calibrated by comparing simulated daily discharges with natural flow derived from observed streamflow records at Lematang Rotan and Komering Campaka as shown in Figure 4.3.2-1. Through a lots of model parameter sensitivity checks, it was found that the gap between the observed hydrograph and the simulated one at Lematang Rotan mainly depended upon the uncertainty of the rainfall data sets. There are many diversion channels that connect Komering River and Ogan River and affected the streamflow observed at Komering Campaka. Considering these two conditions, the calibration result expressed in Figure 4.3.2-1 was accepted. Then, calibrated model parameters for soil type, vegetation class, and land-use type are summarized in Tables 4.3.2-1~4.

CHAPTER 4 CLIMATE CHANGE IMPACT ASSESSMENT AND HYDROLOGICAL SIMULATION

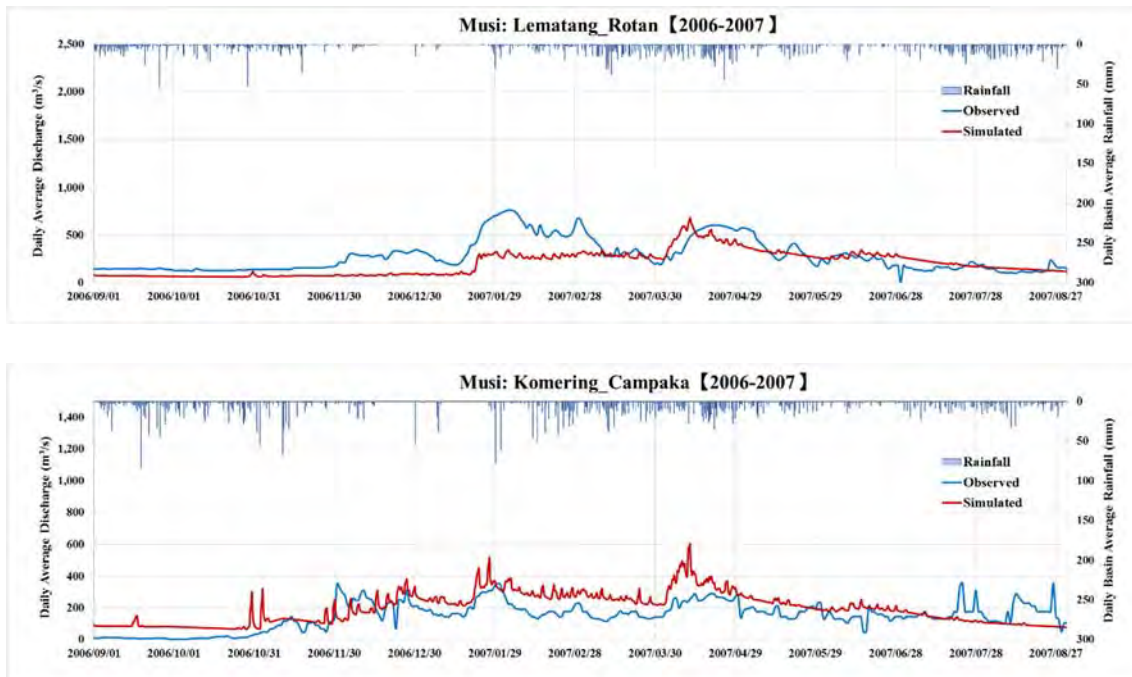


Figure 4.3.2-1 Comparison between observed and simulated natural flows at Lematang Rotan and Komering Campaka from September 2006 to August 2007. Red solid line: simulated discharge with observed rainfall; Blue solid line: observed discharge.

CHAPTER 4 CLIMATE CHANGE IMPACT ASSESSMENT AND HYDROLOGICAL SIMULATION

Table 4.3.2-1 Soil parameters for the Musi River basin model

| Soil Classification | | Soil water parameters | | | | | | | |
|---------------------|--------------------------|-------------------------|------------------------|-------------------------|-------------------------|---|---|---|---|
| FAO soil code | Soil Class (FAO) Symbols | theta_s | theta_r | alpha | n | ks1 | ks2 | ksg | GWcs |
| | | Saturated water content | Residual water content | van Genuchten parameter | van Genuchten parameter | Saturated Hydraulic conductivity for soil surface [mm/hr] | Saturated Hydraulic conductivity for unsaturated zone [mm/hr] | Hydraulic conductivity for unconfined aquifer [mm/hr] | coefficient for aquifer storage [m ³ /m ³] |
| - | - | - | - | - | - | calibrated | calibrated | calibrated | - |
| 3653 | Vp39-3b | 0.661 | 0.069 | 0.024 | 1.583 | 28.598 | 2.860 | 100.0 | 0.150 |
| 3747 | Jd12-2/3 | 0.716 | 0.080 | 0.018 | 1.376 | 15.996 | 1.600 | 100.0 | 0.150 |
| 3856 | Th17-2c | 0.735 | 0.058 | 0.020 | 1.569 | 15.431 | 7.443 | 100.0 | 0.150 |
| 4446 | Af11-2/3 | 0.671 | 0.074 | 0.024 | 1.425 | 13.931 | 1.393 | 100.0 | 0.150 |
| 4449 | Af55-3b | 0.679 | 0.075 | 0.024 | 1.435 | 14.399 | 1.440 | 100.0 | 0.150 |
| 4450 | Af56-2a | 0.637 | 0.068 | 0.026 | 1.677 | 35.745 | 3.575 | 100.0 | 0.150 |
| 4451 | Af57-2a | 0.673 | 0.077 | 0.023 | 1.502 | 22.574 | 2.257 | 100.0 | 0.150 |
| 4461 | Ao104-2/ | 0.686 | 0.074 | 0.021 | 1.492 | 20.811 | 2.081 | 100.0 | 0.150 |
| 4462 | Ao105-2/ | 0.693 | 0.071 | 0.022 | 1.526 | 28.969 | 2.897 | 100.0 | 0.150 |
| 4468 | Ap25-2/3 | 0.649 | 0.069 | 0.025 | 1.556 | 22.722 | 2.272 | 100.0 | 0.150 |
| 4475 | Be116-2c | 0.663 | 0.066 | 0.018 | 1.521 | 29.982 | 2.998 | 100.0 | 0.150 |
| 4479 | Bh17-2bc | 0.714 | 0.077 | 0.016 | 1.457 | 19.976 | 1.998 | 100.0 | 0.150 |
| 4490 | Fo101-2b | 0.732 | 0.089 | 0.025 | 1.400 | 22.975 | 2.297 | 100.0 | 0.150 |
| 4506 | Gh20-3a | 0.709 | 0.083 | 0.018 | 1.357 | 13.079 | 1.308 | 100.0 | 0.150 |
| 4551 | Od20-a | 0.703 | 0.085 | 0.019 | 1.403 | 20.222 | 2.022 | 100.0 | 0.150 |
| 4563 | Qc59-1ab | 0.647 | 0.062 | 0.027 | 2.156 | 15.361 | 8.636 | 100.0 | 0.150 |
| 4580 | Tv38-1bc | 0.707 | 0.054 | 0.022 | 1.719 | 15.162 | 8.516 | 100.0 | 0.150 |
| 6997 | WATER | 0.661 | 0.069 | 0.024 | 1.583 | 28.598 | 2.860 | 100.0 | 0.150 |

Table 4.3.2-2 Soil depth in the Musi River basin model

| Soil depth | |
|-----------------------|--------------|
| surface+root+deep [m] | acquirer [m] |
| 2 | 4 |

Table 4.3.2-3 Vegetation parameters for the Musi River basin model

| Sib2 Reclassification | Sstmax |
|--------------------------------|--------|
| Broadleaf Deciduous Trees | 10 |
| Broadleaf and Needleleaf Trees | 15 |
| Short Vegetation/C4 Grassland | 5 |
| Shrubs with Bare Soil | 5 |
| Dwarf Trees and Shrubs | 5 |
| Agriculture or C3 Grassland | 150 |

Table 4.3.2-4 Land-use parameters for the Musi River basin model

| Surface roughness | River roughness |
|-------------------|-----------------|
| 0.01 | 0.02 |

CHAPTER 4 CLIMATE CHANGE IMPACT ASSESSMENT AND HYDROLOGICAL SIMULATION

(3) Model Validation

We applied the calibrated model to a long-term simulation from 1986 to 2013. The upper two in Figure 4.3.2-2 shows the simulated daily streamflow (orange line) in comparison with the observed streamflow (black dot and line) at Lematang Rotan and Komering Campaka. The discrepancies between the observed data and the simulated output may originate from the lack of river channel storage due to the model simplification. To express the storage effect, nine-day running averaging was applied to the model output. The result corresponds to the observed data as shown in the lower two graphs in Figure 4.3.2-2.

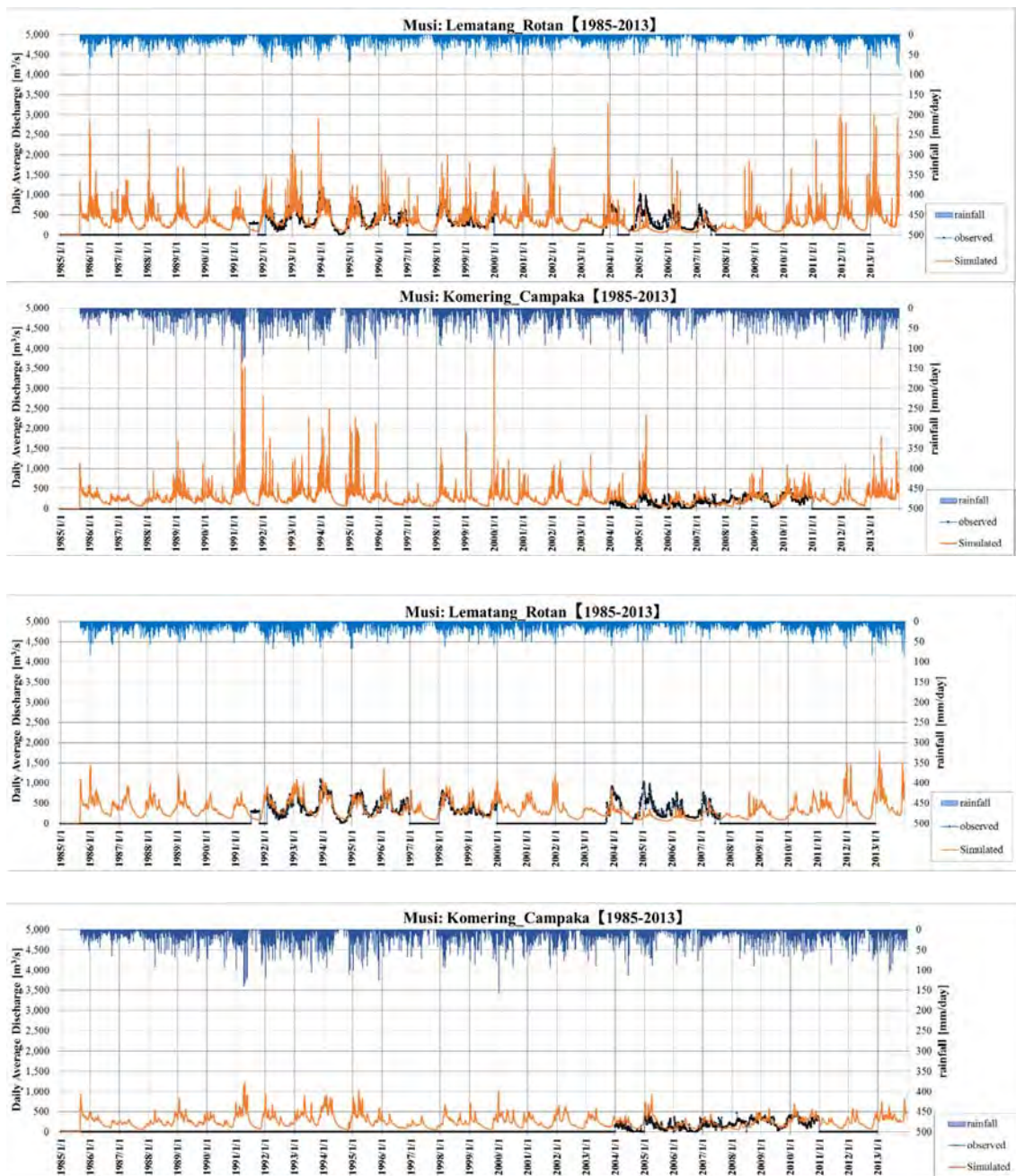


Figure 4.3.2-2 Comparison between observed and simulated natural flows at Lematang Rotan and

CHAPTER 4 CLIMATE CHANGE IMPACT ASSESSMENT AND HYDROLOGICAL SIMULATION

Komerling Campaka from 1986 to 2013. Orange solid line: simulated daily discharge (upper two) and nine day running average (lower two) with observed rainfall; Black dots and line: observed daily discharge.

4.3.3 Selection of Future Scenarios in the Musi River Basin

(1) Future Scenario Selection for Water Resources Management

To select future scenario “Water Resources Management Plan”, we identified two indicators including the 275th and 355th discharge of river flow duration curve. Figure 4.3.3-1 shows box plots for percentage increase of the two indicators of river flow duration curve at the major two points, #200 and #900, in the Musi River basin. Considering the consistent order of the median and 1st and 3rd quartile among the selected three sites, we selected three models to represent High, Medium, and Low scenarios of future discharge as follows:

- “gfdl_2_1” as Low scenario (the safest scenario)
- “ingv_enham4” as Medium scenario (scenario of highest probability)
- “gfdl_2_0” as High scenario (the most hazardous scenario)

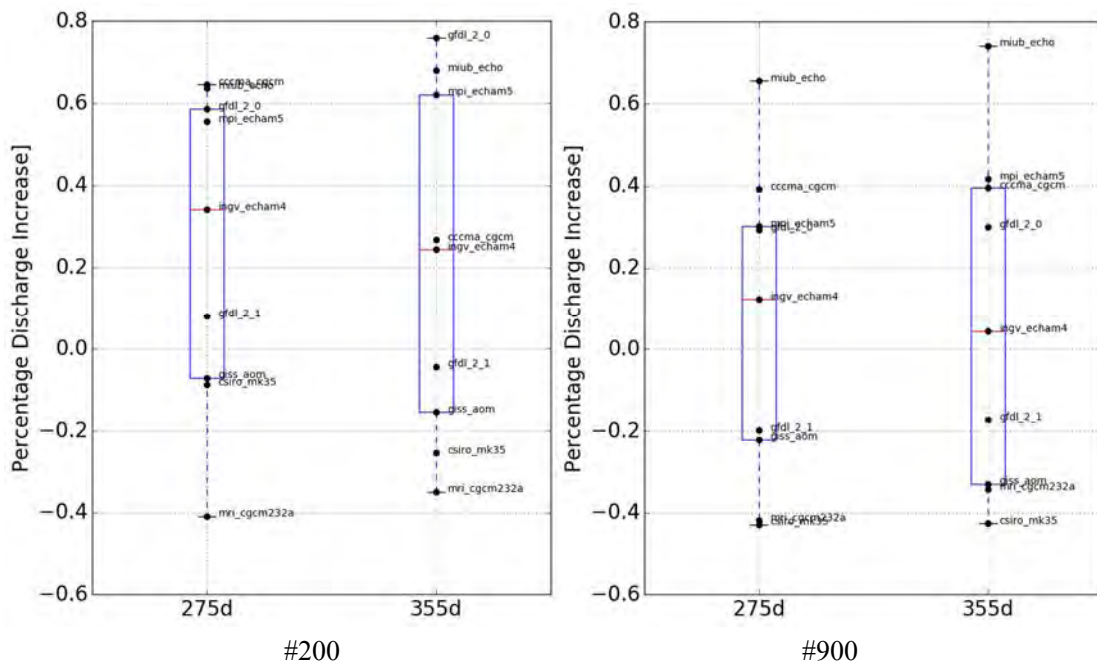


Figure 4.3.3-1 Percentage increase of the two indicators of river flow duration curve at the major two points, #200 (left) and #900 (right), in the Musi River basin.

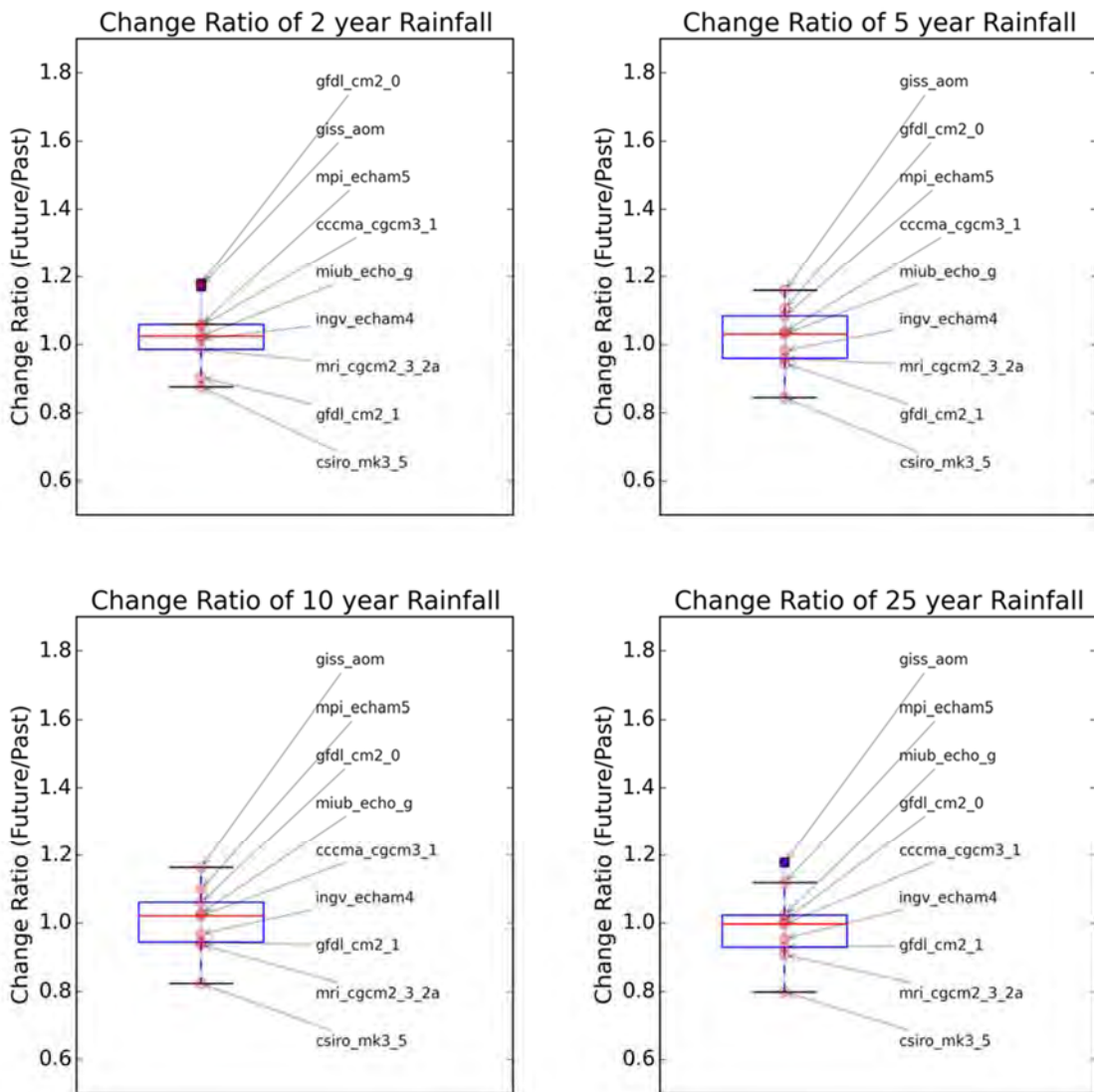
(2) Future Scenario Selection for Flood Risk Management

We evaluated the magnitude of the peak rainfall intensity, which corresponds to the peak flow of

CHAPTER 4 CLIMATE CHANGE IMPACT ASSESSMENT AND HYDROLOGICAL SIMULATION

the flood hydrograph, and then selected five months, November through March, as a design duration. We applied frequency analysis to the basin-averaged five month observed rainfall. Finally, we determined six indicators for selecting future scenarios for flood condition: the change ratio (future/present) of basin-averaged five month observed rainfall of the 2-, 5-, 10-, 25-, 50- and 100-year return period events. Figure 4.3.3-2 shows change ratios (future/present) of extreme rainfall for different return periods. A set of three change factors for extreme rainfall is evaluated for each return period considering the uncertainty of the GCM projection. Considering the consistent order of the median and 1st and 3rd quartile, we selected three models to represent High, Medium, and Low scenarios of future flood as follows:

- “gfdl_2_1” as Low scenario (the safest scenario)
- “miub_echo_g” as Medium scenario (scenario of highest probability)
- “mpi_echam5” as High scenario (the most hazardous scenario)



CHAPTER 4 CLIMATE CHANGE IMPACT ASSESSMENT AND HYDROLOGICAL SIMULATION

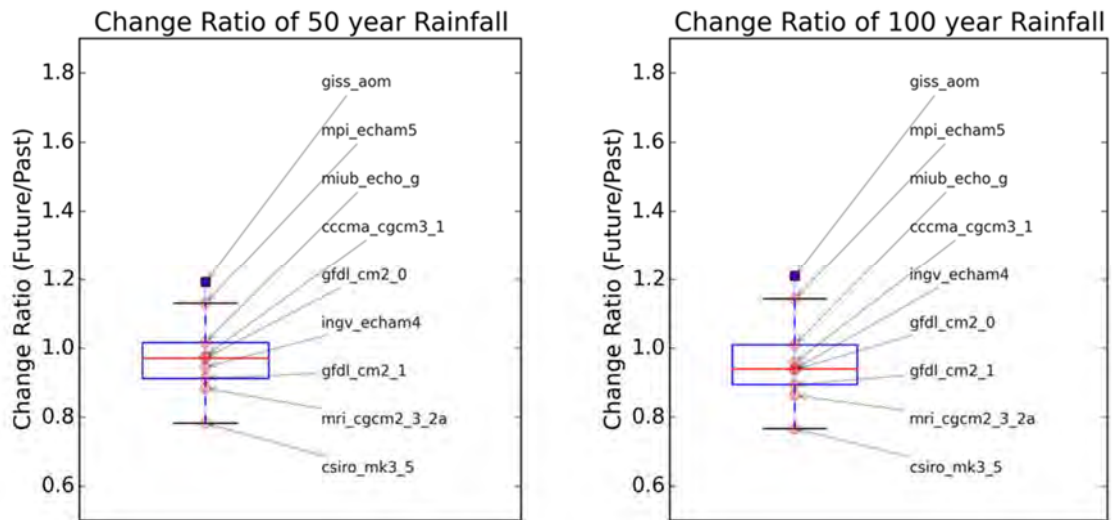


Figure 4.3.3-2 Box plots for change factors (future/present) of extreme rainfall for different return periods

The rainfall record from November 1993 to March 1994, which corresponds to an almost 100 year return period, was selected as a design hyetograph. By multiplying the change factors for extreme rainfall associated with each of the three climate change scenarios shown in Table 4.3.3-1, we ascertained design rainfall for each return period in future.

Table 4.3.3-1 Summary of the change factors for extreme rainfall associated with each of the three climate change scenarios.

| Return period | High scenario (scenario of the most hazardous side) | Medium scenario (scenario of highest probable) | Low scenario (scenario of safest side) | Observed Precipitation |
|---------------|--|---|---|------------------------|
| | [mpi_echam5] | [miub_echo_g] | [gfdl_cm2_1] | [1994] |
| 2 | 0.75 | 0.73 | 0.64 | 0.71 |
| 5 | 0.89 | 0.85 | 0.78 | 0.82 |
| 10 | 0.97 | 0.91 | 0.83 | 0.88 |
| 25 | 1.05 | 0.96 | 0.88 | 0.94 |
| 50 | 1.11 | 1.00 | 0.90 | 0.98 |
| 100 | 1.16 | 1.02 | 0.91 | 1.01 |

CHAPTER 4 CLIMATE CHANGE IMPACT ASSESSMENT AND HYDROLOGICAL SIMULATION

4.3.4 Climate Change Impact Assessment for River Runoff, ET, and Soil Moisture

(1) Simulation of River Flow under Effects of Climate Change

Runoff was simulated by feeding bias-corrected GCM data into the developed basin model. Meteorological forcing datasets (rainfall, temperature, and radiation) were obtained from each GCM. For other required parameters for the WEB-DHM model that were unavailable, the same data used in the calibration stage was applied. Temporal interpolation from daily maximum and minimum data into hourly temperature was implemented based on an empirical model.

Three types of simulations were run, namely, “simQobs”, “simQgcmp”, and “simQgcmf”. The simQobs represents simulated flows from 1986 to 2013 driven by observed meteorological data. The simQgcmp represents simulated flows driven by future meteorological conditions from 1985 to 2000 obtained from bias-corrected GCM outputs. The simQgcmf represents simulated flows for 2050–2065 driven by future meteorological conditions obtained from bias-corrected GCM outputs. As mentioned earlier, the nine GCMs selected in order of performance were used for rainfall-runoff analysis for simQobs and simQgcmf and the three GCMs selected in the section 4.3.3 for simQgcmp.

(2) Changes of Hydrological Parameters

1) Precipitation

Figure 4.3.4-1 shows annual mean changes in projected precipitation for 2050–2065 with respect to 1985–2000 in the Musi River basin. The annual rainfall will decrease in future.

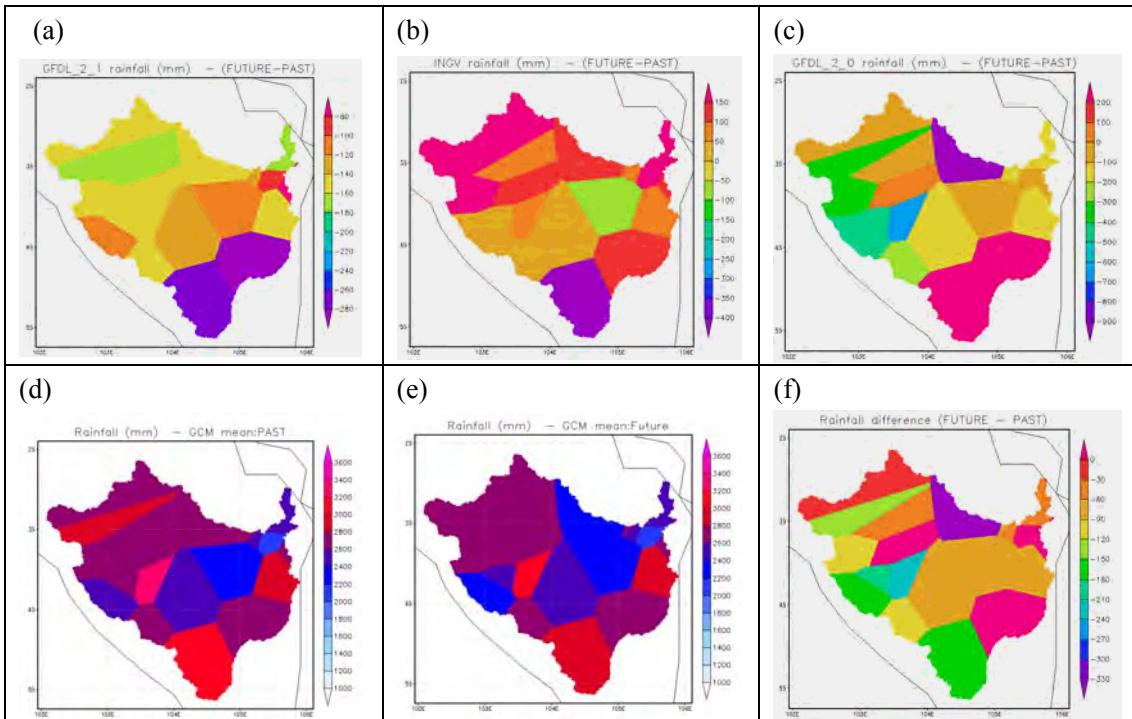


Figure 4.3.4-1 Changes in Precipitation: (a) difference “gfdl_2_1” of annual average for future(2050-2065) minus past(1985-2000); (b) difference “ingv_enham4” of annual average for future(2050-2065) minus past(1985-2000); (c) difference “gfdl_2_0” of annual average for future(2050-2065) minus past(1985-2000); (d) three-model mean of annual average for past (1985-2000); (e) three-model mean

CHAPTER 4 CLIMATE CHANGE IMPACT ASSESSMENT AND HYDROLOGICAL SIMULATION

of annual average for future (2050–2065); (f) difference between (e) and (d).

2) River Runoff

a) Seasonal

To evaluate the magnitude of predicted change and its uncertainty quantitatively, percentage increases for monthly mean discharges were calculated using simQgcmp and simQgcmf. Figure 4.3.4-2 shows percentage increases of monthly mean river discharge from the three selected climate models nearby Palembang (sub-basin #300). According to the figures, the multi-model ensemble median/mean discharge shows an increasing trend in the average from Dismember through May, whereas a decreasing trend from June through November. Therefore, we expect that total discharge in the Musi River basin in the future will likely increase in the second-half rainy season and the first-half dry season and decrease in the first-half rainy season and the second-half dry season. In addition, the multi-model ensemble spread widely, meaning that the uncertainty of monthly discharge trends among the GCMs were very large.

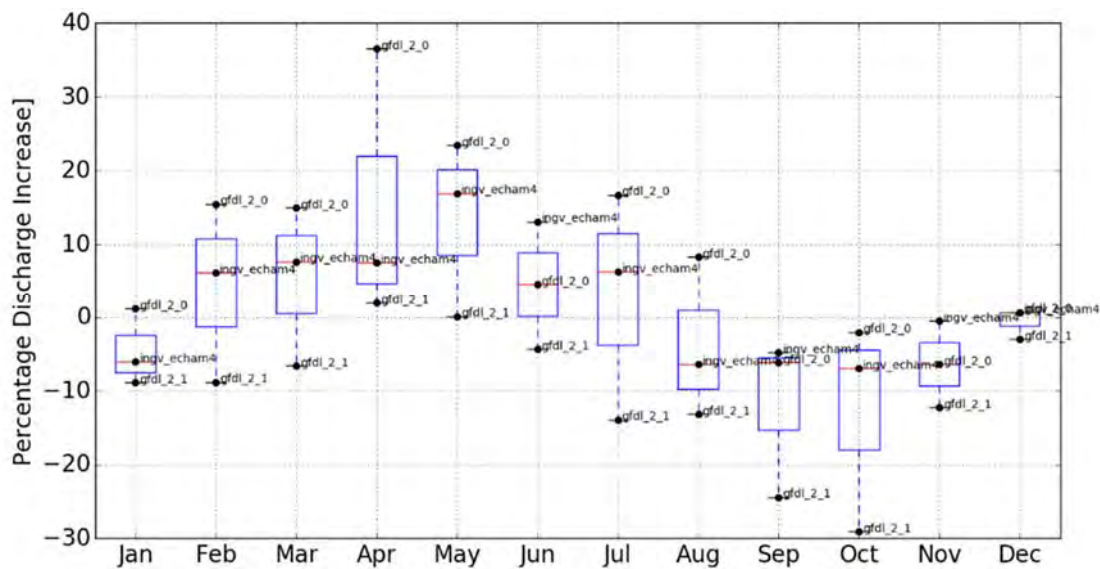


Figure 4.3.4-2 Percentage increases of 16-year mean monthly discharges nearby Palembang (sub-basin #300). Red line: median values; Lower and upper black box edges: first and third quartiles; Upper and lower black lines: highest and lowest values within the 1.5-times inter-quartile range from the third and first quartiles.

b) Annual Flow Duration Curve

In order to evaluate the magnitude of predicted change and its uncertainty quantitatively, percentage increases of discharge at each rank were calculated using present and future discharge. Figure 4.3.4-3 shows the result nearby Palembang (sub-basin #300). The multi-model ensemble mean of the percentage of increase (black thick line) is positive and negative in case of the exceedance

CHAPTER 4 CLIMATE CHANGE IMPACT ASSESSMENT AND HYDROLOGICAL SIMULATION

probability less and larger than 50%, respectively. Therefore, we expect that the low flow discharge will likely decrease, whereas the high flow discharge will likely increase. In addition, the pattern of the change varied GCM by GCM as shown in Figure 4.3.4-3, meaning that discharge trends among the GCMs were inconsistent.

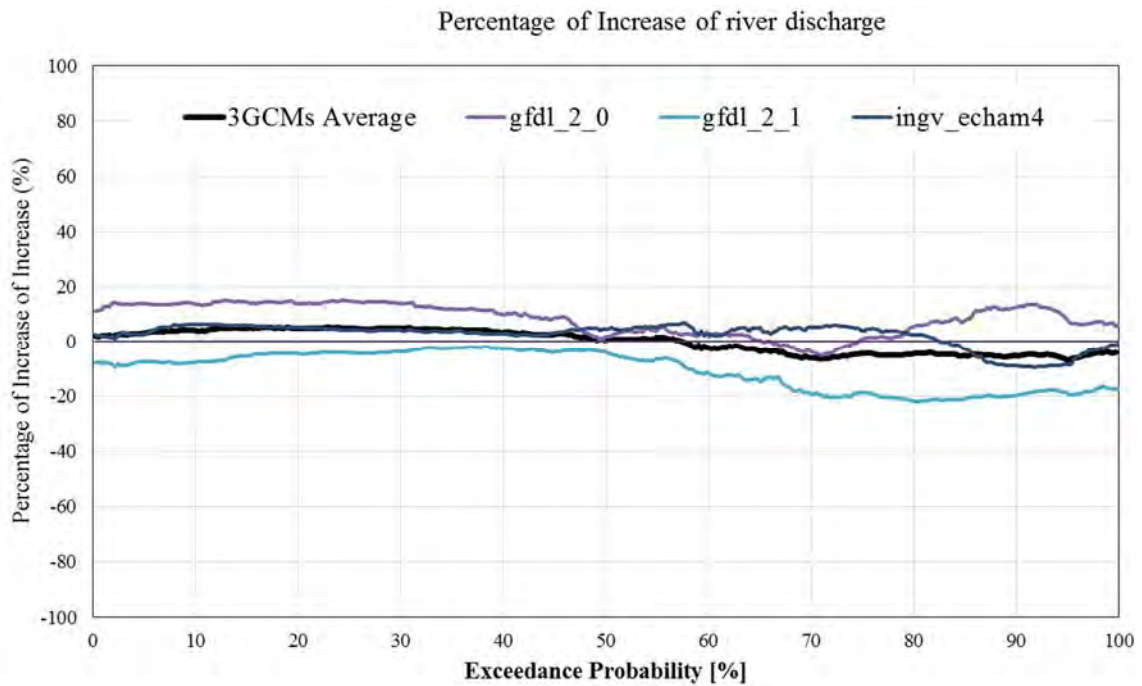


Figure 4.3.4-3 Percentage increases of river discharge nearby Palembang (sub-basin #300) from the past, 1985-2000 to the future, 2050-2065. Black solid line: average the three GCMs.

c) Drought

Climate change impacts on droughts in the Musi River basin are some of the most important concerns. To evaluate changes in drought discharge, the following indices were used.

- Annual drought discharge (average of 355th rank of daily discharge)
- Number of days in a year in which river discharge is less than the present drought discharge

Table 4.3.4-1 lists the calculated drought indices at nearby Palembang (sub-basin #300) for each climate simulation. The change in the annual drought discharge is very small but all of the selected models show the increase of the number of days in a year in which river discharge is less than the present drought discharge. It is very likely that the drought period will become longer in future in the Musi Basin.

CHAPTER 4 CLIMATE CHANGE IMPACT ASSESSMENT AND HYDROLOGICAL SIMULATION

Table 4.3.4-1 Drought indices at nearby Palembang (sub-basin #300)

| | Annual Drought Discharge (m ³ /s) [Average 355 th rank] | | Average number of days with river discharge below the present drought discharge | |
|-------------|--|--------|---|--------|
| | Present | Future | Present | Future |
| gfdl_2_0 | 771.4 | 774.6 | 32 | 33 |
| gfdl_2_1 | 625.5 | 647.5 | 47 | 51 |
| ingv_echam4 | 875.8 | 822.4 | 26 | 41 |

3) Surface Air Temperature

Figure 4.3.4-4 shows annual mean changes in surface air temperature for 2050–2065 relative to 1985–2000. The multi-model mean was calculated using the three selected GCMs. To consider spatial distribution of the change in the annual mean surface air temperature over the basin, we need to correct the effect of elevation.

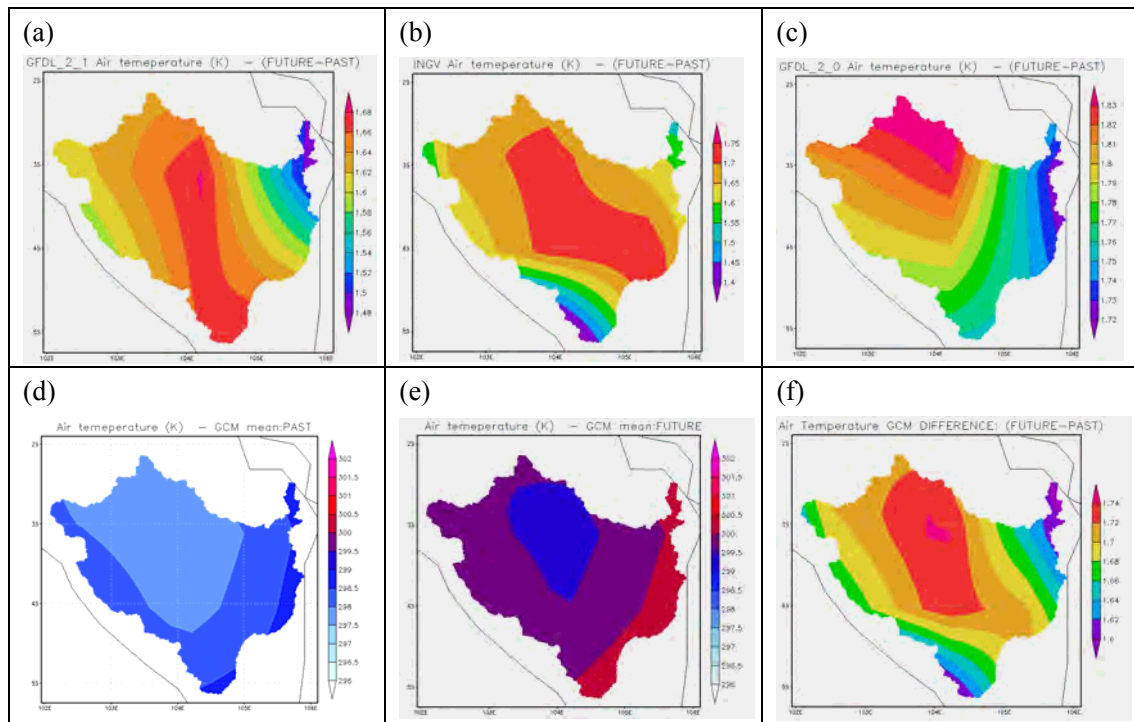


Figure 4.3.4-4 Changes in Surface Air Temperature: (a) difference “gfdl_2_1” of annual average for future(2050-2065) minus past(1985-2000); (b) difference “ingv_enham4” of annual average for future(2050-2065) minus past(1985-2000); (c) difference “gfdl_2_0” of annual average for future(2050-2065) minus past(1985-2000); (d) three-model mean of annual average for past (1985-2000); (e) three-model mean of annual average for future (2050–2065); (f) difference between (e) and (d).

CHAPTER 4 CLIMATE CHANGE IMPACT ASSESSMENT AND HYDROLOGICAL SIMULATION

4) Evapotranspiration (ET)

Figure 4.3.4-5 shows annual mean changes of projected evapotranspiration (ET) for 2050–2065 with respect to 1985-2000 in the Musi River basin. There was an increased trend of ET in both river basins. ET will increase in the whole basin but the change is relatively small.

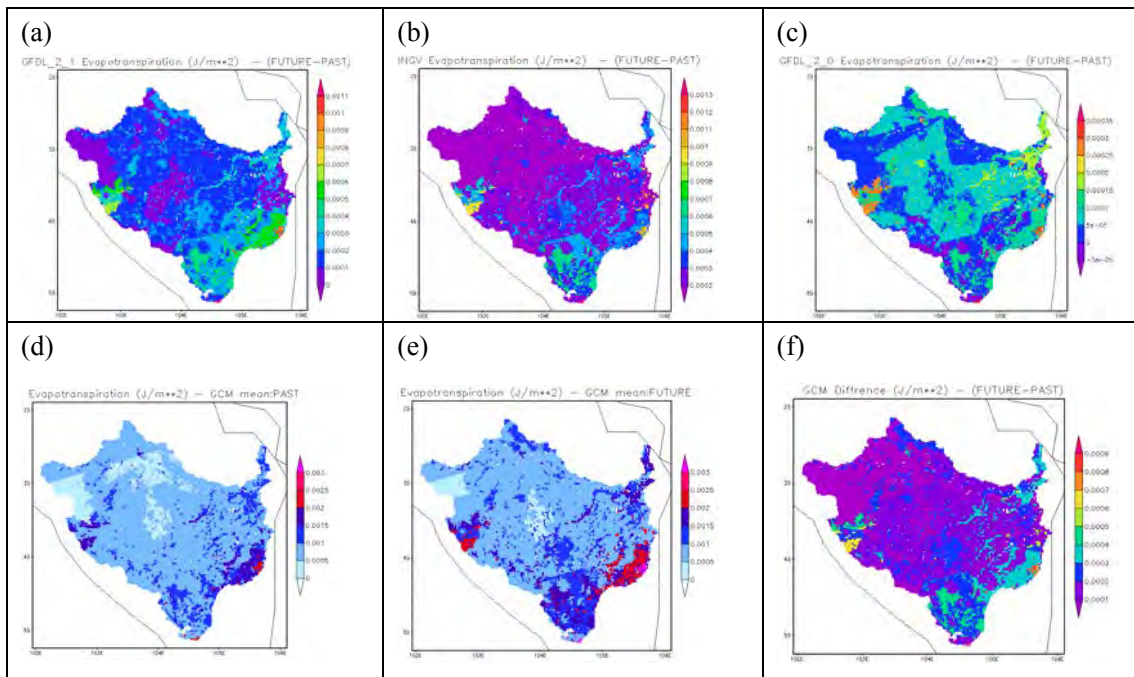


Figure 4.3.4-5 Changes in Evapotranspiration (ET): (a) difference “gfdl_2_1” of annual average for future(2050-2065) minus past(1985-2000); (b) difference “ingv_enham4” of annual average for future(2050-2065) minus past(1985-2000); (c) difference “gfdl_2_0” of annual average for future(2050-2065) minus past(1985-2000); (d) three-model mean of annual average for past (1985-2000); (e) three-model mean of annual average for future (2050–2065); (f) difference between (e) and (d).

5) Soil Moisture

The WEB-DHM model is also capable of simulating soil moisture and its changes. Figure 4.3.4-6 shows annual mean changes in soil moisture for 2050–2065 relative to 1985–2000 in the Musi River basin. The average change is very small.

CHAPTER 4 CLIMATE CHANGE IMPACT ASSESSMENT AND HYDROLOGICAL SIMULATION

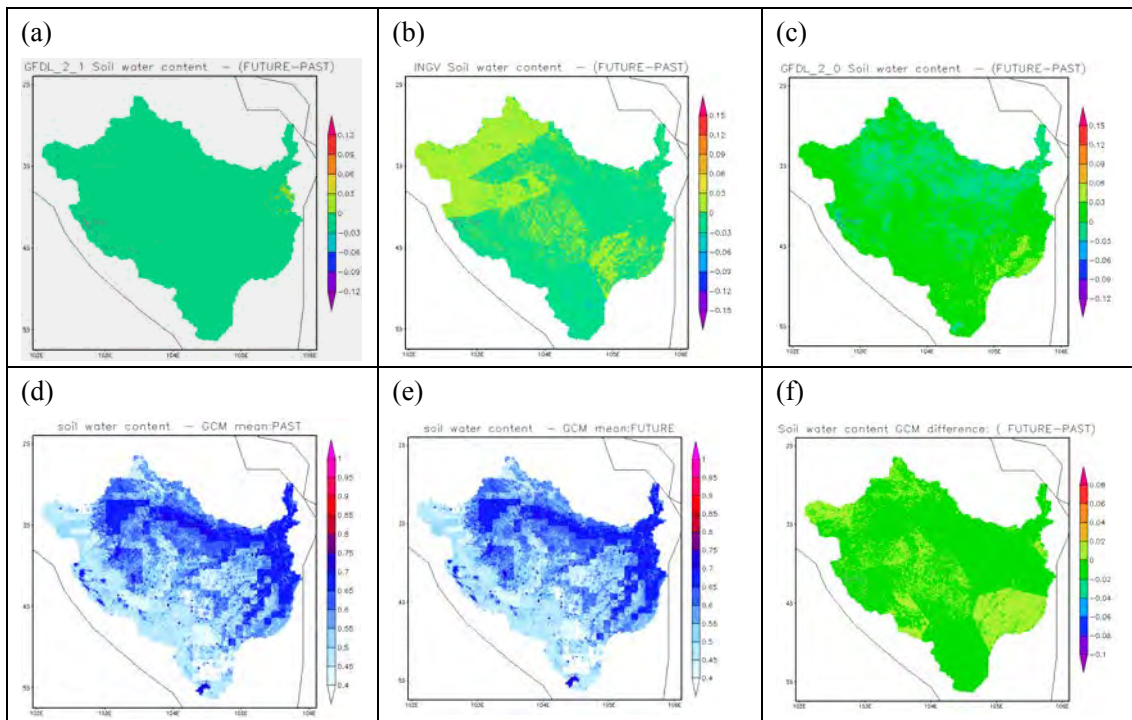


Figure 4.3.4-6 Changes in Soil Moisture: (a) difference “gfdl_2_1” of annual average for future(2050-2065) minus past(1985-2000); (b) difference “ingv_enham4” of annual average for future(2050-2065) minus past(1985-2000); (c) difference “gfdl_2_0” of annual average for future(2050-2065) minus past(1985-2000); (d) three-model mean of annual average for past (1985-2000); (e) three-model mean of annual average for future (2050–2065); (f) difference between (e) and (d).

(4) Summary of Climate Change Impact in the Musi River Basin

We evaluated climate change impacts on water resources in the Musi River basin. Through multi-model ensemble analyses, we quantitatively evaluated the projected changes and their uncertainty. The projected change of water resources is summarized below.

- i. Annual rainfall will decrease very likely.
- ii. Monthly averaged discharge will decrease in the first-half rainy season and the second-half dry season, whereas will increase in the second-half rainy season and the first-half dry season.
- iii. Low flow discharge will likely decrease, whereas high flow discharge will likely increase.
- iv. It is very likely that the drought period will become longer in future
- v. The changes in ET and soil moisture, which are closely related with rice production, are very small.

CHAPTER 4 CLIMATE CHANGE IMPACT ASSESSMENT AND HYDROLOGICAL SIMULATION

4.3.5 Runoff Analysis for Flood Risk Assessment

Runoff calculations were done to evaluate future river flood conditions based on the methodology described in section 4.3.3. We evaluated the magnitude of basin-averaged five month rainfall for 2-, 5-, 10-, 25-, 50- and 100-year return periods (hereafter referred to as T-year return period) using observed daily rainfall records. The stretch/shorten ratio for T-year return period for the present flood condition was calculated as a ratio of the basin-averaged five month rainfall intensity for T-year return period to the peak rainfall intensity of the flood event. By scaling it with the change ratio for T-year return period, the stretch/shorten ratio for T-year return period for the future flood conditions was evaluated. The calculated stretch/shorten ratios are summarized in Table 4.3.5-1.

Runoff calculations were conducted for the future/present flood event with 2-, 5-, 10-, 25-, 50- and 100-year return periods. The impact of climate change on the flood regime was evaluated by comparing simulated flood discharge with different extreme rainfall scenarios (present and three set of future scenarios). The simulated hydrograph for the past and the future three scenarios are shown in Figures 4.3.5-1~4. Table 4.3.5-1 shows the intensity and change ratios of simulated flood peak discharges for different future scenarios and different return periods at the nearby Palembang (sub-basin #300). The results indicate severe flooding conditions in the future climate. Inundation simulation will be carried out using the evaluated present/future flood hydrograph and future flood risk will be analyzed in the subsequent study component for “Water Resources Management Plan”.

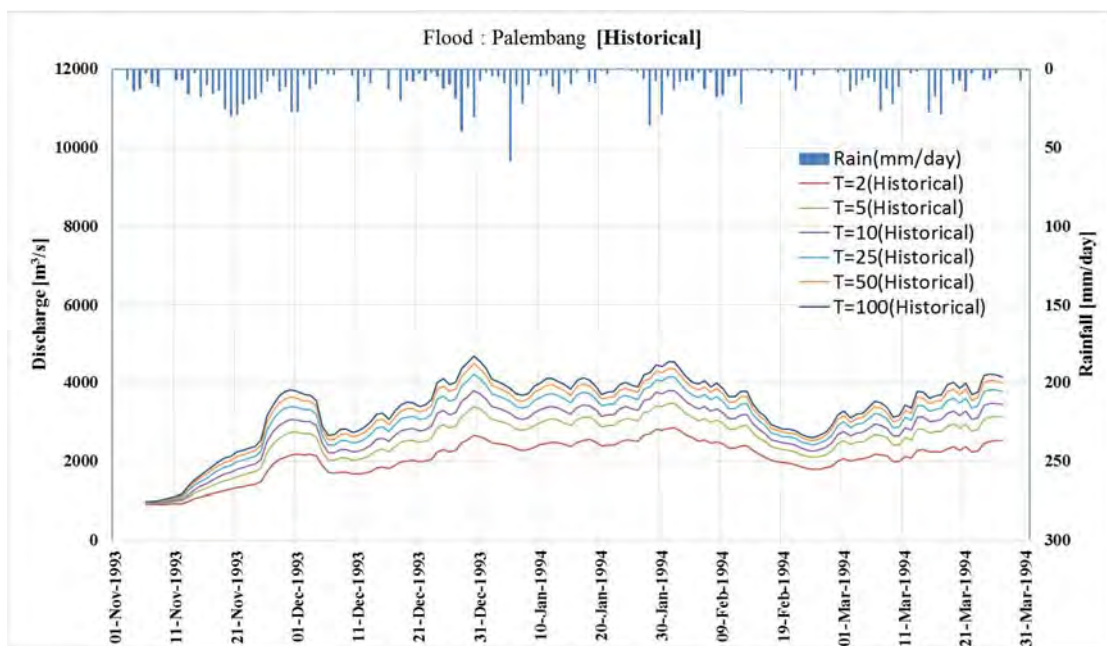


Figure 4.3.5-1 Results of runoff simulations using historical data for different return periods and different scenarios at the nearby Palembang (sub-basin #300).

CHAPTER 4 CLIMATE CHANGE IMPACT ASSESSMENT AND HYDROLOGICAL SIMULATION

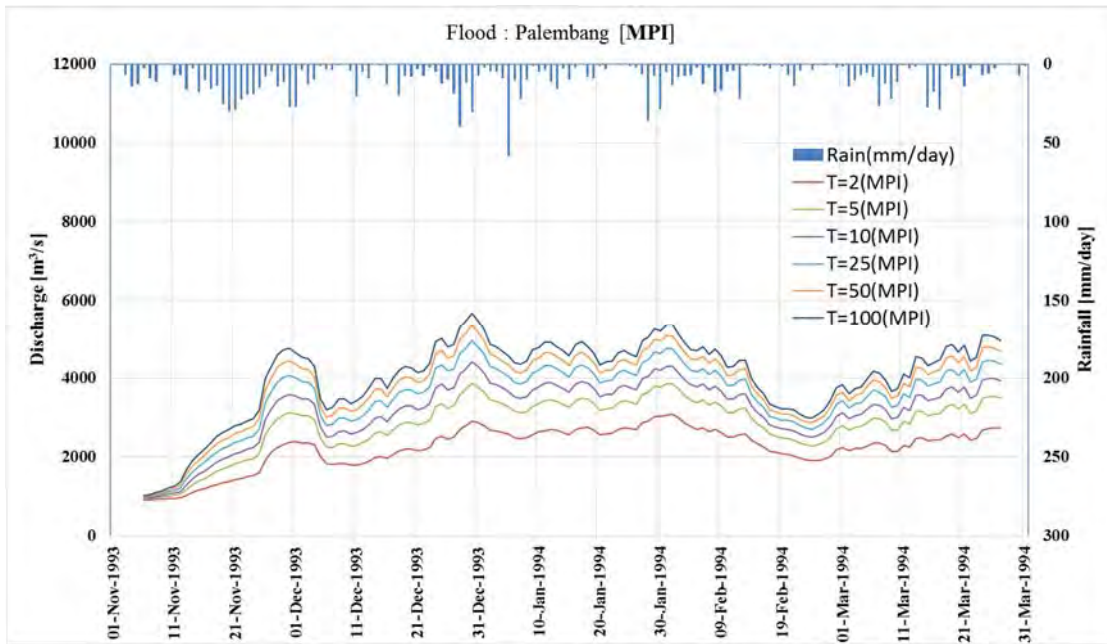


Figure 4.3.5-2 Results of runoff simulations using MPI (scenario of the most hazardous side) data for different return periods and different scenarios at the nearby Palembang (sub-basin #300).

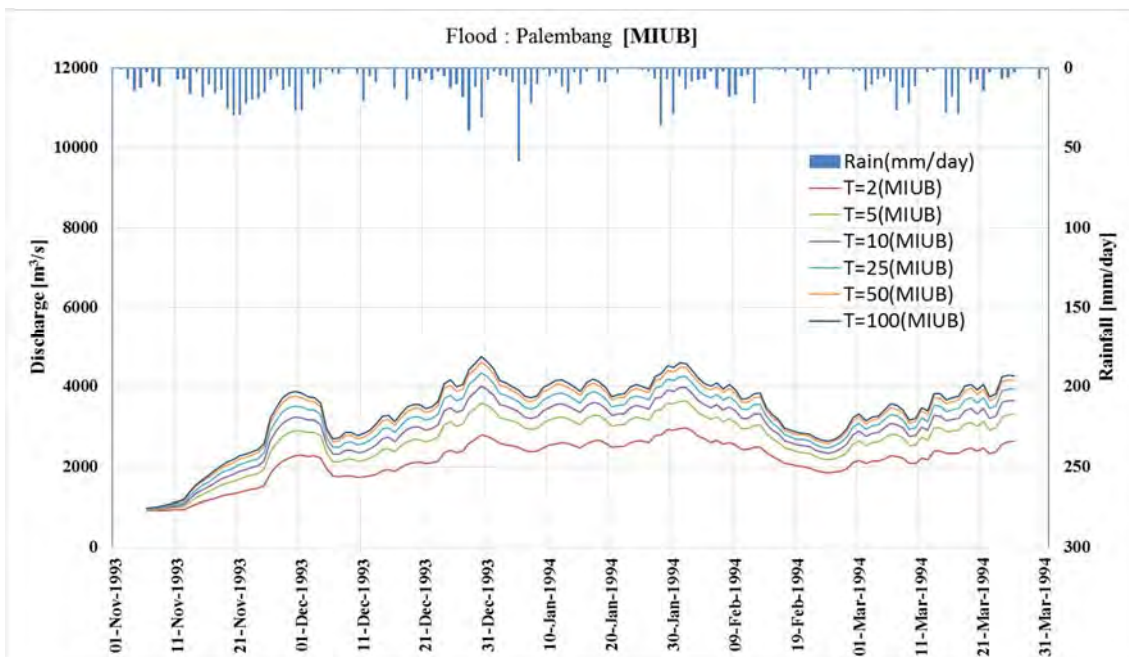


Figure 4.3.5-3 Results of runoff simulations using MIUB (scenario of highest probable) data for different return periods and different scenarios at the nearby Palembang (sub-basin #300).

CHAPTER 4 CLIMATE CHANGE IMPACT ASSESSMENT AND HYDROLOGICAL SIMULATION

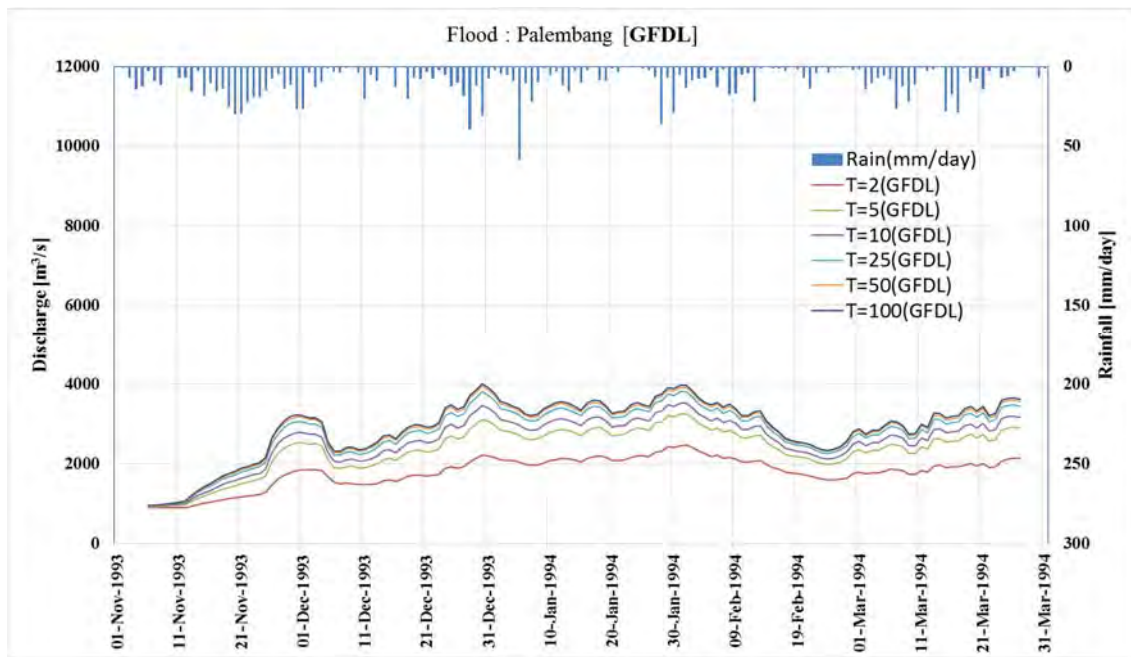


Figure 4.3.5-4 Results of runoff simulations using GFDL (scenario of safest side) data for different return periods and different scenarios at the nearby Palembang (sub-basin #300).

Table 4.3.5-1 Intensity and change ratios of simulated flood peak discharges for different future scenarios and different return periods at the nearby Palembang (sub-basin #300).

| Return Period | Peak Discharge(m ³ /s) | | | | Change Ratio of Peak Discharge (Future/Historical) | | |
|---------------|-----------------------------------|-----------------|------------------|------------------|--|------------------|------------------|
| | Historical | Future(H) [MPI] | Future(M) [MIUB] | Future(L) [GFDL] | Future(H) [MPI] | Future(M) [MIUB] | Future(L) [GFDL] |
| T=2 | 2,860 | 3,080 | 2,970 | 2,470 | 1.08 | 1.04 | 0.86 |
| T=5 | 3,470 | 3,870 | 3,640 | 3,250 | 1.12 | 1.05 | 0.94 |
| T=10 | 3,810 | 4,420 | 4,010 | 3,530 | 1.16 | 1.05 | 0.93 |
| T=25 | 4,220 | 4,960 | 4,350 | 3,810 | 1.18 | 1.03 | 0.90 |
| T=50 | 4,490 | 5,350 | 4,620 | 3,940 | 1.19 | 1.03 | 0.88 |
| T=100 | 4,690 | 5,680 | 4,760 | 4,010 | 1.21 | 1.01 | 0.86 |

CHAPTER 4 CLIMATE CHANGE IMPACT ASSESSMENT AND HYDROLOGICAL SIMULATION

4.4 Implementation of Climate Change Impact Assessment on Food Production: Musi River Basin

4.4.1 Implementation of Field Survey Required for Preparing a Crop Model and Establishment of the Method

The crop simulation model needs information on agricultural management such as rice variety, growing season, and amount of fertilizer as input data, plus actual values of growth and yield of rice as validation data. In addition to this information for the model, field surveys of actual water use are needed for development of an irrigation module. Accordingly, we assisted the consultant in charge of “Water resources management plan” as the other part of this project to establish methods (manuals) for those surveys.

(1) Selection of the outsourcing contractor to conduct field survey

We conducted technical support activities in Indonesia to establish and practice field surveying as referred to in Appendix B. We were introduced to the Suboptimal Land Research Center of Sriwijaya University, which is a candidate contractor for outsourcing field surveys. After several discussions with the consultant and the candidate, we established a preliminary method of field surveying for collecting information for the aforementioned purpose. The detailed methodology was referred to in Section 4.4.4. Because better candidates were hard to find, we recommended the Suboptimal Land Research Center at the Sriwijaya University as the outsourcing contractor to the consultant.

Besides this activity, we conducted preliminary field surveys to formulate the concept of a coupling hydrologic and rice growth model. Information on the surveys is given in the following sections.

(2) Collection of governmental data

Since governmental data is quite important and informative, we recommended the consultant to collect the data. The collected data were referred to in Section 4.4.4. Since land-use maps were of insufficient quality, we synthesized the maps from the Department of Agriculture and Kementerian Pertanian and BAPPEDA.

(3) Summary of Field Survey Results

In this section, we present some of results obtained by the above mentioned field survey. Table 4.4.1-1 shows difference in yield and fertilizer amounts between locations obtained through farmers’ interviews. The fertilizer amount varied among locations but it was not consistent with the yield. The inconsistency may be derived from difference in soil fertility. Although the field surveys were planned to include soil surveys, only some of the recommended data was obtained (Figure 4.4.1-1). The analysis of difference in rice productivity between locations needs further study.

CHAPTER 4 CLIMATE CHANGE IMPACT ASSESSMENT AND HYDROLOGICAL SIMULATION

Table 4.4.1-1 Difference in rice yield and fertilizer between ecotypes and locations, obtained through farmers' interview.

| Ecotypes | Location | Cropping | Yield (t ha ⁻¹) | Fertilizer (N kg ha ⁻¹) |
|-------------------|-----------------|----------|--------------------------------|---|
| Rainfed | Leumping | | 4.2 | 60.8 |
| | | 1st | 4.2 | 59.8 |
| | | 2nd | 4.3 | 61.8 |
| Irrigated | Belitang | | 4.2 | 91.4 |
| | | 1st | 4.2 | 62.8 |
| | | 2nd | 4.1 | 68.3 |
| | Musi Rawas | | 4.2 | 120.0 |
| | | 1st | 3.8 | 123.4 |
| | | 2nd | 4.6 | 116.6 |
| Tidal swamp | Telang Upang | | 3.9 | 84.2 |
| | | | 5.0 | 117.7 |
| | | | 2.8 | 50.6 |
| Fresh water swamp | Rambutan | | 2.9 | 65.4 |

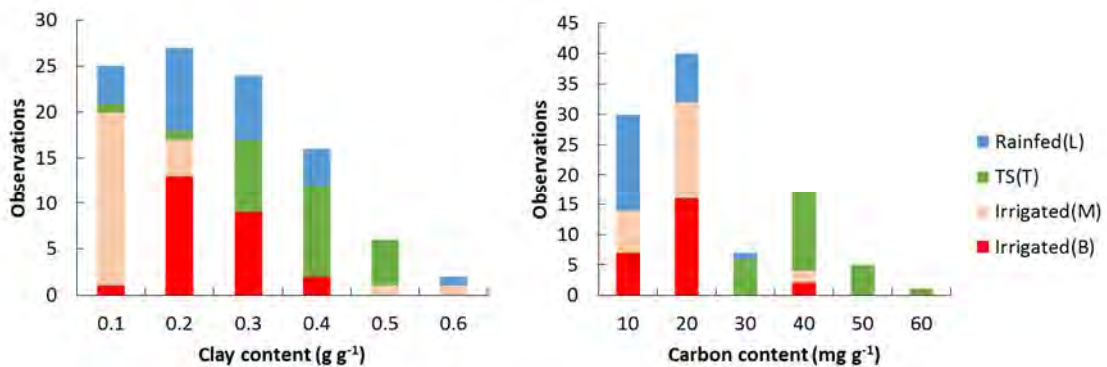


Figure 4.4.1-1 Difference in soil clay and carbon content between locations obtained through field surveys.

The field survey also showed the difference in yield between locations and farmers (Figure 4.4.1-2). The sampled yield obtained by field survey was consistent with the yield obtained through farmers' interviews except for Musi Rawas. Since the most sampled yield in Musi Rawas recorded more than 8 t ha⁻¹, the data may include some errors.

The governmental data showed the area of paddy fields classified into four ecotypes: rainfed, irrigated, tidal swamp, and freshwater swamp for each kabupaten (Table 4.4.1-2). The kabupaten where a majority of paddy fields are classified as fresh water swamps, e.g. Muara Enim, had a peak planting time in June (Figure 4.4.1-2); those in the tidal swamp ecotype, e.g. Banyuasin, had a large peak around November and a small peak around June; those in the rainfed ecotype, e.g. Lahat, had relatively

CHAPTER 4 CLIMATE CHANGE IMPACT ASSESSMENT AND HYDROLOGICAL SIMULATION

unclear peaks but were similar to those in the tidal swamp ecotype; and those in the irrigated ecotype, e.g. Pagar Alam, did not have any clear peaks.

Table 4.4.1-2 Area of paddy fields classified into four ecotypes—tidal swamp, irrigated, rainfed, and fresh water swamp (FWS)—in each kabupaten.

| | Tidal Swamp | Irrigated | Rainfed | FWS | Total |
|--------------------|-------------|-----------|---------|---------|---------|
| BANYUASIN | 143,454 | 0 | 10,122 | 44,982 | 198,558 |
| Pagar Alam | 0 | 3,292 | 200 | 0 | 3,492 |
| LAHAT | 0 | 25,610 | 2,685 | 490 | 28,785 |
| MUARA ENIM | 0 | 4,111 | 5,635 | 24,407 | 34,153 |
| MUSI BANYUASIN | 42,081 | 399 | 830 | 29,566 | 72,876 |
| MUSI RAWAS | 0 | 14,592 | 12,223 | 24,082 | 50,897 |
| OGAN ILIR | 0 | 0 | 1,000 | 67,544 | 68,544 |
| OGAN KOMERING ILIR | 26,785 | 650 | 56,463 | 73,308 | 157,206 |
| Ogan Komering Ulu | 1,476 | 2,259 | 1,636 | 0 | 5,371 |
| OKU Selatan | 0 | 9,872 | 1,512 | 70 | 11,454 |
| OKU TIMUR | 0 | 26,139 | 30,765 | 23,007 | 79,911 |
| PALEMBANG | 26 | 0 | 189 | 7,813 | 8,028 |
| PRABUMULIH | 0 | 300 | 50 | 875 | 1,225 |
| Total | 213,822 | 87,224 | 123,310 | 296,144 | 720,500 |

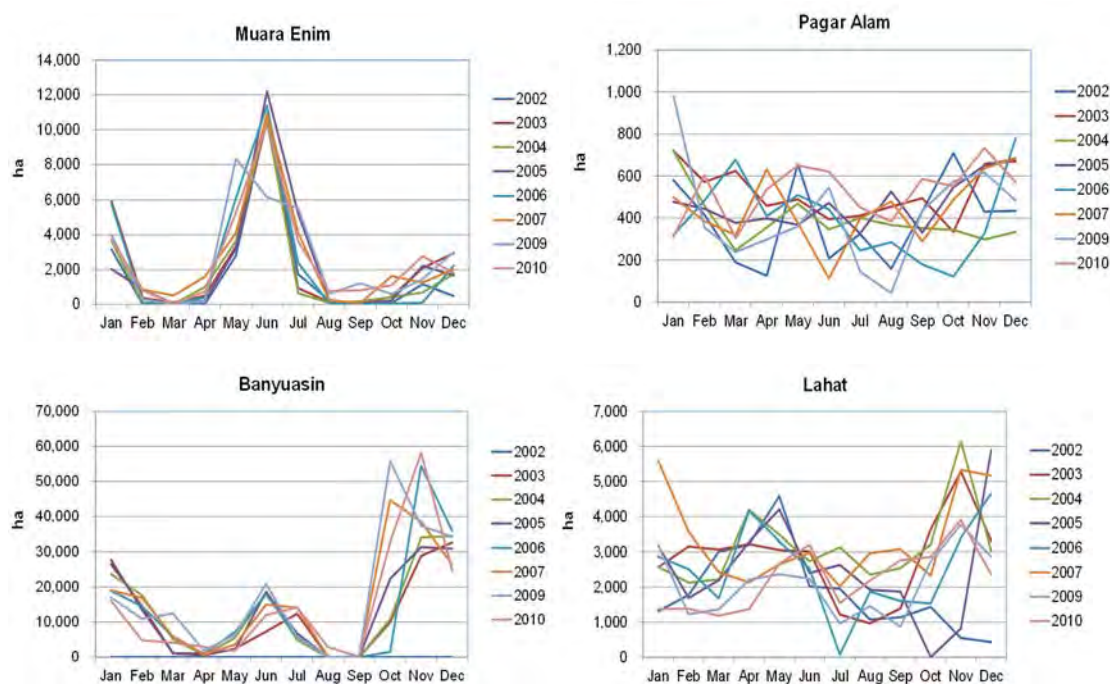


Figure 4.4.1-2 Planting times of rice in each kabupaten. A majority of paddy fields in Mura Enim were classified as fresh water swamp ecotypes; those in Pagar Alam as irrigated; those in Banyuasin as tidal swamp; and those in Lahat as rainfed (see Table 4.4.1-2).

CHAPTER 4 CLIMATE CHANGE IMPACT ASSESSMENT AND HYDROLOGICAL SIMULATION

The above-mentioned data was classified not only into kabupaten but also into ecotypes. However, the yield data was only classified into kabupaten. To assess water use, and to develop strategies for production improvement, yield data classified into ecotypes is recommended. The governmental data showed the differences in yield between kabupaten (Figure 4.4.1-3), and the rapid increase in yield from 2000.



Figure 4.4.1-3 Statistical yield in each kabupaten.

4.4.2 Development of a Coupling Hydrologic and Rice Growth Model

(1) Model Structure

To address water and food security under climate change, we developed a coupling hydrologic and rice growth model. Since a hydrologic model outputs soil moisture and river discharge, we can use them as input for the crop and irrigation models, respectively. By coupling these three models, we can solve for the entire system, which links precipitation to soil moisture, river discharge, irrigable water, and crop growth (including evapotranspiration and leaf area index (LAI) growth; Figure 4.4.2-1).

Model coupling is based on the Water and Energy Budget-based Distributed Hydrological Model (WEB-DHM), which calls Simulation Model for Rice-Weather Relations (SIMRIW)-rainfed as a subprogram. The overall structure of the coupling model is shown in Figure 4.4.2-2.

CHAPTER 4 CLIMATE CHANGE IMPACT ASSESSMENT AND HYDROLOGICAL SIMULATION

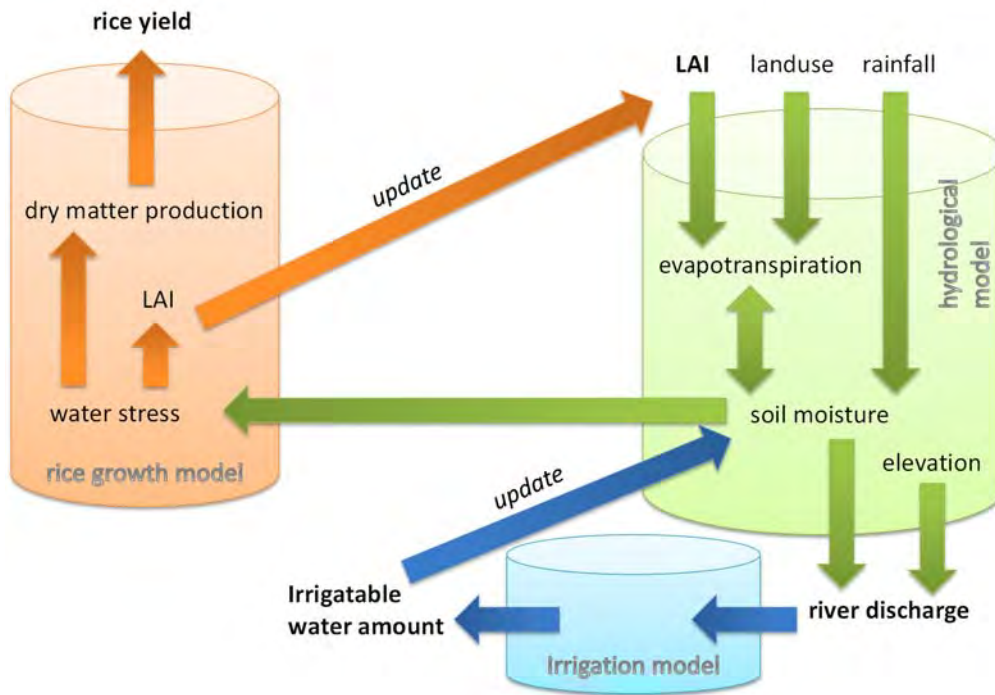


Figure 4.4.2-1 Linkage between hydrologic, irrigation, and crop models

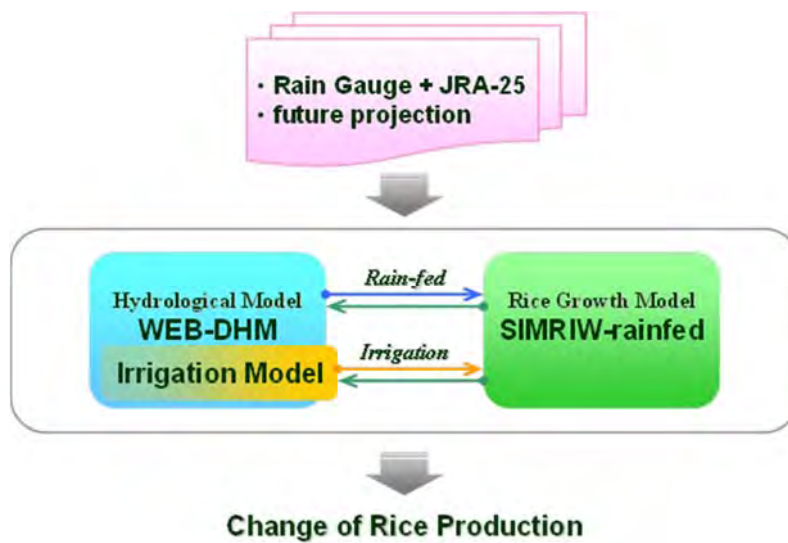


Figure 4.4.2-2 Model Overview

The model has five components:

1. WEB-DHM
2. SIMRIW-rainfed
3. Paddy model
4. Coupling system
5. Irrigation model (for “irrigated paddy”, “tidal water swamp”, and “freshwater swamp”)

CHAPTER 4 CLIMATE CHANGE IMPACT ASSESSMENT AND HYDROLOGICAL SIMULATION

Here, WEB-DHM (1), SIMRIW-rainfed (2), and irrigation model (5) are the core models and the paddy model (3) is incorporated within WEB-DHM (1). The coupling is done through the coupling system (4).

1) WEB-DHM

Please refer to Section 4.1.3.

2) SIMRIW-rainfed

This simulation model for rice growth and yield under rainfed conditions was originally developed on the basis of data obtained in northeast Thailand. The model has six parts: phenological development, nitrogen uptake, water stress, leaf area expansion, dry matter production, and yield formation (Figure 4.4.2-3). However, preliminary investigations in the targeted area (Section 3.1.3) classified paddy fields in the Musi River Basin into four ecotypes: irrigated, rainfed, tidal swamp, and freshwater swamp. Accordingly, submodels corresponding to these ecotypes were developed and incorporated in the model.

The model requires field and cultivar parameters. Since the major cultivar, Ciherang, appeared to be the same in both the Citarum and Ciherang river basins, default parameter sets were prepared based on our previous study in the Citarum River basin. The parameter sets for other cultivars, Ciliwung, Impari 4, Impara 3, Mekkongga, IR48, and IR64, were estimated on the basis of previous documents. To obtain field parameters, several categories of field data, such as soil and plant, are necessary. However, sufficient data was not observed by the field survey (See Section 4.4.1). Here, we applied a technological coefficient for each ecotype, which represents the difference in productivity.

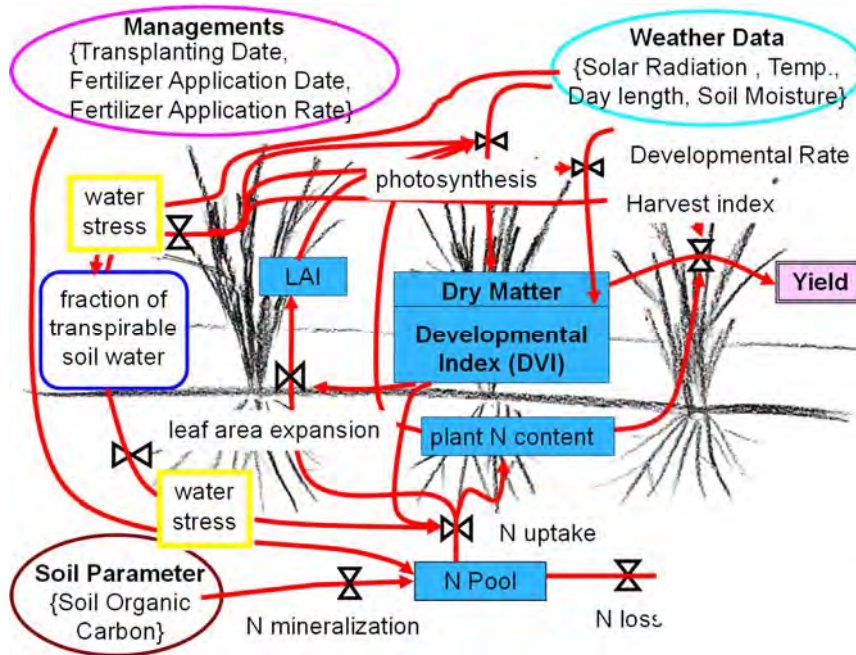


Figure 4.4.2-3 Overview of SIMRIW-rainfed.

3) Paddy model

Since Simple Biosphere 2 (SiB2, one of the components of WEB-DHM) has no paddy scheme, we introduced a paddy model into it (Figure 4.4.2-4). This model has four characteristics:

i) Existence of dike and surface storage water

One of the unique aspects of a paddy is that it has a dike. Because of this dike, the paddy can hold water that will evaporate and infiltrate. We presently assume all “paddy” grids to be surrounded by dikes of 10 cm in height. If water flows into a paddy grid above this depth, residual water leaves as surface flow. In other words, the dike can hold water until the water depth reaches 10 cm.

ii) Evaporation

When there is water stored on the surface, we calculate its evaporation by a bulk transfer method.

iii) Transpiration

For the calculation of transpiration from rice crops, we followed the SiB2 method and simply adjusted the parameters for such crops. For the calculation of transpiration from rice crops, we followed the SiB2 method and simply adjusted the parameters for such crops.

iv) Infiltration

When there is water stored on the surface, we also calculate its infiltration. We assume that this stored water infiltrates the surface soil layer quickly. If that layer is saturated, residual water returns to the surface stored water.

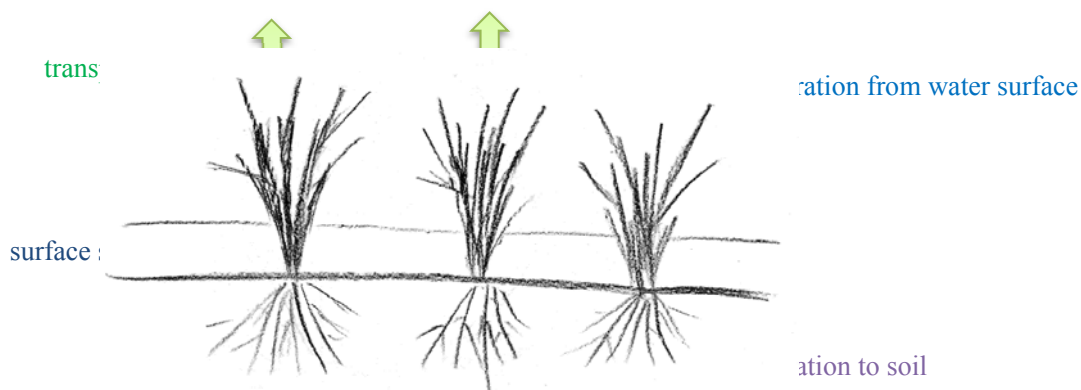


Figure 4.4.2-4 Overview of the paddy scheme.

4) Coupling system

An overview of the coupling system is described in Figure 4.4.2-5. The model calls SIMRIW-rainfed for every paddy grid of the WEB-DHM and calculates the increase of LAI and dry matter

production of rice. The calculated LAI is returned to the WEB-DHM and the updated LAI is used within that model to calculate hillslope and river channel flows. Evapotranspiration, photosynthesis, and respiration are calculated within the SiB2 incorporated in WEB-DHM, and updated soil moisture is passed to SIMRIW-rainfed (Figure 4.4.2-5). Thus, soil moisture, LAI, and forcing data are passed between WEB-DHM and SIMRIW-rainfed. Since LAI is calculated within SIMRIW-rainfed, we no longer need it from satellite data. We can also calculate it for future conditions.

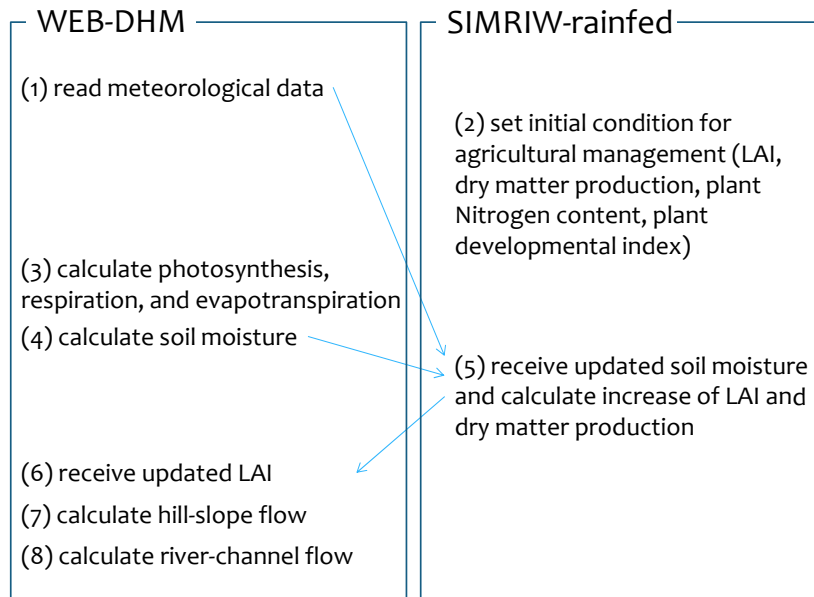


Figure 4.4.2-5 Overview of the coupling system

5) Irrigation Model

(i) Irrigated paddy

We have developed a simple irrigation model. One of the key procedures in this model is to correlate intake weirs and paddies (Figure 4.4.2-6), as follows. For each paddy cell, we must predefine the locations of intake weirs, from which farmers take irrigation water. For modeling, we assumed a “virtual” irrigation channel so that water taken from a river channel goes onto paddy fields directly and rapidly, without any losses from evaporation and infiltration.

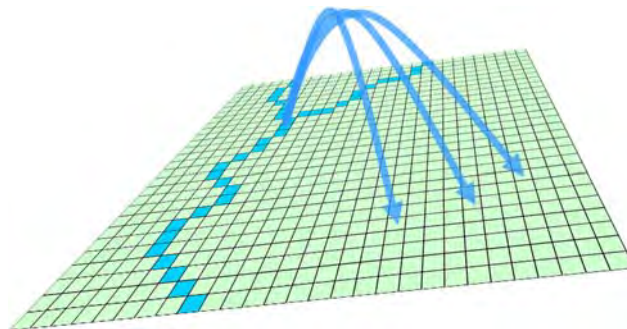


Figure 4.4.2-6 Definition of relationship between intake weirs and paddy cells

CHAPTER 4 CLIMATE CHANGE IMPACT ASSESSMENT AND HYDROLOGICAL SIMULATION

For defining locations of intake weirs, we assume that they can take water wherever a river channel exists. However, since WEB-DHM can calculate river discharge only at individual “flow intervals,” we can define only one intake weir per flow interval. Thus, we took only the uppermost river grid as an intake weir for each flow interval (Figure 4.4.2-7).

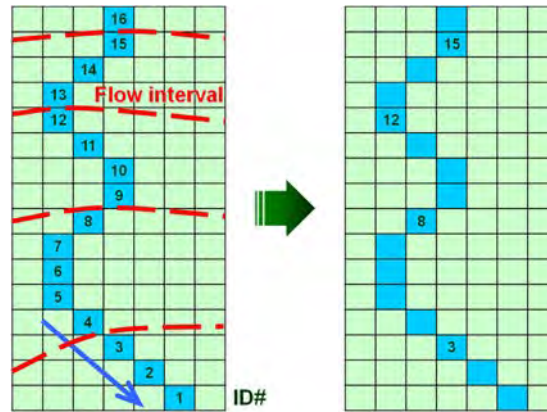


Figure 4.4.2-7 Identification of intake weir locations

Each intake weir is correlated to paddy cells by the following procedure (Figure 4.4.2-6): (i) The correlation procedure proceeds from downstream to upstream. (ii) For paddy cells that have been allocated an intake weir downstream, no intake weir will be allocated by the procedures for upstream. Assuming a red cell is the target weir (Figure 4.4.2-8(b)) and brown cells have already been assigned intake weirs by the downstream procedure, brown cells can no longer take water from the red cell. Then, we lift the red cell upward by 2 m (assuming pump irrigation) and check elevation at eight surrounding cells, except at brown cells. If these cell elevations are lower than the lifted red cell, river water irrigates these cells (yellow cells). Afterward, we examine elevations of cells surrounding the yellow grids. If the surrounding grid has lower elevation than the yellow grid, we assume that the former grid can take water from the red cell. We continue this procedure for surrounding grids and find cells that can be irrigated from the red cell. Finally, pink cells are defined such that they can introduce water from the red cell. (iii) We then proceed to the next target cell, which is located on the upper stream of the previous target cell.

Since the output of this procedure can be read by Windows Excel, we can edit the results with Excel by manually referring to the actual situation.

CHAPTER 4 CLIMATE CHANGE IMPACT ASSESSMENT AND HYDROLOGICAL SIMULATION

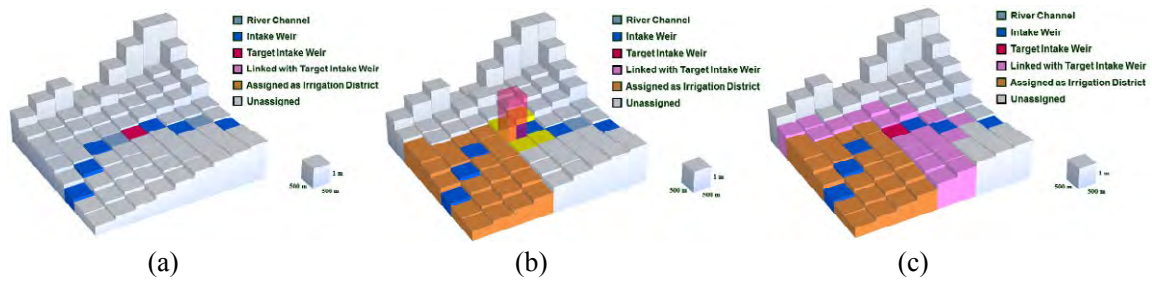


Figure 4.4.2-8 Allocation of intake weir to paddy grids.

The water allocation rule in our model is shown in Figure 4.4.2-9. The basic concept is that we provide irrigation water to each paddy field proportional to the amount of water demand. First, we derive water demand for each paddy grid by subtracting current from designed water depths. In this procedure, we consider maximum flow velocity at the intake and do not allow the system to take irrigation water beyond its velocity. Then, we sum water demand for one target intake weir and obtain total water demand for that intake. Next, we check river flow at the target intake weir and subtract environmental flow from it. The residual water is “available” for irrigation. Finally, we calculate the ratio of available water to total demand and multiply that ratio by the demand of each paddy grid. Thus, the allocated irrigation amount for each paddy field is just proportional to its original demand. This represents a type of “equality principle” for water allocation.

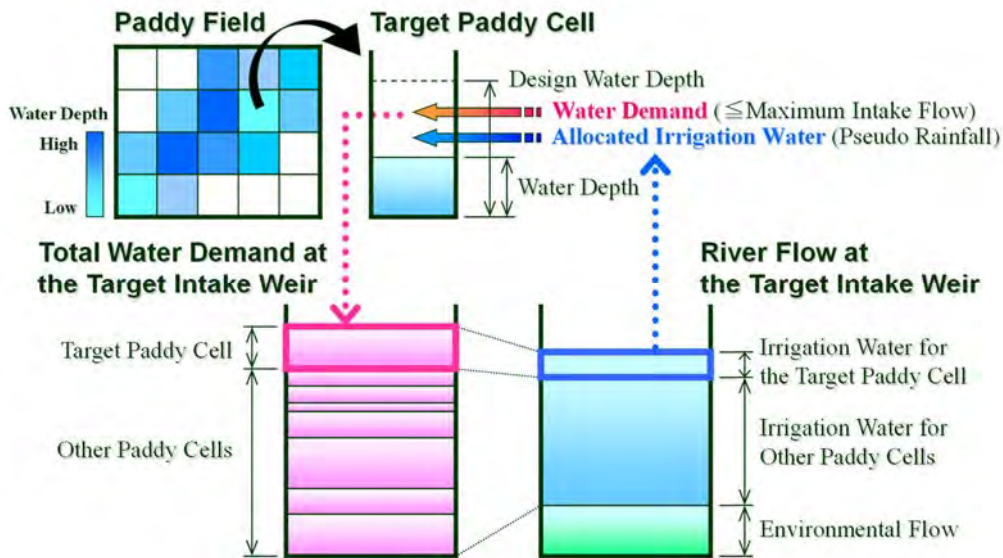


Figure 4.4.2-9 Water allocation rule in the irrigation model

(ii) Tidal swamp

The concept of an irrigation model for tidal swamp paddies is that if the water level of a river, after consideration of the tidal effect, exceeds a threshold value, paddies can introduce irrigation water from the river (Figure 4.4.2-10). Since there is backwater from the sea that is limitless, river discharge does not decrease even though irrigation is applied. Since water levels at river mouth and water channels in

CHAPTER 4 CLIMATE CHANGE IMPACT ASSESSMENT AND HYDROLOGICAL SIMULATION

tidal swamp areas were not available in the present, paddy fields in the tidal swamp ecotype was simulated similarly to those in the irrigated ecotype in the current study.

The simulation for this study

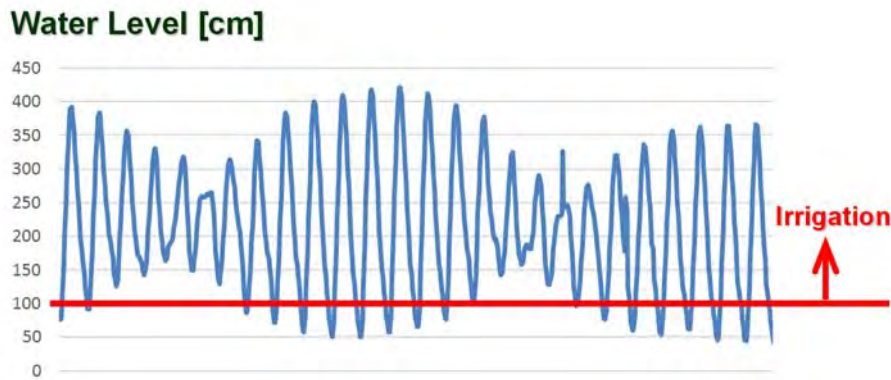


Figure 4.4.2-10 Water allocation rule in the irrigation model

(iii) Freshwater swamp

The concept of an irrigation model for fresh water swamp paddies is that water is available if the water depth is positive, but rice is damaged if the water depth exceeds the threshold value. To simulate water depth, water movement should be simulated, and the simulation needs digital elevation map on the order of cm. However, such maps were not obtained in the present. Here, we simulated water availability in fresh water swamp paddies similarly to that in rainfed paddies.

(2) Validation of the Coupling Hydrologic and Rice Growth Model and Determination of Technological Coefficient for Each Ecotype.

1) Condition of the simulation

If we use properly scientific observed data, the simulation can follow actual growth and obtained field parameters that represent the productivity of each field (Figure 4.4.2-11). However, sufficient data sets had not been obtained by the field survey (See Section 4.4.1). We employed the technological coefficient for each ecotype, which represent differences in productivity between ecotypes as we mentioned above. To obtain the coefficient, we selected the points 4° 05' S 104° 40' E, 3° 47' S 104° 54' E, 3° 02' S 104° 50' E, 2° 30' S 104° 58' E, 2° 39' S 104° 53' E, and 3° 10' S 102° 56' E for Belitang, Leumping, Rambutan, Upang, Telang, and Musi Rawas, respectively. Rice production was simulated from September 1st, 1985 to December 31st, 2012 as the present climate. The planted date was set by November 1st (Days of Year <DOY> = 305) for rainfed, irrigated, and tidal swamp ecotypes in rainy season and May 1st (DOY = 121) for all ecotypes for the dry season on the basis of governmental data. The technological coefficients were obtained as the rates of average simulated yield against the observed yield for each location and summarized for each ecotype. The yield data obtained through farmers' interviews was used as the observed yield, because the governmental data

CHAPTER 4 CLIMATE CHANGE IMPACT ASSESSMENT AND HYDROLOGICAL SIMULATION

was not obtained for each ecotype and the sampled yield data from the field survey seemed to have errors (Section 4.4.1).

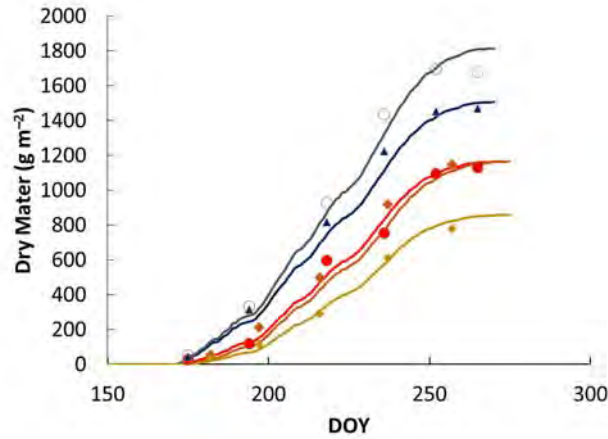
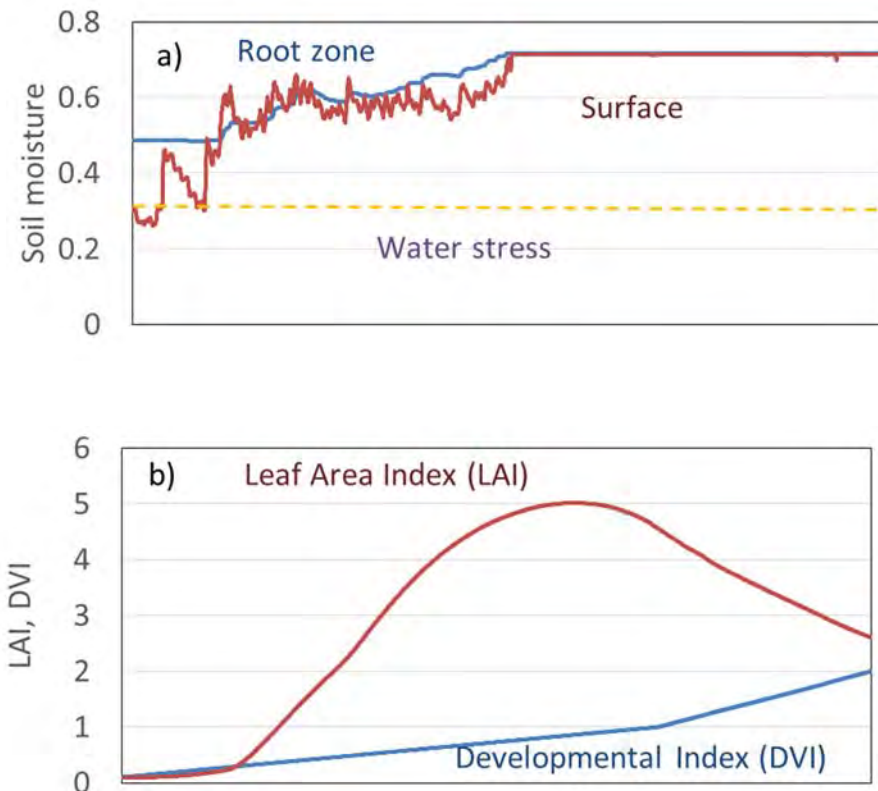


Figure 4.4.2-11 Simulation of rice above ground dry matter production (lines) in farmers' fields in the Musi River Basin. Symbols are the data obtained from farmers' fields through the field survey (Section 4.4.1). Each color indicates each farmer field. DOY: Days of year.



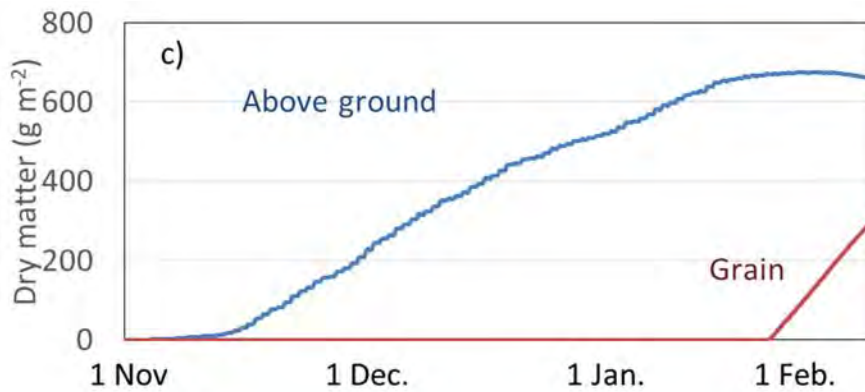


Figure 4.4.2-12 Simulation example. Rice planted in Lemping (Rainfed ecotype) in November 1st, 2009 simulation. (a) Soil moisture in the surface (red) and the root zone (blue); (b) LAI (red) and Developmental index (blue; 1, heading and 2, maturity); (c) Grain (red) and above ground (blue) dry matters.

2) Samples of the simulation

Figure 4.4.2-12 is a simulation example. In this case, rice was planted before precipitation at the beginning of the rainy season, making soil moisture adequate for the growth. Inadequate soil moisture caused water stress during vegetative growth, and decreased LAI and above-ground dry matter. However, the saturated soil moisture was maintained from one month before heading to maturity, and grain production was not affected by water. Since the above ground dry matter did not exceed 700 g m⁻² (7 t ha⁻¹), the yield was only 300 g m⁻² (3 t ha⁻¹).

3) The technological coefficient

The average yield simulated from from September 1st, 1985 to December 31st, 2012 ranged from 304 g m⁻² in Lemping, planted May 1st, to 406 g m⁻² in Musi Rawas, planted May 1st (Figure 4.4.2-13). Because Lemping was classified into the rainfed ecotype, water was often inadequate for production. Accordingly, Lemping also showed the largest standard deviation by years.

The technological coefficient was obtained as the rates of average simulated yields against the observed yields for each location and summarized for each ecotype. The average yield in the rainfed ecotype included non-yields due to severe water stress. However, we did not conduct field surveys where severe water stress caused non-yields. Accordingly, we excluded non-yields in the calculation of technological coefficients. The coefficients were 1.065, 1.181, 0.821, and 1.130 for irrigated, rainfed, fresh water swamp, and tidal swamp ecotypes, respectively.

CHAPTER 4 CLIMATE CHANGE IMPACT ASSESSMENT AND HYDROLOGICAL SIMULATION

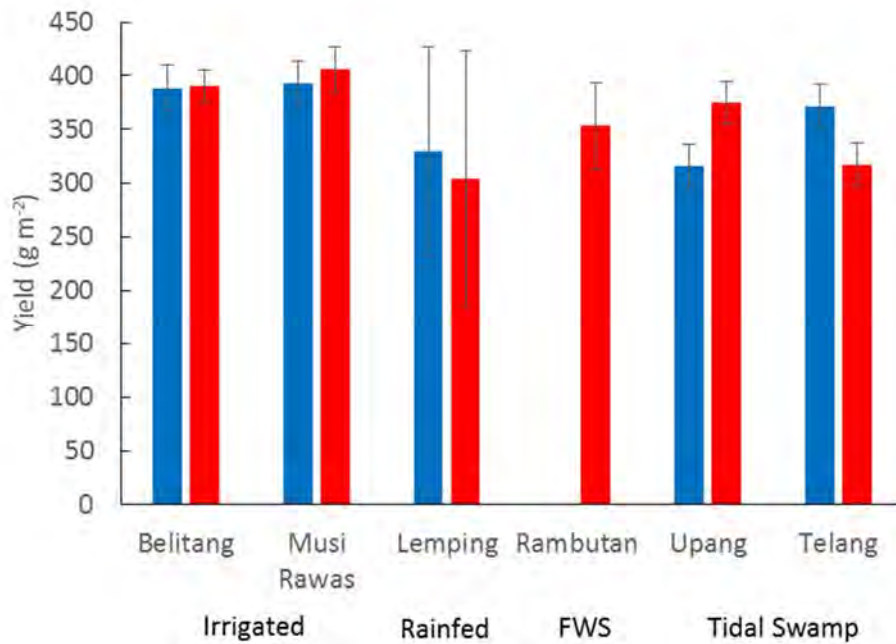
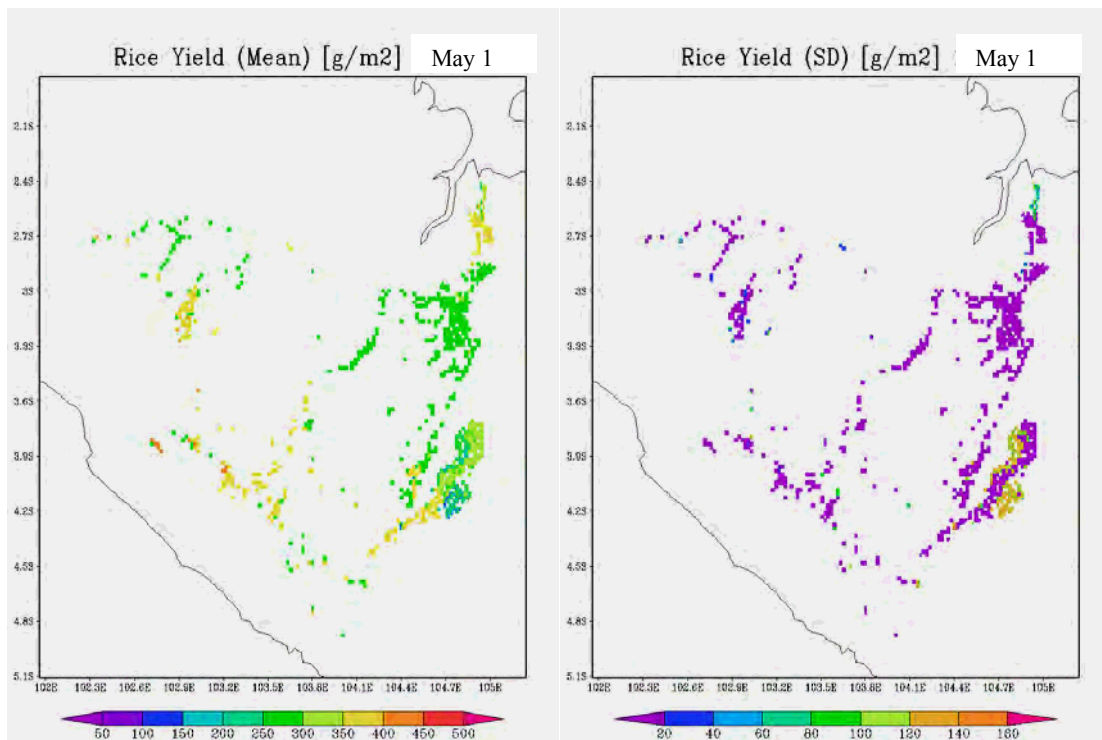


Figure 4.4.2-13 The average yield simulated from September 1st, 1985 to December 31st, 2012. Error bars are s.d. and mean yearly variations. The planted dates were November 1st (Blue) and May 1st (Red).



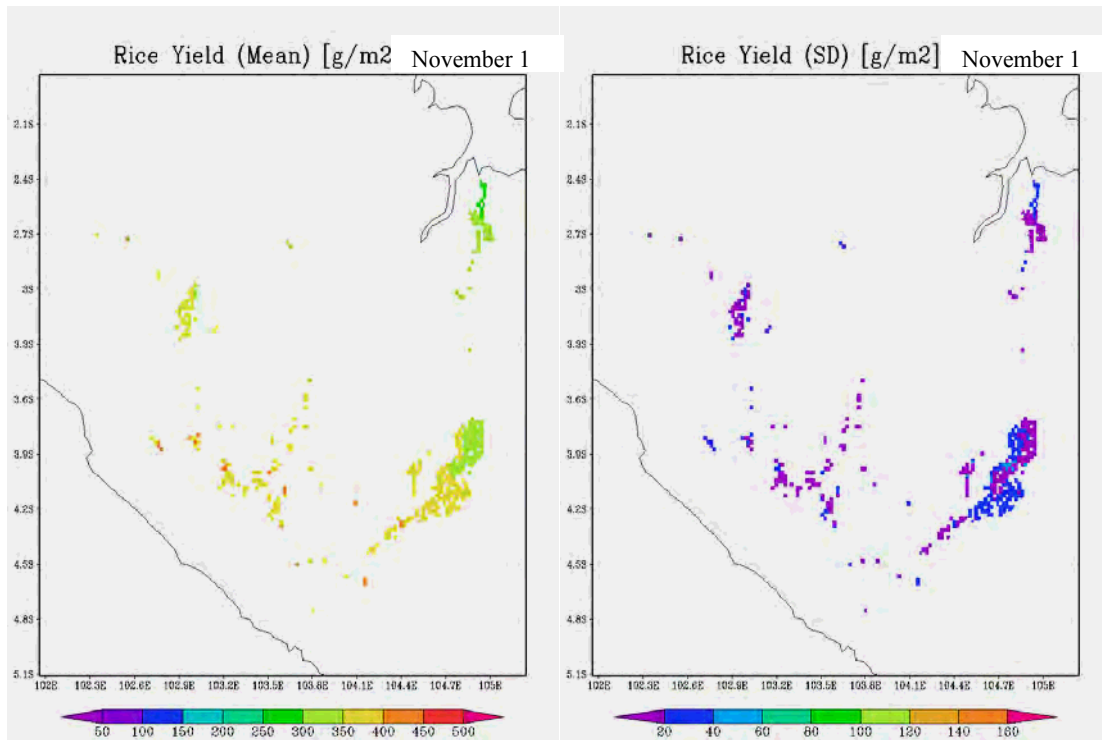


Figure 4.4.2-14 Spatial distribution of rice yields. Simulations were conducted for the period from September 1st, 1985 to December 31st, 2012 under the present climate conditions. Planting dates were set at May 1st (Days of Year <DOY> = 121, dry season; above) and November 1st (DOY = 305, rainy season; below). The yields (left) and the standard deviation (right) were calculated for the period.

4) Spatial distribution of simulated yields

After incorporating the technological coefficients, the Coupling Hydrologic and Rice Growth Model simulated rice yields from September 1st to December 31st, 2012 under the present climate conditions (Figure 4.4.2-14). The yields varied not only by the technological coefficients but also by soil moisture and solar radiation, which were derived from the hydrologic model, WEB-DHM. Several points showed the higher yields exceeding more than 500 g m⁻² due to sufficient soil moisture with higher solar radiation. The yields in the rainfed ecotype were lower in the dry season than in the rainy season (also see Figure 4.4.3-4) because insufficient soil moisture caused yield loss as described in the above section. The yields in the tidal swamp ecotype were higher in the dry season than in the rainy season due to higher solar radiation. The yields in the irrigated ecotype were similar during the dry and rainy seasons. Larger standard deviations, meaning yearly variations, were observed in the rainfed ecotype as described in the above section.

The yearly trends in yields averaged for whole ecotypes are shown in Figure 4.4.2-15. The largest yield depletion was observed in 1997. The year was reported as El Nino, of which magnitude was the largest in observation history. Although severe droughts were reported around the world, statistical yields did not imply such phenomena. Methodology for statistical data seems to be necessary. The

CHAPTER 4 CLIMATE CHANGE IMPACT ASSESSMENT AND HYDROLOGICAL SIMULATION

simulated yields did not show any similarity with the statistical yields, but showed a similarity with the statistical harvested area. The correlation coefficient between the simulated yield and the statistical harvested area was 0.57 ($P < 0.01$). Excluding the effect of soil moisture, lower simulated yield was derived from lower solar radiation, which was ordinarily accompanied by greater precipitation. The greater precipitation may cause floods and decrease the harvested area. Estimations of flood damage and flooded areas are recommended for the Coupling Hydrologic and Rice Growth Model, which will be developed in a further study.

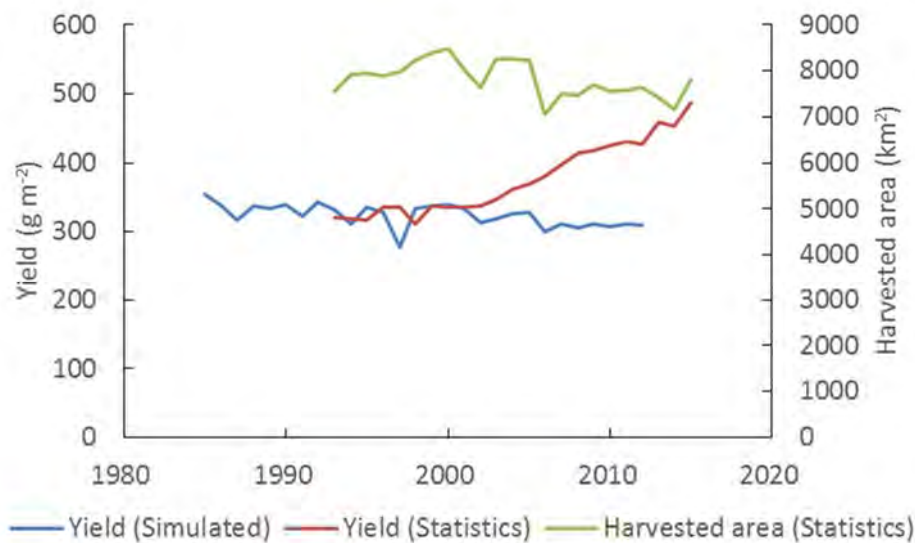


Figure 4.4.2-15 Trends of simulated and observed yields and the harvested area.

4.4.3 Implementation of Impact Assessment for Rice Production by the Coupling Model

(1) Simulation conditions

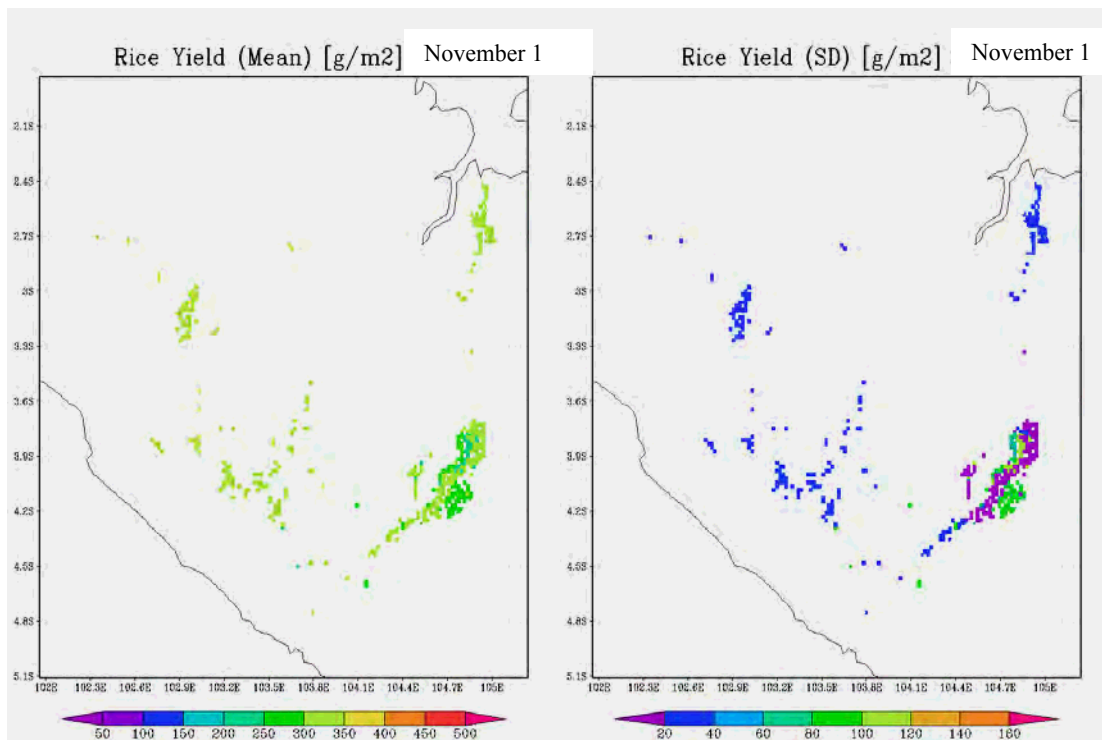
Three GCM scenarios, *gfdl_2_0*, *gfdl_2_1*, and *ingv_enham4*, were selected to predict future climate as mentioned in the previous section (Section 4.3.4). The scenarios consisted of predicted weather data for present and future, from January 1st 1985 to December 31st 2000, and from January 1st 2050 to December 31st 2065, respectively. Planted dates were set at November 1st (Days of Year $\langle \text{DOY} \rangle = 305$) for rainfed, irrigated, and tidal swamp ecotypes in the rainy season and May 1st ($\text{DOY} = 121$) for all ecotypes in the dry season. These are the same as validations for the present climate. The technological coefficients were set as the values determined under the present climate, namely 1.065, 1.181, 0.821, and 1.130 for irrigated, rainfed, fresh water swamp, and tidal swamp ecotypes, respectively. The climate impacts for the future were assessed against the present both were generated by the GCM scenarios.

CHAPTER 4 CLIMATE CHANGE IMPACT ASSESSMENT AND HYDROLOGICAL SIMULATION

(2) Impact assessment

Simulated yields under present and future climates were shown in Figure 4.4.3-1 and 4.4.3-2 as examples, which were simulated under the GCM scenario gfdl_2_1. The simulation results were summarized in Figure 4.4.3-3. The yields under future climates decreased slightly in irrigated, fresh water swamp, and tidal swamp ecotypes due to higher temperature.

The effects of climate change were obvious in rainfed ecotypes in which yield was affected by precipitation through soil moisture. The yield simulated under GCM scenario gfdl_2_0 showed less standard deviation (yearly variation) in rainy season than that under the present climate. Larger yearly variation were predicted in dry season production under GCM scenario gfdl_2_1 and in rainy season under GCM scenario ingv_echam 4. The reduction was derived from lower average and larger standard deviation in soil moisture in the middle of rainy season, February and March (Figure 4.4.3-4). On the other hand, soil moisture remained high and stable at the beginning of dry season, May and June. If GCM scenarios gfdl_2_1 or ingv_echam 4 are true, adjustments to planting dates and growth duration are necessary.



CHAPTER 4 CLIMATE CHANGE IMPACT ASSESSMENT AND HYDROLOGICAL SIMULATION

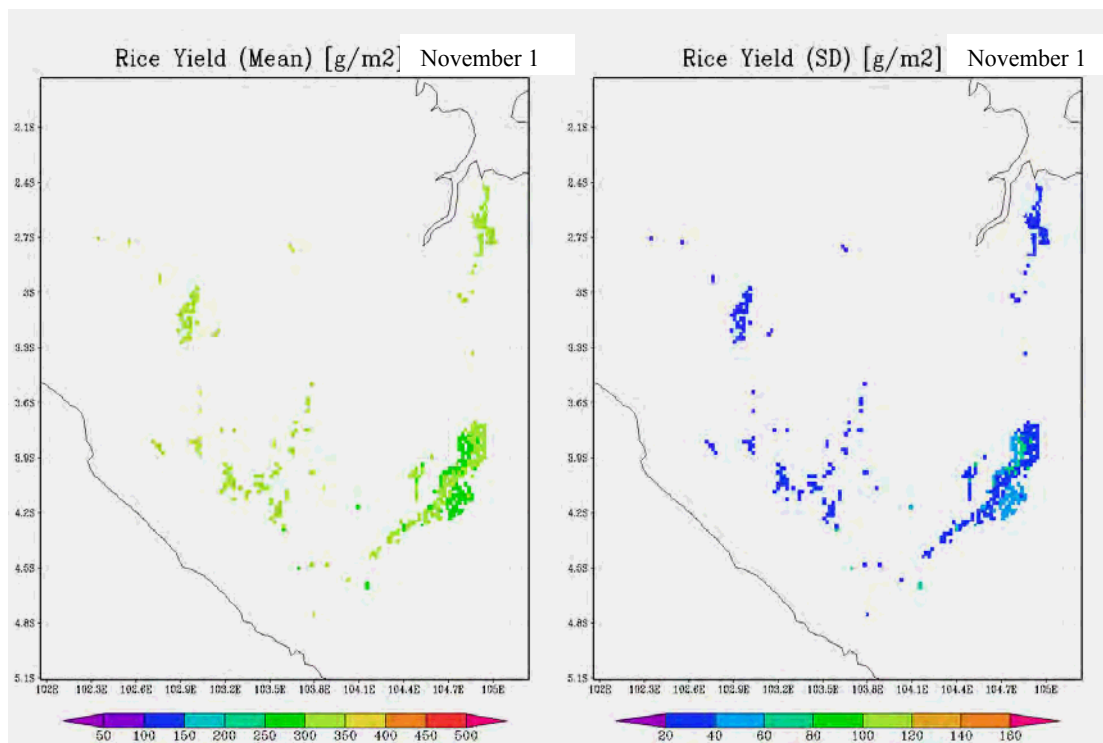


Figure 4.4.3-1 Distribution of simulated yields under the present (above) and future climate (below) in GCM scenario gfdl 2_1. Simulations were conducted for the period from January 1st, 1985 to December 31st, 2000 under the present climate conditions; and the period from January 1st, 2050 to December 31st, 2065 under the future climate conditions. Planting dates were set at November 1st (DOY = 305, rainy season). The yields (left) and the standard deviation (right) were calculated for the period.

CHAPTER 4 CLIMATE CHANGE IMPACT ASSESSMENT AND HYDROLOGICAL SIMULATION

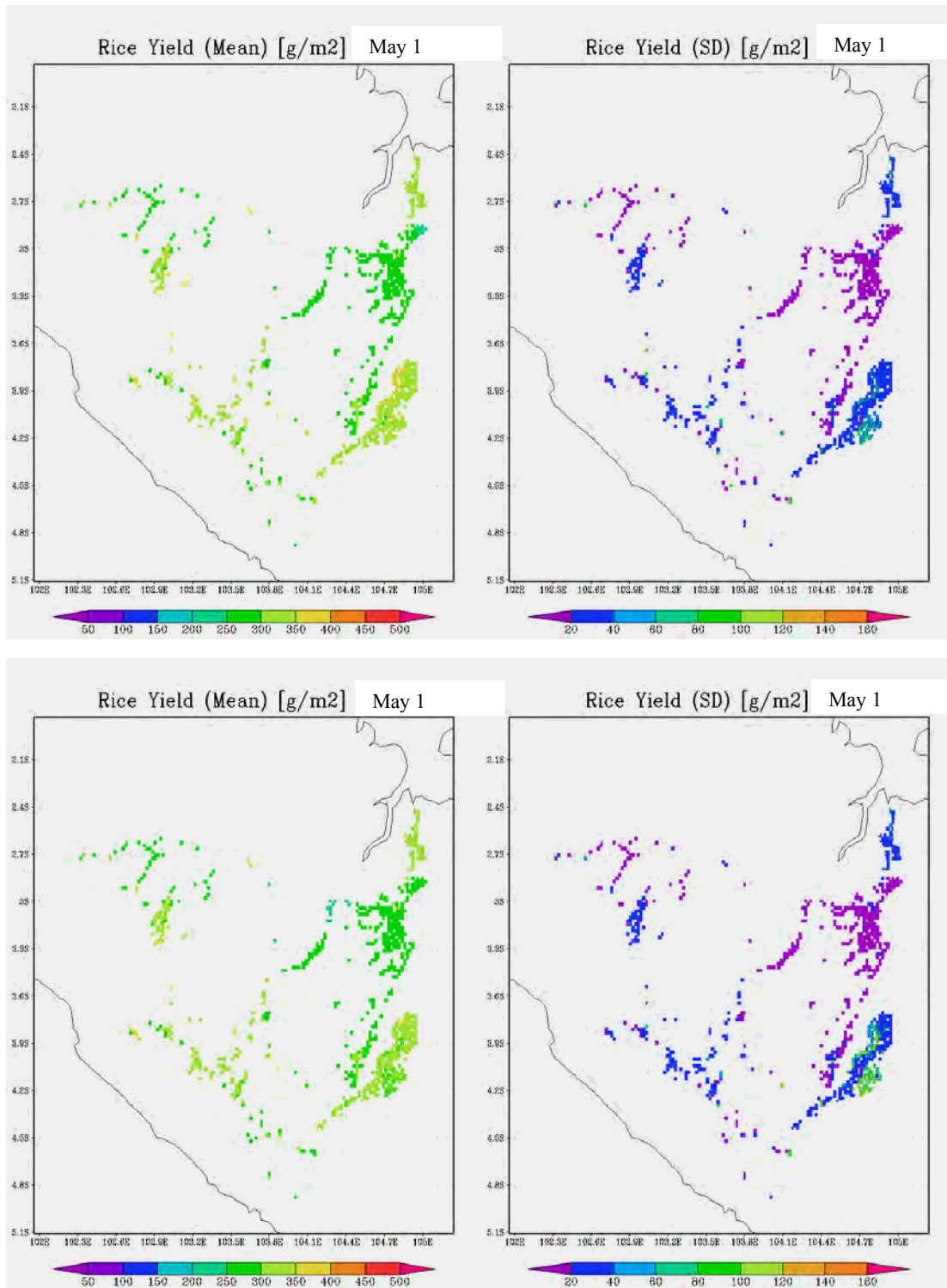


Figure 4.4.3-2 Distribution of simulated yields under the present (above) and future climate (below) in GCM scenario gfdl 2_1. Simulations were conducted for the period from January 1st, 1985 to December 31st, 2000 under the present climate conditions; and the period from January 1st, 2050 to December 31st, 2065 under the future climate conditions. Planting dates were set at May 1st (DOY = 121, dry season). The yields (left) and the standard deviation (right) were calculated for the period.

CHAPTER 4 CLIMATE CHANGE IMPACT ASSESSMENT AND HYDROLOGICAL SIMULATION

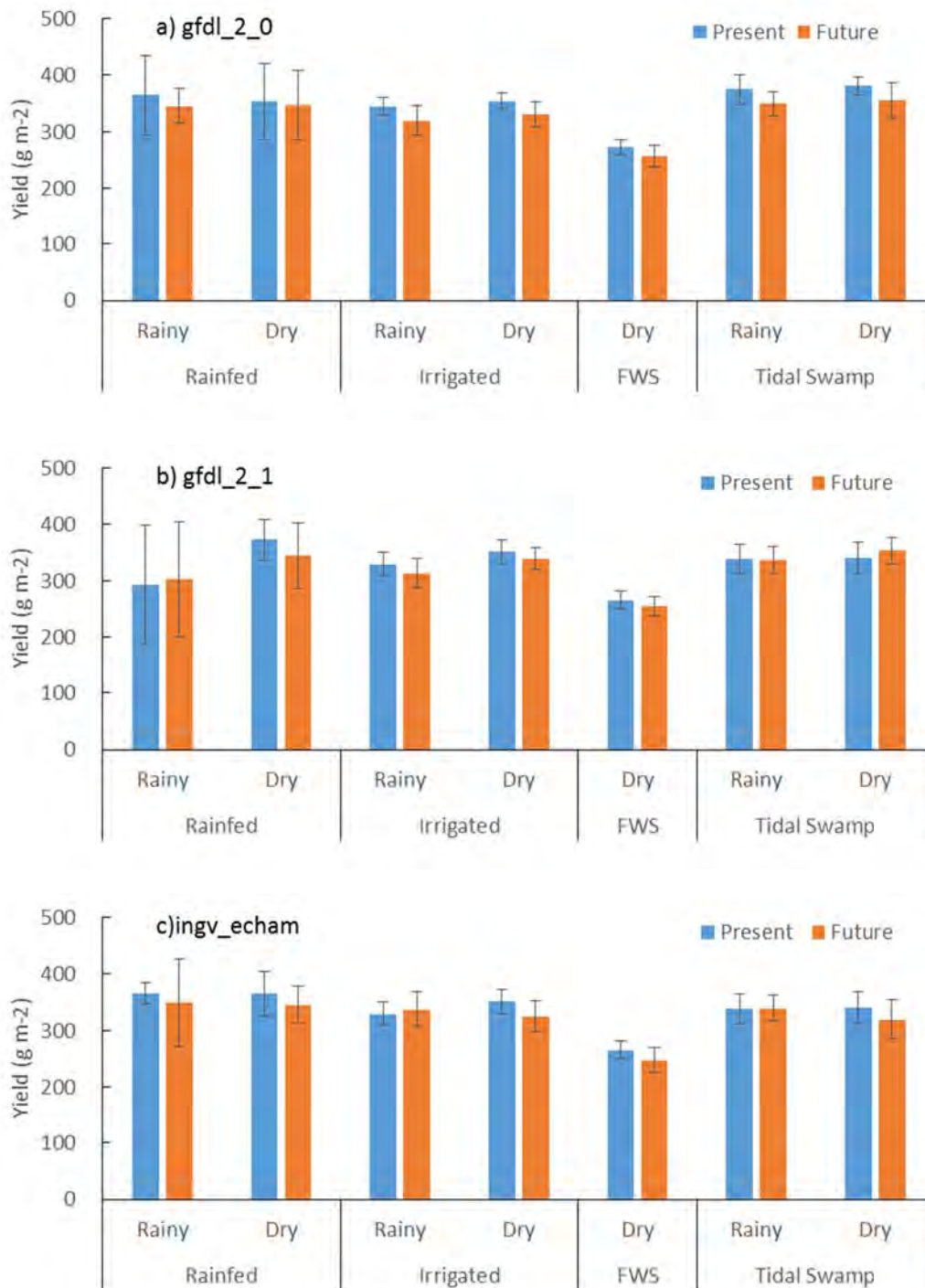


Figure 4.4.3-3. Simulated yields under future climates against those under the present climate by GCM scenarios, (a) gfdl_2_0, (b) gfdl_2_1 and (c) ingv_echam. Simulations were conducted for the period from January 1st, 1985 to December 31st, 2000 under the present climate conditions; and the period from January 1st, 2050 to December 31st, 2065 under the future climate conditions. Planting dates were set at November 1st (rainy season) and May 1st (dry season).

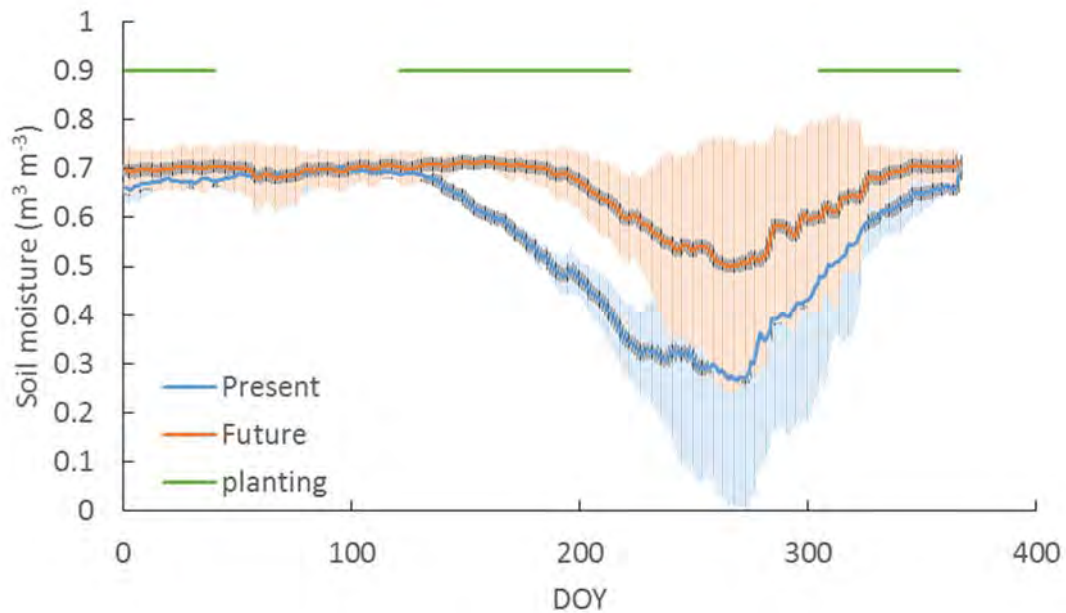


Figure 4.4.3-4 Comparison of soil moisture under present and future climates at Leumping (Rainfed ecotype). GCM scenario gfdl_2_1 was used. DOY: Days of year.

4.4.4 Designing of Technology Education System for Wide Area Management

As described in the previous sections, the following procedures are necessary to assess the climate impact on rice production in wide areas: (1) data collection from farmer's fields (2) collection of government data, (3) parameterization for the model, and (4) application of the model. Here we described each item in detail by referring the present study as examples. The strategy and tasks to design a technology education system were summarized in (5).

(1) Data collection from farmer's fields

Information items that should be collected in the fields and the collection method were determined as the following four topics in this study.

- (i) Selection of 150 sample fields from six locations (25 field each), i.e., the Telang, Upang, Rambutan, Leumping, Belitang, and Musi Rawas areas specified in Figure 4.4.4-1. Paddy fields are governmentally and agro-ecologically classified into four ecotypes (tidal swamp, fresh water swamp, irrigated, and rainfed). Because of the area and importance, we selected two tidal swamp and two irrigated locations. The farmer's fields ordinarily show quite large variations; 25 fields for each location is considered the minimum number.
- (ii) Analyzing and compiling soil data namely water contents, texture, constituents (C-organic, N-total, P-Bray, K-dd, Na, Ca, Mg, CEC, Al-dd, H-dd) and properties (pH H₂O, pH KCl, permeability, pF) specified in the "Data Sheet" and "Survey Method" of Figures 4.4.4-2 and 4.4.4-3. These items

CHAPTER 4 CLIMATE CHANGE IMPACT ASSESSMENT AND HYDROLOGICAL SIMULATION

to be analyzed were determined according to standard soil analysis items in the Suboptimal Land Research Center at the Sriwijaya University. Soil texture and C-organic are considered necessary items, because these are important factors to determine water status and soil fertility for the plants. The other items are necessary for further consideration: if some soil factors constraint rice productivity, the factors must be incorporated into the model. The constraint information will be obtained from the model validation. In particular, salinity is considered one constraint factor for rice production in tidal swamp areas, recommending analysis for cation concentration.

- (iii) Analyzing and compiling plant data: dried weights and nitrogen contents of biomass plus leaf area for two weeks, six weeks, heading time of plants, straw and grain yields (dried weights), and nitrogen contents of straw and grain at harvest time as specified in the “Data Sheet” and “Survey Method” of Figures 4.4.4-2 and 4.4.4-3.

The plant data is necessary to calibrate and validate the model.

- (iv) Analyzing and compiling data on agriculture management through interview surveys as specified in the “Data Sheet” and “Survey Method” in Figures 4.4.4-2 and 4.4.4-3.

The management data is necessary as the input data for the model.

- (v) Preparation of “Progress Report No.1”, “Progress Report No.2”, and “Final Report” with compiled data sheets.

In order to use the data systematically, compiling the data is quite important. Based on the duration and the due date, the reports were determined to divide into three.



Figure 4.4.4-1 Location map for sample survey fields

| following items are for irrigated and tidal swamp area | | | |
|--|--------------------|-------|------------------------------|
| 12 Plants Data | 2nd season | | unit |
| 13 Dried weight | 2w | | $g\ m^{-2}$ |
| | 6w | | $g\ m^{-2}$ |
| | Heading | | $g\ m^{-2}$ |
| | Maturity | Straw | $g\ m^{-2}$ |
| | | Grain | $g\ m^{-2}$ |
| 14 Nitrogen concn | 2w | | $g\ g^{-1}$ |
| | 6w | | $g\ g^{-1}$ |
| | Heading | | $g\ g^{-1}$ |
| | Maturity | Straw | $g\ g^{-1}$ |
| | | Grain | $g\ g^{-1}$ |
| 15 Leaf area | 2w | | $m^2\ m^{-2}$ |
| | 6w | | $m^2\ m^{-2}$ |
| | Heading | | $m^2\ m^{-2}$ |
| | | Straw | $g\ g^{-1}$ |
| | | Grain | $g\ g^{-1}$ |
| 16 Interviews | 2nd season | | |
| | Transplanting date | | |
| | Harvesting date | | |
| | date | kind | amount(kg ha ⁻¹) |
| 1st Fertilizer | | | |
| | date | kind | amount(kg ha ⁻¹) |
| 2nd fertilizer | | | |
| | date | kind | amount(kg ha ⁻¹) |
| 3rd fertilizer | | | |
| | date | kind | amount(kg ha ⁻¹) |
| 3rd fertilizer | | | |
| | date | kind | amount(kg ha ⁻¹) |
| Irrigation(apply condition, times, water depth etc.) | | | |

| 12 Plants Data | 1st season | | unit |
|--|--------------------|-------|------------------------------|
| 13 Dried weight | 2w | | $g\ m^{-2}$ |
| | 6w | | $g\ m^{-2}$ |
| | Heading | | $g\ m^{-2}$ |
| | Maturity | Straw | $g\ m^{-2}$ |
| | | Grain | $g\ m^{-2}$ |
| 14 Nitrogen concn | 2w | | $g\ g^{-1}$ |
| | 6w | | $g\ g^{-1}$ |
| | Heading | | $g\ g^{-1}$ |
| | Maturity | Straw | $g\ g^{-1}$ |
| | | Grain | $g\ g^{-1}$ |
| 15 Leaf area | 2w | | $m^2\ m^{-2}$ |
| | 6w | | $m^2\ m^{-2}$ |
| | Heading | | $m^2\ m^{-2}$ |
| 16 Interviews | 1st season | | |
| | Transplanting date | | |
| | Harvesting date | | |
| | date | kind | amount(kg ha ⁻¹) |
| 1st Fertilizer | | | |
| | date | kind | amount(kg ha ⁻¹) |
| 2nd fertilizer | | | |
| | date | kind | amount(kg ha ⁻¹) |
| 3rd fertilizer | | | |
| | date | kind | amount(kg ha ⁻¹) |
| Irrigation(apply condition, times, water depth etc.) | | | |

| | | | |
|-----------------------|-------------------|-------|---------------|
| 1 ID: | | | |
| 2 Location name: | | | |
| 3 Field no. | | | |
| 4 GPS | Latitude | | |
| | Longitude | | |
| 5 Soil Data | | | unit |
| 6 Water content | | | $g\ g^{-1}$ |
| 7 Texture | Sand | | $g\ g^{-1}$ |
| | Silt | | $g\ g^{-1}$ |
| | Clay | | $g\ g^{-1}$ |
| 8 C/N | Total C | | $mg\ g^{-1}$ |
| | Total N | | $mg\ g^{-1}$ |
| 9 Soil organic carbon | | | $mg\ g^{-1}$ |
| 10 Permeability | Crop layer | | $m\ s^{-1}$ |
| | Sub-soil layer | | $m\ s^{-1}$ |
| 11 pF soil moisture | Crop layer | | |
| | pF=0 | | $m^3\ m^{-3}$ |
| | pF=1.8 | | $m^3\ m^{-3}$ |
| | pF=4.2 | | $m^3\ m^{-3}$ |
| | Sub-soil layer | | |
| | pF=0 | | $m^3\ m^{-3}$ |
| | pF=1.8 | | $m^3\ m^{-3}$ |
| | pF=4.2 | | $m^3\ m^{-3}$ |
| 12 Plants Data | 1st season | | unit |
| 13 Dried weight | 2w | | $g\ m^{-2}$ |
| | 6w | | $g\ m^{-2}$ |
| | Heading | | $g\ m^{-2}$ |
| | Maturity | Straw | $g\ m^{-2}$ |
| | | Grain | $g\ m^{-2}$ |

Figure 4.4.4-2 Sample of a data sheet

CHAPTER 4 CLIMATE CHANGE IMPACT ASSESSMENT AND HYDROLOGICAL SIMULATION

| | |
|---|--|
| 1 ID | ID is named by the combination of initial letter of location name, hyphen and field no. |
| 2 Location name | Location name is selected from the list. |
| 3 Field no. | Field is numbered from 1 to 25. The order is determined by the Surveyor. |
| 4 GPS | Geographic location is measured by GPS instrument. The instrument is provided from Kyoto University (if necessary. And must be returned after the project finished). |
| 5 Soil | Soil is collected and prepared for analysis on the basis of standard method. Namely. Soils for texture, C/N and soil organic carbon analysis are collected from 3 points in a fields, and air-dried after mixing. Soils for analysis of permeability and pF soil moisture relations are sampled by using 100-ml core-sampler at 2 layers. One layer is at 7.5 cm depth (5–10 cm) for cropping layer, and another layer is at 30 cm (27.5 – 32.5 cm). |
| 6 Water content | Water content is determined after air-dried before analysis of texture, C/N and soil organic carbon for calibration. |
| 7 Texture | Texture (content of sand, silt and clay) is determined by pipette method. |
| 8 C/N | Total C and N contents would be determined by CN analyzer. Otherwise, the method is determined before analysis. |
| 9 Soil organic carbon | Soil organic carbon is determined by Walkely method. Otherwise, the method is determined before analysis. |
| 10 Permeability | Permeability (hydraulic water conductivity) for saturated soil is determined by constant-head method. |
| 11 pF and soil moisture relation | pF (water potential) and soil moisture relation is determined by suction pressure and centrifugation methods. |
| 12 Plant | Plant sample are collected from 1 m ² for each field. Samples at maturity are divide into grain and straw. |
| 13 Dried weight | Dried weight per unit area is determined after 72h drying in oven. Calculation from fresh weight and moisture content in sub sample is also possible. |
| 14 Nitrogen concentration | Nitrogen concentration of dried samples is determined by NC analyzer or Kjeldahl method. Otherwise the method is determined before analysis. |
| 15 Leaf area | Leaf area per unit area is determined by using canopy analyzer LAI2200. The analyzer is provided from Kyoto University. The measurement method is instructed by Dr. Iskandar Lubis of IPB. The instruction opportunity also provided from Kyoto University. |
| 16 Interviews | Interviews are conducted by the surveyors. Information about fertilizer is necessary for each fertilizer type, e.x. NPK Kujang, Urea, SP36 etc. Irrigation strategy, e.x. apply condition, time, water depth, will be described in text. |

Figure 4.4.4-3 Survey method

(2) Collection of governmental data

The government data listed in Figure 4.4.4-4 was collected. The usage of data was mentioned in the previous sections.

CHAPTER 4 CLIMATE CHANGE IMPACT ASSESSMENT AND HYDROLOGICAL SIMULATION

| No. | Title | Organization | Data type |
|-----|--|---|---------------|
| 1 | Law of the Republic of Indonesia No.7 of 2004 Regarding Water Resources | Presidential Secretariat | Electric File |
| 2 | Irrigation, Government Regulation No.20/2006 dated May 30, 2006 | Business News 7394-7395/2-8-2006 | Electric File |
| 3 | Overview of Indonesia Water System and Policies | Ir. M. Donny Azdan, Ph.D | Electric File |
| 4 | The Status and Challenges of Water Infrastructure Development in Indonesia | Sugiyanto and Candra R. Samekto Nippon Koei | Electric File |
| 5 | Climate Change Risk and Adaptation Assessment (South Sumatera), Sectoral Report Agriculture, June 2012 | Ministry of Environment | Electric File |
| 6 | Climate Change Risk and Adaptation Assessment (South Sumatera), Sectoral Report Climate Analysis and Projection, June 2013 | Ministry of Environment | Electric File |
| 7 | Climate Change Risk and Adaptation Assessment (South Sumatera), Sectoral Report Water, June 2014 | Ministry of Environment | Electric File |
| 8 | Profil Balai Wilayah Sungai Sumatera VIII | Direktorat Jenderal Sumber Data Air, Departemen Pekerjaan Umum | Electric File |
| 9 | Potensi Pengembangan Lahan Rawa Lebak Di Sumatera Selatan | Pemerintah Provinsi Sumatera Selatan, Dinas Pertanian Tanaman Pangan & Hortikultura | Electric File |
| 10 | Kalender Tanam Terpadu, MT III 2013 | Badan Penelitian Dan Pengembangan Pertanian | Electric File |
| 11 | Budidaya Padi Di Lahan Rawa Lebak Dengan Pendekatan Pengelolaan Tanaman Terpadu | BPTP, Sumatera Selatan | Electric File |
| 12 | PROGRAM DAN KEGIATAN PRODUKSI PADI DI SUMATERA SELATAN | Badan Penelitian Dan Pengembangan Pertanian | Electric File |
| 13 | PROGRAM/KEGIATAN TANAMAN PANGAN TAHUN 2013 PRODUKSI PADI DAN PALAWIJA | Pemerintah Provinsi Sumatera Selatan, Dinas Pertanian Tanaman Pangan & Hortikultura | Electric File |
| 14 | Produksi Tanaman Bahan Makanan 2002 | Badan Pusat Statistik, Sumatera Selatan | Paper |
| 15 | Produksi Tanaman Bahan Makanan 2003 | Badan Pusat Statistik, Sumatera Selatan | Paper |
| 16 | Produksi Tanaman Bahan Makanan 2004 | Badan Pusat Statistik, Sumatera Selatan | Paper |
| 17 | Produksi Tanaman Bahan Makanan 2005 | Badan Pusat Statistik, Sumatera Selatan | Paper |
| 18 | Produksi Tanaman Bahan Makanan 2006 | Badan Pusat Statistik, Sumatera Selatan | Paper |
| 19 | Produksi Tanaman Bahan Makanan 2007 | Badan Pusat Statistik, Sumatera Selatan | Paper |
| 20 | Produksi Tanaman Bahan Makanan 2008 | Badan Pusat Statistik, Sumatera Selatan | Paper |
| 21 | Produksi Tanaman Bahan Makanan 2009 | Badan Pusat Statistik, Sumatera Selatan | Paper |
| 22 | Produksi Tanaman Bahan Makanan 2010 | Badan Pusat Statistik, Sumatera Selatan | Paper |
| 23 | Luas Lahan Menurut Penguannya 2002 | Badan Pusat Statistik, Sumatera Selatan | Paper |
| 24 | Luas Lahan Menurut Penguannya 2003 | Badan Pusat Statistik, Sumatera Selatan | Paper |
| 25 | Luas Lahan Menurut Penguannya 2004 | Badan Pusat Statistik, Sumatera Selatan | Paper |
| 26 | Luas Lahan Menurut Penguannya 2005 | Badan Pusat Statistik, Sumatera Selatan | Paper |
| 27 | Luas Lahan Menurut Penguannya 2006 | Badan Pusat Statistik, Sumatera Selatan | Paper |
| 28 | Luas Lahan Menurut Penguannya 2007 | Badan Pusat Statistik, Sumatera Selatan | Paper |
| 29 | Luas Lahan Menurut Penguannya 2008 | Badan Pusat Statistik, Sumatera Selatan | Paper |
| 30 | Luas Lahan Menurut Penguannya 2009 | Badan Pusat Statistik, Sumatera Selatan | Paper |
| 31 | Luas Lahan Menurut Penguannya 2010 | Badan Pusat Statistik, Sumatera Selatan | Paper |
| 32 | Luas Lahan Menurut Penguannya 2011 | Badan Pusat Statistik, Sumatera Selatan | Paper |

Figure 4.4.4-4 List of government data

CHAPTER 4 CLIMATE CHANGE IMPACT ASSESSMENT AND HYDROLOGICAL SIMULATION

(3) Parameter optimization for the model

The method to estimate coupling model parameters from the above information was mentioned in the previous sections. The model has 3 categories for parameters: irrigation, field, and cultivar. Irrigation parameters were optimized from the management data described in 4.4.2 (1)-5). Field parameters, which represent soil fertility and water holding capacity, can be optimized on the basis of the relationship between soil and plant data (Figure 4.4.2-11). Cultivar parameters, which represent performance of cultivars under the given conditions, were derived from the previous study and the previous documents (Section 4.4.2 (1) -2)).

(4) Application of the model

Textbooks was prepared for the method for inputting the climate conditions at present and the future into the coupling model of WEB-DHM and SIMRIW-rainfed and the method for impact assessment of food production under climate change. The text was provided in JICA Training in Japan (Section 4.5.2).

(5) Strategy and tasks to design technology education system

Full-scale optimization for the coupling model needs all data described above. The concept of the method of optimization was taught to members from Indonesia in JICA Training in Japan (4.5.2). The training courses were oriented toward future leaders.

The data related to soil, plant, and agricultural management has been collected by several Ministry of Agriculture institutes depending on the purpose, but were not integrated. Development of an integrated data system is desired.

Because full-scale optimization needs a lot of data to be corrected, the sub scale of optimization seems to be reasonable. Once the evaluation system on the basis of the coupling model has been established, the system might be applicable to other areas with the sub scale of optimization. The sub scale of optimization can be developed on the basis of government data, and can be summarized as textbooks. To ensure the accuracy of the model output, improvements in government data as described in 4.4.4-(2) are strongly recommended.

The impact assessment has been designed to produce information for decision makers. Accordingly, if the purpose of the assessment is clarified by the decision makers, the model should be set according to the purpose. The procedure of setting of the parameters and conditions has already been taught in the JICA Training. Although the application of the model can be managed by technical experts, further improvements to the system need collaborations with researchers. For example, the latest information on future climates is provided by researchers. Down-scaling from the information to the targeted area also requires researches' help. Constraints for rice production will be revealed by researchers' analyses as described in Section 4.4.3. The establishment of such a community where decision makers, technical experts, and researchers can collaborate to assess the climate change impact will be necessary.

CHAPTER 4 CLIMATE CHANGE IMPACT ASSESSMENT AND HYDROLOGICAL SIMULATION

4.5 Implementation of Capacity Development

The capacity development program of the project, including training courses, seminars, and workshops, was conducted effectively by using individual experiences and human networks.

4.5.1 Implementation of the Seminar in Indonesia

The climate change seminars were carried out.

Seminars on “Climate Change Impact Analysis and Hydrological Simulation” were held in Jakarta, and also in Surabaya and in Palembang as major bases for Brantas and Musi river basins. Details of the seminars are given in Table 4.5.1-1 and Appendix A.

Participants in the seminars included related development partners and Indonesian organizations. Each seminar took up about a half day.

The study team was dispatched based on the reporting schedule, seminars, and meetings in Indonesia over the course of the study. Appendix-A also details these dispatches individually.

The study was initiated in June 2013 and the first dispatches were between June 23 and 26 in Jakarta. In addition to a kickoff meeting, the first seminar was held with relevant organizations on the Indonesian side on June 24.

During the second dispatch in May 2014, two climate change seminars were held in Jakarta and Surabaya each. Main topics were climate change impact assessments and hydrological simulations. Project progress was explained and some results of a case study in the Brantas river basin were shown. Another effort including crop model development for agriculture in the Musi river basin was also briefly described.

Table 4.5.1-1 Outlines of Climate Change Seminars

| Dispatch Date | Seminar location | Mission / Seminar topics |
|--|---|---|
| First dispatch June 23 to 26, 2013 (4 days) | - Jakarta June 24, 2013 | Kickoff meeting, Inception Report submission and first seminar for assessing climate change impacts and integration in Water Resources Management Plan. <Main Seminar topics> 1) Project outline (objectives, significance, contents, and others) 2) Methods of assessment of climate change impacts and runoff analysis |
| Second dispatch May 18 to 22, 2014 | - Jakarta May 19, 2014 - Surabaya May 20, 2014 | Interim Report submission and to hold seminars in Jakarta and in Surabaya. <Main Seminar topics> 1) Results of assessment of climate change impacts |

CHAPTER 4 CLIMATE CHANGE IMPACT ASSESSMENT AND HYDROLOGICAL SIMULATION

| | | |
|--|---|---|
| (5 days) | | and runoff analysis for Brantas River basin 2) Findings and study results of the project |
| Third dispatch February 2 to 4, 2017 (3 days) | - Palembang February 2, 2017- Jakarta February 3, 2017 | Draft Final Report submission and to hold seminars in Jakarta and in Palembang. <Main Seminar topics> 1) Results of assessment of climate change impacts and runoff analysis for Musi River basin 2) Comprehensive summary of the study including applications to other river basins |

In order to maintain better communication between both sides, two midterm meetings for limited people were added as below (Table 4.5.1-2). It is meaningful to share the status of the project at appropriate times and to have some talks to rediscover each responsibility.

Table 4.5.1-2 Outlines of Midterm Meetings

| Dispatch Date | Seminar location | Mission / Seminar topics |
|-----------------------------|--|---|
| 20 August, 2015 (3 days) | - Jakarta | Interim Report Meeting, in 2015. <Main Discussion> - Interim progress report of the study - Challenge points of Musi River Basin in this study - Expected the project scheduling |
| July, 2016 (4 days) | - Jakarta July 27, 2016 - Palembang July 28, 2016 | Interim Report Meeting, in 2016. <Main Discussion> - Interim explanation of Musi river basin outputs and overall schedule of the project by the study leaders. - Climate Change Seminar in Palembang |

4.5.2 Implementation of Training in Japan (Assistance)

As mentioned in Section 3.3, JICA country-focused training courses “Simulation and Evaluation of Climate Change Impacts by Downscaling and Hydrological Modeling” were conducted. These training courses were initially planned by JICA and the Water Resources Management Plan team (Component-2), following Table 4.5.2-1 tentatively.

Table 4.5.2-1 Program of Climate Change Impact Assessment and Runoff Analysis (Tentative)

| | |
|--------------|--|
| Course Title | Simulation and Evaluation of Climate Change Impacts by Downscaling and Hydrological Modeling |
| Trainee | 4 persons in total. |
| Period | 4 weeks x 2 times (The same trainees should be invited twice) |

CHAPTER 4 CLIMATE CHANGE IMPACT ASSESSMENT AND HYDROLOGICAL SIMULATION

| | |
|---------|---|
| Purpose | To learn methods for assessment of climate change impacts and runoff analysis |
| Topics | First 4 weeks: Learning methods through lectures and practices Second 4 weeks: Deep understanding through study work by trainees |
| Trainer | The study team “Climate Change Impact Assessment and Runoff Analysis” |

Source: JICA Project Team

The study team cooperated with the Water Resources Management Plan team (Component-2) to arrange the detailed schedules and to draft materials for these trainings courses. Each of them was practically implemented as in the outline shown in Table 4.5.2-2.

Table 4.5.2-2 Program of training on climate change impact assessment

| Item | 1st Training-1 | 1st Training-2 * ¹ | 2nd Training |
|-----------------------------|---|---|---|
| Trainee | Group (4 people) | Individual (1 person) | Group (3 people) |
| Period | 4 weeks (April, 2014) | 2 months (January to March, 2015) | 4 weeks (May to June, 2015) |
| Course Title | Simulation and Evaluation of Climate Change Impacts by Downscaling and Hydrological Modeling | | |
| Objectives | To build up technical knowledge for the trainees: (1) To assess climate change impacts in consideration of uncertainty in climate change impacts (2) To consider adaptation measures based on quantitative assessment of climates impacts | | |
| Topics and Items | < Learning methods through lectures and practices > 1) Overview of climate system and climate change impact assessment 2) Bias collection, dam operation 3) WEB-DHM training for Musi River and Brantas River Basins (introduction, preparation of input data) 4) Evaluation of future conditions using WEB-DHM with GCM data 5) Crop model/coupled water-rice model with irrigation module | | < Deep understanding through study work by trainees > 1) Analysis of climate change 2) Overview of WEB-DHM 3) Study result of Brantas River Basins with WEB-DHM 4) Work on development of WEB-DHM 5) Study on Agriculture field in Musi river basin |
| Trainer | Study Team for “Climate Change Impact Assessment and Runoff Analysis” | | |
| Place | Tokyo | Tokyo | Tokyo, Tsukuba |
| Visiting, Observation Trips | — | - JMA - Tanashi Observation Field * ² | - ICHARM - JAXA - JMA |

CHAPTER 4 CLIMATE CHANGE IMPACT ASSESSMENT AND HYDROLOGICAL SIMULATION

Source: JICA Project Team

[Note]

- *1: Conducted by the framework of JICA and the University of Tokyo.
- *2: The experimental field of University of Tokyo, Nishi-Tokyo city, Tokyo.

The study team implemented the country-focused training courses three times. Local Indonesian operational staff were invited twice each time during the training session on assessment of climate change impacts. In terms of accumulating related knowledge and analysis techniques effectively, same trainees were permitted to both training courses attached to counterpart organizations. Knowledge and technology transfer were conducted on a daily basis in each training period.

< 1st: Learning methods through lectures and practices >

The first training course of four weeks, from March 31 to April 26, 2014, which was the responsibility for the study team (Component-1) focused on WEB-DHM principles and application for the three weeks. The other one week was allocated for coupling a crop model.

After the first training course, similar content to the first was conducted for BMKG staff individually in The University of Tokyo in Japan, from January 29 to March 21, 2015, accepting strong demand from Indonesia side. The framework of JICA and the University of Tokyo conducted this training from the research and development point of view, including science and practical and operational areas, spending more than the previous time to promote a more effective and efficient implementation of the project.

< 2nd: Deep understanding through study work by trainees >

The 4-week training course from May 27 to June 24, 2015 was our responsibility again, focused on deepening understanding through study work by the attendees.

The study team members gave lectures and presentations that included study and survey methods, explanations of deliberation processes and results, and introduction of actual cases in Japan or other countries, with individual topics and subjects related to the expertise and experiences of each study team member. To improve technical knowledge, understanding, and practical skills, appropriate texts, research papers, and materials were provided to trainees for their own training and discussions.

As well as the implementation and operations described above, observation trips were arranged and attendees visited some agencies and facilities. Details of these country-focused training courses are given in Appendix C.

CHAPTER 4 CLIMATE CHANGE IMPACT ASSESSMENT AND HYDROLOGICAL SIMULATION

4.5.3 Handbook for Assessing and Integrating Climate Change Impacts into Water Resources Management Plan (Assistance)

The project will prepare recommendations for the guidelines to be applicable to the POLAs (Water Resources Management Strategic Plan) and RENCANAs (Water Resources Management Implementation Plan) in other river basins in Indonesia, taking climate change issues into account.

To comply with the guidelines, a handbook is essential for technical transfers to other basins in Indonesia.

The study team was in charge of development of the handbook covered in the study area to cooperate with the Water Resources Management Plan team as well as the country-focused training courses above mentioned.